Protein interaction studies of the voltage-dependent calcium channel beta subunit

Adrian Butcher

A thesis submitted in fulfilment of the requirements for the degree of Doctor of Philosophy at the University of London

2006

Department of Pharmacology
Andrew Huxley Building
University College London
Gower Street
London, W1E 6BT

ProQuest LLC
789 East Eisenhower Parkway
P.O. Box 1346
Ann Arbor, MI 48106-1346

Declaration

I, Adrian Butcher confirm that the work presented in this thesis is my own. Where information has been derived from other sources, I confirm that this has been indicated in the thesis

Adrian Butcher

Abstract

Voltage dependent calcium channels (VDCCs) are heteromultimeric membrane proteins which open to allow Ca^{2+} entry upon depolarisation of the plasma membrane. The β subunit of voltage-dependent calcium channels interacts with the alpha interaction domain (AID) in the I-II linker of the pore forming α1 subunit and regulates trafficking and biophysical properties of these channels.

A surface plasmon resonance binding assay has been developed to measure the interaction between the I-II linkers of Ca_V 1.3, Ca_V 2.1 and Ca_V2.2 and Ca_Vβ1b, Ca_Vβ2a and Ca_Vβ3 and the dissociation constants (K_D) for these interactions have been calculated and were found to be between 12.1 and 20nM. The assay was then extended to measure the interaction between the I-II linkers of Ca_V 1.3 and Ca_V 2.2 and G protein βγ subunits. The dissociation constant for G βγ binding to the I-II linker of Ca_V2.2 was calculated to be 62.2nM whereas no interaction was detected between the I-II linker of Ca_V1.3 and Gβγ.

The effects of specific mutations within AID on Ca_Vβ subunit binding and calcium channel trafficking were measured using surface plasmon resonance and cell surface biotinylation assays. Mutation of tryptophan within AID abolished Ca_Vβ binding and reduced the amount of Ca_V2.2 channels in the plasma membrane whereas mutation of tyrosine reduced the affinity of Ca_Vβ for AID by 24 fold but had no effect on the biophysical properties or trafficking of Ca_V2.2 expressed in tsA 201 cells.

Activation of phosphoinositide 3-kinase (PI3 kinase) promotes translocation of VDCC's to the plasma membrane, this mechanism involves protein kinase B and is specific for calcium channels containing the Ca_Vβ2a subunit. Co-expression of PI3 kinase resulted in increased phosphorylation on serine 574 of Ca_Vβ2a and protein kinase B was found to co-precipitate with Ca_Vβ2a.

Finally, a proteomic approach was used to identify proteins which may interact with Ca_Vβ subunits. Ca^{2+}/calmodulin dependent kinase II was found to interact specifically with the C-terminus of Ca_Vβ1b.

Acknowledgements

I would like to thank Professor Annette Dolphin for the opportunity to work in the lab and for help and support during the PhD project. I am also enormously grateful to all members of the ACD lab for their help and advice during my time there, especially to Nick Berrow, Mark Richards, Jerome Leroy, Karen Page, Manuela Nito-Rostro, Stuart Martin, Patricia Viard and Wendy Pratt. I wish all members of the ACD lab the best of luck in whatever they may do in future.

I would also like to thank my parents for their generosity and support whilst I have been studying, especially during the time that I have been writing and thanks also to my aunt and uncle who generously supported me when I first moved to London.

Contents

List of Figures

List of Tables

List of Abbreviations

ABP	AID binding pocket
AID	Alpha interaction domain
AMPA	Alpha-amino-3-hydroxy-5-methyl-4-isoxazolepropionic acid
AMP	Adenosine monophosphate
cAMP	Cyclic adenosine monophosphate
ATP	Adenosine triphosphate
BAD	Bcl-2 like agonist of cell death
BCA	Bicinchoninic acid
BHK	Baby hamster kidney
BIA	Biomolecular interaction analysis
BID	Beta interaction domain
BSA	Bovine serum albumin
C-terminus	Carboxyl terminus
CaM kinase II	Ca^{2+}/calmodulin dependent protein kinase II
CHAPS	3-[(3-Cholamidopropyl)dimethylammonio]-1-propanesulfonate
CHCB2/HP1γ	Chromobox protein 2/heterochromatin protein γ
CM	Carboxymethyl
C	Cytosine
Dlg	Disks large protein
DNA	Deoxyribonucleic acid
cDNA	Complimentary DNA
DMEM	Dulbecco's modified eagle medium
DMSO	Dimethysulphoxide
DRG	Dorsal root ganglion
DTT	Dithiothreitol
EA2	Episodic ataxia type-2
EDC	N-ethyl-N'-(dimethylaminopropyl)-carbodiimide
EDTA	Ethylenediaminetetraacetic acid
ER	Endoplasmic reticulum
FHM	Familial hemiplegic migraine
FRET	Fluorescence resonance energy transfer

G	Guanine
G protein	GTP binding protein
Gβγ	GTP binding protein βγ subunit
GAKIN	Guanylate kinase associated kinesin
GK	Guanylate kinase
GKAP	Guanylate kinase associated protein
GLUT4	Glucose transporter protein 4
GPCR	G protein coupled receptor
GSK-3	Glycogen synthase kinase-3
GST	Glutathione-s-transferase
GTP	Guanine triphosphate
HEK	Human embryonic kidney
HEPES	(N-(2-Hydroxyethyl)piperazine-N'-(2-ethanesulfonic acid)
His tag	Hexahistidine tag
HRP	Horse radish peroxidase
HVA	High voltage activated
IFC	Integrated microfluidic cartridge
IGF-1	Insulin like growth factor
ILK	Integrin linked kinase
IP3	Inositol triphosphate
IPTG	Isopropyl-1-thio-β-D-galatopyranoside
I-V	Current-voltage
KDa	Kilodaltons
LTD	Long Term depression
LTP	Long term potentiation
LVA	Low voltage activated
mA	Milliamps
MAGUK	Membrane associated guanylate kinase
MALDI	Matrix Assisted Laser Desorption Ionisation
MCS	Multiple cloning site
MES	2-(N-Morpholino)ethanesulfonic acid 4-Morpholineethanesulfonic acid
MIDAS	Metal ion dependent adhesion site

MOPS	3-(N-Morpholino)propanesulfonic acid 4-Morpholinepropanesulfonic acid
mRNA	Messenger RNA
mTOR	Mammalian target or rapamycin
N-terminus	Amino terminus
NHS	*N*-hydroxysulfosuccinimide
Ni NTA	Nickel nitrillotriacetic acid
NMDA	N-methyl-D-aspartate
NusA	N utilisation substance protein
^{32}P	Phosphate isotope 32
^{33}P	Phosphate isotope 33
PBS	Phosphate buffered saline
PCR	Polymerase chain reaction
PDK-1	Phosphoinositide dependent kinase
PI3 Kinase	Phosphoinositide 3-kinase
PKB	Protein kinase B
PMCA	Plasma membrane calcium ATPase
PMF	Peptide mass fingerprinting
PSD-95	Post synaptic density-95
PVDF	Polyvinyldeneflouride
RACE	Rapid amplification of cDNA ends
RNA	Ribonucleic acid
ROC	Receptor operated calcium channel
RyR	Ryanodine receptor
SAP-97	Synapse-associated protein-97
SCA6	Spinocerebellar ataxia type 6
SCID	Severe combined immunodeficiency
SDS PAGE	Sodium dodecyl sulphate polyacrylamide gel electrophoresis
SERCA	Sarco-endoplasmic reticulum calcium ATPase
SH2	Src homology-2
SH3	Src homology-3
SOC	Store operated calcium channel
SPR	Surface plasmon resonance
SV40	Simian virus 40

TAE	Tris acetate EDTA
TE	Tris EDTA
TGFβ	Target growth factor β
TIR	Total internal reflectance
TOF	Time of flight
V	Volts
VDCC	Voltage dependent calcium channel
VWA	Von Willebrand factor-A
UV	Ultraviolet
ZO-1	Zona occludens-1

Chapter 1:
General Introduction

1.1 Intracellular calcium homeostasis

From prokaryotic to eukaryotic organisms, calcium ions are important and versatile signalling agents. In mammalian cells, Ca^{2+} ions are involved in many cellular processes including gene transcription, hormone secretion, muscle contraction cellular proliferation and neurotransmitter release (Bootman, 2001). Intracellular Ca^{2+} concentrations are usually around 100nM whilst the concentration in the extracellular space can be up to 2mM (Clapham, 1995). Although Ca^{2+} ions are essential for life, high levels of intracellular Ca^{2+} are extremely toxic and result in cell death. It is therefore not surprising that nature has developed specialised mechanisms for controlling the levels of intracellular Ca^{2+} as well as utilising the steep concentration gradient for signalling and information transfer.

Intracellular Ca^{2+} can be derived from two sources. Channels in the endoplasmic reticulum such as the inositol trisphosphate (IP3) receptor or the ryanodine (RyR) receptor allow release of Ca^{2+} from internal stores within the endoplasmic reticulum into the cytoplasm in response to certain stimuli. Extracellular calcium is delivered to the cytoplasm via Ca^{2+} influx channels in the plasma membrane. Several types of influx channel contribute to the elevation of cytosolic Ca^{2+}, these include voltage dependent calcium channels (VDCC) which are activated in response to depolarisation of the plasma membrane. Receptor-operated Ca^{2+} channels (ROCs) are activated in response to agonist binding to the extracellular side of the plasma membrane. Receptor operated channels include the N-methyl-D-aspartate (NMDA) receptor and the nicotinic acetylcholine receptor. Store-operated calcium channels (SOC) allow influx of calcium from the extracellular space in response to depletion of Ca^{2+} from intracellular stores. First discovered in non-excitable cells (Hoth *et al.*, 1992), and later described in other cell types (Skryma *et al.*, 2000; Albert et al., 2002; Hunton et al., 2004; reviewed by Bolotina, 2004). The molecular identity of the channels and the mechanism by which store depletion is sensed has only recently been discovered. Feske et al, (2006) reported that the genetic defect responsible for severe combined immunodeficiency (SCID) in humans is also responsible for store operated Ca^{2+} current. The protein named orai1 is the product of the ORAI1 gene and expression of orai1 in SCID T cells restored store operated Ca^{2+} current. Previous studies had identified STIM1 as a calcium sensor which can migrate from the ER to the plasma membrane upon Ca^{2+} depletion (Zhang *et al.*, 2005) and subsequent studies have shown that orai1 and stim1 functionally interact

(Peinelt *et al.*, 2006) and reconstitute store operated Ca^{2+} channels (Soboloff *et al.*, 2006). Mechanically-activated calcium channels are activated in response to stretch, stress or shape change in cells such as tracheal epithelia (Boitano *et al.*, 1992).

As Ca^{2+} ions can be extremely toxic, rises in cytosolic Ca^{2+} are rapidly buffered such that only 0.25-1% of the ions which enter the cytoplasm remain free (Neher, 1995). Calcium buffering is carried out, at least in part, by a large group of calcium binding proteins known as the "EF hand" family. The family is named after the E and F regions of parvalbumin which contains two α helices separated by a Ca^{2+} binding loop. The Ca^{2+} binding loop is composed of amino acid residues containing side chain oxygen groups such as glutamate (Krestinger, 1980) as between 4 and 12 oxygen atoms are required to coordinate a single Ca^{2+} ion (Fasman, 1989). Members of the EF hand family include calmodulin which is ubiquitous and can change its conformation upon Ca^{2+} binding and can act as a calcium sensor, calbindin, calretinin and parvalbumin (Heizmann *et al.*, 1991; Baimbridge *et al.*, 1992; Lewit-Bentley, 2000). The Ca^{2+} buffering mechanism means that Ca^{2+} ions diffuse slowly in the cytoplasm relative to unbuffered signalling molecules such as IP3. The range of action is therefore very short and the majority of its signalling action takes place at or around its site of entry into the cytoplasm.

Mechanisms have also evolved to actively extrude Ca^{2+} ions from the cytoplasm. In the endoplasmic reticulum, the sarco-endoplasmic reticulum calcium ATPase (SERCA) pump uses energy in the form of ATP to sequester Ca^{2+} ions from the cytoplasm into the endoplasmic reticulum where they are again buffered by Ca^{2+} binding proteins such as calreticulin and calsequestrin which bind Ca^{2+} ions with low affinity but high capacity (Baksh *et al.*, 1991; Michalak *et al.*, 1998). Plasma membrane calcium ATPase (PMCA) pumps perform a similar function but extrude cytosolic Ca^{2+} ions into the extracellular space (Brandt and Vanaman, 1996). Operating in parallel to these pumps in most cell types it the Na^{+}/Ca^{2+} exchanger, this exchanger can move Ca^{2+} into or out of the cytoplasm depending upon the electrochemical gradient. Under normal physiological conditions, the exchanger effectively extrudes Ca^{2+} ions from the cytoplasm in exchange for Na^{+} ions at a rate of 1 Ca^{2+} for 3 Na^{+}. The direction of exchange can be reversed in response to high intracellular Na^{+} ion concentrations. Finally, mitochondria, as well as being the cellular power houses may play a role in intracellular Ca^{2+} homeostasis.

Figure 1.1

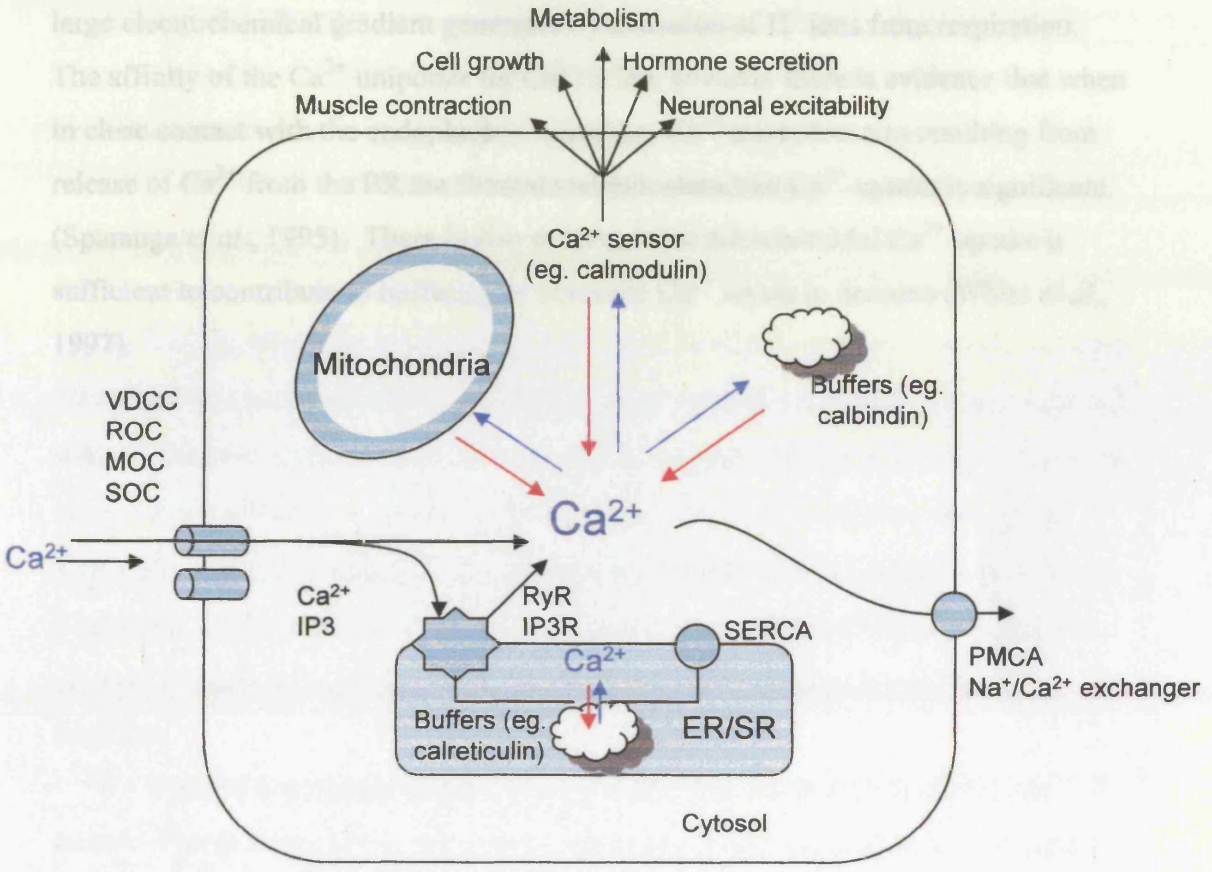

Figure 1.1. Summary of main processes which contribute cytosolic Ca^{2+} homeostasis. VDCC voltage dependent calcium channel; ROC receptor operated calcium channel; MOC mechanically operated calcium channel; SOC store operated calcium channel; RyR ryanodine receptor; IP3R inositol 1,4,5 trisphosphate receptor; ER/SR endoplasmic/sarcoplasmic reticulum; SERCA sarco-endoplasmic reticulum calcium ATPase; PMCA plasma membrane calcium ATPase. Reproduced from Bootman, (2001) with modifications.

Mitochondria can accumulate Ca^{2+} up to concentrations of 500μM in the mitochondrial matrix, the Ca^{2+} enters via a Ca^{2+} uniporter and entry is driven by the large electrochemical gradient generated by extrusion of H^{+} ions from respiration. The affinity of the Ca^{2+} uniporter for Ca^{2+} is low however there is evidence that when in close contact with the endoplasmic reticulum, Ca^{2+} microdomains resulting from release of Ca^{2+} from the ER are formed and mitochondrial Ca^{2+} uptake is significant (Sparanga *et al.*, 1995). There is also evidence that mitochondrial Ca^{2+} uptake is sufficient to contribute to buffering of cytosolic Ca^{2+} levels in neurons (White *et al.*, 1997).

1.2 Voltage dependent calcium channels

Voltage dependent calcium channels (VDCCs) open to allow Ca^{2+} entry upon depolarisation of the plasma membrane. Voltage dependent calcium channels play major roles in normal physiological processes such as muscle contraction, gene transcription, electrical signalling and hormone secretion (Catterall, 2000) and in the pathological processes of many diseases. They are major routes of Ca^{2+} entry in excitable cells and their presence has been said to define an excitable cell (Hille, 2001).

Voltage dependent calcium channels are heteromultimeric membrane proteins composed of a pore-forming α1 subunit, a cytoplasmic β subunit, an extracellular α2 subunit linked to a transmembrane δ subunit by at least one disulphide bond. In some cases a transmembrane γ subunit is also present. The transmembrane topology of VDCCs is shown in figure 1.2. Genes encoding 10 different α1 subunits, 4 different β subunits, 4 α2δ subunits and 8 putative gamma subunits have been identified and cloned. In addition many splice variants for each class of subunit have been described.

Voltage dependent calcium channels were first discovered in crustacean muscle (Fatt & Katz, 1953), the muscle was found to still generate action potentials when sodium was omitted from the bathing solution. Nearly 30 years later, the first biochemical analysis was performed on channels purified form solubilised skeletal muscle transverse tubules (Curtis & Catterall, 1983). Analysis by SDS PAGE revealed an α subunit, a β subunit, a δ and a γ subunit and showed α1 and β subunits to be substrates for cAMP-dependent phosphorylation (Curtis & Catterall, 1985). Subsequent biochemical analysis revealed the α subunit to consist of two proteins α1 and α2δ (Takahashi *et al.*, 1987). α2δ was largely extracellular, heavily glycosylated and a disulphide linked heterodimer of α2 and δ. The α1 subunit was designated the pore-forming subunit as it bound to radiolabelled 1,4 dihydropyridines.

1.2.1 Voltage dependent calcium channel classification

VDCCs were originally classified according to their biophysical and pharmacological properties. In skeletal, cardiac and smooth muscle, L-type calcium currents were so called because of their long lasting nature, this is due to slow voltage dependent inactivation. L-type calcium currents are inhibited by dihydropyridines,

Figure 1.2

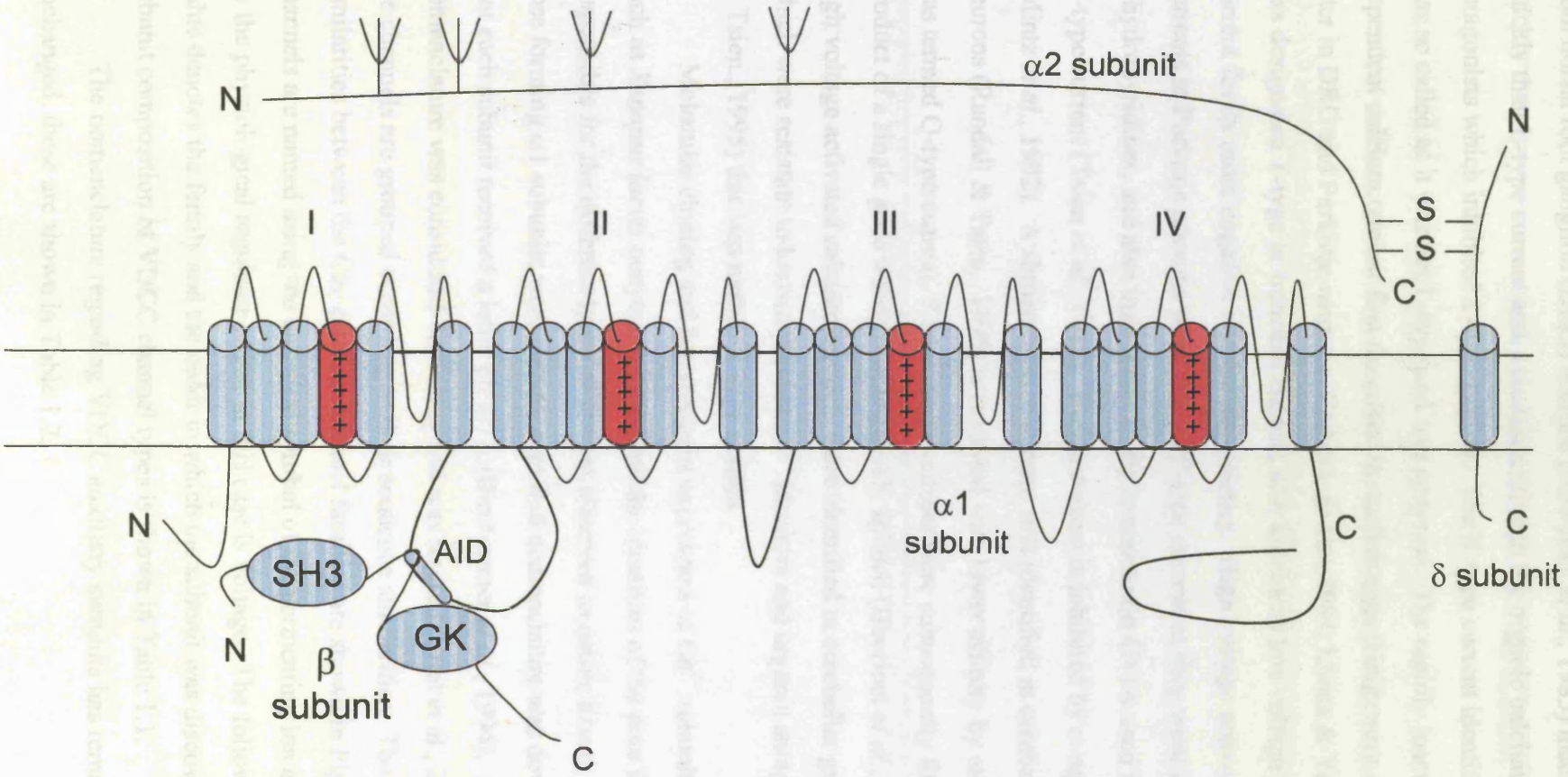

Figure 1.2. Subunit composition of HVA calcium channels. The pore forming α1 subunit consists of 24 membrane spanning segments, transmembrane segments marked in red represent the voltage sensor. The α1 subunit is associated with an extracellular α2 subunit which is linked to the transmembrane δ subunit by a disulphide bond. The cytoplasmic $Ca_V\beta$ subunit associates with the α1 subunit primarily via the highly conserved AID motif located within the cytoplasmic linker between transmembrane domains I and II.

phenylalkylamines and benzothiazipines (Reuter, 1983). Calcium currents recorded from dorsal root ganglion (DRG) neurons (Nowycky *et al.*, 1985) inactivated more quickly than L-type current and were insensitive to the organic calcium channel antagonists which inhibited L-type current. The N-type current identified in this way was so called as it was not L-type and was neuronal. The rapidly inactivating voltage dependent calcium current first described in starfish eggs (Haigawara *et al.*, 1975) and later in DRG and Purkinje neurons (Carbone & Lux,1984; Llinas & Yarom, 1981) was designated T-type or transient current, also known as low voltage activated current for its more negative voltage dependency. High voltage activated calcium currents in Purkinje neurons were termed P-type current as they were insensitive to dihydropyridines, and also insensitive to the ω-conotoxin GVIA used to distinguish N-type current (Tsien *et al.*, 1988). P-type current is inhibited by ω-agatoxin IVA (Mintz *et al.*, 1992). A similar type of current first identified in cerebellar granule neurons (Randall & Tsien., 1995) is inhibited with lower affinity by ω-agatoxin IVA was termed Q-type current, P and Q-type current were subsequently found to be the product of a single gene which is alternatively spliced (Bourinet *et al.*, 1999). Other high voltage activated calcium currents were identified in cerebellar granule neurons which were resistant to known peptide Ca^{2+} blockers and organic antagonists (Randall & Tsien., 1995) this was named R-type current.

Molecular cloning and heterologous expression of Ca^{2+} subunits in systems such as *Xenopus laevis* oocytes has revealed the identities of the pore forming α1 responsible for the different types of current observed in native tissue. As more new pore forming α1 subunits were cloned, a unified nomenclature was developed such that each subunit received a letter eg. α1A (Birnbaumer *et al.*, 1994). However this nomenclature was considered confusing and was revised (Ertel et al., 2000) such that the channels are grouped according to their sequence similarities. The sequence similarities between the Ca_V calcium channel families are shown in Figure 1.3. The channels are named using the chemical symbol of the permeating ion eg. Ca followed by the physiological regulator which in this case is voltage. The following numerical value denotes the family and the order in which the subunit was discovered. The subunit composition of VDCC channel types is shown in Table 1.1.

The nomenclature regarding VDCC auxiliary subunits has remained unchanged, these are shown in Table 1.2.

Table 1.1

Ca^{2+} channel	Current type	Tissue specificity	Selective blocker	ıFunction	Reference
$Ca_V1.1$	L	Skeletal muscle	Dihydropyridines	E/C coupling Ca^{2+} homeostasis Gene expression	Tanabe et al., (1987)
$Ca_V1.2$	L	Cardiac muscle Endocrine CNS	Dihydropyridines	E/C coupling Hormone secretion Gene expression	Koch et al., (1990)
$Ca_V1.3$	L	Endocrine CNS	Dihydropyridines	Hormone secretion Gene expression	Williams et al., (1992)
$Ca_V1.4$	L	Retina	Dihydropyridines	Tonic neurotransmitter release	Strom et al., (1998)
$Ca_V2.1$	P/Q	CNS	ω-agatoxin IVA	Neurotransmitter release	Mori et al., (1991)
$Ca_V2.2$	N	CNS	ω-conotoxin GVIA	Neurotransmitter release	Dubel et al., (1992)
$Ca_V2.3$	R	CNS	SNX 482	$Ca2^{2+}$ dependent action potentials Neurotransmitter release	Soong et al., (1994)
$Ca_V3.1$	T	Cardiac muscle Skeletal muscle CNS	Mibefradil	Pacemaker activity	Perez-Reyes et al., (1998)
$Ca_V 3.2$	T	Cardiac muscle CNS	Mibefradil	Pacemaker activity	Cribbs et al., (1998)
$Ca_V3.3$	T	CNS	Mibefradil	Pacemaker activity	Lee et al., (1999)

Table 1.1. Voltage dependent calcium channels are grouped into one of three families according to their sequence similarities. The table shows a list of the pore forming α1 subunits, the type of current they mediate, their tissue specificity and their selective pharmacological blocker.

Table 1.2

Subunit	Function	Tissue specificity	Reference
α2δ-1	Trafficking of $Ca_V\alpha1$ subunit Increase in current amplitude Hyperpolarise voltage dependence of activation	Brain, Heart, Skeletal muscle	Gurnett et al.,1996
α2δ-2	Increase in current amplitude	Lung, testis, brain, heart, pancreas, prostate, skeletal muscle, spinal cord	Klugbauer et al., 1999
α2δ-3	Increase in current amplitude Hyperpolarise voltage dependence of activation	Brain, heart, skeletal muscle	Klugbauer et al., 1999
α2δ-4	Increase in current amplitude	Heart, skeletal muscle, intestine, fetal liver, erythroblasts, adrenal gland, pituitary	Qin et al., 2002
β1	Trafficking of α1 subunit to plasma membrane Increases current amplitude Activation / inactivation kinetics and voltage dependence	Skeletal muscle (β1a), Brain (other β1 isoforms)	Bogdanov et al., 2000
β2	Trafficking of α1 subunit to plasma membrane Increases current amplitude Activation / inactivation kinetics and voltage dependence	Heart, lung, trachea, aorta, brain	Chien et al., 1998
β3	Trafficking of α1 subunit to plasma membrane Increases current amplitude Activation / inactivation kinetics and voltage dependence	Smooth muscle, trachea, aorta, lung, brain	Brice et al., 1999
β4	Trafficking of α1 subunit to plasma membrane Increases current amplitude Activation / inactivation kinetics and voltage dependence	Brain	Brice et al., 1999
γ1	Inhibitory effects	Skeletal muscle	Jay et al., 1990
γ2	Inhibitory effects Trafficking of AMPA receptors	Brain	Letts et al., 1998
γ3	Activation and inactivation kinetics	Brain	Klugbauer et al., 2000
γ4	Inactivation kinetics	Heart, lung, brain, prostate, spinal cord	Klugbauer et al., 2000
γ5	Activation and inactivation kinetics ($Ca_V3.1$)	Brain	Klugbauer et al., 2000
γ6	Reduction in current amplitude (LVA channels)	Heart, skeletal muscle, brain	Chu et al., 2002
γ7	Reduction in current amplitude	Brain, heart, lung, testis	Moss et al., 2002
γ8	As γ2, γ3 and γ4	Brain, testis, spinal cord	Klugbauer et al., 2000

Table 1.2. Auxiliary subunits of voltage dependent calcium channels. Adapted from Arikkath & Campbell, (2003)

Figure 1.3

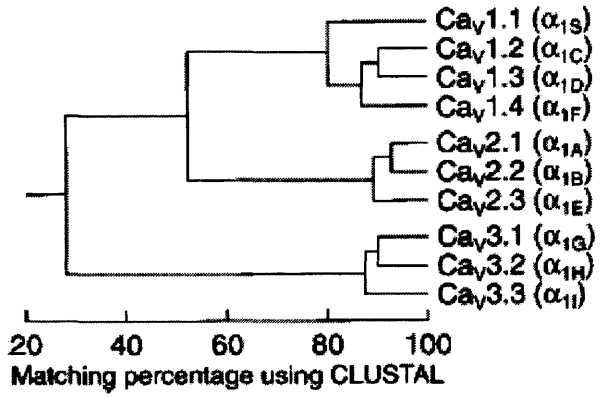

Figure 1.3. Phylogenetic diagram showing the sequence similarities between the Ca_V calcium channel families. Only the transmembrane and pore forming loop are compared. Within each family, the sequence similarity is greater than 80%. Between families the sequence identities are 52% between Ca_V 1 and Ca_V 2 families and 28% between the Ca_V 3 family and the Ca_V 1 2 families. Taken from Ertel et al., (2000).

1.2.2 The pore forming α1 subunit

The VDCC α1 subunit is composed of approximately 2000 amino acid residues giving it a molecular weight of about 250 kilo Daltons (kDa). The polypeptide chain is arranged into 24 transmembrane helices which in turn are arranged into 4 homologous domains connected by cytoplasmic linkers. In addition there are a cytoplasmic N- and C-termini (Figure 1.2), this domain architecture is similar to the voltage gated sodium channel (Yu & Catterall, 2003). The 4th transmembrane segment of each domain contains charged residues and serves as the voltage sensor. Under the influence of the electric field, the voltage sensor rotates outwards and causes the channel to open. The 5th and 6th transmembrane segments form the inner lining of the pore, a membrane associated loop known as the P-loop between segments 5 and 6 contains a conserved glutamate residue which enables the pore's selectivity for Ca^{2+} (Yang *et al.*, 1993). The T-type channel family have two aspartate residues and two glutamate residues rather than 4 glutamate residues in the selectivity filter, it is this which gives rise to their altered ion permeation characteristics (Tavelera et al., 2001).

The I-II linker of all HVA Ca^{2+} channels contains a highly conserved 18 amino acid motif known as the alpha interaction domain (AID) (Pragnell *et al.*, 1994). The AID is the primary site of interaction with the $Ca_V\beta$ subunit which binds to AID with very high affinity (De Waard *et al.*, 1995). Binding of the $Ca_V\beta$ subunit has substantial effects on the biophysical properties of HVA α1 subunit including increased plasma membrane expression and induction of hyperpolarising shifts in the voltage dependence of activation, voltage dependence of inactivation and voltage dependence of steady state inactivation (Catterall, 2000; Dolphin, 2003). In the Ca_V2 family of HVA Ca^{2+} channels the AID also contains a QQXXR motif which has been shown to be involved in interaction with βγ subunits of heterotrimeric G proteins (De Waard *et al.*, 1997). Although the sites of interaction of $Ca_V\beta$ and G protein βγ overlap in Ca_V2 AID, whether these subunits can bind AID at the same time remains controversial (Meir *et al.*, 2000; Sandoz *et al.*, 2004).

Detailed structural information regarding the structure of the ion conducting pore and the voltage sensor of voltage gated potassium channels from both prokaryotes and eukaryotes has been determined using x-ray crystallographical studies (Doyle *et al.*, 1998; Jiang *et al.*, 2003). However, detailed structural

information about VDCCs is still not available probably due to their large and complex nature and difficulties with overexpression and subsequent purification. Some low resolution data have been obtained from analysis of purified dihydropyridine receptor complexes from skeletal and cardiac muscle by electron microscopy (Murata *et al.*, 2001; Wang *et al.*, 2002; Wolf *et al.*, 2003; Wang *et al.*, 2004). These data provide some information about the overall dimensions of the dihydropyridine receptor complex and labelling studies revealed the approximate positions of some auxiliary subunits (Wolf *et al.*, 2003; Wang *et al.*, 2002). There was however substantial variation between the structures presented and there is no consensus on whether the channels are monomeric, dimeric or exist as oligomers under physiological conditions (Wang *et al.*, 2004). Higher resolution structures and clearer labelling studies are necessary to provide more detailed information about the pore forming α1 subunit.

1.2.3 The Ca_V1 family

In humans the Ca_V1 family of calcium channels consists of four members. All members of this family are high voltage activated, mediate L-type current and are sensitive to dihydropyridines. The $Ca_V1.1$ channel is expressed in skeletal muscle and is involved in excitation-contraction coupling. $Ca_V1.1$ links directly with the ryanodine receptors in the sarcoplasmic reticulum acting primarily as a voltage sensor, coupling membrane depolarisation to release of Ca^{2+} from intracellular stores (Schwartz *et al.*, 1985), influx of Ca^{2+} through the channel is secondary to its role as a voltage sensor.

Expressed in a variety of cells including cardiac muscle, smooth muscle and neurons (Perez-Reyes *et al.*, 1990; Mori *et al.*, 1993) $Ca_V1.2$ does function as a Ca^{2+} channel. $Ca_V1.2$ is involved in cardiac excitation-contraction coupling and is modulated by β-adrenergic agonists acting via cyclic AMP dependent protein kinase which enhances calcium current through $Ca_V1.2$ and consequently increases cardiac contractility producing a positive inotropic effect (Morad *et al.*, 1981). In neurons, $Ca_V1.2$ is involved in coupling membrane depolarisation to regulation of gene expression (Weick *et al.*, 2003).

Ca_V 1.3 is expressed in many of the same tissues as $Ca_V1.2$. $Ca_V1.3$ is responsible for a major fraction of L-type Ca^{2+} current in neurosecretory and neuronal

cells (Dolphin,1999; Hell *et al.*, 1993) and is also expressed in hair cells of the inner ear and in cardiac sino atrial nodes where it is involved in pacemaker activity (Scholze *et al.*, 2001; Kollmar *et al.*, 1997).

Originally thought to only be expressed in retinal tissue, Ca_V 1.4 is also expressed in spleen, spinal cord, bone marrow and thymus (McRory *et al.*, 2004). Missense mutations in Ca_V 1.4 have been implicated in the human condition incomplete X-linked congenital stationary night blindness. $Ca_V1.4$ has only recently been functionally characterised (Koschak *et al.*, 2003; McRory *et al.*, 2004) and was found, unlike other L-type Ca^{2+} channels to display very slow voltage dependent inactivation and no calcium dependent inactivation (Koschak *et al.*, 2003; McRory *et al.*, 2004).

1.2.4 The Ca_V2 family

The three members of the Ca_V 2 family are mainly expressed in neuronal tissue. These channels are predominantly localised in the synaptic terminals where they control release of neurotransmitters and regulate synaptic communication (Catterall, 1999; Seager and Takahashi, 1998). A common feature of the Ca_V 2 family is their susceptibility to modulation by βγ subunits of heterotrimeric G proteins coupled to G protein coupled receptors (GPCRs) (Dolphin, 1986; Ikeda and Schofield, 1989). Modulation by G proteins manifests itself as a slowing of current activation kinetics and a shift in the current-voltage relationship to more depolarised potentials (Bean, 1989), recovery from inactivation is both time and depolarisation dependent and can be removed by large depolarising pulses (Ikeda, 1991). Multiple structural determinants have been implicated in the modulation of Ca_V 2 family by G proteins. The cytoplasmic linker between domains I and II of all members of the Ca_V 2 family has been shown to interact directly with the G protein βγ subunit (De Waard *et al.*, 1997; Zamponi *et al.*, 1997; Bell *et al* 2001). Additional binding sites have been demonstrated in the C-terminus (Kinoshita *et al.*, 2001; Qin *et al.*, 1997) however, other groups have demonstrated full G protein modulation of Ca_V 2.2 in a construct where the C-terminus was removed (Stephens *et al.*, 1998). The N-terminus of all channels of the Ca_V 2 family contains the motif YKQSIAQRART which has been shown to be essential for G protein modulation (Canti *et al.*, 1999; Dolphin, 2003). Removal of the Ca_V 2.2 N-terminus abolishes G protein modulation (Page *et*

al; 1998) and replacement of the N-terminus of other classes of channel with that of $Ca_V2.2$ enabled the chimeric channels to be modulated by G proteins (Canti *et al.*, 1999). More recently Agler et al. (2005) demonstrated using yeast two hybrid assays and mammalian cell flourescence resonance energy transfer (FRET), interactions between $G\beta\gamma$, the $Ca_V2.2$ N-terminus and the Ca_V I-II linker and the $Ca_V2.2$ N-terminus and the Ca_V I-II linker. A model is proposed in which the N-terminus acts as a G-protein $\beta\gamma$ gated inhibitory module which binds to the I-II linker to inhibit the channel.

$Ca_V2.1$ is present throughout the brain and central nervous system (Mori *et al.*, 1991) and is involved in neurotransmitter release. As mentioned previously Ca_V 2.1 channels mediated P/Q type current and alternative splicing gives rise to two distinct channel types (Bourinet *et al.*, 1999) which are blocked by ω-agatoxin IVA with different affinities. $Ca_V2.1$ channels interact with proteins involved in exocytosis via a site on the cytoplasmic II-III linker (Walker and DeWaard,1998; Seager *et al.*, 1998). Mutations within CACNA1A, the human gene which codes for $Ca_V2.1$ have been linked to three autosomal dominant neurological disorders in humans, these are episodic ataxia type-2 (EA2), familial hemiplegic migraine (FHM) and spinocerebellar ataxia type 6 (SCA6) (Zhuchenco *et al.*, 1997; Ophoff *et al.*, 1996).

The $Ca_V2.2$ channal is responsible N-type current, $Ca_V2.2$ channels are primarily expressed in nerve terminals where they are involved in release of neurotransmitters (Dunlap *et al.*,1995). Ca_V 2.2 appears to be less involved in neurotransmitter release than $Ca_V2.1$ channels as $Ca_V2.2$ does not couple so efficiently with the exocytotic machinery as $Ca_V2.1$ (Mintz *et al.*, 1995; Qian *et al.*, 2000).

The $Ca_V2.3$ channels mediate R-type current and are specifically inhibited by a 41 amino acid peptide toxin isolated from the African tarantula, *Hysterocrates gigas* (Newcomb *et al.*, 1998). $Ca_V2.3$ channels are mainly localised in neuronal cell bodies (Yokoyama *et al.*, 1995) but are also present in some nerve terminals (Wu *et al.*, 1999; Dietrich *et al.*, 2003).

1.2.5 The Ca_V3 family

The Ca_V 3 family of Ca^{2+} channels is the most recent family to be cloned and characterised (Perez-Reyes *et al.*, 1998; Cribbs *et al.*,1998; Lee *et al.*,1999). The family consists of three members (Perez-Reyes, 1999) all of which mediate T-type current. T-type current activates from small depolarisations and at more negative membrane potentials than HVA current and inactivates rapidly. Unlike HVA Ca^{2+} channels members of the Ca_V3 family do not seem to require the presence of any known calcium channel auxiliary subunits for normal plasma membrane expression or function. Members of the Ca_V3 family are expressed in many tissue types, especially in heart and brain and particularly in tissues which display spontaneous electrical activity such as the sinoatrial nodal cells of the heart and thalamic neurons (Hugenard., 1996). When expressed in HEK-293 cells, $Ca_V3.1$ and $Ca_V3.2$ both produced large transient currents and are likely to be involved in pacemaker activity (Chemin *et al.*, 2001), this role was confirmed for $Ca_V3.1$ when generation of a $Ca_V3.1$ knockout mouse displayed no burst mode firing of action potentials in thalamocortical relay neurons (Kim *et al*,. 2001). In contrast, Ca_V 3.3 exhibited a degree of facilitation and produced a sustained calcium entry and is capable of generating sustained electrical activity associated with pacemaker activity (Chemin *et al.*, 2001).

1.3 Ca^{2+} channel auxiliary subunits

1.3.1 The γ subunit

The γ subunit is the smallest of the VDCC auxiliary subunits with a molecular weight of between 25 and 35 kDa. The γ subunit was first described as a protein which copurified with the dihydropyridine receptor complex from skeletal muscle (Campbell *et al.*, 1989). Molecular cloning of this subunit, termed γ1, revealed a protein containing 4 transmembrane segments and intracellular N-and C-termini. Some time later, a neuronal γ subunit was identified and cloned (Letts *et al.*,1998), this gene is mutated in the mutant mouse *stargazer* and thus, the gene product is known as "stargazin". More recently six new putative γ subunits have been identified and cloned (Klugbauer *et al.*, 2000; Burgess *et al.*, 2001; Moss *et al.*, 2002).

The function of the γ subunit as a Ca^{2+} channel subunit remains to some extent controversial but some functional effects have been described. In mice where γ1 expression is eliminated, dihydropyridine sensitive Ca^{2+} current in isolated myotubules was increased and the voltage dependence of steady state inactivation was shifted to more depolarised potentials suggesting that γ1 serves to decrease Ca^{2+} entry (Freise *et al.*, 2000). The neuronal γ2 subunit has a small but significant effect upon P/Q type current in BHK cells (Letts *et al.*, 1998) and γ 3, γ4 and γ5 subunits will associate with and exert some effects upon currents mediated by $Ca_V2.1$ and $Ca_V2.2$ (Sharp *et al.*, 2001; Klugbauer *et al.*, 2000; Rousset *et al.*, 2001). In addition, there are reports of modulatory effects of γ subunits upon T-type currents in coexpression studies (Klugbauer *et al.*, 2000; Green *et al.*, 2001; Lacinova, 2000). There is also evidence that the neuronal γ2 subunit is involved in trafficking of alpha-amino-3-hydroxy-5-methyl-4-isoxazolepropionic acid (AMPA) receptors to the plasma membrane (Chen *et al.*, 2000) and this is now accepted to be the main role for γ2, γ3, γ4 and γ8 (Nicoll, Tomita and Bredt, 2006; Tomita *et al.*, 2006; Rouach *et al.*, 2005; Tomita *et al.*, 2005).

1.3.2 The α2δ subunit

The α2δ subunit is a highly glycosylated protein which is encoded by a single gene. The α2δ subunit gene product is highly post-translationally processed and cleaved (Jay *et al.*, 1991) to yield an entirely extracellular α2 subunit which is joined to the δ subunit by a disulphide bond. The δ subunit anchors the α2 subunit to the plasma membrane via a single transmembrane segment. Four α2δ subunit genes have so far been cloned and characterised (Ellis *et al.*, 1998; Klugbauer *et al.*, 1999; Qin *et al.*, 2002). α2δ-1 appears to be expressed in most tissue types (Barclay *et al.*, 2001) where as α2δ-2 and α2δ-3 expression is restricted mostly to the brain (Barclay *et al.*, 2001; Klugbauer *et al.*, 1999). The α2δ-4 subunit appears to be localised to specialised cell types such as pituitary gland, adrenal gland, colon and liver (Qin *et al.*, 2002). In co-expression studies, when expressed with a pore forming α1 and $Ca_V\beta$ subunit, α2δ subunits increase the current density and shift the voltage dependence of activation to more hyperpolarised potentials (Felix *et al.*, 1997; Hobom *et al* 2000; Klugbauer *et al.*, 1999). There is also an increase in dihydropyridine binding sites in the plasma membrane suggesting that the number of channels in the membrane is increased and that α2δ may have a role in Ca^{2+} channel trafficking (Shistik *et al.*, 1995). A recent study by Canti et al. (2005) showed that the Von Willebrand factor-A (VWA) domain which is present in all α2δ subunits contains a metal ion dependent adhesion site (MIDAS). When mutated so that it can no longer bind divalent cations, the mutant α2δ subunit no longer enhanced Ca^{2+} currents mediated by $Ca_V1.2$, Ca_V 2.1 or $Ca_V2.2$. The authors suggest that it is the interaction between the MIDAS motif and the $Ca_V\alpha1$ subunit which promotes trafficking to the plasma membrane.

1.3.3 The Ca_V β subunit

Beta subunits of voltage dependent calcium channels are small (55-75 kDa) entirely cytoplasmic proteins which have substantial effects upon the trafficking and biophysical properties of high voltage activated calcium channels. The $Ca_V\beta$ subunit binds with high affinity to a highly conserved motif within the cytoplasmic linker between domains I and II of HVA Ca^{2+} channels known as the alpha interaction domain (AID) (DeWaard *et al.*, 1995).

The β subunit associated with the skeletal muscle dihydropyridine receptor was the first to be identified (Takahashi *et al.*, 1987). The gene encoding $Ca_V\beta1a$ was subsequently cloned and characterised (Ruth *et al.*, 1989) and shortly afterwards three more $Ca_V\beta$ subunits were cloned based on their homology with $Ca_V\beta1$ (Castellano *et al.*, 1993; Hullin *et al.*, 1992; Perez-Reyes *et al.*, 1992). Alignments of the four $Ca_V\beta$ subunit gene sequences revealed the presence of five amino acid sequence similarity domains (D1-D5) (Birnbaumer et al., 1998) of which two, D2 and D4 are encoded by 4 and 6 exons respectively and are highly conserved (Figure 1.4). Alternative splicing can occur in the variable regions D1, D3 and D5 giving rise to many splice variants for each $Ca_V\beta$ subunit including one, $Ca_V\beta2a$ which can be palmitoylated at its N-terminus (Chien *et al.*, 1998).

1.3.3.1 Tissue distribution and subcellular localisation of $Ca_V\beta$ subunits

All four $Ca_V\beta$ subunits have been shown to be expressed in the brain (Ludwig *et al.*, 1997). Using specific antibodies and riboprobes for $Ca_V\alpha1$ subunits as well as $Ca_V\beta$ subunits, an expression profile was generated which suggested that whilst $Ca_V\beta3$ associates predominantly with $Ca_V2.2$ and $Ca_V\beta4$ associates with $Ca_V2.1$, a $Ca_V\beta$ subunit may associate with any HVA $Ca_V\alpha1$ subunit. This was confirmed by the findings that L-type channels, $Ca_V2.1$ and $Ca_V2.2$ immunprecipitated from brain were associated with multiple $Ca_V\beta$ subunits (Pichler *et al.*, 1997; Scott *et al.*, 1996; Liu *et al.*, 1996).

The $Ca_V\beta1a$ subunit is expressed in skeletal muscle and appears to be the only β subunit expressed in this tissue. Mice in which the $Ca_V\beta1$ gene is deleted die at birth from asphyxia and the amount of $Ca_V1.1$ in the myotubes is undetectable,

Figure 1.4

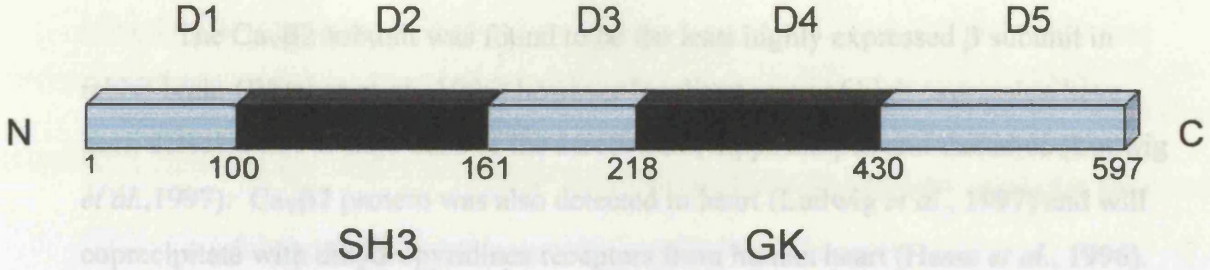

Figure 1.4. Linear model of $Ca_V\beta 1b$ produced from alignment of known $Ca_V\beta$ subunit sequences. $Ca_V\beta$ subunits contain five amino acid sequence similarity domains (D1-D5), two of which (D2 and D4) are highly conserved and form SH3 and GK domains respectively. The numbers represent the number of amino acid residues in each domain of $Ca_V\beta 1b$. Data are taken from Dolphin, (2003)

highlighting the important role of the $Ca_V\beta$ in calcium channel trafficking (Gregg *et al* 1996). The $Ca_V\beta1b$ subunit is more widely expressed, being present in brain, ventricular, spleen and cardiac tissue (Powers *et al.*, 1992; Scott *et al.*,1996; Hullin *et al.*, 1999; Hullin *et al.*, 2003).

The $Ca_V\beta2$ subunit was found to be the least highly expressed β subunit in rabbit brain (Witcher *et al.*, 1995) however localised areas of high expression have been detected in Purkinje cells of the cerebellum, hippocampus and thalamus (Ludwig *et al.*,1997). $Ca_V\beta2$ protein was also detected in heart (Ludwig *et al.*, 1997) and will coprecipitate with dihydropyridines receptors from human heart (Hasse *et al.*, 1996). However, coexpression of the cardiac $Ca_V1.2$ with $Ca_V\beta2a$ does not produce channels with the biophysical properties of endogenous cardiac Ca^{2+} channels (Wei *et al.*, 2000). Recently, Colecraft et al. (2002) used 5' rapid amplification of cDNA ends (5' RACE) PCR to clone a new $Ca_V\beta2$ splice variant named $Ca_V\beta2b$. Expression of $Ca_V\beta2b$ in heart cells yielded channels with biophysical properties which closely resembled those of native cardiac Ca^{2+} channels. The authors suggest that it is $Ca_V\beta2b$ rather than $Ca_V\beta2a$ which is the major $Ca_V\beta2$ variant expressed in cardiac tissue and it is for this reason that previous attempts to isolate $Ca_V\beta2a$ from cardiac tissue (Qin *et al.*, 1998) have been unsuccessful. Mice in which the gene coding for $Ca_V\beta2$ has been inactivated have been generated and this mutation was found to be lethal (Ball *et al.*, 2002). By placing the β2 gene under the control of a myosin heavy chain promoter and thereby restricting the expression to the heart, the authors were able to rescue the mice and study the effects of $Ca_V\beta$ in the retina. The $Ca_V\beta2$ deficient mice showed abnormal retinal function and abnormal distribution of the retinal calcium channel $Ca_V1.4$ suggesting that $Ca_V\beta2$ is the primary β subunit expressed in retina.

The $Ca_V\beta3$ subunit is strongly expressed in the brain where it appears to be associated with the majority (56%) of $Ca_V2.2$ subunits (Scott *et al.*, 1996) but also associates with $Ca_V2.1$. $Ca_V\beta3$ is also expressed in aorta, lung, trachea and β cells of the pancreas and is considered to be the $Ca_V\beta$ subunit which associates with $Ca_V1.2$ in smooth muscle (Hullin *et al.*, 1992; Collin *et al.*, 1994; Berggren *et al.*, 2004). Mice lacking a $Ca_V\beta3$ subunit have been generated and characterised in detail with regard to cardiovascular function and glucose homeostasis. The $Ca_V\beta3$ deficient mouse

showed little phenotype (Murakami *et al.*, 2000), there was no difference in smooth muscle contraction or sensitivity of muscle contraction to L-type Ca^{2+} channel blockers compared to wild type mice and the authors concluded that there may be some compensation by other $Ca_V\beta$ subunits such as $Ca_V\beta2a$. The $Ca_V\beta3$ deficient mice did show an increase in blood pressure in response to a high salt diet suggesting a possible role for $Ca_V\beta3$ in salt sensitivity hypertension (Murakami *et al.*, 2000). Whilst there was no difference in smooth muscle contraction, western blotting and dihydropyridine binding experiments showed reduced expression of L-type Ca^{2+} channel $\alpha1$ subunits in the plasma membrane of cells of the aorta, electrophysiological experiments revealed a 30% reduction in Ca^{2+} current density (Murakami *et al.*, 2003). The impact of $Ca_V\beta3$ disruption on pain processing was also investigated. Pain processing was found to be reduced or dampened in $Ca_V\beta3$ deficient mice which expressed only low levels of $Ca_V2.2$ in DRG neurones compared to wild type mice and whilst no reduction in expression was observed in $Ca_V2.1$ channels, a depolarising shift in their voltage dependence of activation and a change in the voltage dependence of facilitation of compound Ca^{2+} currents was reported.

The $Ca_V\beta4$ subunit is also strongly expressed in the brain, particularly in the cerebellum (Ludwig *et al.*, 1997) and has also been detected in kidney, testis, retina and lymphocytes (Escayg *et al.*, 1998). Three splice variants of $Ca_V\beta4$ have been cloned and characterised, all are expressed in the brain, eye, heart and lung but the truncated $Ca_V\beta4_c$ isoform is expressed in cochlea and is the only $Ca_V\beta4$ isoform expressed in this tissue (Hibino *et al.*, 2003). The variants $Ca_V\beta4_a$ and $Ca_V\beta4_b$ differ slightly in their N-terminal regions and this has been shown to have effects on the voltage dependence of activation and inactivation of $Ca_V2.1$ and $Ca_V2.2$ with channels containing $Ca_V\beta4_a$ showing a more depolarised voltage dependence of activation and inactivation than those with $Ca_V\beta4_b$ (Helton *et al.*, 2002). The $Ca_V\beta4_c$ isoform is truncated within its guanylate kinase like domain and perhaps not surprisingly has little effect upon Ca^{2+} currents. However, this isoform was found to be recruited to the nucleus of tSA-201 cells and to attenuate the gene silencing activity of chromobox protein 2/heterochromatin protein 1γ (CHCB2/HP1γ) (Hibino *et al.*, 2003).

The $Ca_V\beta$ subunit has no predicted transmembrane regions and is regarded as a cytoplasmic protein. However, the N-terminus of the $Ca_V\beta2a$ isoform contains two cysteines as positions 3 and 4 which can be palmitoylated (Chien *et al.*, 1996). This

palmitoylation directs $Ca_V\beta2a$, when expressed alone, to the plasma membrane (Chien *et al.,* 1995; Bogdanov *et al.*, 2000) whereas a palmitoylation deficient mutant in which cysteine 3 and 4 are changed to serine shows a more diffuse pattern of expression (Leroy *et al.*, 2005). The $Ca_V\beta3$ and $Ca_V\beta4$ subunits show a more diffuse localisation throughout the cytoplasm when expressed in COS-7 cells with some staining observed in the nucleus (Bogdanov *et al.*, 2000). Plasma membrane expression has also been observed for $Ca_V\beta1b$ when expressed alone In COS-7 cells (Brice *et al.*, 1997). The determinant for this localisation was identified as a highly acidic 11 amino acid motif in the C-terminus of $Ca_V\beta1$ which when deleted reduced membrane expression and when transferred to $Ca_V\beta3$, promoted localisation of $Ca_V\beta3$ to the plasma membrane (Bogdanov *et al.*, 2000).

Recently, five splice variants of $Ca_V\beta2$ have been cloned ($Ca_V\beta2_{a\text{-}e}$) and their subcellular localisation characterised (Takahashi *et al.*, 2003). Of the five isoforms, both the palmitoylatable $Ca_V\beta2a$ isoform and the non-palmitoylatable $Ca_V\beta2e$ isoform showed distinct plasma membrane localisation when fused to the fluorescent protein GFP and expressed alone in HEK 293 cells. The other three isoforms showed a more diffuse cytoplasmic localisation. Interestingly and in agreement with other studies (Brice *et al*; 1997; Bogdanov *et al*; 2000), the subcellular localisation of the $Ca_V\beta2$ subunit isoform did not affect its ability to traffic $Ca_V\alpha1$ subunits to the plasma membrane nor did the presence of a $Ca_V\alpha1$ subunit change the subcellular distribution of the $Ca_V\beta$ subunit isoform (Takahashi *et al.*, 2003).

1.3.3.2 $Ca_V\beta$ subunit structure

As previously mentioned, the primary structure of the $Ca_V\beta$ subunit contains five domains, two of which are highly conserved (Birnbaumer, 1998). The first insights into the structure of the $Ca_V\beta$ subunit came from homology models made by Hanlon et al. (1999). Using homology searches and threading algorithms, structural predictions were made which assigned the D2 domain as an Src Homology-3 (SH3) domain and the D4 domain as being similar to the yeast Guanylate Kinase (GK). This domain structure places the $Ca_V\beta$ subunit in the membrane associated guanylate kinase (MAGUK) family of proteins. The N-terminus of $Ca_V\beta1b$ upon which the model was based was predicted to contain a putative Post Synaptic Density protein 95 (PSD-95), Discs large protein (dlg) and Zona occludens-1 (ZO-1) (PDZ) domain. However, this N-terminal region is poorly conserved among $Ca_V\beta$ subunits and is subject to alternative splicing and thus this homology is not conserved.

The MAGUK family of proteins always contain a 300 amino acid region with homology to yeast GK. This family of proteins are believed to be ubiquitous scaffolding molecules and other members include PSD-95, PSD-93, SAP 97 and CASK. In the GK domain of MAGUK proteins GK is catalytically inactive, this is the case for $Ca_V\beta$ subunits in which the glycine-rich ATP binding motif is not conserved. The MAGUK family of proteins also always contain at least one PDZ domain, although probably absent in $Ca_V\beta$ subunits, PDZ domains are involved in protein-protein interactions at sites of cell-cell contact such as synapses, neuromuscular junctions and tight junctions (Garner *et al.*, 2000). Interaction of PDZ domains with their protein partners usually occurs via short C-terminal sequences, these interactions also occur with a relatively low affinity (low μM range) (Harris and Lim, 2001). SH3 domains are also involved in protein-protein interaction and have been found to bind to polyproline motifs (P X X P). However, these types of interaction are rarely found in MAGUK proteins (Funke, Dakoji & Bredt, 2005). Instead, many ligands have been found to interact with the GK domain, these include guanylate kinase associate protein (GKAP) (Kim *et al.*, 1997), A kinase anchoring protein (AKAP) (Colledge *et al.*, 2000) and guanylate kinase associated kinesin (GAKIN) (Hanada *et al.*, 2000). In addition to binding to its many protein partners, GK will interact with SH3 in an intramolecular fashion (Shin *et al.*, 2000), this

intramolecular interaction appears to be essential for some functions of MAGUK proteins (McGee *et al.*, 1999; Shin *et al.*, 2000). This certainly appears to be the case for $Ca_V\beta$ subunits as the SH3 and GK domains have been shown to interact with one another (Opatowsky *et al.*, 2003; Takahashi *et al* 2004). Although some modulatory effects were observed using the GK domain alone (Maltez *et al.*, 2005), this interaction is required to fully reconstitute the trafficking and modulatory effects characteristic of $Ca_V\beta$ subunits (Takahashi *et al.,* 2004; Maltez *et al.*, 2005; Takahashi *et al.*, 2005).

Recently, three groups reported the crystal structures of $Ca_V\beta2$, $\beta3$ and $\beta4$ core domains (Chen *et al.*, 2004; Van Petegem *et al.*, 2004; Opatowsky *et al.*, 2004). By removing the highly variable N and C-termini and either truncating the central variable region or using $Ca_V\beta$ subunit isoforms in which this was very short, the authors were able to generate constructs from which structural data could be obtained, in one study, the two conserved domains were expressed as separate entities and resulting complex was crystallised. The structures were also presented as complexes with AID peptides, revealing the exact nature of the $Ca_V\beta/Ca_V\alpha1$ interaction.

The structure of $Ca_V\beta3$ core complexed with AID peptide is shown in Figure 1.5. The structure shows that the $Ca_V\beta$ subunit core does indeed contains two interacting domains, the SH3 domain consists of four β strands and two long α helices which extend away from the SH3. The second α helix ($\alpha2$, Figure 1.4) joins to the non-conserved central variable region, the C-terminal residues of which form the fifth β strand of SH3 ($\beta5$, Figure 1.4). The central β strands of the SH3 are arranged in a similar fashion to those of other MAGUK proteins such as PSD-95 whose structure was also recently solved (McGee *et al.*, 2001). However unlike other MAGUK proteins, $Ca_V\beta$ has a long α helix at its N-terminus ($\alpha1$ Figure 1.4), this structure seems to be in place of a PDZ domain which would be N-terminal to the SH3 in other MAGUK proteins. There are also differences in the orientation of the SH3 relative to the GK domain, the orientation of SH3 in $Ca_V\beta$ is shifted by approximately 90° compared to PSD-95.

The main revelation of the structure concerns the nature of AID peptide binding. All three structure clearly show the AID peptide tightly embedded in a deep

Figure 1.5

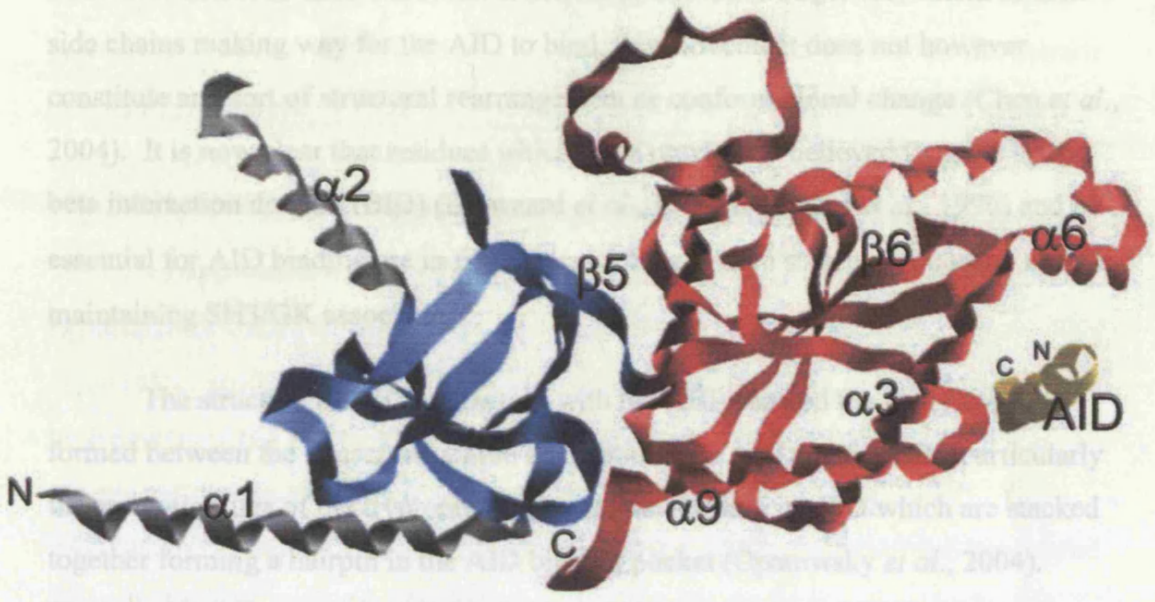

Figure 1.5. The structure of $Ca_V\beta 2a$ core in complex with the $Ca_V1.1$ AID peptide is shown as a ribbon diagram with the SH3 domain marked in blue, the GK domain is marked in red and the AID peptide in yellow. The SH3 and GK domains are closely associated and the AID peptide fits into a deep groove on the reverse side of the GK domain termed the aid binding pocket (ABP). The central variable region of the $Ca_V\beta$ subunit is not shown but would occur between helix α2 and β strand β5. The structural elements are numbered according to Chen et al., (2004).
Taken from Richards, Butcher and Dolphin, (2004)

groove in the GK domain now termed the AID binding pocket (ABP) (Van Petegem *et al.*, 2004). Comparison of $Ca_V\beta$ structures with and without AID present show small movement of three backbone α helices in GK and a larger movement of their side chains making way for the AID to bind, this movement does not however constitute any sort of structural rearrangement or conformational change (Chen *et al.*, 2004). It is now clear that residues which were previously believed to make up the beta interaction domain (BID) (De waard *et al.*, 1994; De waard *et al.*, 1996) and be essential for AID binding are in fact critical for $Ca_V\beta$ core structural integrity and for maintaining SH3/GK association.

The structure of AID interacting with the ABP showed the many contacts formed between the conserved amino acid residues in AID and the ABP particularly the aromatic rings of the tryptophan and tyrosine residues of AID which are stacked together forming a hairpin in the AID binding pocket (Opatowsky *et al.*, 2004). These residues have previously been shown to be essential for AID/$Ca_V\beta$ interaction (Pragnell *et al.*, 1994; Witcher *et al* 1995; De Waard *et al.*, 1995) and more recently the conserved tryptophan was shown to be essential for binding and modulation of $Ca_V2.2$ (Leroy *et al.*, 2005) whilst the conserved tyrosine is necessary only for maintenance of the high affinity interaction between AID and the ABP (Butcher *et al.*, 2006).

Recently, the structure of the N-terminus of $Ca_V\beta4_a$ was solved by nuclear magnetic resonance (NMR) spectroscopy (Vendel *et al.*, 2006). This region represents the highly variable D1 domain (Figure 1.3) and was previously believed not to contain significant secondary structure as it is so poorly conserved across the $Ca_V\beta$ subunit family. The structure of the $Ca_V\beta4_a$ N-terminus was shown to contain two antiparallel β sheets and two α helices which form an independent protein module separate from that of the $Ca_V\beta$ subunit core. The authors speculate that this module may participate in protein-protein interactions either within the $Ca_V\beta$ subunit or with other proteins and contribute to $Ca_V\beta$ subunit function.

1.3.3.3 $Ca_V\beta$ subunit function

$Ca_V\beta$ subunits have substantial effects on the plasma membrane localisation and biophysical properties of the HVA $\alpha 1$ subunit with which they are expressed. In systems where HVA Ca^{2+} channel $\alpha 1$ subunits are expressed without $Ca_V\beta$ subunits or when the amounts of $Ca_V\beta$ subunits are depleted in native tissue, the result is a reduction in macroscopic Ca^{2+} current, reduced trafficking to the plasma membrane and slowed activation kinetics (Singer *et al.*, 1991; Berrow *et al.*, 1995; Brice *et al.*, 1997). Coexpression of $Ca_V\beta$ subunits has since been shown to increase functional expression of $Ca_V\alpha 1$ at the plasma membrane (Brice *et al.*, 1997; Bichet *et al.*, 2000) and a recent study in which mutations were introduced into $Ca_V2.2$ such that it could no longer bind to $Ca_V\beta$ resulted in substantially reduced levels of $Ca_V2.2$ in the plasma membrane along with reduced current density (Leroy *et al.*, 2005). The mechanism by which $Ca_V\beta$ mediated its trafficking effects is unclear but it has been suggested that an endoplasmic reticulum (ER) retention signal present in the I-II linker of HVA Ca^{2+} channels is masked by $Ca_V\beta$ subunit binding (Bichet *et al.*, 2000) causing the $Ca_V\alpha 1$ to be released from the ER to proceed to the plasma membrane. However, the AID does not contain any known ER retention signal (Dolphin, 2003) and interestingly, recent work in which part of the I-II linker of $Ca_V2.2$ including AID was transferred to $Ca_V3.1$ which does not require $Ca_V\beta$ subunits for efficient trafficking did not result in decreased plasma membrane expression of the chimeric channels (Arias *et al.*, 2005). These results suggest that the signal for ER retention may lie elsewhere or be masked by regions of the $Ca_V\beta$ subunit other than the ABP.

In addition to increasing the number of functional channels at the plasma membrane, $Ca_V\beta$ subunits also hyperpolarise the voltage-dependence of activation and steady-state inactivation (Dolphin, 2003). In other words, the channels with which they are associated require smaller membrane depolarisations to activate or open, this would manifest itself as a leftward shift in the current-voltage relationship on a plot where the normalised current traces are plotted against the test potential.

There is little difference in the effects of any $Ca_V\beta$ subunit on the voltage dependence of activation (Dolphin, 2003) but there are differences in steady-state inactivation, which are due to determinants in both $Ca_V\alpha 1$ and $Ca_V\beta$ subunits. For

example, the voltage-dependence of steady state-inactivation of $Ca_V2.2$ and $Ca_V2.3$ were shown by Canti et al. (2000) to be hyperpolarised by all $Ca_V\beta$ subunits except $Ca_V\beta2a$ which shifted the steady-state inactivation process in the depolarising direction by approximately +10 mV. This effect had previously been shown for $Ca_V\alpha1.2$, $Ca_V2.1$ and $Ca_V2.3$ by other groups (De Waard and Campbell, 1995; Cens *et al.*, 1998). The determinant for the unique behaviour of $Ca_V\beta2a$ was shown to be its ability to be palmitoylated which when removed caused $Ca_V\beta2a$ to behave like other $Ca_V\beta$ subunits with regard to steady-state inactivation (Canti *et al.*, 2000).

All HVA $Ca_V\alpha1$ subunits have the intrinsic ability to inactivate without the need for accessory subunits (Stotz and Zamponi, 2001). The determinants involved in voltage-dependent inactivation have been investigated in detail and several regions of the channel have been shown to be important. By using chimeric channels of $Ca_V2.1$ and $Ca_V2.3$, Zhang et al. (1994) reported that the differences in inactivation kinetics were due to determinants within the sixth transmembrane segment of domain I and a short sequence within the I-II linker. Subsequent studies have implicated all four transmembrane domains as determinants in voltage dependent inactivation with domains II and III being particularly important (Spaetgens *et al.*, 1999). Other determinants have been reported in the cytoplasmic C-terminus of $Ca_V1.2$ and the I-II linker of $Ca_V2.1$ (Soldatov *et al.*, 1998; Herlitz *et al.*, 1997) and a single amino acid change in $Ca_V2.1$ is known to change the properties of $Ca_V2.1$ from Q-type to non-inactivating P-type (Bourinet *et al.*, 1999). Despite this intrinsic ability of the $Ca_V\alpha1$ subunit, $Ca_V\beta$ subunits have substantial effects upon the kinetics of voltage-dependent inactivation (Stotz & Zamponi., 2001). Coexpression of either $Ca_V\beta1$ or $Ca_V\beta3$ causes a substantial increase in inactivation rates whereas $Ca_V\beta2a$ dramatically slows inactivation kinetics and $Ca_V\beta4$ produces a moderate slowing. The ability of $Ca_V\beta2a$ to slow inactivation kinetics has again been shown to be due to its palmitoylation (Qin *et al.*, 1998) as prevention or removal of palmitoylation reduces the effect of slowed inactivation kinetics induced by $Ca_V\beta2a$ (Stephens *et al.*, 2000). On the basis of results regarding the properties of $Ca_V\beta2a$ and the I-II linker in voltage dependent inactivation, a model is proposed whereby the I-II linker acts as an inactivation gate (Restituto *et al.*, 2000; Stotz *et al.*, 2000). This is consistent with evidence that $Ca_V\beta$ subunits bind to the I-II linker and exert substantial effects upon

voltage-dependent inactivation and also with data regarding $Ca_V\beta 2a$ which whilst tethered to the plasma membrane due to its palmitoylation, restricts the movement of the I-II linker and thus slows inactivation (Restituto *et al.*, 2000).

1.3.3.4 Role of $Ca_V\beta$ subunits in modulation by G proteins and facilitation

As described previously, the Ca_V2 family of HVA Ca^{2+} channels can be modulated by $\beta\gamma$ subunits of heterotrimeric G proteins (Dolphin., 2003). Although important determinants of G protein modulation have been identified in the I-II linker (De Waard *et al.*, 1997), the N-terminus (Canti *et al.*, 1999) and in some channels the C-terminus (Qin *et al.*, 1997), the $Ca_V\beta$ subunit also plays an important role in G protein modulation.

Canti et al. (2000) demonstrated by coexpression studies in *Xenpus laevis* oocytes that all $Ca_V\beta$ subunits antagonised G protein mediated inhibition of $Ca_V2.2$, this result had previously been reported by other groups who had reported substantial increases in G protein mediated inhibition in the absence of $Ca_V\beta$ subunits (Bourinet *et al.*, 1996) and interpreted the results as simply a competition between $Ca_V\beta$ and $G\beta\gamma$ for sites on the $Ca_V\alpha 1$ subunit. However, Canti et al, (2000) noted that the effects were voltage-dependent and activation of G proteins antagonises the $Ca_V\beta$ mediated hyperpolarisation of $Ca_V2.2$. Furthermore, the presence of $Ca_V\beta$ increases the rate of dissociation of $G\beta\gamma$ from $Ca_V2.2$ during a depolarising prepulse and the authors therefore concluded that both $Ca_V\beta$ and $G\beta\gamma$ bind to the channel at the same time. Unbinding of $G\beta\gamma$ from the channel is measured as facilitation and manifests itself as an increase in current following a large depolarising prepulse. It is believed that the prepulse removes bound $G\beta\gamma$, thus, the amount of facilitation observed represents the amount of $G\beta\gamma$ bound to the channel. The idea that both $Ca_V\beta$ and $G\beta\gamma$ can occupy the channel together is still controversial. Displacement of G $\beta\gamma$ was demonstrated using fluorescence resonance energy transfer (FRET) by Sandoz et al. (2004), the authors suggested that displacement of $Ca_V\beta$ from the I-II linker is a key step in G protein regulation of $Ca_V2.1$ calcium channels. However, this contradicts findings of Hummer et al. (2003) who found, again using FRET that $Ca_V\beta$ and G protein β can bind to the I-II linker at the same time. A recent study by Leroy et al., (2005) showed using a $Ca_V2.2$ channel in which the conserved tryptophan in the I-II

linker is mutated to alanine thus preventing $Ca_V\beta$ binding that the channel was still inhibited by $G\beta\gamma$. However, the inhibition was not voltage-dependent, but coexpression of $Ca_V\beta 2a$ which is targeted to the plasma membrane by its palmitoylation restored all elements of G protein modulation. The authors conclude that $Ca_V\beta$ subunits are essential for removal of inhibition by $G\beta\gamma$ and that in this system the effects mediated by $Ca_V\beta$ are probably via low affinity interactions with $Ca_V2.2$ at sites other than the AID.

1.3.3.5 Novel functions of $Ca_V\beta$ subunits

In addition to the well established role of $Ca_V\beta$ subunits in Ca^{2+} channel trafficking and modulation, some recent studies have highlighted novel functions which seem to involve $Ca_V\beta$ subunits. Some of these functions do result in regulation of VDCC $\alpha 1$ subunits but others involve different protein partners and are not directly related to $Ca_V\alpha 1$ function. Beguin et al. (2001) identified by yeast two hybrid and immunoprecipitation a small GTP binding protein known as GEM which interacted with $Ca_V\beta 3$. Further experiments showed that the interaction was not restricted to $Ca_V\beta 3$ but GEM could also bind $Ca_V\beta 1$ and $Ca_V\beta 2$. The outcome of the interaction which was to prevent channel trafficking to the plasma membrane was also not restricted to any particular class of channel as it occurred for both L and non L-type channels but not T-type channels (Finlin *et al.*, 2003). Another novel protein partner was reported by Viard et al. (2004). The authors showed that Protein kinase B/Akt, a protein kinase downstream of PI3 kinase co-precipitated with $Ca_V\beta 2a$ and can phosphorylate $Ca_V\beta 2a$ in its C-terminus. The result is increased trafficking of $Ca_V\beta 2a$ containing Ca^{2+} channel complexes to the plasma membrane. Hibino et al. (2003) isolated a short splice variant of $Ca_V\beta 4$ from cochlea and showed that in yeast 2 hybrid assays this variant interacted with a nuclear protein involved in gene silencing. Subsequent experiments showed that this splice variant is preferentially targeted to the nucleus and could regulate the gene silencing activity of chromobox protein 2 (CHCB2). Finally, the $Ca_V\beta 3$ knockout mouse studied by Berggren et al. (2004) showed a more efficient glucose homeostasis compared to wildtype mice. The authors showed that $Ca_V\beta$ was able to negatively modulate the formation of inositol

1,4,5-trisphosphate ($InsP_3$) and so negatively modulate the release of Ca^{2+} ions from intracellular stores However, the mechanism by which this occurs is as yet unknown.

1.4 Aims of this work

The initial aim of this work was to develop a surface plasmon resonance (SPR) binding assay to study the interaction of $Ca_V\beta$ subunits with the highly conserved AID motif located within the I-II linker if HVA Ca^{2+} channels. Surface plasmon resonance has advantages over other biochemical binding assays as there is no requirement for fluorescent or radio-labelling and the assay allows on- and off-rates to be measured and a dissociation constant (K_D) for the interaction to be calculated. This involves production of I-II linker fusion proteins containing the entire I-II linker of L-type ($Ca_V1.3$) and non L-type ($Ca_V2.1$ and $Ca_V2.2$) channels and the production of purified $Ca_V\beta$ subunits. The assay was then extended to examine the interaction of purified G protein $\beta\gamma$ subunits with the purified I-II linkers. The assay was then extended further to examine the effects of mutating the conserved tryptophan and tyrosine residues in the I-II linker on $Ca_V\beta$ subunit binding. These residues have previously been shown to disrupt $Ca_V\beta$ subunit binding (Pragnell *et al.*, 1994; Witcher et al 1995; De Waard *et al.*, 1995). Next, the effects of introducing these mutations into the I-II linker of full length $Ca_V2.2$ were investigated with regard to the ability of $Ca_V\beta$ subunits to traffic the mutated channels to the plasma membrane. This was studied by western blotting with anti $Ca_V2.2$ antibodies and cell surface biotinylation assays.

The second part of this work focuses specifically on the $Ca_V\beta2a$ subunit. It was recently reported that activation of phosphoinositide 3-kinase (PI3 kinase) promotes translocation of VDCC's to the plasma membrane (Viard *et al.*, 2004). This mechanism was shown to involve protein kinase B and to be specific for channels containing the $Ca_V\beta2a$ subunit. Biochemical assays were developed to investigate the interaction between $Ca_V\beta2a$ and protein kinase B, these include metabolic labelling of transfected cells with ^{33}P, western blotting with phospho-specific antibodies, *in vitro* phosphorylation and immunoprecipitation.

Finally, in view of recent findings that the $Ca_V\beta$ subunit may have functions other than trafficking and modulation of $Ca_V\alpha1$ subunits (Beguin *et al.*, 2001; Finlin *et al.*, 2003, Hibino *et al.*, 2003; Viard *et al.*, 2004), it was highly desirable to identify other proteins which may interact with the $Ca_V\beta$ subunit. To this end, a proteomic approach was used to identify unknown proteins which coprecipitate with $Ca_V\beta$ subunits from immunoprecipitation and pull down experiments.

Chapter 2:

Materials and methods

2.1 Molecular Biology

2.1.1 Suppliers

All reagents used in these experiments were purchased from Sigma Aldrich Company LTD and were of the highest purity available.

2.1.2 Water

The water used for both molecular biology and tissue culture was prepared using a Milli-Q Ultrapure Water Purification System (Millipore). The water quality was 18MΩ/cm^2 and was filtered through a 0.22μm membrane prior to use.

2.1.3 Deoxyribonucleic Acid

The following cDNA's were used in these experiments. $Ca_V2.2$ from rabbit (D14157) (Fujita *et al.*, 1993). $Ca_V\beta1b$ from rat (X61394) (Pragnell *et al.*, 1991). $Ca_V\beta2a$ from rat (M80545) (Perez-Reyes *et al.*, 1992). $Ca_V\beta3$ from rat (M88751) (Castellano *et al.*, 1993). $\alpha2\delta2$ from mouse (Barclay *et al.*, 2001). $Ca_V2.1$ from rabbit (X57689) (Mori *et al.*, 1991). $Ca_V1.3$ from human (M76558) (Williams *et al.*, 1992). PI3 kinase regulatory subunit P101γ from pig (Y10742) (Stephens *et al.*, 1997). PI3 kinase catalytic subunit P110γ from Human (X83368) (Stoyanov *et al.*, 1995). Akt 1/PKBα from mouse was purchased from Upstate Cell Signalling Solutions (Charlottesville, VA) (Franke *et al.*, 1995). Green fluorescent protein (GFP-mut3b) (U73901) (Cormack *et al.*, 1997).

2.1.4 Expression vectors

2.1.4.1 Eukaryotic expression vectors

The expression vector pMT2 (Swick *et al.*, 1992) was used for expression of proteins in eukaryotic cell lines. This vector contains the SV40 origin of replication and so can replicate in cells expressing the SV40 large T antigen. Originally developed as a *Xenopus laevis* oocyte expression vector, pMT2 expresses well in both COS-7 and tsA 201 cells. pMT2 has been modified in our laboratory to contain additional restriction endonuclease sites in its multiple cloning site (MCS) this increases its versatility and facilitates the subcloning of large cDNA fragments. In these experiments, pMT2 was used for the expression of all cDNA constructs in

mammalian cells with the exception of PI3 kinase regulatory subunit P101γ which was in pcDNA3.

2.1.4.2 Prokaryotic expression vectors

Prokaryotic expression vectors enable foreign proteins to be expressed in bacterial cells, the host cells are usually *E.coli.* In these experiments, three prokaryotic expression vectors were used all of which were used because they provided high level protein expression under the control of the isopropyl-1-thio-β-D-galactopyranoside (IPTG) inducible *lac* operon.

The *lac* operon consists of three contiguous genes which encode β-galactosidase, *lacY* lac permease *lacZ* and lac transacetylase *lacA*. A fourth gene *lacI* is situated upstream. *LacI* encodes a repressor protein which under conditions of no lactose binds to the promoter region of the operon, upstream from the three contiguous genes known as the *lac* operator. When lactose or its non-metabolisable analogue IPTG are present, the lac repressor protein preferentially binds this and the promoter region becomes available for RNA polymerase to begin transcription. In inducible expression vectors, the *lac* promoter is replaced with the T7 promoter and the three genes involved in lactose metabolism replaced with a cloning site into which foreign genes can be inserted.

The three prokaryotic expression vectors used in these studies were pET28, pETM6T1 and pGEX-2T. The pET28 vector contains a versatile multiple cloning site under the control of the T7 promoter and genes of interest can be expressed with either N-terminal or C-terminal $His_{(6)}$ tags. The pETM6T1 vector was a generous gift of Dr Andrei Okorokov, (Wolfson Institute for Biomedical Research, University College London) and is a modified version of pET44b. This vector contains an N-terminal $His_{(6)}$ tag followed by the 495 amino acid NusA solubility tag. The gene of interest is inserted between the NusA and an optional C-terminal $His_{(6)}$ tag, this vector is also under the control of the T7 promoter. The pGEX-2T vector was used to generate GST fusion proteins. pGEX-2T contains an N-terminal Glutathione-s-transferase fusion tag, expression is IPTG inducible and under the control of a hybrid *tac* promoter (a hybrid of the *E. coli trp* and *lac* promoters) (De Boer *et al.*, 1983).

2.1.5 Polymerase chain reaction (PCR)

Polymerase chain reaction (PCR) was used to amplify DNA sequences of interest from cDNA templates. PCR was used to introduce point mutations, to engineer epitope tags into genes of interest or to introduce restriction endonuclease sites to facilitate subcloning. In all cases two oligonucleotide primers were used which flanked the region of interest in the 3' and 5' direction and the primers contained at least 18 base pairs which were complimentary to the target sequence. All primers were obtained from Invitrogen and were purified by polyacrylamide gel electrophoresis (PAGE) if they exceeded 25 base pairs in length. The *Pyrococcus furiosus* (*Pfu*) DNA polymerase was used in all PCR reactions and was purchased from Stratagene. The *Pfu* DNA polymerase possesses 3' to 5' exonuclease proofreading activity that enables the polymerase to correct nucleotide-misincorporation errors. This means that *Pfu* DNA polymerase-generated PCR fragments will have fewer errors than *Taq*-generated PCR inserts. All PCR reactions contained 5% dimethyl sulfoxide (DMSO), as addition of DMSO can promote DNA "melting" in GC rich DNA sequences. PCR reactions were set up as follows in a reaction volume of 100µl.

Components	**Concentration**
10 x *Pfu* reaction buffer	10µl
Deoxynucleotide triphosphate	0.5mM each
Forward primer	40µmol
Reverse primer	40µmol
Pfu DNA polymerase	5 units
Template DNA	0.5µg
DMSO	5µl

The reaction mixture was split into two 200µl PCR tubes and subjected to the following conditions using a thermal cycler.

Time	Temperature °C	Step	Cycles
3 min	98	Initial melt	1
20 sec	98	Melting	25
20 sec	55	Annealing	25
As required	72	Extension	25
5 min	72	Final extension	1

For all primer combinations tested, an annealing temperature of 55°C was used and was found not to give rise to significant non-specific priming. The resulting PCR products were purified using a rapid PCR purification kit (Marligen Bioscience Inc, 2502 Urbana Pike Ijamsville, USA) according to the manufacturer's protocol and were eluted in ultra pure water.

2.1.6 Agarose gel electrophoresis

DNA fragments were separated by electrophoresis on 0.7 – 2% agarose minigels. The electrophoresis buffer was Tris-acetate EDTA (TAE) and contained 10mM Tris acetate pH 7.4 and 1mM ethylenediaminetetraacetic acid (EDTA). Staining was performed after electrophoresis using a solution of 1µg/ml Ethidium bromide dissolved in TAE. Stained gels were viewed using a UV transilluminator.

2.1.7 DNA extraction from agarose gels

DNA fragments of interest were extracted from agarose gels using a Rapid Gel Extraction kit (Marligen Bioscience Inc, 2502 Urbana Pike Ijamsville, USA) according to the manufacturer's protocol and were eluted in ultra pure water.

2.1.8 DNA modifying enzymes

Restriction endonucleases were used to cleave double stranded DNA in specific positions. All restriction endonucleases were purchased from Invitrogen LTD (3, Fountain Drive, Inchinnan Business Park, Paisley, UK) and were used according to manufacturer's instructions. DNA ligation was performed using T4 DNA ligase purchased from Invitrogen LTD. Ligation reactions contained 1 unit of T4 DNA ligase in 10µl reaction volume, ligation reactions were performed at 16°C overnight.

2.1.9 Bacterial cultures

For routine subcloning and propagation of expression vectors, One Shot TOP10 chemically competent *E.coli* were used (Invitrogen LTD), cells were transformed according to manufacturer's instructions. Mini cultures were set up in 5ml Lysogeny broth (LB) (Bertani, 1951) containing appropriate antibiotics. Cultures were grown at 37°C overnight in a shaking incubator. For propagation of plasmids, 50µg/ml Ampicillin or 30µg/ml Kanamycin were used.

2.1.10 DNA purification

Plasmid DNA was purified from *E.coli* minicultures using a Rapid plasmid purification kit (Marligen Bioscience Inc) according to manufacturer's instructions, plasmid DNA was eluted in 50µl Tris-EDTA (TE) and stored at -20°C. Large scale plasmid DNA was purified from 200ml cultures using High Purity Plasmid Purification kits (Marligen Bioscience Inc) according to manufacturer's instructions. Purified DNA was adjusted to 1 µg/µl and stored at -20°C.

2.1.11 Generation of epitope tagged constructs and fusion proteins

2.1.11.1 GST fusion proteins

The cytoplasmic linker between domains I and II of $Ca_V1.3$, $Ca_V2.1$ and $Ca_V2.2$ were amplified by PCR using primers which introduced *Bam*HI and *Eco*RI restriction sites into the 5' and 3' ends respectively. The resulting PCR products were ligated into *Bam*HI and *Eco*RI cut pGEX-2T to create GST Ca_VI-II linker fusion proteins. The resulting constructs were verified by DNA sequencing.

2.1.11.2 NusA fusion proteins

The cytoplasmic linker between domains I and II of $Ca_V2.2$ was amplified by PCR using primers which introduced *Eco*RI restriction sites into the 5' and 3'ends. The resulting PCR product was inserted into pETM 6T1 which had been made linear by digestion with *Eco*RI to create NusA $Ca_V2.2$ I-II linker fusion protein. Mutations within the I-II linker fusion protein which changed tryptophan 391 to alanine, tyrosine 388 to serine and tyrosine 388 to phenylalanine were made by site directed mutagenesis.

2.1.11.3 HA tagged constructs

Wildtype $Ca_V\beta2a$ and $Ca_V\beta2a$ S574A were amplified by PCR using primers which introduced *Eco*RI restriction sites into the 5' and 3' ends and in addition, modified the N-terminus of $Ca_V\beta2a$ to remove the first methionine, introduce an HA tag and to change cysteine 3 and 4 to serine. The N-terminus of HA tagged $Ca_V\beta2a$ and $Ca_V\beta2a$S574A now reads MYPYDVPDYAQSSGLVH.

Wildtype protein kinase B in expression vector pUSEamp was amplified by PCR using primers which introduced *Eco*RI restriction sites into the 5' and 3' ends and also introduced an HA tag to the N-terminus of the protein. The resulting PCR products were ligated into pMT2 which had been made linear with *Eco*RI. All HA tagged constructs were verified by DNA sequencing.

2.1.11.4 $His_{(6)}$ tagged constructs

As described previously, the prokaryotic expression vector pET28 was used to generate all $His_{(6)}$ tagged constructs used in these experiments. $His_{(6)}$ tagged $Ca_V\beta1b$ (H6Cβ1b) was made by amplifying $Ca_V\beta1b$ by PCR using primers which removed

the existing stop codon, replacing it with a $His_{(6)}$ tag followed by a new stop, the forward and reverse primers also contained *Nco*I and *Eco*RI restriction sites respectively to facilitate subcloning into pET28. $His_{(6)}$ tagged $Ca_V\beta3$ (H6Cβ3) was made by two rounds of PCR, the first amplified the 5' end of $Ca_V\beta3$ removing an internal *Afl*III restriction site. The second round used the product from the first round of PCR as forward primer and a reverse primer which included a $His_{(6)}$ tag and an *Eco*RI restriction site. H6Cβ3 was subcloned into pET28 using *Nco*I and *Eco*RI restriction sites. $His_{(6)}$ tagged $Ca_V\beta2a$ was amplified by PCR using primers which introduced EcoRI restriction sites into both the 5' and 3' ends. The resulting PCR product was subcloned into pET28 in frame with the N-terminal $His_{(6)}$ tag encoded by the vector.

2.1.11.5 $Ca_V\beta$ C-terminus and ΔC-terminus constructs

The $His_{(6)}$ tagged C-terminus of $Ca_V\beta1b$ was generated by digesting $Ca_V\beta1b$ in pET28 with N*co*I, this removed the majority of $Ca_V\beta$ coding region. The resulting construct contained 166 residues of $Ca_V\beta1b$ C-terminus fused to a C-terminal $His_{(6)}$ tag. $Ca_V\beta1b$ without a C-terminus (H6Cβ1b ΔC-terminus) was generated by PCR using a reverse primer which truncated $Ca_V\beta1b$ at the end of the GK like domain introducing a C-terminal $His_{(6)}$ tag followed by a stop codon.

The C-termini of $Ca_V\beta2a$ and $Ca_V\beta2a$S574A were amplified by PCR using primers which introduced *Eco*RI into the 3' and 5' ends. The resulting PCR products were subcloned into pET28 using EcoRI, the resulting constructs contained an N-terminal $His_{(6)}$ encoded by the vector.

2.1.11.6 Site Directed Mutagenesis

Site directed mutagenesis was used to create point mutations in $His_{(6)}$ tagged $Ca_V\beta2a$ to create $Ca_V\beta2a$S574A and also to change tryptophan 391 to alanine and tyrosine 388 to serine or phenylalanine in $Ca_V2.2$ NusA I-II linker fusion constructs. Point mutations were made using the QuickChange Site Directed Mutagenesis kit (Stratagene). The technique is PCR based and involves the use of a pair of complimentary DNA primers both of which harbour the intended mutation. PCR followed by *Dpn*I digestion of methylated template DNA results in mutated plasmids

consisting of "nicked" circular strands. The mutated plasmid is introduced without the need for ligation into XL1 blue *E.coli* which repair and propagate the plasmid. All constructs generated this way were verified by DNA sequencing

2.1.12 DNA sequencing

DNA sequencing was performed using a PCR based method. The reaction mixture contains a mix of standard deoxynucleotide triphosphates and fluorescent dideoxyribonucleotide triphosphates. The polymerase and fluorescent nucleotide mix used was BigDye version 3.1 (Applied Biosystems). DNA sequencing reactions were set up in the following way.

Component	Concentration
Template DNA	0.5μg
Primer	4pmol
BigDye Version 3.1	4μl
Water	To 10μl

The reaction mixture was subjected to the following reaction conditions using a thermal cycler.

Time	Temperature (°C)	Step	Cycles
2 min	98	Initial melt	1
20 sec	98	Melt	25
20 sec	50	Annealing	25
4 min	60	Extension	25
4 min	60	Final extension	1

The resulting products were precipitated using sodium acetate and ethanol and finally washed with 70% ethanol to remove traces of salt. The DNA sequences were analysed using an ABI PRISM 3100 Genetic Analyzer (Applied Biosystems) according to the manufacturer's instructions. The resulting sequence data was inspected using Chromas version 1.45 software and sequence alignments against the corresponding sequence obtained from GenBank were made using Omiga software.

2.2 Protein Chemistry

2.2.1 Bacterial strains and cultures

E.coli BL21-CodonPlus-RIL (Stratagene) bacteria were used as the host strain for large scale protein production. BL21-CodonPlus-RIL *E.coli* contain extra copies of the *arg*U, *ile*Y and *leu*W transfer RNA genes. This enables this strain to recognise arginine codons AGA and AGG, the isoleucine codon AUA and the leucine codon CUA. These codons can restrict translation of heterologous proteins from certain organisms causing expression of truncated protein products or no expression at all.

For protein expression, single colonies of *E.coli* BL21-CodonPlus-RIL containing the plasmid of interest were picked and cultured overnight in LB pH7.4 in a shaking incubator at 37°C. The following day, the saturated cultures were diluted 1:10 in LB pH5.5 containing the appropriate antibiotics and 1%w/v glucose. The cultures were grown at 37°C until the optical density at 560nm was between 0.5 and 0.6. Cultures were then cooled to 22°C and protein production was induced by addition of IPTG to a final concentration of 0.5mM for $Ca_V\beta$ subunit constructs and 0.1mM for all other constructs. Protein expression was allowed to proceed for 4 hours before cultures were harvested by centrifugation at 10,000 x g for 5 min. Pelleted cultures were stored at -80°C until required.

2.2.2 Ni-NTA chromatography

Ni-NTA chromatography was used to purify expressed proteins carrying hexahistidine tags from bacterial lysates. Metal ions can be divided into three groups based on their preferential reactivity towards nucleophiles (Pearson, 1973) Iron, Calcium and Aluminium are known as hard metal ions and react preferentially with oxygen. Intermediate metal ions include copper, nickel, zinc and cobalt coordinate oxygen, nitrogen and sulphur. As there are limited numbers of cysteines exposed on the surface of proteins, histidines are a major target for intermediate metal ions (Chaga, 2001). The use of engineered affinity tags and immobilised metal affinity chromatography (IMAC) was first demonstrated by Hochuli et al. (1988), the technique is now widely used in the purification of recombinant proteins. In these experiments, nickel complexed with nitrilotriacetic acid (NI-NTA) (Qiagen) was used

as this forms stronger complexes with the metal ion than some other adsorbents leading to less metal ion leaching during use.

For purification of all $Ca_V\beta$ subunit constructs, frozen *E.coli* pellets were thawed on ice and resuspended in 10ml of buffer containing 20mM Tris pH 8.0, 150mM NaCl, 1mM dithiothreitol (DTT) and 20mM imidazole. Complete EDTA free protease inhibitor cocktail (Roche Diagnostics) was present in all buffers at a concentration of 1 tablet per 50ml buffer. The cells were lysed by sonication for two pulses of two min, the cells were rested on ice between pulses. The lysates were cleared by centrifugation for 20 min at 20,000 x g at 4°C. The cleared lysate was loaded onto a 1ml NI-NTA column which had been pre-equilibrated with buffer containing 20mM Tris pH 8.0, 150mM NaCl, 1mM DTT, 20mM Imidazole. The column was washed with 25 volumes of equilibration buffer before elution with 5 volumes of equilibration buffer containing 400mM imidazole. The eluate from the column was collected in 1ml aliquots and stored at 4°C until required.

For purification of NusA fusion constructs, the initial cell lysis was performed as for $Ca_V\beta$ subunit constructs. After centrifugation the resulting pellet was washed once in 10ml lysis buffer and resuspended in 10ml buffer containing 20mM (N-(2-Hydroxyethyl)piperazine-N'-(2-ethanesulfonic acid) (HEPES) pH 8.0, 150mM NaCl, 1mM DTT, 20mM imdazole and 1.5% 3-[(3-Cholamidopropyl)dimethylammonio]-1-propanesulfonate (CHAPS), and was incubated for1 hour at 4°C on a rolling platform. After centrifugation at 20,000 x g for 20 min, the resulting supernatant was diluted 1:1 with lysis buffer and loaded onto a 1ml Ni-NTA column which had been pre-equilibrated with lysis buffer containing 0.5% CHAPS. The column was washed with 25 volumes of lysis buffer containing 0.5% CHAPS before proteins were eluted in 4 volumes of lysis buffer containing 0.5% CHAPS and 400mM imidazole. The column eluates were collected in 1ml aliquots and stored at 4°C until required.

2.2.3 Glutathione Sepharose chromatography

Glutathione-s-transferase (GST) fusion proteins were purified using glutathione sepharose 4b beads. This type of separation is known as affinity

chromatography and is based on the high affinity of GST for its substrate peptide glutathione. Glutathione is a tripeptide of glutamate, cysteine and glycine, its physiological role is as an antioxidant protecting cells from toxins such as free radicals. Glutathoine-s-transferase catalyses the conjugation of toxins with glutathione via the sulphydril group on the peptide, thus aiding cellular detoxification (Douglas, 1987; Martinez-lara *et al.*, 2002).

Frozen *E.coli* pellets were thawed on ice and resuspended in 10ml of buffer containing 20mM Tris pH 7.4, 150mM NaCl, 1mM DTT, 1mM EDTA, 1% n-lauryl sarcosine. Cells were lysed by sonication for two pulses of two min followed by incubation on a rolling platform for 10 min at 4°C. Triton X-100 was added to a final concentration of 1% and the cell lysates was re-sonicated for 2 min. The lysate was cleared by centrifugation at 20,000 x g for 20 min at 4°C. The resulting supernatant was loaded on to a 1ml glutathione sepharose column which had been pre-equilibrated with buffer containing 20mM Tris pH 7.4, 150mM NaCl 1mm DTT, 1mM EDTA 0.1% tritonX-100. The column was washed with 25 volumes of equilibration buffer and eluted in 4 volumes of buffer containing 20mM tris pH8.0, 150mM NaCl, 1mM DTT, 1mM EDTA, 0.1% tritionX-100, 5mM reduced glutathione. The eluate was collected in 1ml aliquots and stored at 4°C until required. The purified GST fusion proteins remained soluble in elution buffer, addition of 1% n-lauryl sarcosine and 1% Triton X-100 was not necessary to keep proteins soluble for subsequent experiments

2.2.4 Polyacrylamide gel electrophoresis – SDS PAGE

SDS polyacrylamide gel electrophoresis (PAGE) was performed on NuPAGE Bis-Tris gels 10 well mini gels (Invitrogen) with a running buffer of NuPAGE MOPS or NuPAGE MES depending upon the required resolution. The NuPAGE system is based on the system described by Laemmli. (1970) with some modifications. The Laemmli system used Tris-Glycine polyacrylamide gels cast at a pH of 8.7 which increased to 9.5 during electrophoresis. In addition, the Laemmli sample buffer was at pH 6.8 where disulphide bonds are poorly reduced leading to reduced resolution. NuPAGE Bis-Tris gels are cast at a lower pH and the pH of the gel during electrophoresis is around neutral. The change in buffer composition and pH gives

greater resolution of protein bands and means that higher concentrations of protein can be separated without loss of resolution. For resolution of large proteins, NuPAGE MOPS was used, the working concentration contained 50mM 3(N-morpholino) propane sulphonic acid (MOPS), 50mM Tris, 3.4mM SDS, 1mM EDTA pH 7.4. For smaller proteins, NuPAGE MES running buffer was used the working concentration contained 50mM 2-(morpholino) ethane sulphonic acid (MES), 50m Tris, 3.4mM SDS, 1mM EDTA pH 7.3. Protein samples were prepared by addition of the appropriate volume of 4 x NuPAGE LDS sample buffer followed by NuPAGE reducing agent, samples were heated to 80°C for 5 min prior to loading. Gels were run at a constant voltage of 200 V.

After electrophoresis, protein bands were visualised by staining with coomassie blue. This was done using SimplyBlue safe stain (Invitrogen) according to manufacturer's instructions.

2.2.5 Western blotting

For western blotting, proteins were transferred from polyacrylamide gels to polyvinyldeneflouride (PVDF) membrane. This was used in preference to nitrocellulose membrane as it has a higher binding capacity for protein. The transfer was made using a semi dry blotting apparatus (Biorad) with NuPAGE transfer buffer (Invitrogen). Working concentrations of transfer buffer contained 25mM Bicine, 25mM Bis-Tris, 1mM EDTA, 10% methanol and 0.001% SDS.

For transfer of one gel, 3 pieces of Whatman filter paper (8.5 cm by 7.5cm) were soaked in transfer buffer and placed on the platinum anode. A sheet of PVDF membrane cut to the same size and pre-soaked in methanol before being placed on the filter paper. The gel was pre-soaked in transfer buffer for 5min prior to being placed on the membrane and a further 3 pieces of soaked filter paper were placed on the gel. The circuit was completed by addition of the stainless steel cathode to the gel sandwich. The apparatus was run at a constant current of 5mA/h per cm^2 of gel with the voltage limited to 25 V.

The membrane was removed from the transfer apparatus and blocked for 1 hour in a buffer containing 20mM Tris pH 7.4, 500mM NaCl, 5% bovine serum albumin (BSA) and 0.05% Tween-20. The blocked membrane was placed in a 50 ml tube and primary antibodies were diluted 1:1000 in antibody diluent which consisted of 20mM Tris pH7.4, 500mM NaCl, 5% BSA, 10% goat serum, and 0.5% nonioinic detergent Igepal. The primary antibodies used in these experiments are listed in Table 2.1. The membrane was incubated with primary antibody overnight at room temperature on a rolling platform. The membrane was washed 3 times for 15 minutes with wash buffer (20mM Tris pH 7.4, 500mM NaCl) and secondary antibody was diluted 1:1000 in antibody diluent and incubated with the membrane for 1 hour at room temperature on a rolling platform. The membrane was then washed again 3 times for 15 min. The secondary antibodies used were goat anti rabbit conjugated to horse radish peroxidase (HRP) or goat anti mouse conjugated to HRP depending on the origin of the primary antibody.

Immunoreactive bands were revealed using ECL plus western blotting detection reagent (GE Healthcare) according to the manufacturers instructions. ECL plus is primarily a very sensitive chemiluminescent detection reagent, that is, the peroxidase coupled to the secondary antibody catalyses a reaction involving peroxide and luminol which emits light which can then be detected using photographic film. The ECL plus chemical reaction however also has a fluorescent component. The fluorescent component of the reaction was imaged directly using a Typhoon 9210 variable mode phosphorimager.

2.2.6 Autoradiography and Densitometry

For analysis of proteins containing incorporated ^{33}P, protein samples were separated by SDS PAGE as described above. As ^{33}P emits a weak radioactive signal, even a thin layer of polyacrylamide can interfere with the detection of labelled proteins. To avoid this, the proteins were transferred to PVDF membrane as described above. Labelled proteins were detected by exposing the membranes to a storage phosphor screen (Molecular Dynamics, Amersham Biosciences) overnight. The radioactive bands were revealed by scanning the storage phosphor screen using a Typhoon 9210 variable mode phosphorimager.

For analysis of ^{32}P labelled proteins, it was not necessary to transfer the proteins to a PVF membrane. The SDS PAGE gels were placed on a square of Whatman filter paper, covered in a plastic membrane and dried. The dried gels were exposed to a storage phosphor screen overnight and the screens were scanned with a Typhoon 9210 variable mode phosphorimager to reveal the radioactive bands.

Images of western blots and storage phosphor screens were inspected and quantified using ImageQuant 5.2 software (Molecular Dynamics, Amersham Bioeciences). Band intensities were compared after subtraction of the background signal which was measured at the same point on the gel as the protein of interest but in a lane where the protein of interest is not present.

Table 2.1

Primary antibody	Source	Description	Working dilution	Supplier
Anti $Ca_V\beta 2a$	Rabbit	Affinity purified	1:1000	Chein *et al.*,1996
Anti $Ca_V2.2$	Rabbit	Affinity purified	1:1000	Raghib *et al.*, 2001
Anti Akt/PKBα	Rabbit	Affinity purified	1:1000	Cell Signalling Technology
Anti-phospho-Akt/PKBα (Ser473)	Rabbit	Affinity purified	1:1000	Cell Signalling Technology
Anti-phospho-Akt/PKBα (Thr308)	Rabbit	Affinity purified	1:1000	Cell Signalling Technology
Anti HA	Rat	Monoclonal, Affinity purified	1:1000	Roche
Anti Glu-Glu	Mouse	Monoclonal, Afffinity purified	1:1000	Advanced Targeting Systems
Anti PI3 kinase p110	Rabbit	Affinity purified	1:1000	Santa Cruz Biotechnology

Table 2.1. The primary antibodies used for western blotting in these experiments are listed above.

2.2.7 Mammalian tissue culture and transfection

In these experiments, COS-7 and tsA201 cells were used. COS-7 cells are African green monkey kidney cells which have been transformed with an origin defective SV40 virus (Gluzman, 1981). Cells were cultured in Dulbecco's modified eagle medium (DMEM) (Invitrogen) supplemented with 10% new born calf serum (Invitrogen), 2mM glutamine, 5 units/ml penicillin and 0.5μg/ml streptomycin. Cells were cultured in $75cm^2$ at 37°C in 5% CO_2 and diluted 1:12 when confluent.

TsA201 cells are SV40 transformed human embryonic kidney (HEK) cells which express the temperature sensitive T antigen. TsA201 cells were cultured in DMEM supplemented with 2mM glutamine, 10% foetal bovine serum (Invitrogen), 5 units/ml penicillin and 0.5μg/ml streptomycin. Cells were cultured in $75cm^2$ flasks at 37°C in 5% CO_2 and diluted 1:12 when confluent.

COS-7 cells were transfected using Geneporter (Gene Therapy Systems) according to the manufacturer's instructions. TsA201 cells were transfected using FuGENE 6 transfection reagent (Roche Diagnostics) according to the manufacturer's instructions. Both COS-7 and tsA201 cells were split 1:6 prior to transfection and were used 48 hours after transfection.

2.2.8 Immunoprecipitation and Co-immunoprecipitation

Immunoprecipitation was performed to isolate epitope tagged proteins from transfected mammalian cell lysates. Proteins of interest were engineered to contain the HA epitope tag derived from the influenza virus haemaglutinin protein. The antibodies used for immunoprecipitation were Rat monoclonal anti HA high affinity antibodies (Clone 3F10) (Roche Diagnostics). This antibody was selected specifically because its high affinity for the HA epitope sequence, this means that lower working concentrations can be used and less cross reactivity is observed, this is highly desirable in immunoprecipitation experiments.

For immunoprecipitation of HA tagged $Ca_V\beta 2a$ subunits, transfected COS-7 cells were used 48 hours post transfection. The cells were washed three times with phosphate buffered saline (PBS) and resuspended in 1ml of lysis buffer containing 20mM Tris pH 7.4, 150mM NaCl, 1mM EDTA, 1% Igepal, 1mM sodium orthovanadate, 50μM cantharidic acid, 20μM bromotetramisole oxalate and protease inhibitors. Cells were disrupted by passing them through a fine needle until the solution was homogeneous and the cell lysate was cleared by centrifugation at 20,000 x g for 20 min at 4°C. The protein concentration of the resulting supernatant was determined using the bicinchoninic acid (BCA) kit. HA tagged $Ca_V\beta 2a$ subunits were precipitated from 500μg of supernatant using 3μg anti HA antibody, complexes were formed during incubation for 5 hours on a rolling platform. Immune complexes were recovered by addition of 50 μl protein G agarose which had been pre-equilibrated with lysis buffer and incubation for a further 2 hours at room temperature. Immune complexes were washed three times for 15 min with lysis buffer and once with lysis buffer containing 0.5 M NaCl before resuspension in 100μl NuPAGE LDS sample buffer.

The same procedure was performed for co-immunoprecipitation experiments where COS-7 cells were transfected with either HA $Ca_V\beta 2a$ and wildtype Akt/PKBα or HA tagged Akt/PKBα and untagged $Ca_V\beta 2a$.

2.2.9 Cell surface biotinylation

Cell surface biotinylation was used to measure the plasma membrane expression of $Ca_V2.2$ constructs. The technique takes advantage of the reagent sulfosuccinimidyl-2-(biotinamido)ethyl-1,3-dithiopropionate (EZ link sulfo-NHS-SS-biotin) (Pierce). This reagent is a thiol cleavable, water soluble biotinylation reagent which contains an *N*-hydroxysulfosuccinimide (NHS) ester group which reacts with the ε-amine of lysine residues to produce a stable product. Although soluble in water, the biotinylation reagent will not cross the plasma membrane so only lysine residues exposed on the surface of proteins in the plasma membrane will be labelled. The structure of sulfosuccinimidyl-2-(biotinamido)ethyl-1,3-dithiopropionate is shown in Figure 2.1. After labelling, proteins containing the biotin label can be precipitated using streptavidin coupled to agarose beads, the presence of a disulphide linkage between the NHS group and the biotin group means that the precipitated proteins can be liberated from the streptavidin agarose by treatment with strong reducing agents.

TsA201 cells in 75cm^2 flasks were transfected with $Ca_V2.2$ DNA and accessory subunits in the following ratio: 10μg $Ca_V2.2$ pMT2, 7μg $Ca_V\beta$ pMT2, 7μg α2δ2 pMT2. After 48 hours, the cells were washed three times with PBS prior to labelling with 2ml per flask PBS pH 8.0 containing 800μM sulfosuccinimidyl-2-(biotinamido)ethyl-1,3-dithiopropionate, the reaction was allowed to proceed at room temperature for 15 min. The reaction was terminated by addition of 10ml 100mM glycine in PBS. Labelled cells were collected by centrigugation at 1000 x g for 5 min at 4°C and washed a further three times with PBS to remove unincorporated biotinylation reagent which would interfere with subsequent precipitation.

Labelled cells were lysed by addition of 750μl of lysis buffer containing 20mM Tris pH 7.4, 150mm NaCl, 1mM EDTA, 1.5% Triton X-100 and protease inhibitors followed by brief sonication. After centrifugation at 20,000 x g for 20 min at 4°C the protein concentration of the resulting supernatant was determined using the bicinchoninic acid (BCA) kit (Pierce). Biotinylated proteins were precipitated by incubating 500μg of whole cell lysate with 50μl streptavidin agarose beads (Pierce) for 3 hours at room temperature on a rotating platform. The streptavidin agarose precipitates were washed 3 times for 10 min with lysis buffer before biotinylated

Figure 2.1

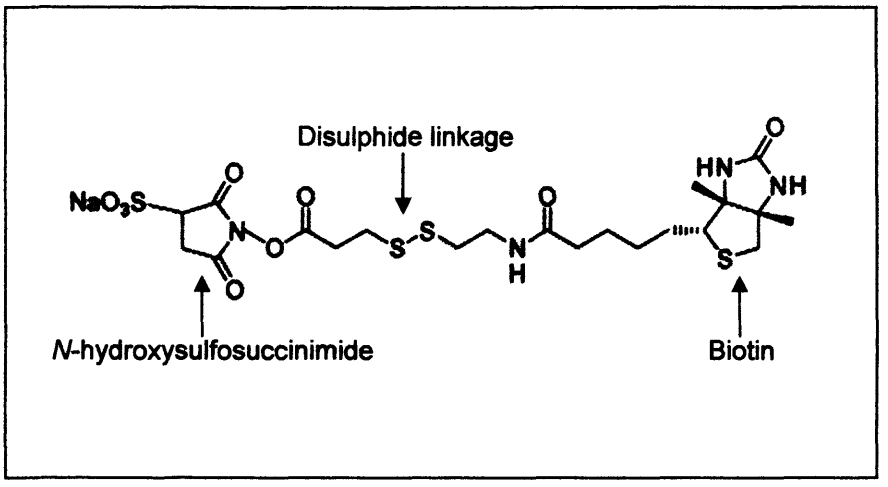

Figure 2.1. The molecular structure of sulfosuccinimidyl-2-(biotinamido)ethyl-1,3-dithiopropionate (EZ link sulfo-NHS-SS-biotin) used in cell surface biotinylation experiments. The biotin group, the *N*-hydroxysulfosuccinimide group and the disulphide linkage are indicated.

proteins were liberated from the beads by addition of 50µl lysis buffer containing 100mM DTT and incubation for 30 min at room temperature. As a control for cell leakiness, western blotting was performed on samples of precipitated proteins using antibodies to the cytoplasmic protein kinase Akt.

2.2.10 ^{33}P metabolic labelling

Metabolic labelling was used to measure the change in incorporation of phosphate into $Ca_V\beta2a$ constructs. Transfected COS-7 cells in 75cm^2 flasks were transfected and used for ^{33}P labelling after 48 hours.

Cells were washed three times with phosphate free Dulbecco's modified Eagle's medium (DMEM) (ICN Biochemicals, Irvine, California.) containing 10% dialysed FBS (Invitrogen) and incubated in phosphate free media for 1 hour. The medium was replaced with phosphate free DMEM containing 30µCi/ml [^{33}P] orthophosphate and incubated for a further 6 hours. Labelled cells were washed twice with Tris Buffered Saline (TBS) containing protease inhibitors and 1mM EDTA, harvested by centrifugation for 5 min at 1000 x g and either processed immediately as described in the protocol for immunoprecipitation or stored at -80°C until required.

2.2.11 *In vitro* phosphorylation

Phosphorylation *in vitro* was performed using recombinant Protein kinase B purified from insect cells (Upstate Biotechnology) and a recombinant positive control substrate BAD purified from *E.coli* (Upstate Biotechnology). The test substrates were $Ca_V\beta2a$ C-terminus and $Ca_V\beta2a$ S574A C-terminus, both were over expressed in *E.coli* and purified by Ni-NTA chromatography as described.

Each reaction contained 2µg of substrate protein and 0.4µg purified kinase in a total volume of 40µl. The kinase and substrate were diluted in assay buffer which contained 20mM MOPS, 25mM β-glycerophosphate, 1mM sodium orthovanadate, 5mM EDTA and 1mM DTT. γ-^{32}P ATP was diluted to 1µCi/µl in Mg/ATP (75mM $MgCl_2$, 500µM cold ATP in assay buffer) and 10 µl were added to each reaction. Diluted ATP was the last component to be added to the reaction mixture. Reactions were incubated at 30°C for 15 min and stopped immediately by addition of an equal

volume of 2 x SDS sample buffer followed by heating to 80°C for 5 min. Reaction mixtures were separated by SDS PAGE and phosphate incorporation was revealed by autoradiography and quantified using ImageQuant 5.2.

2.2.12 Precipitation of unknown proteins from native tissue

Purified $Ca_V\beta 1b$ subunit and N-terminal and C-terminal portions of the $Ca_V\beta 1b$ subunit were used as bait in attempts to capture an identify novel binding partners for the $Ca_V\beta 1b$ subunit from mouse brain lysates.

The $Ca_V\beta 1b$ constructs were expressed and purified by Ni-NTA chromatography as described above. The purified proteins were then immobilised onto 1ml HiTrap NHS-activated columns (GE Healthcare). The columns were activated and the immobilisation performed according to the manufacturers instructions. The columns contain agarose beads coupled to epichlorohydrin and are activated by N-hydroxysuccinimide (NHS), the proteins are coupled to the matrix via free primary amine groups. Prior to coupling, the bait proteins were dialysed into coupling buffer which was composed of 200mM sodium hydrogencarbonate, 500mM NaCl pH8.3. Approximately 2mg of each bait protein was applied to each column and as a control, 1 column was activated and blocked but no protein was immobilised. Analysis of the column eluate by using the BCA protein assay and comparing protein concentrations before and after immobilisation showed that greater than 90% of the bait protein bound to the column. After immobilisation and blocking, the columns were washed with 5 volumes of 20mM glycine pH2.2 to remove any non-specifically bound proteins.

The brains of 10 adult C57BLKs/J mice (Naggert *et al.*, 1995) were washed with TBS and homogenised in 20ml buffer containing 20mM Tris pH7.4, 150mM NaCl, 1mM EDTA, 1% CHAPS and protease inhibitors. The homogenate was cleared by centrifugation at 20,000 x g for 30 min at 4°C. The resulting supernatant was divided into 4 equal parts and the same volume of lysate was applied to each column. The columns were washed with 20 volumes of lysis buffer and eluted in 3 volumes of 20mM glycine pH2.0 containing 0.5% CHAPS. The pH of the eluates was immediately neutralised by addition of 1M Tris pH7.4.

2.2.13 Identification of unknown proteins

Samples containing unknown proteins were prepared and analysed by SDS PAGE. Electrophoresis and subsequent staining with coomassie blue was performed under sterile conditions using equipment which had not previously been used for analysis of protein samples thus keeping contamination to a minimum. Protein bands of interest were excised from the polyacrylamide and stored at -80°C until required.

Unknown proteins were analysed by Matrix Assisted Laser Desorption Ionisation Time of Flight (MALDI-TOF) mass spectroscopy by Dr Dinah Rahman (Section of Proteomics, MRC Clinicial Sciences Centre, Imperial College London). The resulting spectra were analysed using Mascot software (Matrix Science, www.matrixscience.com).

2.3 Surface plasmon resonance spectroscopy

Surface plasmon resonance experiments were performed on a BIAcore 2000 machine (BIAcore AB), using CM5 research grade sensor chips. The BIAcore 2000 machine is able to regulate the temperature of the integrated microfluidic cartridge (IFC) and so all binding experiments were performed at a constant temperature of 25°C. The CM5 Sensor chip is composed of a thin gold conducting film to which a layer of carboxymethyl dextran is coupled, the chip is enclosed in a protective plastic case. When docked with the machine, the chip is removed from the case and pressed against the IFC to make the flow cells or channels in which the binding events take place and are monitored. A diagram of the IFC, flow cells and sensor chip surface is shown in figure 2.2.

The surface of the CM5 sensor chips was prepared for the immobilisation of antibodies or ligand proteins by treating the surface with a mixture of 50mM N-hydroxysuccinimide (NHS) and 200mM N-ethyl-N'-(dimethylaminopropyl)-carbodiimide (EDC). The EDC/NHS mixture reacts with the carboxyl groups on the carboxymethyl dextran, modifying them to amine reactive NHS esters. The EDC first reacts with the carboxyl group on the dextran forming unstable intermediates which are susceptible to attack by amines, the NHS is present to stabilise the intermediates and promote the reaction yield (Staros *et al.*, 1986).

Following chip surface activation, anti GST antibodies were injected at a concentration of 10μg/ml for 10 minutes. The antibodies were diluted in a buffer

Figure 2.2

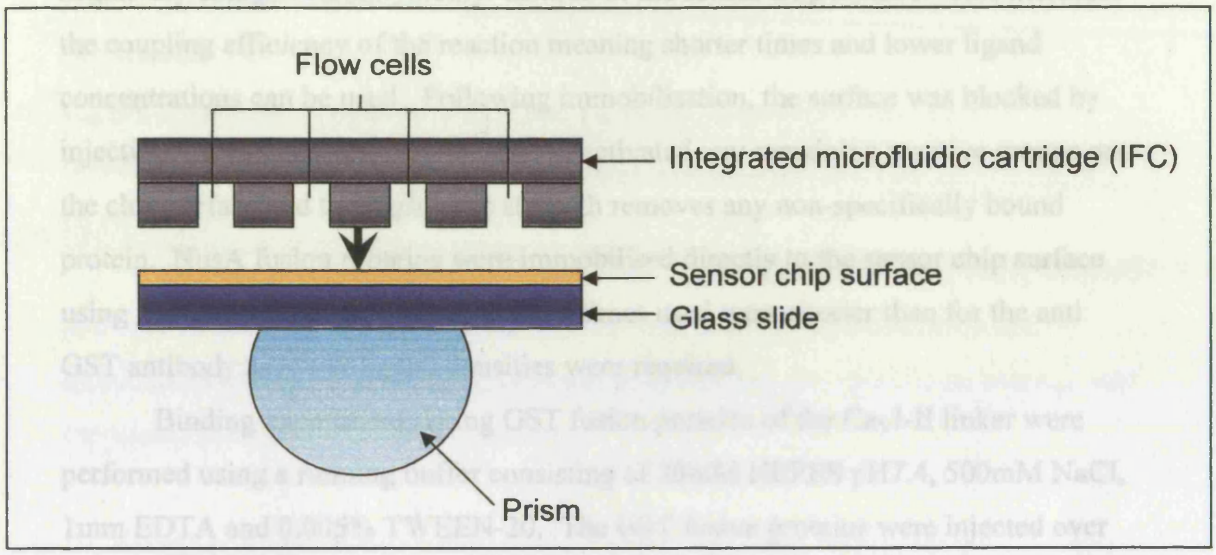

Figure 2.2. In the BIAcore 2000 machine, binding experiments are performed in flow cells which are formed when the sensor chip surface is pressed against the integrated microfluidic cartridge (IFC). Buffer and interacting partners are delivered via the IFC to the sensor chip surface where other interacting partners or "ligands" are immobilised. Redrawn from BIAcore applications handbook.

containing 10mM sodium acetate pH4.0 prior to injection. The lowered pH causes the proteins to become slightly positively charged and therefore attracted to the negatively charged carboxymethyl dextran of the sensor chip surface. This increases the coupling efficiency of the reaction meaning shorter times and lower ligand concentrations can be used. Following immobilisation, the surface was blocked by injecting 1M Ethanolamine pH8.5 this deactivated any remaining reactive groups on the chip surface and the high ionic strength removes any non-specifically bound protein. NusA fusion proteins were immobilised directly to the sensor chip surface using the same chemistry but the contact times used were shorter than for the anti GST antibody as lower ligand densities were required.

Binding experiments using GST fusion proteins of the Ca_VI-II linker were performed using a running buffer consisting of 20mM HEPES pH7.4, 500mM NaCl, 1mm EDTA and 0.005% TWEEN-20. The GST fusion proteins were injected over the immobilised antibody at a concentration of 10μg/ml until 150 RU of protein was bound. The $Ca_V\beta$ subunits were diluted to the appropriate concentrations in running buffer and injected for 5 min at 50μl/min followed by a dissociation period of 5 min at the same flow rate. For NusA Ca_VI-II linker fusions, a buffer consisting of 20mM HEPES pH 7.4, 150mM NaCl, 1mM EDTA, 0.1% CHAPS was used. The $Ca_V\beta$ subunits were diluted in running buffer injected for 5 min at 50μl/min. After each round of binding experiments, the chip surface was washed with 20mM glycine pH2.0 followed by running buffer until a stable baseline was obtained upon which to perform the next experiments.

BIAcore sensorgrams were initially analysed using BIAevaluation 3.0 software (BIAcore, AB). The software allows each set of curves to be aligned such that the injection start point is set to zero seconds in the x axis and zero response in the y axis. This allows the sensorgrams to be aligned relative to one another. Once aligned, any non-specific binding can is subtracted by subtracting the signal from the reference or negative control flow cell which contained GST alone in the GST fusion protein experiments and NusA alone in the NusA fusion protein experiments.

Once aligned, the BIAevaluation software made fits to the sensorgrams to determine the observed rate of analyte accumulation $k_{on\ (obs)}$ and the rate of dissociation k_{off}. The fits were made using a model of 1:1 interaction where the on

and off rates are fitted to single exponentials. The BIAevaluation software uses the following equations:

Association: $R = R_{eq}\,(1\text{-}e^{-(kon(obs)(t\text{-}t0))})$

Dissociation: $R = R_0 e^{-kd(t\text{-}t0)}$

R_{eq} is the response at equilibrium, R and R_0 are the responses at time t and t_0 respectively. From these values, the specific on rate k_{on} and the dissociation K_D can be calculated.

The raw data from the sensorgrams was exported and evaluated using Origin 5 software (Microcal). Single exponential fits were made to the association and dissociation phases of the sensorgrams and from this data the specific on rate k_{on} was calculated using the following equation:

$$k_{on} = \frac{k_{on(obs)} - k_{off}}{[Ca_V\beta]}$$

The dissociation constant K_D was calculated as

$$K_D = \frac{k_{off}}{k_{on}}$$

The data from the NusA fusion proteins was evaluated further by plotting the responses 250 seconds after the start of perfusion and plotting them against $Ca_V\beta$ concentration. The resulting curves were fitted to a hyperbola function:

$$Y = \frac{B_{max} \cdot [\beta]}{K_D + [\beta]}$$

where Y is the response at 250 seconds and B_{max} is the maximum response.

Chapter 3:

Surface plasmon resonance spectroscopy

3.1 Introduction

High voltage activated calcium channels are associated with a regulatory beta subunit. The $Ca_V\beta$ subunit binds to a highly conserved 18 amino acid motif in the intracellular linker between domains I and II of high voltage activated (HVA) calcium channels known as AID (Alpha Interaction Domain) (Pragnell *et al.*, 1994). An alignment of L-type and non L-type calcium channel AID motifs is shown in figure 3.1. $Ca_V\beta$ subunit binding to AID generally increases plasma membrane expression and causes a shift in the voltage dependence of activation and inactivation to more negative potentials (Catterall, 2000). Early work described the binding site on the $Ca_V\beta$ subunit as a 41 amino acid sequence BID (Beta Interaction Domain) (De Waard *et al.*, 1994, 1995). The BID was reported to contain several residues which were critical for binding to AID (De Waard et al., 1995, 1996). However, more recent structural studies on $Ca_V\beta2$, $Ca_V\beta3$ and $Ca_V\beta4$ (Van Petegem *et al.*, 2004; Opatowsky *et al.*, 2004; Chen *et al.*, 2004) have shown that the site of interaction of $Ca_V\beta$ with AID is a groove on the GK like domain termed the AID binding pocket (ABP) (Van Petegem *et al.*, 2004) and the residues previously believed to be important for binding were actually involved in maintaining the structural integrity of the GK module. The structures, all of which show $Ca_V\beta$ subunits in complex with an AID peptide also show the importance of the conserved tryptophan in AID, it is deeply buried in the binding groove forming multiple interactions with surrounding amino acid residues, these findings confirm those of other studies which have shown this conserved tryptophan to be essential for $Ca_V\beta$ subunit binding (Pragnell *et al.*, 1994; Berrou *et al.*, 2002; Leroy *et al.*, 2005).

The AID binds to $Ca_V\beta$ with very high affinity. This was demonstrated firstly by De Waard et al. (1995). Using glutathione-S-transferase fusion proteins of AID_A and *in vitro* translated ^{35}S labelled $Ca_V\beta$ subunits, the dissociation constants (K_D) for $Ca_V\beta$ subunits binding to AID_A were found to be between 2.6 and 76 nM. The $Ca_V\beta4$ subunit bound with the highest affinity and $Ca_V\beta3$ with the lowest affinity, $Ca_V\beta2a$ and 4 were reported to bind with two different affinities. More recently, similar experiments have been performed using surface plasmon resonance binding assays to determine the dissociation constants. Interactions between $Ca_V2.1$ AID and $Ca_V\beta4$ (Geib *et al.*, 2002), $Ca_V2.2$ AID and $Ca_V\beta1b$ (Leroy *et al.*, 2005), $Ca_V1.3$ AID and $Ca_V\beta1b$ (Bell *et al.*, 2001) and between $Ca_V2.2$ AID and $Ca_V\beta3$ (Canti *et al.*,

2003) have been measured. In all cases the dissociation constants were found to be between 5nM and 20nM. Measurements of AID peptide binding to $Ca_V\beta$ have also been made by fluorescence polarisation spectroscopy (Opatowsky *et al.*, 2003; Opatowsky *et al.*, 2004), the dissociation constants were found to be 16 and 26 nM.

Figure 3.1 Alignment of L-type and non L-type AID motifs of HVA calcium channels. Conserved residues are shown in red, non-conserved in black. The sequence within AID of non L-type channels involved in interaction with βγ subunits of heterotrimeric G proteins is underlined.

The intracellular linker between domains I-II of non L-type calcium channels will also bind to βγ dimers of heterotrimeric G proteins (De Waard *et al.*, 1997; Zamponi *et al.*,1997), this has been shown using overlay assays (De Waard *et al.*, 1997) and also by Bell et al. (2001) using surface plasmon resonance studies. The proposed site of interaction is within the conserved AID motif (Figure 3.1) and contains the sequence Q Q X X R which has previously been shown to be involved in interaction with G protein βγ subunits (Chen *et al.*, 1995). Although the I-II linker has been shown to be important for G protein modulation of the Ca_V2 class of calcium channels (De Waard *et al.*, 1997; Zamponi *et al.*, 1997; Herlitz *et al.*, 1997), other regions of the channels especially the N-terminus have been shown to be involved (Canti *et al.*, 1999; Agler *et al.*, 2005).

The experiments described here were performed to investigate the interaction of purified $Ca_V\beta$ subunits with the GST fusion proteins of the I-II loop of HVA calcium channel α1 subunits. The binding experiments were performed using surface plasmon resonance which allows on- and off- rates to be measured and a dissociation constant (K_D) for the interaction to be calculated. In addition, the interaction of G

protein βγ subunits with the I-II linkers of Ca_V 1.3 and Ca_V 2.2 was measured and compared.

3.2 Results

3.2.1 Preparation of GST I-II linker fusion proteins and purified $Ca_V\beta$ subunits.

The cytoplasmic linker between domains I and II of Ca_V 1.3, Ca_V 2.1 and Ca_V 2.2 were amplified by polymerase chain reaction (PCR) as described in Chapter 2 using primers which introduced *Bam* HI and *Eco* RI restriction endonuclease sites to the 5' and 3' ends respectively. The resulting PCR products were subcloned in frame with *Schistosoma japonicum* glutathione-S-transferase in the bacterial expression vector pGEX-2T to create GST I-II linker fusion constructs. The GST fusion system was used here for several reasons. Firstly, it enables efficient purification of expressed proteins (Nygren, 1994), secondly it facilitates immobilisation of the "ligand" proteins in the surface plasmon resonance assay and finally, GST can sometimes function to enhance the solubility of its fusion protein partners.

The GST I-II linker fusion proteins were expressed in *E.coli* BL21 (DE3) RIL bacteria and purified by affinity chromatography using glutathione sepharose beads as described in Chapter 2. All Ca_V I-II linker fusion proteins were found to be insoluble despite the presence of GST. No full length GST I-II linker fusion proteins could be purified from the soluble fraction of the bacterial lysates. Instead, the insoluble material recovered after centrifugation of the lysates was treated with 1% Triton X-100 and 1% n-lauryl sarcosine, and proteins were purified from the resulting supernatant. Once purified, the fusion proteins remained soluble in 0.1% Triton X-100. The GST tag was found to contribute to the solubility of the proteins after purification as treatment of the purified proteins with the protease thrombin, which cleaves the protein between the I-II linker and the GST tag, resulted in Ca_V I-II linker protein which was completely insoluble (not shown). Glutathione-s-transferase alone was prepared by expressing empty pGEX2-T in *E.coli* BL21 (DE3) RIL bacteria. Highly purified GST was prepared by affinity chromatography on glutathione sepharose beads (not shown). Treatment with detergents was not necessary as GST was present in the soluble fraction after cell lysis. Samples of the purified GST I-II linker proteins are shown in figure 3.2 *A* after SDS PAGE and staining with coomassie blue.

Calcium channel beta subunits $Ca_V\beta$1b, $Ca_V\beta$2a and $Ca_V\beta$3 were amplified by PCR using oligonucleotide primers which introduced restriction endonuclease sites

Figure 3.2

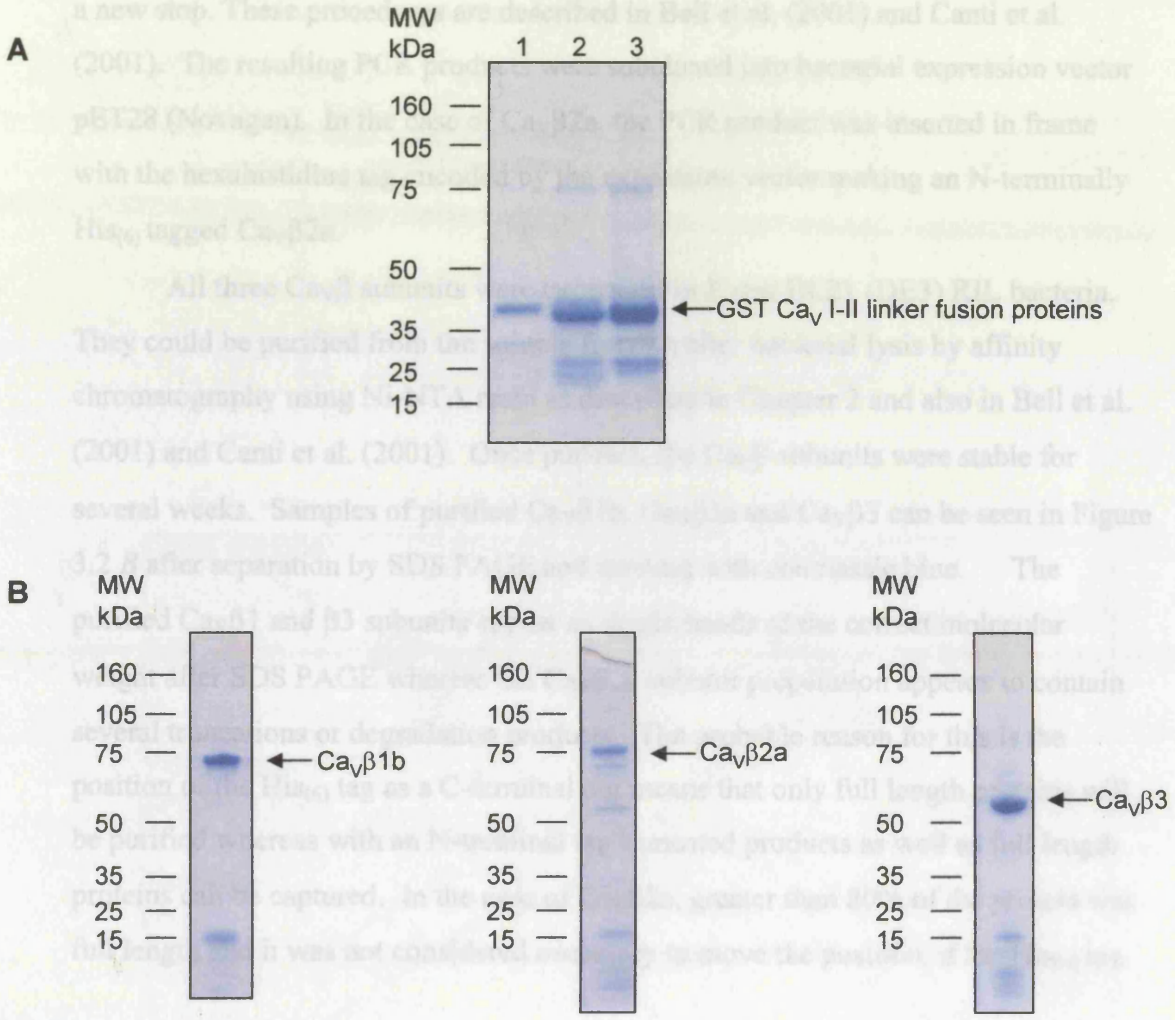

Figure 3.2. A. Coomassie blue stained SDS-PAGE on NuPage 4-12% Bis-Tris gel showing purified GST fusion proteins of $Ca_V2.1$ I-II linker (Lane 1), $Ca_V2.2$ I-II linker (lane 2) and $Ca_V1.3$ I-II linker (lane 3) used in surface plasmon resonance analysis. **B**. Coomassie blue stained SDS-PAGE on NuPage 4-12% Bis-Tris gel showing purified $Ca_V\beta1b$, $Ca_V\beta2a$ and $Ca_V\beta3$ used in surface plasmon resonance analysis. Molecular weight markers are indicated.

into the 3' and 5' ends suitable for subcloning into bacterial expression vector pET28. In the cases of $Ca_V\beta1b$ and $Ca_V\beta3$ a hexahistidine tag was engineered into the reverse primer so that the stop codon was removed and replaced by the $His_{(6)}$ tag followed by a new stop. These procedures are described in Bell et al. (2001) and Canti et al. (2001). The resulting PCR products were subcloned into bacterial expression vector pET28 (Novagen). In the case of $Ca_V\beta2a$, the PCR product was inserted in frame with the hexahistidine tag encoded by the expression vector making an N-terminally $His_{(6)}$ tagged $Ca_V\beta2a$.

All three $Ca_V\beta$ subunits were expressed in *E.coli* BL21 (DE3) RIL bacteria. They could be purified from the soluble fraction after bacterial lysis by affinity chromatography using Ni-NTA resin as described in Chapter 2 and also in Bell et al. (2001) and Canti et al. (2001). Once purified, the $Ca_V\beta$ subunits were stable for several weeks. Samples of purified $Ca_V\beta1b$, $Ca_V\beta2a$ and $Ca_V\beta3$ can be seen in Figure 3.2 *B* after separation by SDS PAGE and staining with coomassie blue. The purified $Ca_V\beta1$ and $\beta3$ subunits appear as single bands of the correct molecular weight after SDS PAGE whereas the $Ca_V\beta2a$ subunit preparation appears to contain several truncations or degradation products. The probable reason for this is the position of the $His_{(6)}$ tag as a C-terminal tag means that only full length proteins will be purified whereas with an N-terminal tag truncated products as well as full length proteins can be captured. In the case of $Ca_V\beta2a$, greater than 80% of the protein was full length and it was not considered necessary to move the position of the $His_{(6)}$ tag.

3.2.2 Surface Plasmon Resonance Spectroscopy

Surface plasmon resonance (SPR) spectroscopy relies on the phenomenon of surface plasmon resonance. The technique allows real time measurement of biological interactions and provides a means for quantifying kinetic and equilibrium constants, without the need for fluorescent or radioactive labels.

Surface plasmon resonance is an optical-electrical phenomenon which arises from the interaction of light with metallic surfaces. Under conditions of total internal reflectance (TIR), energy carried by photons of light is transferred to packets of electrons known as plasmons on the surface of the metal. At the same time, an evanescent electromagnetic wave propagates away from the interface (Figure 3.3 A). Surface plasmon resonance occurs when a thin conducting film is placed at the

Figure 3.3

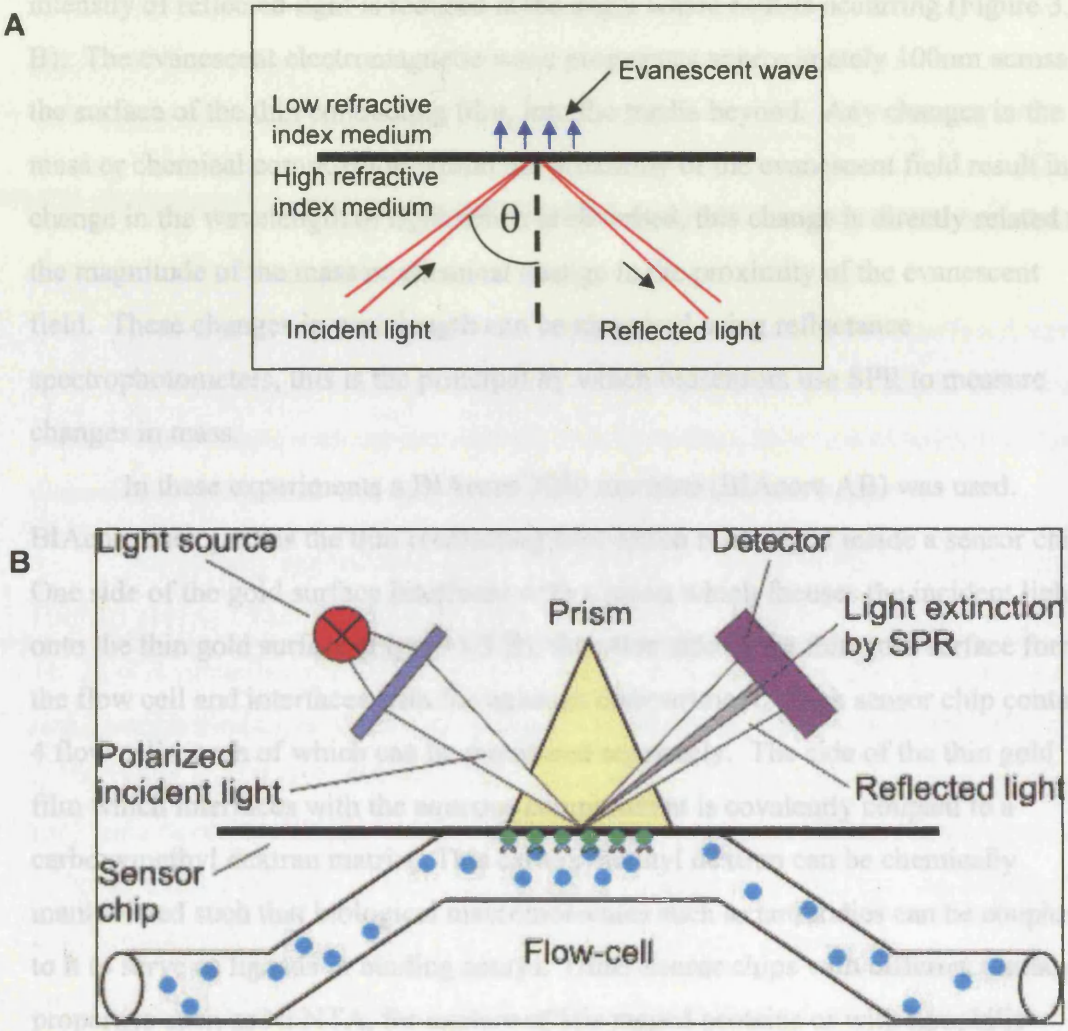

Figure 3.3 A. Propagation of an evanescent electromagnetic wave. At the boundary between high and low refractive index media and under conditions of total internal reflection (TIR) (TIR occurs above the critical angle θ (*theta*)) energy from incident light is transferred to packets of electrons known as plasmons and at the same time, an evanescent electromagnetic wave propagates away from the interface. **B.** Basic principle of the BIAcore system showing polarised incident light being focused onto the surface of a sensor chip. Analyte in the flow cell interacts with the chip surface, this causes a change in mass which changes the position of the light extinction by SPR. (Adapted from Hall, 2001).

interface between two optical media. At angles greater than the TIR angle, the surface plasmons in the thin conducting film couple with the light energy because their frequencies are the same. During this coupling, energy is absorbed and the intensity of reflected light is reduced at the angle where SPR is occurring (Figure 3.3 B). The evanescent electromagnetic wave propagates approximately 100nm across the surface of the thin conducting film, into the media beyond. Any changes in the mass or chemical composition within the proximity of the evanescent field result in a change in the wavelength of light which is absorbed, this change is directly related to the magnitude of the mass or chemical change in the proximity of the evanescent field. These changes in wavelength can be measured using reflectance spectrophotometers, this is the principal by which biosensors use SPR to measure changes in mass.

In these experiments a BIAcore 2000 machine (BIAcore AB) was used. BIAcore uses gold as the thin conducting film which is arranged inside a sensor chip. One side of the gold surface interfaces with a prism which focuses the incident light onto the thin gold surface (Figure 3.3 B), the other side of the thin gold surface forms the flow cell and interfaces with the aqueous compartment. Each sensor chip contains 4 flow cells, each of which can be monitored separately. The side of the thin gold film which interfaces with the aqueous compartment is covalently coupled to a carboxymethyl dextran matrix. This carboxymethyl dextran can be chemically manipulated such that biological macromolecules such as antibodies can be coupled to it to serve as ligands in binding assays. Other sensor chips with different surface properties such as Ni NTA, for capture of His tagged proteins or with lipophilic groups for incorporation of proteins into lipid bilayers are available but in these experiments the standard carboxymethyl dextran CM5 chip was used.

The CM5 sensor chips were prepared as described in Chapter 2. High affinity goat anti-GST antibodies purified from the sera of goats immunized with purified schistosomal GST were covalently coupled to the dextran matrix of all flow cells. The high affinity antibodies are polyclonal and can recognise more than one epitope on GST, thereby improving their capacity for recognizing GST fusion proteins, these antibodies were used to capture the GST fusion proteins. The use of antibodies has several advantages over direct cross-linking of ligand proteins to the surface of the chip. Firstly, the ligand can be removed by washing with glycine pH2.2 and replaced with fresh protein and secondly, the ligand protein is orientated such that the I-II

linker part of the fusion protein is furthest away from the dextran matrix and uniformly presented so binding to the analyte, which in this case is the $Ca_V\beta$ subunit, is not hindered.

Equimolar amounts of GST Ca_V I-II linker fusion proteins were loaded onto individual flow cells and as a control, an equimolar amount of GST alone was loaded onto a flow cell which could then be used as a reference to control for non-specific binding. 100 Response Units (RU) of GST and 150 RU of the GST I-II linker fusion proteins were loaded. 100 RU corresponds to 1ng/nL of protein (Van Der Merwe *et al.*, 2000) this corresponds to approximately 3.4 fmol of each protein.

Solutions of purified $Ca_V\beta$ subunits from 5nM to 200nM were perfused across all flow cells, each injection lasted 5 minutes and was followed by a 5 minute dissociation period. An example sensorgram showing ligand loading, injection of analyte followed by the dissociation phase followed by a regeneration step is shown in Figure 3.4.

Preliminary experiments showed that using a running buffer which contained 10mM HEPES pH7.4, 150mM sodium chloride and 0.005% TWEEN-20, injection of purified $Ca_V\beta$ 1b, 2a or 3 subunits over a flow cell containing just immobilised GST produced substantial non-specific binding (not shown). In a previous study by Geib et al. (2002), 1% glycerol, 0.1% Triton X-100 and 200mM sodium chloride were included in the running buffer, this may have been for a similar reason. Subsequent experiments showed that inclusion of 500mM sodium chloride in the running buffer virtually abolished the non-specific binding to GST without affecting the GST I-II linker / $Ca_V\beta$ subunit interaction.

Under these conditions, specific, concentration dependent binding of $Ca_V\beta$1b, $Ca_V\beta$2a and $Ca_V\beta$3 subunits was observed to the GST I-II linkers of Ca_V1.3, Ca_V2.1 and Ca_V2.2 but negligible concentration-dependent binding was seen in the flow cell containing GST only. The signal from the GST only negative control flow cell was subtracted from the data obtained from the $Ca_V\beta$ subunits binding to the GST Ca_V I-II linker fusion proteins. The resulting sensorgrams were aligned using BIAevaluation 3.0 software (BIAcore AB) and are shown in Figures 3.5, 3.6 and 3.7. From the data in these figures, single exponential fits were made to the dissociation phases of the sensorgrams to establish the off rates (k_{off}). The dissociation rates (k_{off}) for GST Ca_V 1.3 I-II linker, GST Ca_V2.1 I-II linker and GST Ca_V2.2 I-II linker binding to 100nM concentrations of $Ca_V\beta$1b, $Ca_V\beta$2a or $Ca_V\beta$3 are shown in table 3.1. There is little variation in the k_{off} for within each Ca_V I-II linker / $Ca_V\beta$ subunit

Figure 3.4

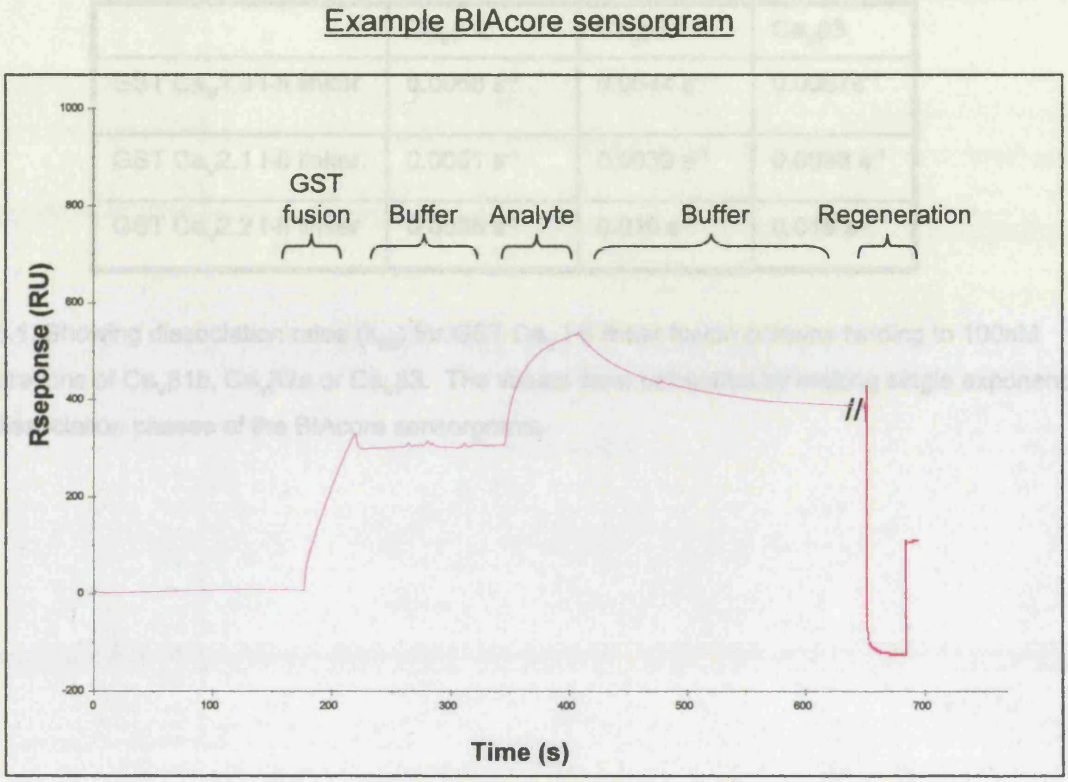

Figure 3.4. Example BIAcore sensorgram. GST fusion proteins are captured via an anti GST antibody, buffer is perfused until the baseline is stable before the required concentration of analyte is injected. Buffer is continually perfused and the dissociation phase is measured for as long as is required. Finally, any remaining ligand/analyte complex is removed with a pulse of 10mM Glycine pH 2.2 and the next cycle can begin.

Table 3.1

	$Ca_V\beta 1b$	$Ca_V\beta 2a$	$Ca_V\beta 3$
GST $Ca_V1.3$ I-II linker	0.0068 s^{-1}	0.0044 s^{-1}	0.0067s^{-1}
GST $Ca_V2.1$ I-II linker	0.0051 s^{-1}	0.0039 s^{-1}	0.0088 s^{-1}
GST $Ca_V2.2$ I-II linker	0.0055 s^{-1}	0.010 s^{-1}	0.018 s^{-1}

Table 3.1. Showing dissociation rates (k_{off}) for GST Ca_V I-II linker fusion proteins binding to 100nM concentrations of $Ca_V\beta 1b$, $Ca_V\beta 2a$ or $Ca_V\beta 3$. The values were calculated by making single exponential fits to the dissociation phases of the BIAcore sensorgrams.

Figure 3.5

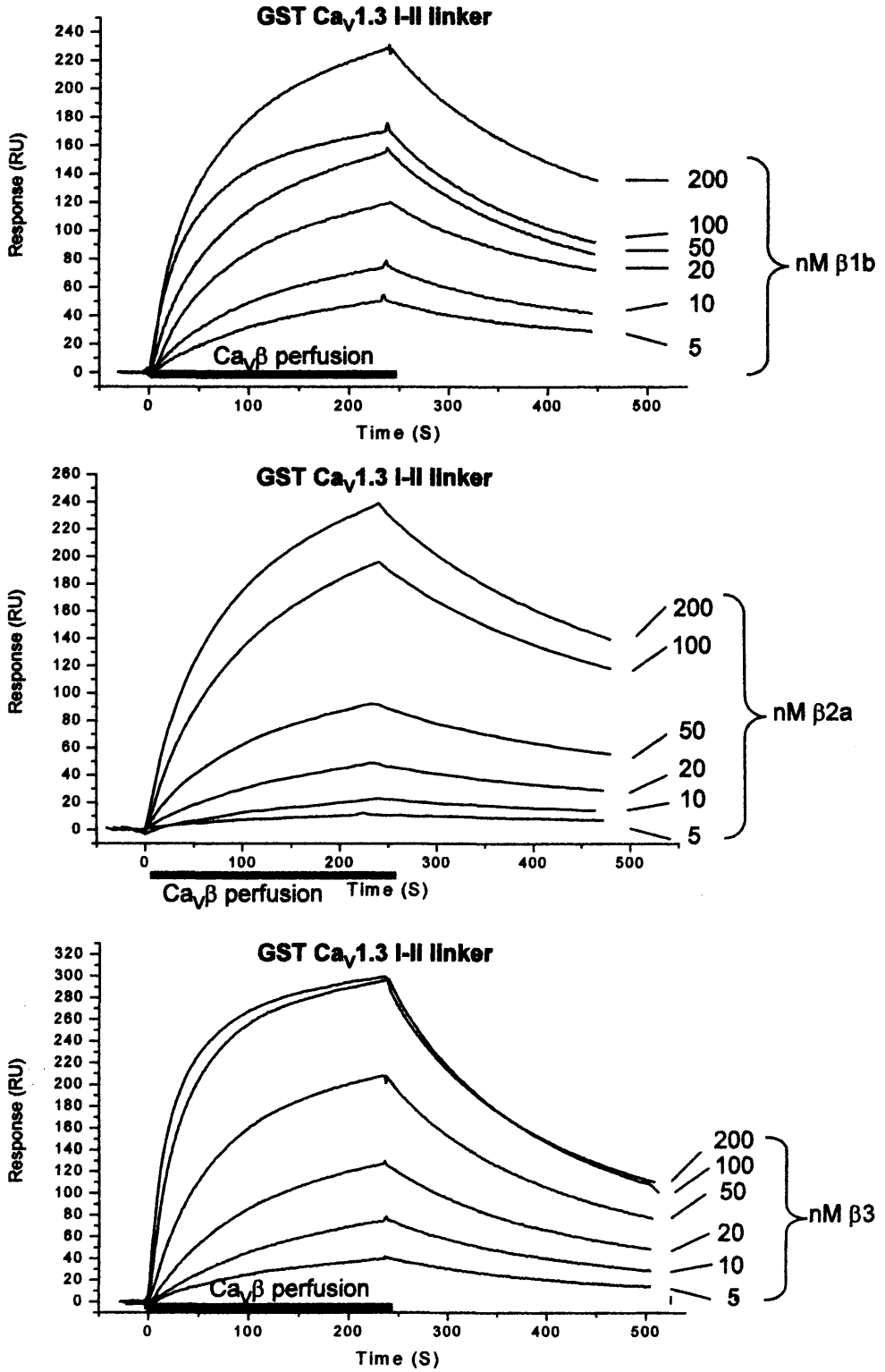

Figure 3.5. Representative BIAcore sensorgrams showing interactions between GST $Ca_V1.3$ I-II linker fusion proteins and $Ca_V\beta1b$ (top panel), $Ca_V\beta2a$ (middle panel) and $Ca_V\beta3$ (bottom panel). Concentrations of 5nM – 200nM (as indicated) were applied.

Figure 3.6

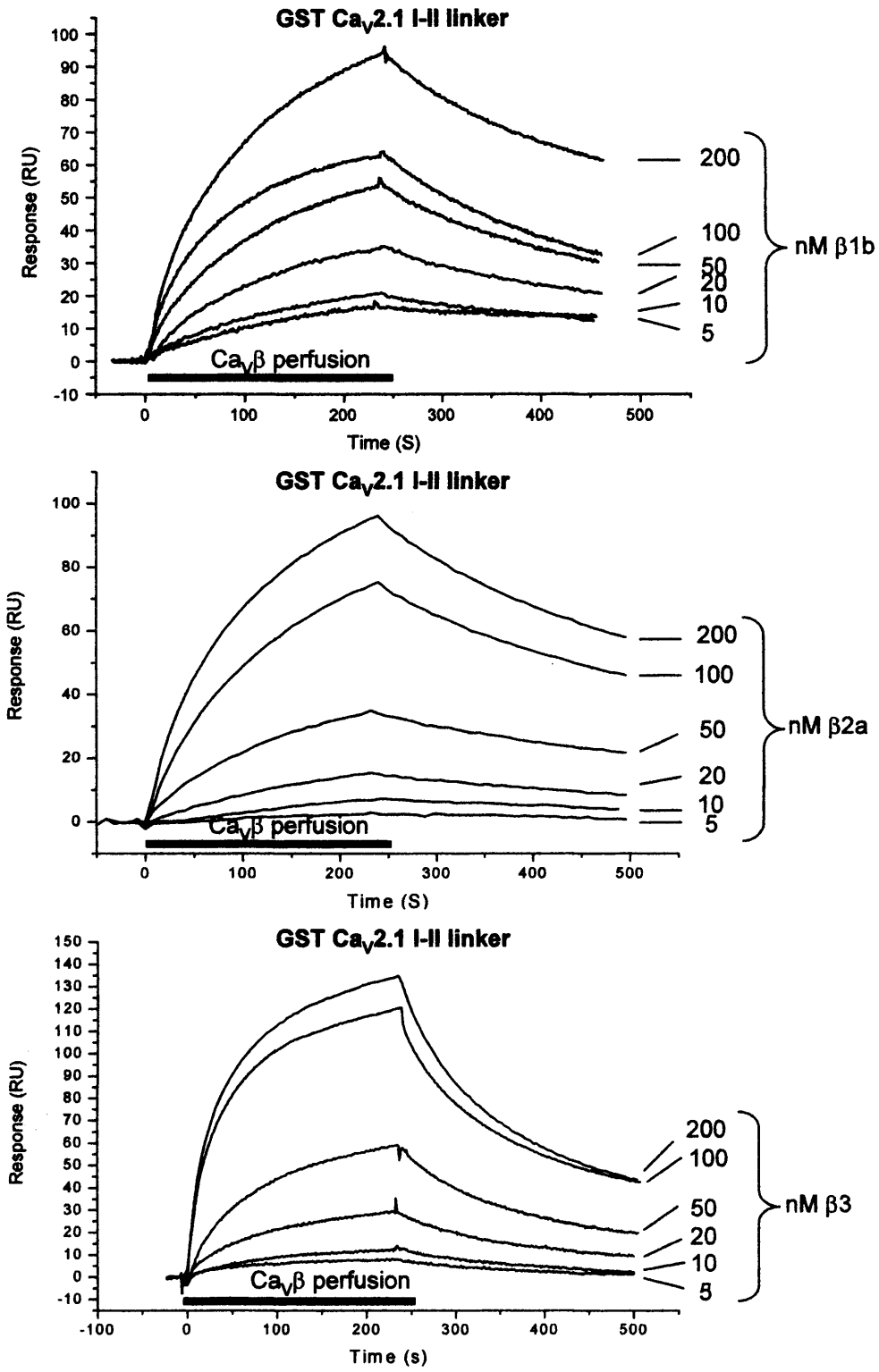

Figure 3.6. Representative BIAcore sensorgrams showing interactions between GST $Ca_V2.1$ I-II linker fusion proteins and $Ca_V\beta1b$ (top panel), $Ca_V\beta2a$ (middle panel) and $Ca_V\beta3$ (bottom panel). Concentrations of 5nM – 200nM (as indicated) were applied.

Figure 3.7

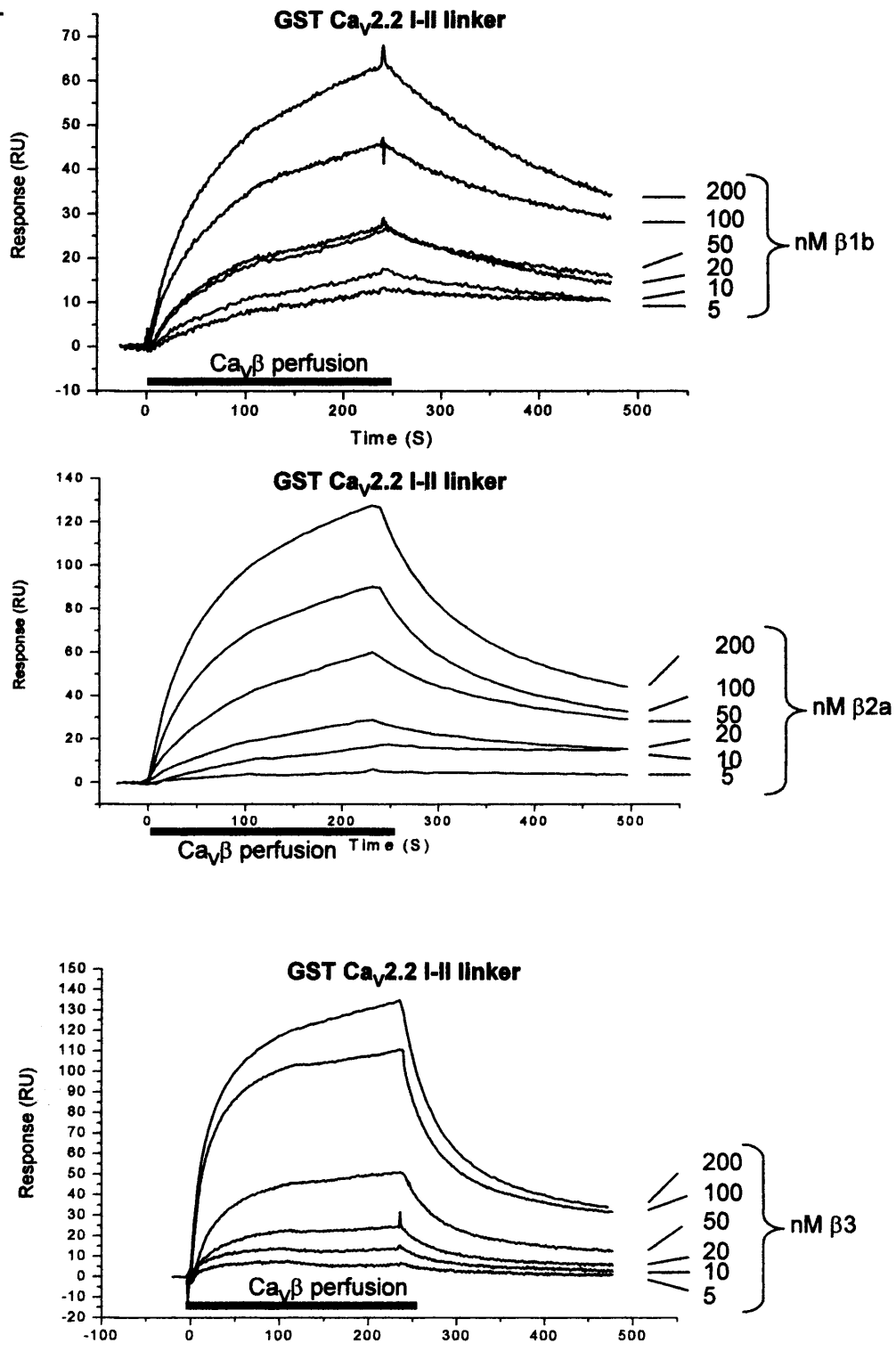

Figure 3.7. Representative BIAcore sensorgrams showing interactions between GST $Ca_V2.2$ I-II linker fusion proteins and $Ca_V\beta1b$ (top panel), $Ca_V\beta2a$ (middle panel) and $Ca_V\beta3$ (bottom panel). Concentrations of 5nM – 200nM (as indicated) were applied.

Table 3.2

	$Ca_V\beta 1b$	$Ca_V\beta 2a$	$Ca_V\beta 3$
GST Ca_V 1.3 I-II linker	13.2 ± 3.6 nM	12.1 ± 3.7 nM	12.7 ± 2.7 nM
GST Ca_V 2.1 I-II linker	13.7 ± 5.4 nM	18.0 ± 3.6 nM	11.9 ± 4.3 nM
GST Ca_V 2.2 I-II linker	17.6 ± 2.0 nM	20.0 ± 2.9 nM	19.0 ± 2.8 nM

Table 3.2. Showing dissociation constants (K_D) calculated from the data shown in figures 3.5, 3.6 and 3.7. Fits were made to each data set using BIAevaluation 3.0 software using a model of 1:1 interaction. Data are mean ± SEM of 4 experiments. All data shown were obtained using the same protein preparations.

Figure 3.8

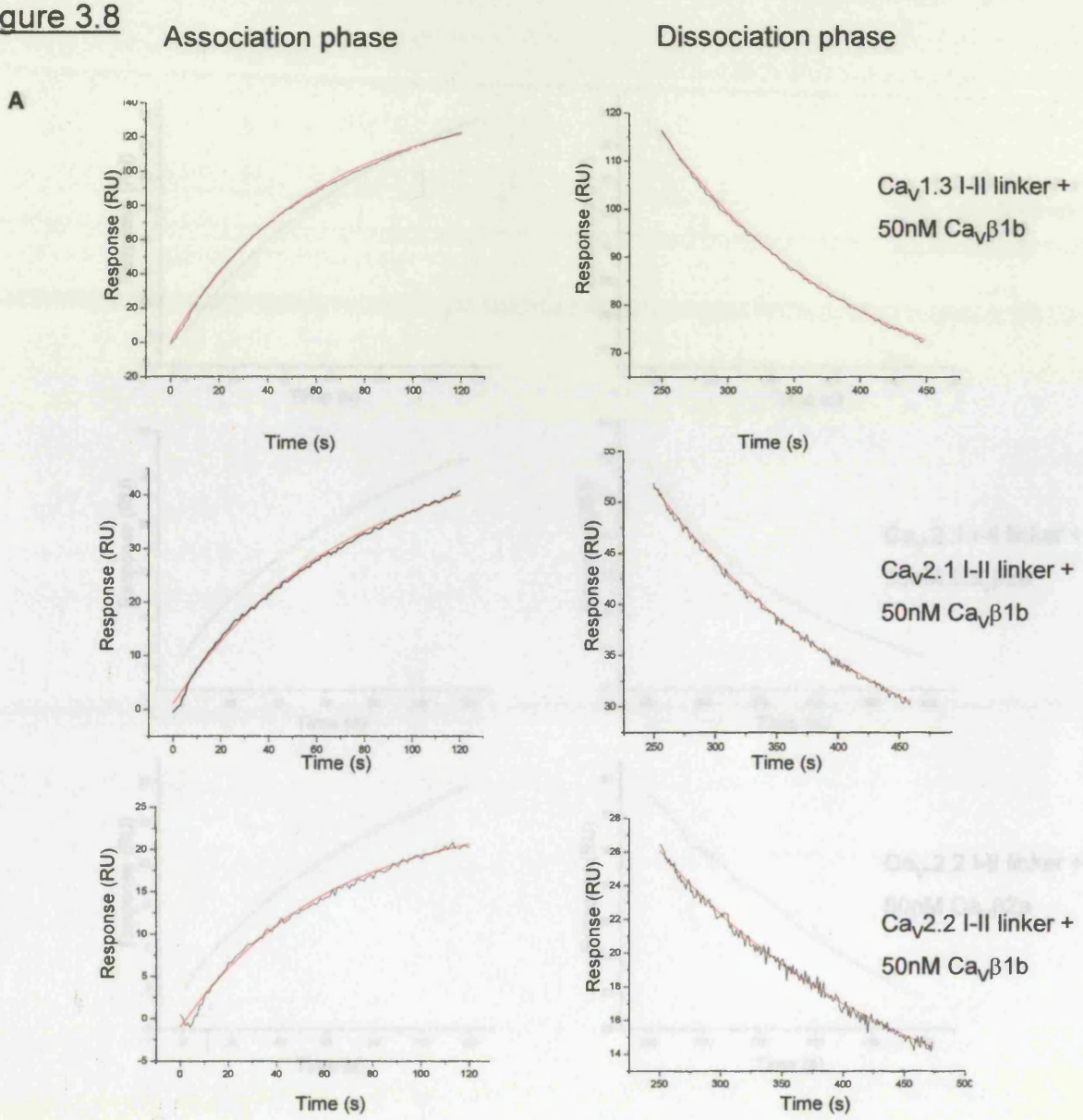

	Ca$_V$β1b concentration (nM)	$k_{on(obs)}$ 1/s	k_{off} 1/s	k_{on} $M^{-1}s^{-1}$	K_D (nM)
GST Ca$_V$1.3 I-II linker	50	0.011	0.006	2×10^5	30
GST Ca$_V$2.1 I-II linker	50	0.013	0.0049	1.62×10^5	30
GST Ca$_V$2.2 I-II linker	50	0.012	0.0046	1.48×10^5	31

B

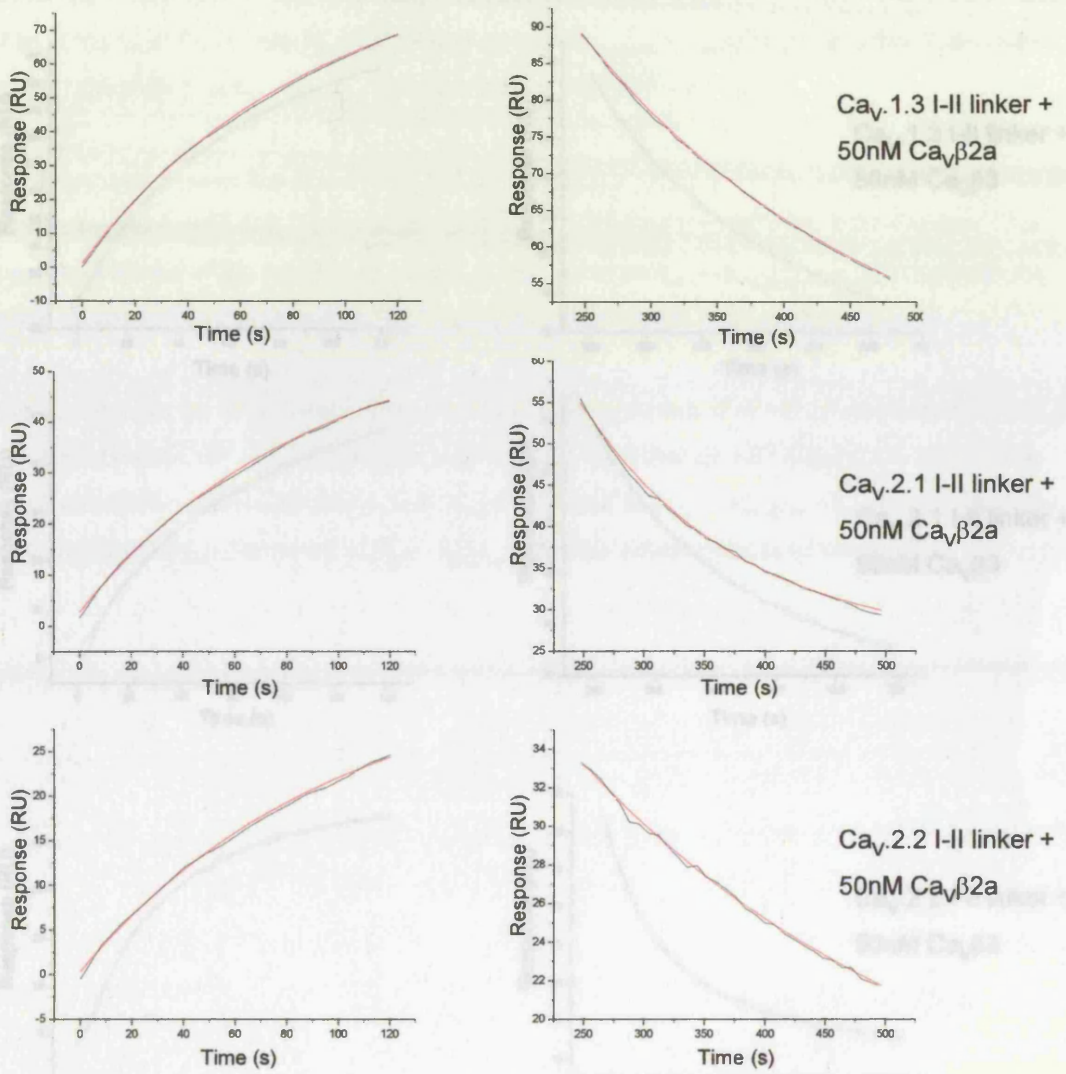

	$Ca_V\beta$2a concentration (nM)	$k_{on(obs)}$ 1/s	k_{off} 1/s	k_{on} $M^{-1}s^{-1}$	K_D (nM)
GST Ca_V1.3 I-II linker	50	0.011	0.0042	1.36×10^5	30
GST Ca_V2.1 I-II linker	50	0.01	0.0031	1.38×10^5	30
GST Ca_V2.2 I-II linker	50	0.011	0.0077	6.6×10^4	116

c

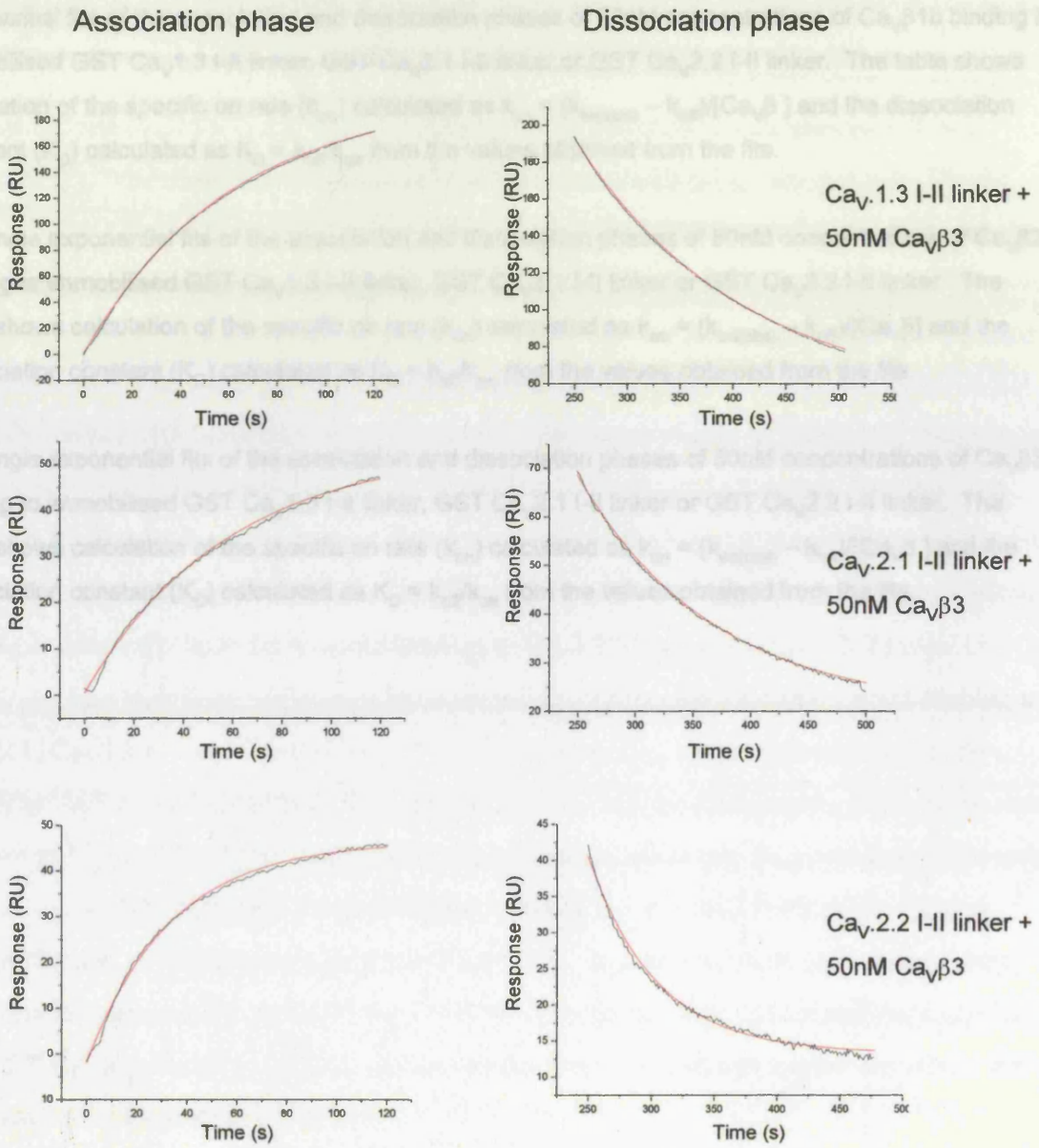

	$Ca_V\beta3$ concentration (nM)	$k_{on(obs)}$ 1/s	k_{off} 1/s	$k_{on} M^{-1}s^{-1}$	K_D (nM)
GST Ca_V1.3 I-II linker	50	0.016	0.0059	2. 02 x 10^5	29
GST Ca_V2.1 I-II linker	50	0.017	0.0085	1.7 x 10^5	50
GST Ca_V2.2 I-II linker	50	0.03	0.018	2.4 x 10^5	75

Figure 3.8. A. Examples of single exponential fits made to BIAcore sensorgrams. A. Single exponential fits of the association and dissociation phases of 50nM concentrations of $Ca_V\beta 1b$ binding to immobilised GST $Ca_V1.3$ I-II linker, GST $Ca_V2.1$ I-II linker or GST $Ca_V2.2$ I-II linker. The table shows calculation of the specific on rate (k_{on}) calculated as $k_{on} = (k_{on(obs)} - k_{off})/[Ca_V\beta\ ]$ and the dissociation constant (K_D) calculated as $K_D = k_{off}/k_{on}$ from the values obtained from the fits.

B. Single exponential fits of the association and dissociation phases of 50nM concentrations of $Ca_V\beta 2a$ binding to immobilised GST $Ca_V1.3$ I-II linker, GST $Ca_V2.1$ I-II linker or GST $Ca_V2.2$ I-II linker. The table shows calculation of the specific on rate (k_{on}) calculated as $k_{on} = (k_{on(obs)} - k_{off})/[Ca_V\beta]$ and the dissociation constant (K_D) calculated as $K_D = k_{off}/k_{on}$ from the values obtained from the fits.

C. Single exponential fits of the association and dissociation phases of 50nM concentrations of $Ca_V\beta 3$ binding to immobilised GST $Ca_V1.3$ I-II linker, GST $Ca_V2.1$ I-II linker or GST $Ca_V2.2$ I-II linker. The table shows calculation of the specific on rate (k_{on}) calculated as $k_{on} = (k_{on(obs)} - k_{off})/[Ca_V\beta\ ]$ and the dissociation constant (K_D) calculated as $K_D = k_{off}/k_{on}$ from the values obtained from the fits.

combination across the range of $Ca_V\beta$ subunit concentrations tested and this is to be expected as the k_{off} should be independent of $Ca_V\beta$ subunit concentration. There was some variation however between the different combinations with Ca_V 2.2 I-II linker / $Ca_V\beta3$ showing the fastest off rate (0.018 s^{-1}) and $Ca_V2.1$ I-II linker / $Ca_V\beta2a$ showing the slowest off rate (0.0039 s^{-1}). The dissociation constants (K_D) were calculated using two methods. Firstly, using the data from Figure 3.5, fits were made as described in Chapter 2 using BIAevaluation 3.0 software. In addition to models of 1:1 stoichiometry, other models were tested however single exponential fits were most appropriate for this data as determined by the chi squared statistical test. The mean K_D values were found to be between 11.9 ± 4.3 nM and 20 ± 2.9 nM, the values calculated for each subunit combination are shown in Table 3.2. Analysis of variance (ANOVA) followed by Tukey's post hoc test was used to analyse the data from Table 3.2. There was no significant difference between the K_D values calculated for $Ca_V\beta1b$ binding to $Ca_V2.1$, $Ca_V2.2$ or $Ca_V1.3$ I-II linker (P = 0.802), no significant difference between the K_D values calculated for $Ca_V\beta2a$ binding to $Ca_V2.1$, $Ca_V2.2$ or $Ca_V1.3$ I-II linker (P = 0.247) and no significant difference between the K_D values calculated for $Ca_V\beta3$ binding to $Ca_V2.1$, $Ca_V2.2$ or $Ca_V1.3$ I-II linker (P = 0.460). Secondly, single exponential fits were made to the first 120 seconds of the association phase and the dissociation phase of the data shown in Figure 3.5. From these fits, the specific association rate (k_{on}) was calculated as $k_{on} = (k_{on(obs)} - k_{off})/[Ca_V\beta]$, and the dissociation constant K_D was calculated as $K_D = k_{off}/k_{on}$. These fits and calculations are shown in Figure 3.8. In addition, these experiments were performed in reverse by immobilising $Ca_V\beta$ subunits on the chip surface and using the GST Ca_V I-II linker proteins as analyte, similar results were obtained and similar K_D values were obtained after evaluation of the data.

These results agree with those of other studies which have shown that the I-II linker of HVA calcium channels binding with high affinity to the $Ca_V\beta$ subunit (De Waard *et al.*, 1995; Bell *et al.*, 2001; Canti *et al.*, 2001; Leroy *et al.*, 2005; Geib *et al.*, 2002; Pragnell *et al.*, 1994; Witcher *et al.*, 1995). There is little variation in the dissociation constants determined here between the combinations of subunits tested although the $Ca_V1.3$ I-II linker may bind $Ca_V\beta$ subunits with a slightly higher affinity than the Ca_V2 class of channels.

3.2.3 Gβγ subunits of heterotrimeric G proteins interact with the I-II linker of $Ca_V2.2$ but not $Ca_V1.3$

Figure 3.9

A

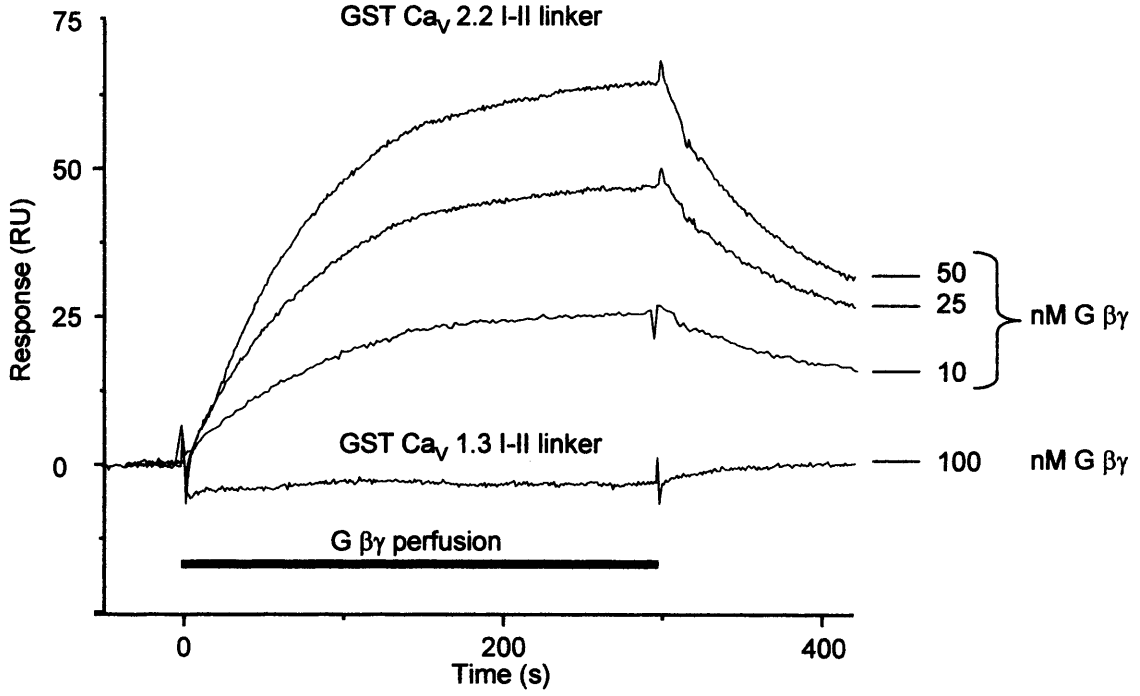

B

	Gβγ concentration (nM)	$k_{on(obs)}$ 1/s	k_{off} 1/s	k_{on} $M^{-1}s^{-1}$	K_D (nM)
GST Ca_V2.2 I-II linker	10	0.0121	0.0104	1.7×10^5	61.1

Figure 3.9.A. Representative BIAcore sensorgrams showing interaction between GST Ca_V2.2 I-II linker and purified G protein βγ subunits. Concentrations of 10nM – 50nM (as indicated) were applied. Also shown is the lack of interaction between GST Ca_V1.3 I-II linker and G protein βγ subunits, no binding was observed even with 100nM Gβγ.

B. Single exponential fits of the association and dissociation phases of 10nM concentration of Gβγ binding to immobilised GST Ca_V2.2 I-II linker. The table shows calculation of the specific on-rate (k_{on}) and the dissociation constant (K_D) from the values obtained from the fits.

In addition to interacting with the $Ca_V\beta$ subunit, the I-II linker of the Ca_V2 class of calcium channels is involved in interaction with the βγ subunits of heterotrimeric G proteins. These interactions have been demonstrated previously using overlay assays (De Waard *et al.*, 1997; Zamponi *et al.*, 1997; Herlitz *et al.*, 1997). The interaction of G protein βγ subunits with the GST I-II linker proteins was investigated using surface plasmon resonance. GST I-II linker fusions of $Ca_V1.3$ and $Ca_V2.2$ and GST alone were prepared as described previously and immobilised via a GST antibody onto a CM5 sensor chip. As before, 150 RU of GST I-

These interactions have been demonstrated previously using overlay assays (De Waard *et al.*, 1997; Zamponi *et al.*, 1997; Herlitz *et al.*, 1997). The interaction of G protein βγ subunits with the GST I-II linker proteins was investigated using surface plasmon resonance. GST I-II linker fusions of $Ca_V1.3$ and $Ca_V2.2$ and GST alone were prepared as described previously and immobilised via a GST antibody onto a CM5 sensor chip. As before, 150 RU of GST I-
II linkers and the corresponding molar equivalent of GST were applied. Prior to injection of βγ subunits, the integrity of the I-II linker fusion proteins was tested by applying a low concentration of purified $Ca_V\beta1b$. $Ca_V\beta1b$ specifically bound to both GST I-II linker fusions (not shown).

G protein βγ subunits purified from bovine brain (Exner *et al.*, 1999) were a generous gift from Professor Bernd Nürnberg (Institut für Pharmakologie, Freie Universität Berlin, Thielallee 69-73, D-14195 Berlin (Dahlem), Germany). The G protein βγ subunits were preparations containing mixed isoforms of β and γ subunits extracted from membranes and stored in detergents. Solutions of purified G βγ subunits from 10nM to 100nM were perfused across all flow cells, each injection lasted 5 minutes and was followed by a 5 minute dissociation period. Specific binding was observed to the GST $Ca_V2.2$ I-II linker whilst minimal binding was observed to the GST only or to the GST $Ca_V1.3$ I-II linker. The signal from the GST only flow cell was subtracted and the resulting sensorgrams were aligned using BIAevaluation 3.0 software (Figure 3.9 *A*). Single exponential fits were made to the association and dissociation phases of the sensorgram obtained from the 10nM injection of Gβγ. From this data, the dissociation constant for Gβγ binding to the GST $Ca_V2.2$ I-II linker was 61.1nM (Figure 3.9 *B*).

3.3 Discussion

High voltage activated calcium channels are associated with a regulatory beta subunit. The intracellular loop between domains I and II contains the AID motif to which $Ca_V\beta$ subunits bind (Pragnell *et al.*, 1994). Binding of $Ca_V\beta$ subunits to the AID motif enhances functional expression of the channels as well as hyperpolarizing the voltage dependence of activation and hyperpolarizing the voltage dependence of steady state inactivation.

Surface plasmon resonance binding assays using GST fusion proteins of the entire I-II linker of Ca_V 1.3, Ca_V2.1 and Ca_V2.2 and purified $Ca_V\beta$1b, $Ca_V\beta$2a or $Ca_V\beta$3 subunits showed the dissociation constant for these interactions to be between 12.1nM and 20nM. These results are in agreement with other studies which have also determined the dissociation constants for AID / $Ca_V\beta$ subunit interactions to be in the low nanomolar range (De Waard *et al.*, 1995; Scott *et al.*, 1996; Geib *et al.*, 2002). De Waard (1995) also found that there was considerable variation between the dissociation constants determined for the four different $Ca_V\beta$ subunits and that $Ca_V\beta$2a and $Ca_V\beta$4 bound with two different affinities suggesting two different binding sites. The data from surface plasmon resonance binding assays described here does not show a substantial difference between the affinities of the different $Ca_V\beta$ subunits for the GST Ca_V I-II linker fusions although Ca_V1.3 I-II linker may bind with a slightly greater affinity than the members of the Ca_V2 class of channels tested here. Although $Ca_V\beta$4 was not tested, the data from the other three $Ca_V\beta$ subunits fitted well to a model of 1:1 interaction. If in the case of $Ca_V\beta$2a or $Ca_V\beta$4, a second beta subunit can bind, the affinity of this interaction may be so low that it cannot be measured by this method.

It seems clear from the data here and from other studies (De Waard *et al.*, 1995; Scott *et al.*, 1996) that all $Ca_V\beta$ subunits are capable of binding to the AID motif of all HVA $Ca_V\alpha$1 subunits. The differences in the non-conserved amino acid residues between the different channel types does not seem to have a substantial effect upon $Ca_V\beta$ binding although one study has implicated the non-conserved residues in the AID motif of Ca_V2.3 as being determinants of voltage dependent inactivation (Berrou *et al.*, 2001). In native tissue the $Ca_V\alpha$1 / $Ca_V\beta$ subunit combinations display a tissue specific distribution with for example, Ca_V1.1 and $Ca_V\beta$1a are predominantly

expressed in skeletal muscle and $Ca_V2.1$ and $Ca_V\beta4$ are predominantly expressed in Purkinje cells of the cerebellum. Interaction of $Ca_V\beta$ with AID promotes trafficking of the $Ca_V\alpha1$ subunit to the membrane as $Ca_V\alpha1$ subunits which cannot interact with $Ca_V\beta$ or $Ca_V\alpha1$ coexpressed with $Ca_V\beta$ subunits which lack the GK domain are not trafficked to the plasma membrane (Leroy *et al.*, 2005; Cohen *et al.*, 2005). As well as interaction with AID, other $Ca_V\alpha1$ / $Ca_V\beta$ subunit interactions have been reported, these include additional $Ca_V\beta$ binding sites within the N and C termini of certain $Ca_V\alpha1$ subunits and elsewhere within the I-II linker (Walker *et al.*, 1999; Stephens *et al.*, 2000; Maltez *et al.*, 2005). The $Ca_V\beta4$ subunit specifically interacts with the C-terminus of $Ca_V2.1$ and regulates the kinetics of voltage dependent inactivation (Walker *et al.*, 1999) and the SH3 domain of $Ca_V\beta2a$ was shown to interact with the I-II linker of $Ca_V2.1$ and increase current amplitude (Maltez *et al.*, 2005). In addition, the $Ca_V\beta2a$ subunit is unique in that it can be palmitoylated at its N-terminus, this has the effect of reducing voltage dependent inactivation (Restituto *et al.*, 2000). As each $Ca_V\beta$ subunit is able to impart specific regulatory properties to particular $Ca_V\alpha1$ subunits (Dolphin, 2003), these secondary interactions may represent the mechanism by which different $Ca_V\beta$ subunits finely adjust the biophysical properties of the $Ca_V\alpha1$.

Surface plasmon resonance binding assays using GST fusion proteins of the entire I-II linker of Ca_V 1.3, $Ca_V2.2$ and G protein $\beta\gamma$ subunits purified from bovine brain showed that the $\beta\gamma$ subunits specifically bound to the $Ca_V2.2$ I-II linker. The K_D for this interaction was calculated to be 62.2 nM. These findings are in agreement with those of previous studies (De waard *et al.*, 1997; Zamponi *et al.*, 1997) which showed that $G\beta\gamma$ binds to the I-II linker of the Ca_V2 class of channels. The lack of interaction of G protein $\beta\gamma$ subunits with the I-II linker of $Ca_V1.3$ is consistent with the findings of Bell et al. (2001). In these studies, the biophysical properties of $Ca_V1.3$ were characterised and this channel was found to be resistant to modulation by G proteins when compared to $Ca_V2.2$.

Although direct binding of G protein $\beta\gamma$ subunits to the I-II linker is an important step in G protein modulation, other regions of the channel have also been shown to be essential determinants. The C-terminus of the Ca_V2 class of channels was shown to bind G protein $\beta\gamma$ subunits via a site in their C-termini (Qin *et al.*,

1997), when this site was removed, G protein modulation was prevented. Subsequent studies revealed an 11 amino acid motif in the N-terminus of $Ca_V2.2$ which is conserved in both $Ca_V2.1$ and 2.3 (Page *et al.*, 1998). Transfer of the N-terminus of $Ca_V2.2$ containing the motif Y K Q S I A Q R A R T to $Ca_V1.2$ which does not show G protein modulation enabled $Ca_V1.2$ to be modulated (Canti *et al.*, 1999), furthermore, mutations within this motif abolished G protein modulation of $Ca_V2.2$.

The AID motif remains an important feature of VDCC modulation, in the case of the Ca_V2 class of channels, it has been shown in this work and by others to bind to both $Ca_V\beta$ and to G protein $\beta\gamma$ subunits. However, whether both $Ca_V\beta$ and G $\beta\gamma$ can bind at the same time remains controversial. As many effects of G protein $\beta\gamma$ binding seem to oppose the effects of $Ca_V\beta$, it was believed that $\beta\gamma$ dimers could displace $Ca_V\beta$ from the I-II linker. However, Canti et al. (1999) showed that a $Ca_V2.2$ channel in which the I-II linker was replaced with that of $Ca_V1.2$ was still substantially modulated by G proteins. Displacement of G $\beta\gamma$ was demonstrated using fluorescence resonance energy transfer (FRET) by Sandoz et al. (2004), the authors suggested that displacement of $Ca_V\beta$ from the I-II linker is a key step in G protein regulation of $Ca_V2.1$ calcium channels. This contradicts findings of Hummer et al. (2003) who found, again using FRET that $Ca_V\beta$ and G protein β can bind to the I-II linker at the same time. This study also reported interaction of G protein β subunit with the C terminus of $Ca_V2.2$ and a possible role for the C-terminus in G protein modulation. The recent structural studies showing AID peptide embedded in the AID binding pocket of $Ca_V\beta$ suggested that either G protein $\beta\gamma$ subunits would be unable to bind to AID in addition to $Ca_V\beta$ or that they would be unable to displace $Ca_V\beta$ (Van Petegem *et al.*, 2004; Opatowsky *et al.*, 2004). This casts doubt on the possibility that G protein $\beta\gamma$ binds to AID at all under physiological conditions where the majority of HVA $\alpha1$ subunits will be associated with $Ca_V\beta$.

Attempts were made here to take advantage of the SPR binding assay developed to measure the interaction of $Ca_V\beta$ and G protein $\beta\gamma$ subunits for AID and perform experiments which might show if G protein $\beta\gamma$ can bind to the I-II linker in addition to $Ca_V\beta$ or if they will displace $Ca_V\beta$ from its binding site. The experiments were performed using the $Ca_V2.2$ I-II linker, $Ca_V\beta1b$ and G protein $\beta\gamma$ subunits all prepared as described previously. Unfortunately, the outcome of these experiments

was impossible to interpret. Although it was possible to demonstrate binding of $Ca_V\beta$ and G $\beta\gamma$ subunits individually, if $Ca_V\beta 1b$ was first bound to the immobilised I-II linker, the outcome of subsequent applications of G protein $\beta\gamma$ subunits could not be measured as the G protein $\beta\gamma$ association phase coincided with the $Ca_V\beta 1b$ dissociation. It was impossible to distinguish between these two events and no further experiments were performed. An alternative strategy would have been to include one component in the running buffer thus holding it at a constant concentration, subsequent injections of the second component could then be made, this however would require preparation of large quantities of either $Ca_V\beta$ or G $\beta\gamma$. Mathematical or physical subtraction of the dissociation curve for one component from the data could also be performed.

It is clear that the mechanism by which the Ca_V2 class of channels interacts with G protein $\beta\gamma$ subunits is highly complex. Recent work revealed interactions between the $Ca_V2.2$ N-terminus, the I-II linker and G $\beta\gamma$ (Agler *et al.*, 2005) and appears to bring together work regarding the role of the N-terminus and the I-II linker. A model is proposed in which the N-terminus acts as an initiatory G protein $\beta\gamma$ binding site and this N-terminus / G protein $\beta\gamma$ complex interacts with the I-II linker to inhibit the channel.

Further work is clearly necessary to understand fully the interactions between the channel domains, accessory subunits and intracellular signalling molecules. Future experiments should perhaps focus on the nature of the interaction between the N-terminus and the I-II linker.

Chapter 4:

The effects of specific mutations within the I-II linker on $Ca_V\beta$ subunit binding and channel trafficking

4.1 Introduction

The $Ca_V\beta$ subunit is responsible for regulation of HVA calcium channels in several ways. $Ca_V\beta$ subunit binding enhances expression of functional channels, modulates their biophysical properties and can promote the voltage dependence of modulation of $Ca_v2.2$ channels by $G\beta\gamma$ dimers (Dolphin, 2003). Studies which originally identified the highly conserved AID motif in the I-II linker of HVA calcium channels to be the $Ca_V\beta$ binding site also identified specific residues which were critical for binding (Pragnell *et al.*, 1994; Witcher et al 1995; De Waard *et al.*, 1995). An alignment of the AID motif from L-type and non L-type HVA calcium channels is shown in figure 4.1. Work by De Waard et al. (1995) showed that a tryptophan to alanine mutation abolished $Ca_V\beta1b$ subunit binding to GST fusion proteins containing the $Ca_V2.1$ AID motif, mutation of isoleucine to alanine also disrupted binding but to a lesser extent. Subsequent studies have shown the tyrosine residue in AID to also be essential for $Ca_V\beta$ binding. Mutation of tyrosine to serine disrupted binding to $Ca_V\beta1b$ and caused a depolarising shift in the voltage dependence of activation and altered the kinetics of inactivation of Ca_V 2.1/$\beta1b$ currents in *Xenopus* oocytes (Pragnell *et al.*, 1994; Witcher et al 1995).

L type	QQLEEDL-GY--WITQAE
Non L-type	QQIERELNGY--WI-KAE

Figure 4.1 Alignment of L type and non L type AID motifs of HVA calcium channels Conserved residues are shown in red, non conserved in black.

These findings would seem to be supported by recent structural studies on $Ca_V\beta$ subunits in complex with AID peptide which showed the aromatic rings of the tryptophan and tyrosine residues to be stacked together forming a hairpin in the AID binding pocket. Figure 4.2 shows a representation of $Ca_V1.1$ AID in complex with $Ca_V\beta3$, the conserved tryptophan and tyrosine residues are indicated. These two residues contribute very significantly to the network of direct and indirect hydrogen bonds and Van der Waals interactions which are formed between AID and $Ca_V\beta$. (Chen *et al.*, 2004; Opatowsky *et al.*, 2004; Van Petegem *et al.*, 2004).

Several studies have disputed the functional importance of the tyrosine residue, Berrou *et al.* (2002) found that although no direct binding of [^{35}S] labelled Cavβ3 subunit to a GST Cav2.3 AID containing the Y to S mutation could be detected, Ca_v2.3 Y383S was still in part modulated by the Ca_vβ3 subunit when co-expressed in *Xenopus* oocytes. Berrou *et al.* (2004) subsequently found that both conserved and nonconserved mutations in Y383 of Ca_v2.3 had little effect on Ca_vβ modulation of whole cell currents in *Xenopus* oocytes but the same mutations in an AID peptide greatly reduced [^{35}S] labelled Cavβ3 binding. In addition, Neuhuber *et al.* (1998) found that whilst Y366S mutation in Cav1.1 prevented co-localization of Cav1.1 with Cavβ1a in the ER of transfected tsA 201 cells, expression of Cav1.1 currents was not affected.

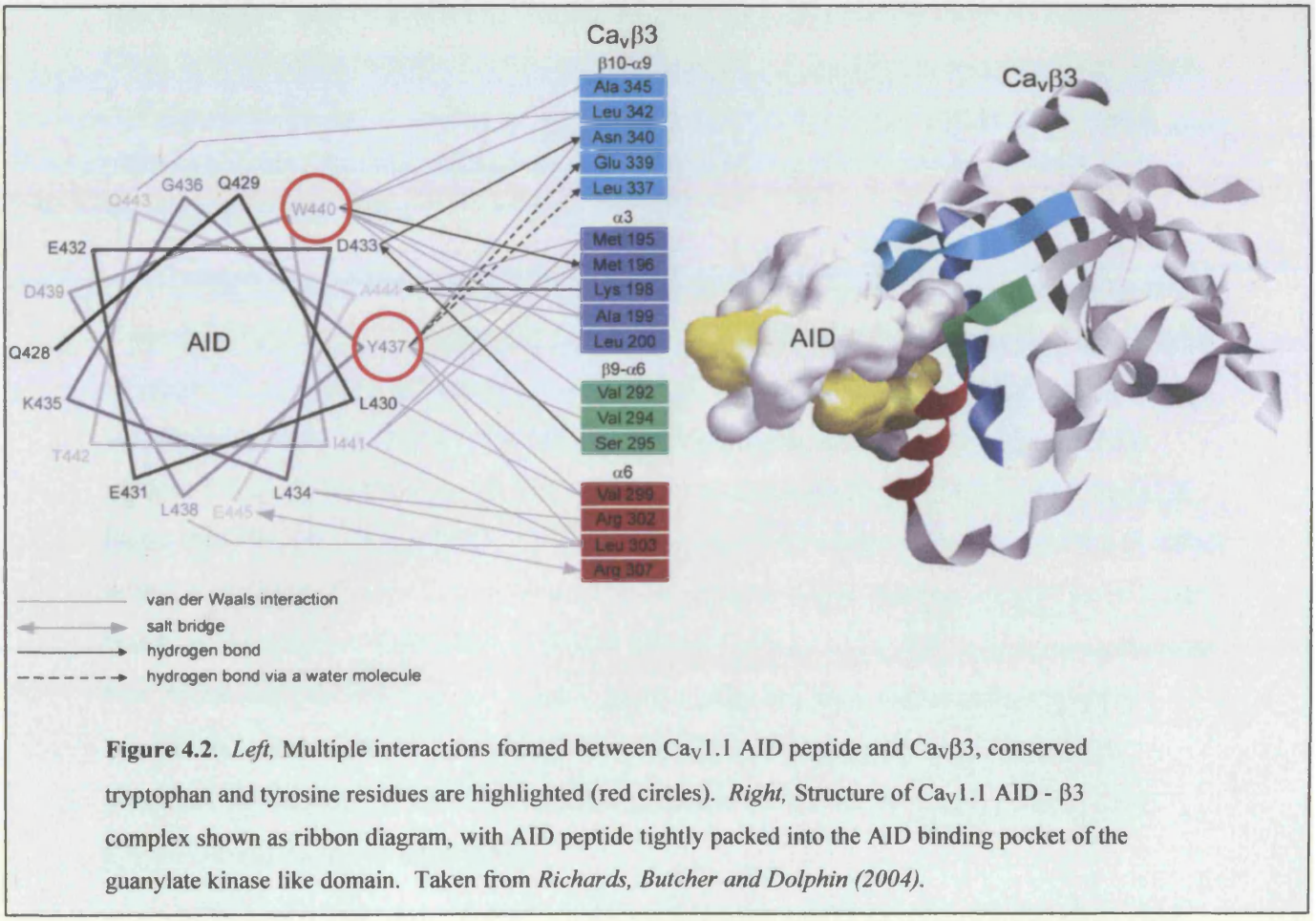

Figure 4.2. *Left,* Multiple interactions formed between Ca_v1.1 AID peptide and Ca_vβ3, conserved tryptophan and tyrosine residues are highlighted (red circles). *Right,* Structure of Ca_v1.1 AID - β3 complex shown as ribbon diagram, with AID peptide tightly packed into the AID binding pocket of the guanylate kinase like domain. Taken from *Richards, Butcher and Dolphin (2004).*

The experiments described here have investigated the effects of mutating tryptophan (W391) to alanine and tyrosine (Y388) to serine or phenylalanine in the I-II linker of Ca_v2.2. The effects of mutating these residues on Ca_vβ subunit binding

has been studied using a surface plasmon resonance binding assay and the effects on trafficking measured using cell surface biotinylation assays. These experiments were done in collaboration with Dr. Jerome Leroy who performed electrophysiological experiments.

4.2 Results

4.2.1 Specific mutation in the I-II linker of $Ca_V2.2$ disrupt $Ca_V\beta1b$ subunit binding

The effects of mutating tryptophan 391 and tyrosine 388 in the I-II linker of $Ca_V2.2$ on $Ca_V\beta1b$ subunit binding were first investigated using a surface plasmon resonance binding assay. Tryptophan 391 and tyrosine 388 in the AID of the full I-II linker of $Ca_V2.2$ were changed by site directed mutagenesis as described in Chapter 2 to alanine and serine or phenylalanine. These residues were chosen as they have previously been used to replace tryptophan and tyrosine at these positions in mutagenesis studies and have been shown to disrupt $Ca_V\beta$ subunit binding. These mutated linkers along with the wild-type I-II linker were joined to the C-terminus of the N utilisation substance protein (NusA), to make NusA $Ca_V2.2$ I-II linker fusion proteins. The expression vector encoding the NusA fusion protein was a modified version pET44(b) (Novagen) and was a generous gift from Dr Andrei Okorokov (Wolfson Institute for Biomedical Research, University College London). NusA was chosen as the fusion protein as it has been shown to enhance solubility of its fusion partners and can be easily purified via an N-terminal $His_{(6)}$ (De Marco *et al.*, 2004; Nallamsetty *et al.*, 2006).

The fusion proteins along with NusA alone and the $Ca_V\beta1b$ subunit were expressed in *E.coli* BL21 (DE3) RIL bacteria and purified by immobilised metal affinity chromatography using Ni-NTA resin as described in chapter 2.2.2. Although fused to a protein which should aid solubility, purification of proteins from the soluble fraction after cell lysis yielded a mixture of products ranging from NusA alone up to and including the full length NusA I-II linker (not shown). The majority of full length NusA I-II linker protein was found associated with the insoluble fraction after cell lysis. Solublisation of this material using 1.5% CHAPS was required prior to purification to ensure efficient capture of the full length fusion proteins. Nus Alone was purified from the soluble fraction after cell lysis without the need for a solublisation step. $Ca_V\beta1b$ was prepared by Ni-NTA chromatography using methods described by Bell *et al* (2001). The purified proteins are shown in Figure 4.3 after SDS PAGE and coomassie blue staining.

The NusA wild-type, Y388F, Y388S I-II loop fusion proteins and NusA only were chemically coupled directly on to the surface of a CM5 sensor chip. 2000 RU (Response Units) of each of the I-II linker proteins was immobilised and the molar equivalent of NusA alone, 1600RU was immobilised as a reference to control for non-specific binding. Solutions

Figure 4.3

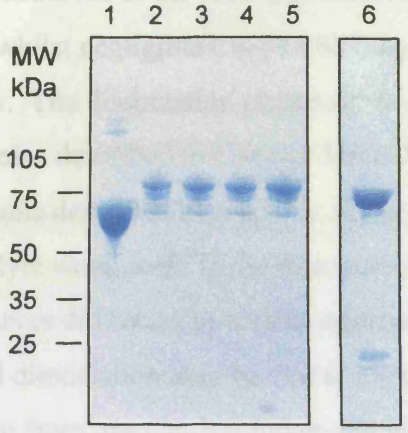

Figure 4.3: Coomassie blue stained SDS-PAGE on NuPage 4-12% Bis-Tris gel showing purified wild-type and mutant NusA I-II linker fusion proteins and the $Ca_V\beta 1b$ subunit used in surface plasmon resonance analysis. NusA only (lane 1), Ca_V 2.2 I-II linker (lane 2), Ca_V2.2Y388F (lane 3), Ca_V2.2Y388S (lane 4), Ca_V2.2W391A (lane 5), $Ca_V\beta 1b$ (lane 6). Molecular weight markers are indicated.

of purified $Ca_V\beta 1b$ subunit from 20nM to 1μM were perfused across all flow cells, each injection lasted 5 minutes and was followed by a 5 minute dissociation period.

Specific binding was observed to the wild-type linker and to both the Y388S and the Y388F mutants (Figure 4.4) whilst negligible $Ca_V\beta 1b$ binding was observed to the flow cell containing NusA only. The dissociation phases of the sensorgrams obtained for the GST Ca_V I-II linker fusion proteins described in Chapter 3 and the NusA I-II linker fusion proteins binding to $Ca_V\beta$ subunits described here appear not to return to baseline when high concentrations of analyte were used. If the dissociation phase was allowed to proceed for sufficient time, the curves did return to a value approaching baseline (not shown). The reason for this slowed dissociation may be that at high concentrations of analyte, the $Ca_V\beta$ subunits can dissociate from one Ca_V I-II linker and bind to another before being washed from the chip surface. An increase in the flow rates used for the experiments may have prevented this phenomenon by washing the analyte from the chip surface before it is able to re-bind.

After subtraction of the signal from the NusA only negative control, single exponential fits were made to the dissociation phases of the sensorgrams, the dissociation rates (k_{off}) for Ca_V 2.2, $Ca_V2.2$ Y388F and Ca_V 2.2 Y388S after a 20nM concentration of $Ca_V\beta$ were 0.0081 s^{-1}, 0.016 s^{-1} and 0.039 s^{-1} respectively, there was little variation in the dissociation rates for each mutant across the range of $Ca_V\beta$ concentrations used in these experiments. Little or no change in the k_{off} is to be expected as this rate should be independent of the $Ca_V\beta$ concentration. The dissociation constant K_D for $Ca_V\beta$ subunit binding to the wildtype $Ca_V2.2$ I-II linker was calculated using the three methods described in chapter 2. Firstly, the data from Figure 4.4 was fitted using the BIAevaluation 3.0 software package (Biacore AB), the K_D values for the wild-type I-II linker, Y388F and Y388S were 11.6 ± 1 nM n=6, 90.4 ± 20 nM n=6 and 209 ± 32 nM n=6 respectively. The K_D values obtained using GST fusions and NusA fusions of wildtype $Ca_V2.2$ I-II binding to $Ca_V\beta 1b$ were compared using analysis of variance (ANOVA) followed by Tukey's post hoc test and were found not to differ significantly (P = 0.177). Secondly, single exponential fits were made to the first 120 seconds of the association phase and the dissociation phase of the data shown in Figure 4.5, the specific association rate, k_{on}, was calculated as $k_{on} = (k_{on(obs)} - k_{off})/[Ca_V\beta]$, and the dissociation constant K_D as $K_D = k_{off}/k_{on}$. These fits and calculations are shown in Figure 4.5. Finally, from the data in Figure 4.4, the responses of the wild-type I-II

Figure 4.4

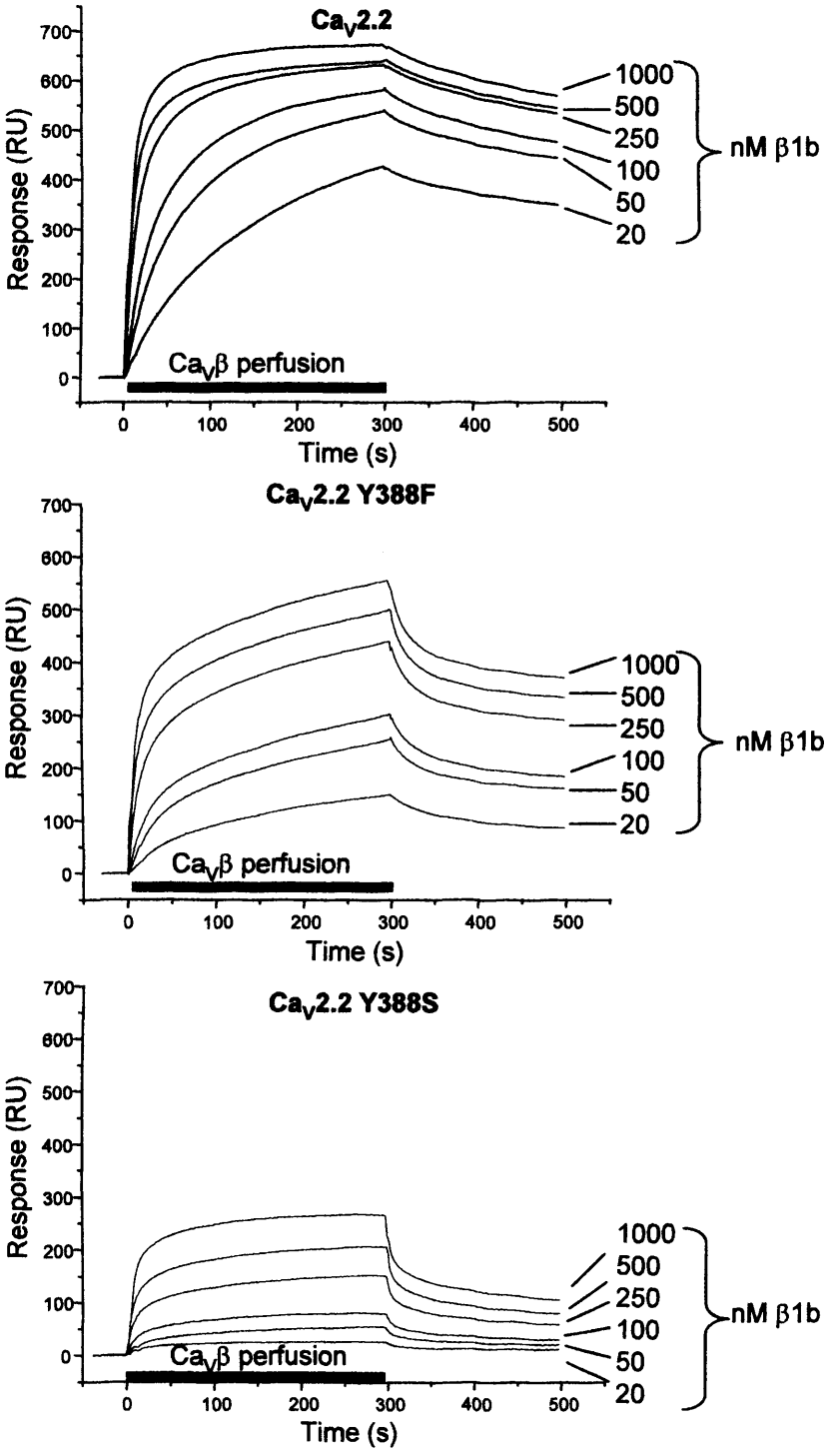

Figure 4.4 Representative Biacore sensorgrams showing interactions between Ca$_V$β1b and NusA I-II linker fusion Proteins from Ca$_V$2.2 (top panel), Ca$_V$2.2 Y388F (middle panel) and Ca$_V$Y388S (bottom panel), concentrations of 20 nM – 1 μM CaVβ1b (as indicated) were applied.

Figure 4.5

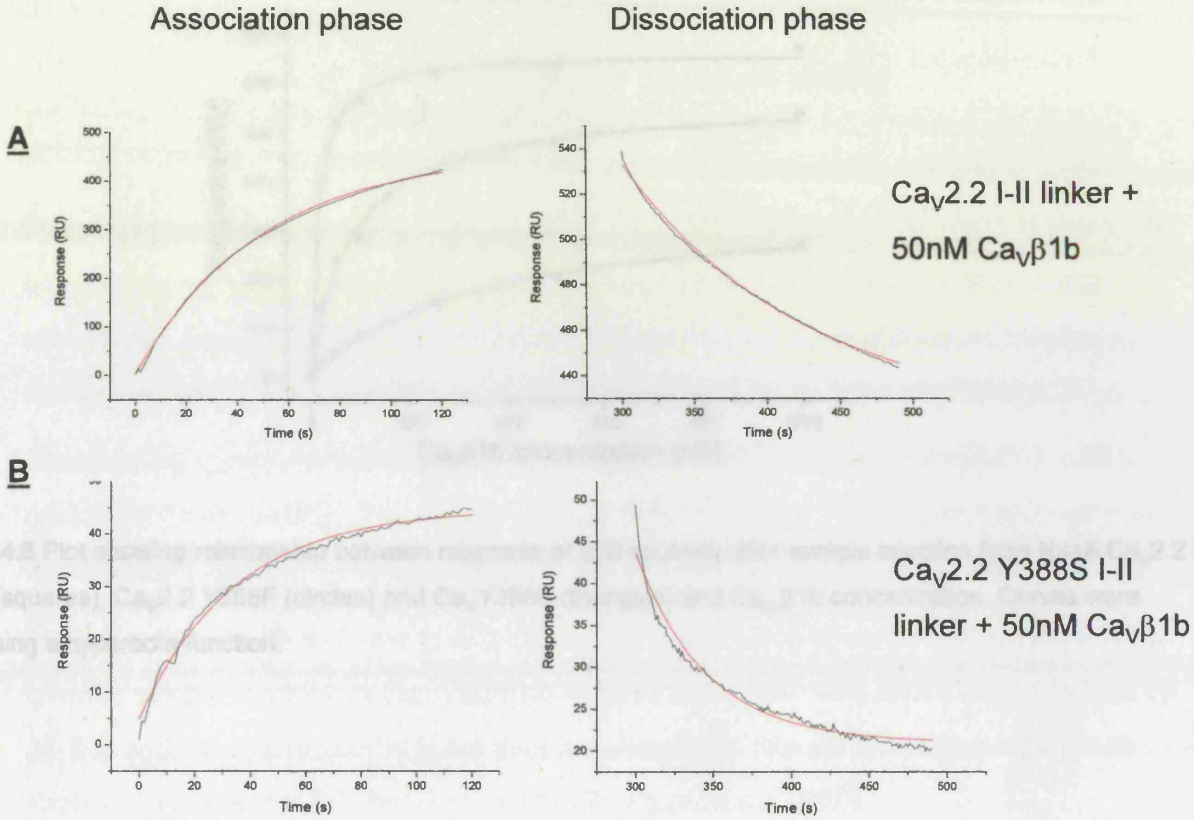

C

Ca$_V$2.2 I-II linker	Ca$_V$β1b concentration (nM)	$k_{on(obs)}$ 1/s	k_{off} 1/s	$k_{on}M^{-1}S^{-1}$	K_D (nM)
Wild-type	50	0.0201	0.0078	2.4×10^5	32
Y388S	50	0.0289	0.0221	1.35×10^5	163

Figure 4.5. Examples of single exponential fits made to Biacore sensorgrams. A. Single exponential fit of the association and dissociation phases of wild-type Ca$_V$2.2 binding to Ca$_V$β1b. B. Single exponential fit of the association and dissociation phases of wild-type CaV2.2Y388S binding to Ca$_V$β1b. C. Table showing calculation of the dissociation constant K_D from the data obtained in A and B

Figure 4.6

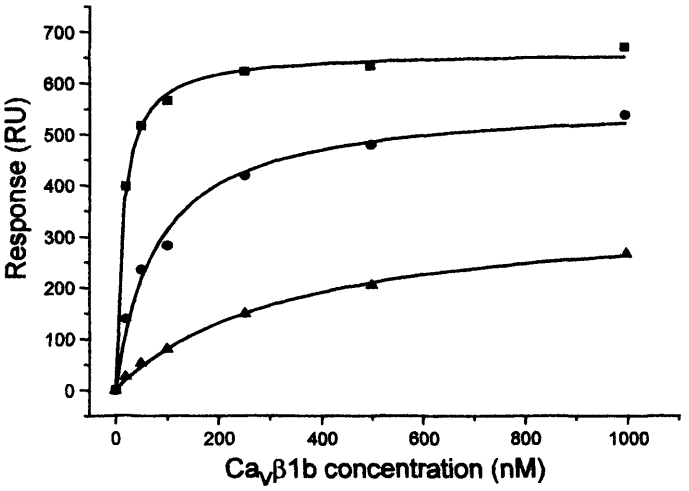

Figure 4.6 Plot showing relationship between response at 250 seconds after sample injection from NusA $Ca_V2.2$ I-II Linker (squares), $Ca_V2.2$ Y388F (circles) and Ca_VY388S (triangles) and Ca_V β1b concentration. Curves were fitted using a hyperbola function.

Figure 4.7

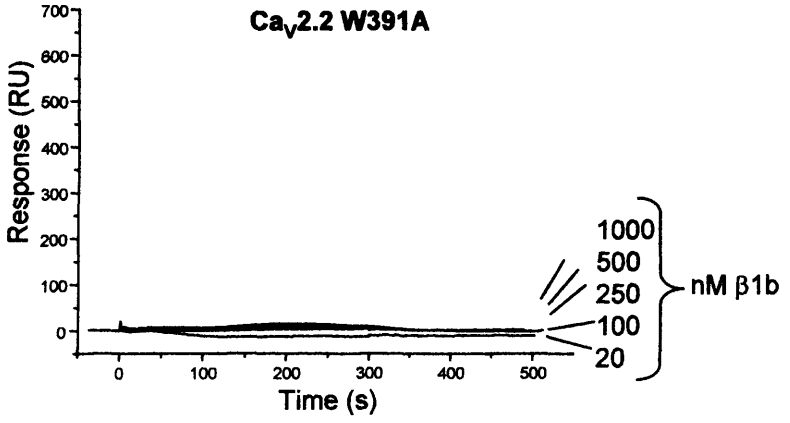

Figure 4.7 Representative Biacore sensorgrams showing lack of interaction between NusA $Ca_V2.2$ W391A I-II linker and $Ca_V\beta 1b$. concentrations of 20 nM – 1 μM $Ca_V\beta 1b$ (as indicated) were applied.

linker and both mutants 250 seconds after the start of perfusion were plotted against $Ca_V\beta$ concentration (Figure 4.6) these curves fitted well to a hyperbola function:

$$Y = \frac{B_{max} \times [\beta]}{K_D + [\beta]} \qquad B_{max} = \text{Maximum binding}$$

From this plot, the dissociation constants K_D for $Ca_V\beta 1b$ binding to wild-type I-II linker and both mutants were 13.7nM, 78nM and 329nM respectively. No binding of the $Ca_V\beta 1b$ subunit was detected to the $Ca_V2.2$W391A I-II linker even at the highest concentration so further analysis was not possible and K_D values could not be determined (Figure 4.7).

These results agree with previous studies which have shown that the tryptophan in AID is critical for $Ca_V\beta$ binding. The affinity of $Ca_V\beta 1b$ for the $Ca_V2.2$ I-II linker calculated from these data are also similar to those found in other studies (De Waard *et al.*, 1995; Bell *et al.*, 2001; Canti *et al.*, 2001; Leroy *et al.*, 2005). The results show however that mutation of the tyrosine residue to serine or phenylalanine reduces the affinity with which $Ca_V\beta$ can bind by 24-fold and 5.6-fold respectively but does not completely prevent interaction as has been suggested previously (Witcher *et al*,. 1995; De Waard *et al.*, 1995).

4.2.2 The effect of specific mutations in AID on Trafficking of $Ca_V2.2$ calcium channels to the plasma membrane.

The W391A mutation abolished $Ca_V\beta 1b$ binding and Y388S mutation reduced the affinity of $Ca_V\beta 1b$ for the $Ca_V2.2$ I-II linker to a greater extent than Y388F. Experiments were performed to establish what effects if any this had on the ability of the β subunit to traffic $Ca_V2.2$W391A and $Ca_V2.2$Y388S channels to the plasma membrane.

Binding of the $Ca_V\beta$ subunit is crucial for $Ca_V2.2$ channel trafficking to the plasma membrane (Bichet *et al.*, 2000; Canti *et al.*, 2001; Leroy *et al.*, 2005). The I-II linker of HVA calcium channels has been suggested to contain an endoplasmic retention signal which causes nascent channels to remain in the ER (Bichet *et al.*, 2000). $Ca_V\beta$ binding to the AID masks

or antagonises this signal causing the channels to be released from the ER and proceed forward to the plasma membrane although no ER retention signal has yet been identified. In experiments in *Xenopus* oocytes, removal of most of the AID sequence of $Ca_V2.1$ or mutation of tyrosine 392 to serine disrupted trafficking to the plasma membrane when coexpressed with $Ca_V\beta3$ (Bichet *et al.*, 2000). The reduction in the affinity of $Ca_V\beta1b$ for W391A and Y388S in $Ca_V2.2$ may therefore be expected to reduce its trafficking effects on the channels.

To investigate the effects on trafficking, a cell surface biotinylation assay was used to measure the expression of $Ca_V2.2$ channels in the plasma membrane of transiently transfected tsA 201 cells. The assay involves treating cells with EZ link sulfo NHS-SS biotin (Pierce, Rockford, IL) which reacts with primary amine groups of lysine residues present in proteins located on the cell surface thus incorporating the biotin label into the protein. Biotinylated surface proteins can then be precipitated using agarose beads coupled to streptavidin which binds biotin with very high affinity (Green, 1990). The amounts of target protein present in the plasma membrane can then be quantified relative to the total amount of protein expressed. This approach has previously been used to study the surface expression of ion channels (Cohen *et al.*, 2005; Ding *et al.*, 2005; Huang *et al* 2004).

Tryptophan 391 was changed to alanine and tyrosine 388 was changed to serine in full length $Ca_V2.2$ using the PCR based site directed mutagenesis technique described in chapter 2. TsA 201 cells were transfected with the following Ca_V calcium channel subunits: $Ca_V2.2$/ $Ca_V2.2$ W391A/Y388S 10μg, 7μg $Ca_V\beta1b$, 7μg $\alpha_2\delta$-2. Empty pMT2 vector (24μg) was used as a negative control or to replace subunits which were omitted. Cell surface biotinylation and precipitation of biotinylated proteins was performed 48 hours after transfection.

4.2.3 $Ca_V2.2$W391A prevents trafficking to the plasma membrane

Western blotting of whole cell lysates (10μg) from transfected tsA201 cells showed no effect of the W391A mutation on the total expression of $Ca_V2.2$ (Figure 4.8, top panel). When cotransfected with $Ca_V\beta1b$, western blot analysis of the biotinylayed proteins using antibodies to the $Ca_V2.2$ II-III linker showed a large reduction in the amount biotinylated $Ca_V2.2$W391A compared to wild-type $Ca_V2.2$. A similar reduction in surface expression was seen for wild-type $Ca_V2.2$ expressed without a $Ca_V\beta$ subunit (Figure 4.8, lower panel). Cotransfection with $Ca_V\beta2a$ resulted in a similar although less drastic reduction in surface

Figure 4.8

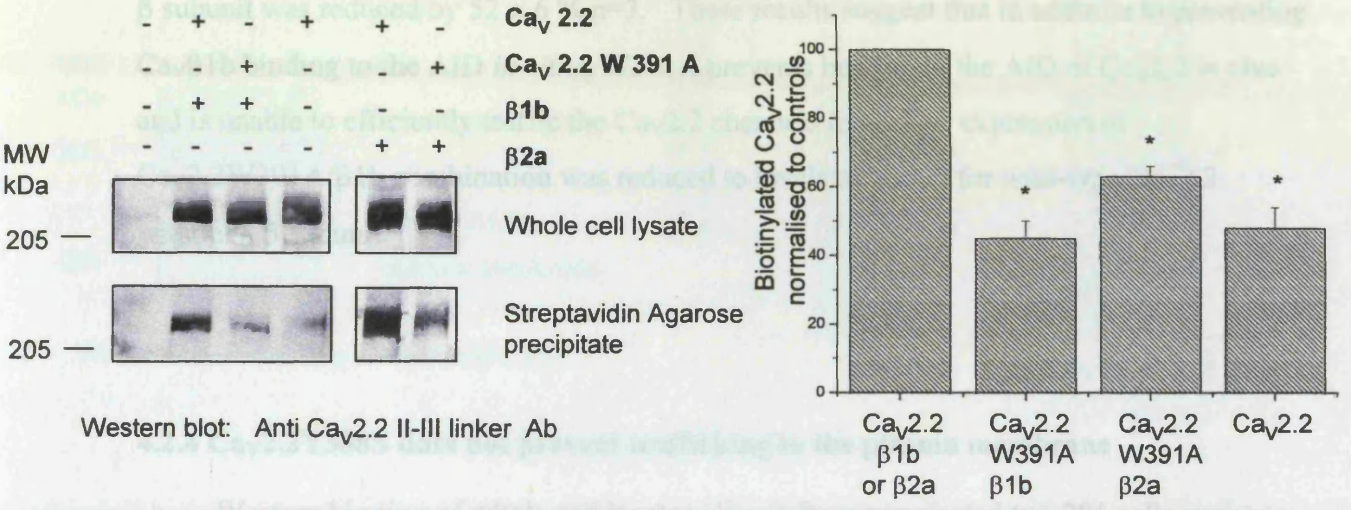

Figure 4.8 Cell surface expression of either $Ca_V2.2$ or $Ca_V2.2W391A$ expressed with α2δ-2 and Ca_Vβ1b or Ca_Vβ2a. *Left,* Total expression of $Ca_V2.2$ is shown by western blot in the upper row and biotinylated $Ca_V2.2$ in the lower row. Cells were transfected with empty Vector (lane 1), $Ca_V2.2$/α2δ-2/β1b (lane 2), $Ca_V2.2W391A$/α2δ-2/β1b (lane 3),$Ca_V2.2$/α2δ-2 (lane 4), $Ca_V2.2$/α2δ-2/β2a (lane 5), $Ca_V2.2W391A$/α2δ-2/β2a (lane 6). *Right panel,* histogram showing quantification of the mean amount of $Ca_V2.2W391A$ expressed at the plasma membrane when expressed alone, with β1b, or β2a given as a percentage of the amount of $Ca_V2.2$ expressed under the same conditions. Data are mean ± SEM of 3 independent experiments. (*) $P < 0.05$ compared to controls.

expression. Expression of channel proteins at the cell surface was quantified using ImageQuant 5.2 (Molecular Dynamics, GE Healthcare) and expressed as a percentage of biotinylated wild-type $Ca_V2.2$ measured under the same conditions (figure 4.8, right). $Ca_V2.2$W391A reduced surface expression by 65 ± 5 % n=3 when coexpressed with β1b and 37 ± 3 % n=3 when coexpressed with β2a, surface expression of wild-type $Ca_V2.2$ without a β subunit was reduced by 52 ± 6 % n=3. These results suggest that in addition to preventing Ca_Vβ1b binding to the AID *in vitro*, W391A prevents binding to the AID of $Ca_V2.2$ *in vivo* and is unable to efficiently traffic the $Ca_V2.2$ channels as surface expression of $Ca_V2.2$W391A/β1b combination was reduced to levels observed for wild-type $Ca_V2.2$ without a β subunit.

4.2.4 $Ca_V2.2$Y388S does not prevent trafficking to the plasma membrane

Western blotting of whole cell lysates (10μg) from transfected tsA 201 cells again showed no effect of the Y388S mutation on the amount of channel protein expressed compared to wild-type $Ca_V2.2$ (Figure 4.9, left panel). Analysis of the biotinylated proteins by the same method showed a consistent elevation in the amount of $Ca_V2.2$ Y388S channel protein present at the plasma membrane (Figure 4.9, lower panel). The amount of Y388S protein at the membrane was quantified relative to wild-type $Ca_V2.2$ and found to be elevated by 38 ± 19% (n=3) (Figure 4.9, right). These results suggest that although the affinity of the Ca_Vβ1b for Y388S is reduced this does not translate into a reduction in the amount of channel protein in the plasma membrane. This suggests that *in vivo* Ca_Vβ1b can still associate with the $Ca_V2.2$Y388S channels and effectively exert its trafficking effects despite a 24-fold decrease in affinity.

Figure 4.9

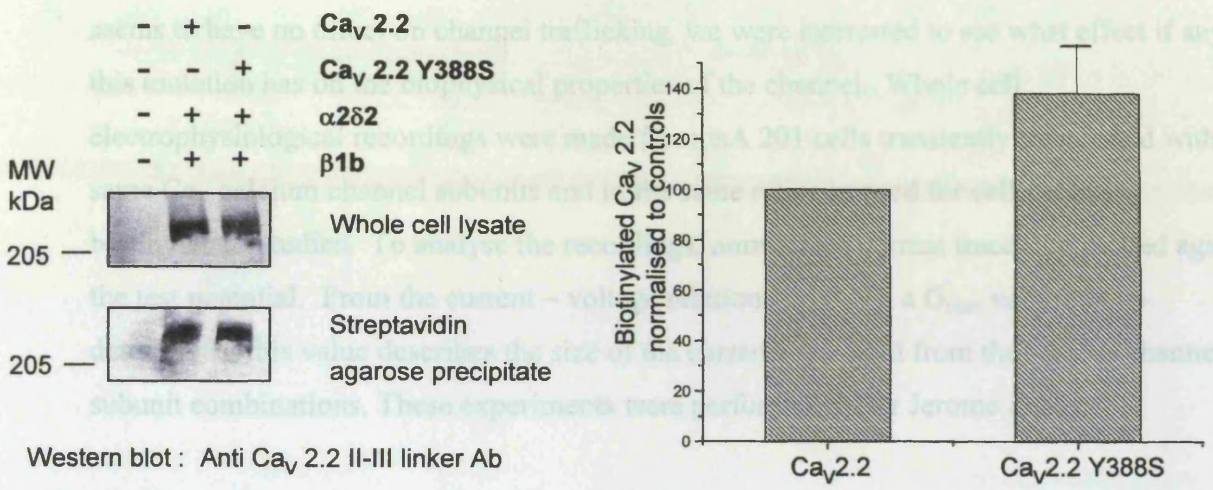

Figure 4.9 Cell surface expression of either Ca_V2.2 or Ca_V2.2Y388S expressed with α2δ-2 and Ca_Vβ1b (left) Total expression of Ca_V2.2 is shown by western blot in the upper row and biotinylated Ca_V2.2 in the lower row. Cells were transfected with empty vector (lane 1), Ca_V2.2/α2δ-2/β1b (lane 2), Ca_V2.2Y388S/α2δ-2/β1b (lane 3) The cell surface expression is increased slightly by the Y388S mutation. *Right panel,* histogram showing quantification of the mean amount of Ca_V2.2Y388S expressed at the plasma membrane when co-expressed with β1b, given as a percentage of the amount of Ca_V2.2 expressed under the same conditions. Data are mean ± SEM of 3 independent experiments, there was no significant difference between the conditions P = 0.110.

4.3 Appendix to Results

4.3.1 The effect of W391A and Y388S mutations on the functional expression of $Ca_V2.2$

Since the Y388S mutation in $Ca_V2.2$ reduces the affinity of $Ca_V\beta1b$ subunit binding but seems to have no effect on channel trafficking, we were interested to see what effect if any this mutation has on the biophysical properties of the channel. Whole cell electrophysiological recordings were made from tsA 201 cells transiently transfected with the same Ca_V calcium channel subunits and in the same ratios as used for cell surface biotinylation studies. To analyse the recordings, normalized current traces are plotted against the test potential. From the current – voltage relationship (I-V), a G_{max} value can be determined, this value describes the size of the currents recorded from the various channel subunit combinations. These experiments were performed by Dr Jerome Leroy.

4.3.2 W391A prevents functional expression of $Ca_V2.2$

Plots of voltage dependence of activation for wild-type $Ca_V2.2$ and $Ca_V2.2$W391A expressed with and without $Ca_V\beta1b$ and β2a and for wild-type $Ca_V2.2$ and $Ca_V2.2$Y388S with and without $Ca_V\beta1b$ are shown in Figure 4.10. Figure 4.10 *A* shows the peak amplitude of the currents recorded from $Ca_V2.2$W391A/β1b/α2δ2 and $Ca_V2.2$/α2δ2 without β1b compared to wild-type $Ca_V2.2$/β1b/α2δ2. The size of the currents from $Ca_V2.2$W391A/β1b/α2δ2 was reduced by 81 ± 3% compared to the $Ca_V2.2$/β1b/α2δ combination to levels comparable with $Ca_V2.2$/α2δ2 without a β subunit. Figure 4.10 *B* shows a similar reduction in current size for the $Ca_V2.2$W391A/β2a/α2δ2 combination compared to $Ca_V2.2$/β2a/α2δ2 the reduction in this case was 72%. These results correlate well with the results from surface plasmon resonance and cell surface biotinylation assays suggesting that the $Ca_V\beta$ subunit can no longer associate with and traffic the $Ca_V2.2$W391A channels.

4.3.3 Y388S has no effect the functional expression of $Ca_V2.2$

Recordings were made from tsA 201 cells transiently transfected with $Ca_V2.2$Y388S and compared to wild-type $Ca_V2.2$. Figure 4.10 *C* shows the peak amplitude of currents recorded from $Ca_V2.2$/β1b/α2δ2 compared to $Ca_V2.2$/α2δ2 without a β subunit and

Figure 4.10

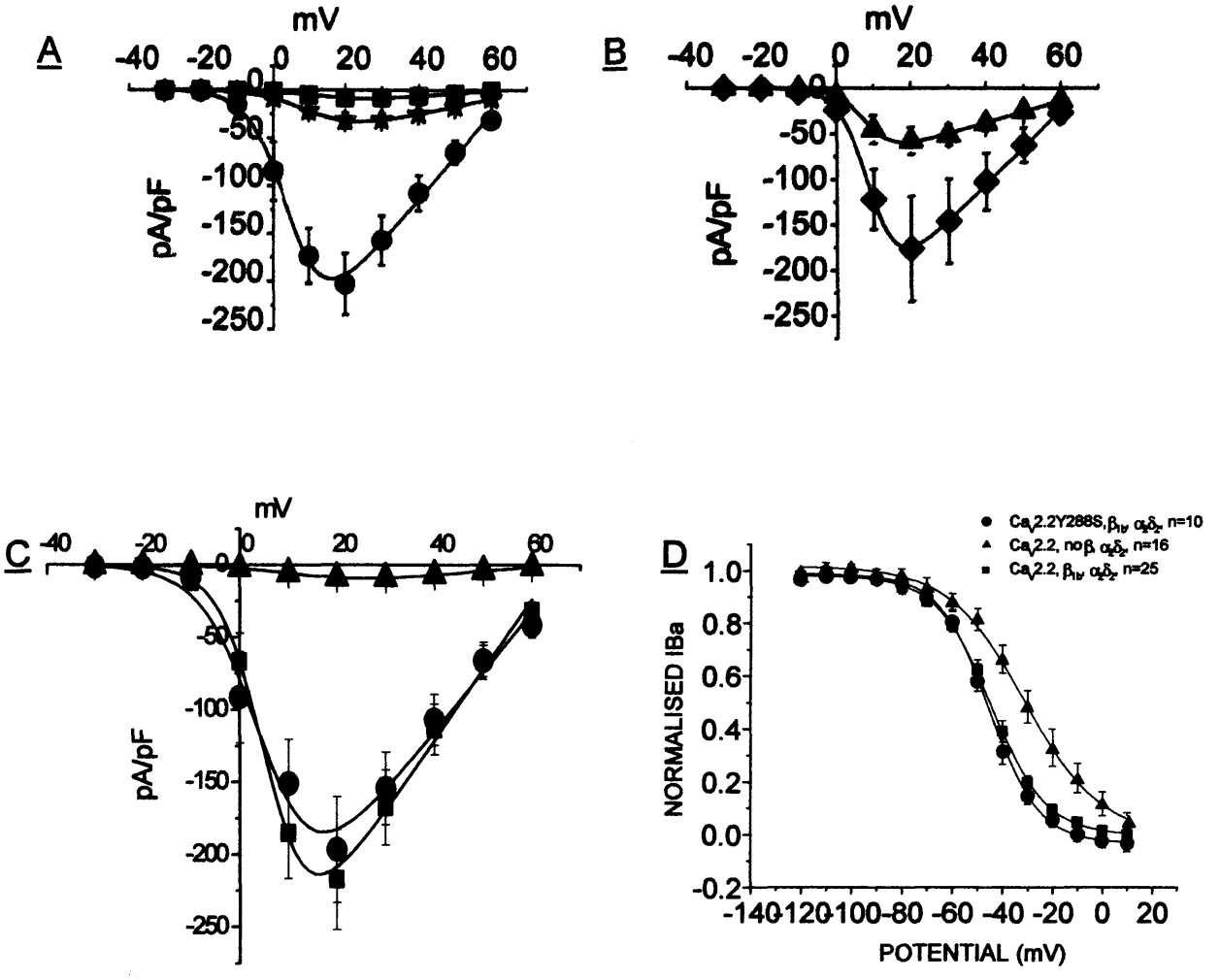

Figure 4.10 Functional expression of $Ca_V2.2$, $Ca_V2.2$W391A and $Ca_V2.2$Y388S. A. Current – Voltage relationship for $Ca_V2.2/\alpha2\delta$-2 (filled squares), compared to $Ca_V2.2/\alpha2\delta$-2/$Ca_V\beta$1b (filled circles) and $Ca_V2.2$W391A/$\alpha2\delta$-2/$Ca_V\beta$1b (filled stars). B. Current – Voltage relationship for Ca_V 2.2/$\alpha2\delta$-2/$Ca_V\beta$2a (filled diamonds), compared to $Ca_V2.2$W391A/$\alpha2\delta$-2/CaVβ2a (filled triangles). Taken from Leroy *et al.* (2005). C. Current – Voltage relationship for $Ca_V2.2/\alpha2\delta$-2/CaVβ1b (filled squares) compared to $Ca_V2.2/\alpha2\delta$-2 (filled triangles) and $Ca_V2.2$Y388S/$\alpha2\delta$-2/CaVβ1b (filled circles). D. Plot showing Voltage dependence of steady state inactivation for $Ca_V2.2/\alpha2\delta$-2/CaVβ1b (filled squares) compared to $Ca_V2.2/\alpha2\delta$-2 (filled triangles) and $Ca_V2.2$Y388S/$\alpha2\delta$-2/$Ca_V\beta$1b (filled circles).

$Ca_V2.2Y388S/\beta1b/\alpha2\delta2$ combination. There is no significant difference between the amplitude of the currents recorded from $Ca_V2.2$ and $Ca_V2.2Y388S$, both are greatly enhanced compared to $Ca_V2.2$ expressed without a β subunit. Figure 4.10 *D* shows the voltage dependence of steady-state inactivation curves for $Ca_V2.2$ and $Ca_V2.2Y388S$, both show a leftward shift to more hyperpolarized potentials compared to $Ca_V2.2$ without a β subunit. This hyperpolarisation of steady state inactivation is a classic feature of $Ca_V\beta$ subunit modulation and suggest that although the $Ca_V\beta$ has reduced affinity for the $Ca_V2.2Y388S$ I-II linker these channels can still be trafficked and normally modulated by the $Ca_V\beta1b$ subunit.

4.4 Discussion

HVA calcium channels are modulated by auxiliary β subunits, $Ca_V\beta$ subunit binding to the AID motif enhances functional expression of the channels as well as hyperpolarizing the voltage dependence of activation and hyperpolarizing the voltage dependence of steady state inactivation. Mutation of a single tryptophan residue, W391 in $Ca_V2.2$ abolished $Ca_V\beta$ subunit binding. The importance of this tryptophan has been shown previously in both biochemical and structural studies and is regarded as the key residue involved in the $Ca_V\beta$/AID interaction (De Waard *et al.*, 1995; Chen *et al.*, 2004; Opatowsky *et al.*, 2004; Van Petegem *et al.*, 2004; Leroy *et al.*, 2005).

Coexpression of $Ca_V2.2$W391A with $Ca_V\beta1b$ reduced trafficking to the plasma membrane and reduced the functional expression compared to wild-type $Ca_V2.2/\beta1b$ combination to levels similar to wild-type $Ca_V2.2$ expressed without a β subunit, so it appears that $Ca_V2.2$W391A cannot be regulated by the $Ca_V\beta1b$ subunit. However, whilst cell surface biotinylation experiments showed that coexpression of $Ca_V\beta2a$ with $Ca_V2.2$W391A also reduced surface expression, subsequent experiments by Dr Jerome Leroy in our laboratory showed that those mutant channels which did reach the plasma membrane were still fully modulated by $Ca_V\beta2a$ (Leroy *et al.*, 2005). This was found to be due to the ability of $Ca_V\beta2a$ to be palmitoylated at its N-terminus. Palmitoylation alters its subcellular location and causes it to be associated with the plasma membrane (Restituto *et al.*, 2000). This presumably brings the $Ca_V\beta2a$ into close proximity with the channels. In agreement with this, non-palmitoylatable $Ca_V\beta2a$ was unable to modulate $Ca_V2.2$W391A, whilst the addition of a palmitoylation motif to $Ca_V\beta1b$ caused it to modulate $Ca_V2.2$W391A channels.

It has previously been proposed that trafficking and modulation by $Ca_V\beta$ are independent processes, Canti et al. (2001) reported that trafficking of $Ca_V2.2$ requires a low concentration of $Ca_V\beta3$ and that the K_D for this process was approximately 17nM. Full modulation was dependent upon a lower affinity interaction with a K_D of approximately 120nM, suggesting an additional $Ca_V\beta$ interaction site on the Ca_V 2.2 protein. Cohen et al. (2005) reported that a small splice variant of $Ca_V\beta1b$ found in heart and named β1d, lacks the GK like domain containing the AID binding pocket and presumably cannot interact with AID. This protein could still modulate the open probability of $Ca_V1.2$ channels whilst having no effect upon channel trafficking, again suggesting secondary sites of interaction between the Ca_V α1 and the β subunit. In addition, $Ca_V\beta$ binding sites other than AID have been

reported in the N and C termini of HVA calcium channels (Walker *et al.*, 1999; Stephens *et al.*, 2000) and elsewhere in the I-II loop (Maltez *et al.*, 2005). Maltez et al. (2005) reported direct binding of the $Ca_V\beta$ subunit SH3 domain to a site in the I-II linker of $Ca_V2.1$ close to but different from the AID motif. The surface plasmon resonance binding assay described here included the entire I-II linker of $Ca_V2.2$ and the full length $Ca_V\beta1b$ yet no binding was detected to the W391A mutant linker even at the highest $Ca_V\beta1b$ concentration tested. This may be due to the affinity of this interaction being too low to measure by this method as the lower limit for weak interactions is approximately 10μM, alternatively, the interaction may be specific for $Ca_V2.1$.

In the case of $Ca_V2.2$W391A/$Ca_V\beta2a$, it is seems that whilst the trafficking effects of $Ca_V\beta$ are virtually abolished by the mutation, palmitoylation increases the local concentration of $Ca_V\beta$ around the channels in the plasma membrane to levels where low affinity interactions sufficient to modulate the channels can occur. It seems clear that the high affinity AID/$Ca_V\beta$ interaction is crucial for channel trafficking and may also serve to bring the $Ca_V\beta$ subunit to a location relative to the channel where secondary, lower affinity interactions can occur.

Mutation of tyrosine 388 to serine had a large effect on its ability to bind $Ca_V\beta1b$ reducing the affinity approximately 24 fold, however binding was not abolished as has been reported previously (Pragnell *et al.*, 1994; Witcher *et al.*, 1995; Berrou *et al.*, 2004; Berrou *et al.*, 2005). Mutation of tyrosine 388 to phenylalanine had a lesser impact upon $Ca_V\beta$ binding, these two residues are similar in structure differing by only one hydroxyl group. This group is reported to form hydrogen bonds to the β subunit via two water molecules (Opatowsky *et al.*, 2004). The moderate reduction in affinity for the phenylalanine mutant may simply reflect the absence of these interactions whilst replacement of tyrosine with serine represents a more drastic structural change preventing AID from interacting properly with the AID binding pocket.

This reduction in affinity caused by Y388S did not result in any detrimental effects on channel function, $Ca_V2.2$Y388S channels were still trafficked to the plasma membrane, expression of functional channels was enhanced and the voltage dependence of steady state inactivation was hyperpolarised when coexpressed with $Ca_V\beta1b$. The lack of effect may be due to the large amounts of $Ca_V\beta$ subunit protein produced in the expression system used in the study. The excess of $Ca_V\beta$ may be sufficient to compensate for the reduction in affinity

of $Ca_V\beta$ for the I-II linker by being able to constantly occupy the AID and so cause the channels to be trafficked and modulated as normal.

To further investigate the trafficking and modulation of $Ca_V\beta 1b$ on $Ca_V2.2Y388S$, an approach similar to that taken by Canti et al. (2001) could be used. Using a *Xenopus* oocyte expression system, the amount of overexpressed $Ca_V\beta$ subunit can be more tightly controlled as the DNA or RNA to be expressed is injected directly into the nucleus or cytoplasm respectively of each oocyte. If the amount of $Ca_V\beta$ could be systematically reduced, the effect on trafficking and modulation of $Ca_V2.2Y388S$ could then be measured relative to the wild-type channel. It may then be possible to determine if there are any functional differences between $Ca_V2.2$ and $Ca_V2.2Y388S$ channels.

Chapter 5:

The role of $Ca_V\beta 2a$ in PI3 kinase induced voltage dependent calcium channel trafficking

5.1 Introduction

Voltage Dependent Calcium Channels (VDCC) are the major route of calcium entry in excitable cells (Catterall, 2000). High Voltage Activated (HVA) calcium channels are primarily modulated by the $Ca_V\beta$ subunit which enhances functional expression as well as hyperpolarizing the voltage dependence of activation and hyperpolarizing the voltage dependence of steady state inactivation, (Walker *et al.*, 1998; Bichet *et al.*, 2000; Leroy *et al.*,2005). This is true of all $Ca_V\beta$ subunits except $Ca_V\beta$2a which slows inactivation and causes a depolarizing shift in the voltage dependence of steady state inactivation (Stea *et al.*, 1994). Calcium influx through VDCC's can also be modulated by extracellular stimuli binding to receptors which in turn relay these signals via signaling intermediates such as heterotrimeric G-proteins and phosphoinositides which can directly or indirectly regulate the channels (Dolphin, 2003; Wu *et al.*, 2002).

The $G\beta\gamma$ dimers of heterotrimeric G proteins inhibit the Ca_V2 class of voltage dependent calcium channels. This inhibition manifests itself as a slowing of the activation kinetics and a shift in the voltage dependence of activation towards more depolarised potentials, for review see (Dolphin, 2003). The molecular mechanism behind this inhibition is complex but has been shown to involve direct binding of the $G\beta\gamma$ dimers to the cytoplasmic linker between domains I and II (De Waard *et al.*, 1997; Zamponi *et al.*, 1997) and also essential determinants in the cytoplasmic N-terminus (Canti *et al.*, 1999; Agler *et al.*, 2005).

Production of $G\beta\gamma$ dimers can modulate voltage dependent calcium channel activity in other ways. Viard et al. (1999) reported that stimulation of the angiotensin receptor $AT1_A$ can mediate an increase in L-type current in vascular myocytes. This effect was shown to be partially due to a $G\beta\gamma$ sensitive phosphoinositide 3-kinase (PI3 kinase) as the effect could be blocked by the PI3 kinase inhibitor wortmannin and mimicked by infusion of the $G\beta\gamma$ sensitive PI3 kinase γ, there was also a component mediated by protein kinase C. In addition, Blair et al. (1997) reported the stimulation of native L and N-type calcium channels in cerebellar granule neurons after treatment with insulin-like growth factor (IGF-1). This effect was also demonstrated to be mediated by PI3 kinase as incubation with the PI3 kinase inhibitor wortmannin or introduction of a dominant negative PI3 kinase abolished the effect.

Phosphoinositide 3-kinases are lipid kinases which phosphoryate the 3' hydroxyl group of the inositol ring of inositol phospholipids, producing Phosphatidylinositol(3)P, Phosphatidylinositol(3,4)P_2 or Phosphatidylinositol (3,4,5)P_3 (Rameh et al., 1999). Phosphoinositide 3-kinase enzymes are divided into three classes, of these, class I PI3 kinases have been the focus of most work as they are coupled to extracellular stimuli. Class I PI3 kinases are further subdivided into class IA and class IB isoforms. Class IA PI3 kinases are composed of one of three regulatory subunits p85α, p85β and p55γ and one of three catalytic subunits p110α, p110β and p110δ. The regulatory subunit interacts with high affinity with the tyrosine phosphorylated sequence pYxxM in the C-termini of receptor tyrosine kinases and other molecules via two Src-homology 2 (SH2) domains (Pawson 1995), this interaction recruits the catalytic p110 subunit to the plasma membrane where it can phosphorylate its lipid substrate. Class IB PI3 kinases are regulated differently, the regulatory p101 subunit interacts with the catalytic p110γ (Krugmann et al., 1999) and this complex can be activated by Gβγ dimers of heterotrimeric G proteins (Brock *et al.*, 2003; Stephens *et al.*, 1997).

Activation of class I PI3 kinases and production of Phosphatidylinositol(3,4)P_2 or Phosphatidylinositol (3,4,5)P_3 causes recruitment of plekstrin homology (PH) domain containing proteins from the cytosol to the plasma membrane. Plekstrin homology (PH) domains are approximately 100 amino acid residue regions which are capable of interacting with phosphoinositides (Haslam *et al.*, 1993). Over 200 genes containing PH domains have been identified in the human genome (Venter *et al.*, 2001), the best characterised of which is the serine / threonine kinase protein kinase B (PKB)/Akt. Membrane recruitment followed by phosphorylation on threonine 308 and serine 473 is required for full activation of PKB, which can then leave the plasma membrane to phosphorylate its many target proteins. Many PKB substrates have so far been identified, these include the Bcl-2 like agonist of cell death (BAD) (Data *et al.*, 1997), glycogen synthase kinase-3 (GSK-3) (Cross *et al.*, 1995) and mammalian target of rapamycin (mTOR) (Sekulic *et al.*, 2000).

Protein kinase B is an important regulator of many important cellular processes such as cell death (Testa *et al.*, 2001), cell cycle progression and cell growth (Blume-Jensen and Hunter., 2001). It is therefore no surprise that changes in PKB activity or the proteins which regulate it are involved in a number of human

cancers and in diabetes (Cheng et al., 1996; Ruggeri et al., 1998; Nicholson and Anderson., 2002; Weston et al., 2001; Brazil and Hemmings., 2001). In addition to these processes, the PI3K/ PKB pathway has been implicated in the trafficking and membrane insertion of certain membrane proteins and ion channels. Kanzaki et al. (1999) reported that a calcium permeable cation channel named growth factor regulated channel (GRC) of the transient receptor potential (TRP) channel family was trafficked to the plasma membrane after stimulation with IGF-1 in Chinese hamster ovary (CHO) cells. Furthermore, this effect was blocked by wortmannin, implicating effectors downstream of phosphoinositide 3-kinase. Lhullier et al. (2002) described the regulation of membrane insertion of calcium-dependent potassium channels (K_{ca}) in response to the target growth factor TGFβ1. Application of TGFβ1 to neurons of the chick ciliary ganglion caused activation of PKB and the mitogen activated protein kinase (MAP) Erk and promoted the insertion of K_{ca} channels into the plasma membrane from intracellular stores. These effects were blocked by the PI3Kinhibitors wortmannin and LY294002. In addition, Wang et al. (1999) reported abolition of translocation of the glucose transporter GLUT4 in L6 myoblast muscle cells in response to insulin treatment after introduction of a dominant negative PKB (AAA-PKB) in which the regulatory phosphorylation sites threonine 308 and serine 473 and phosphate transfer residue lysine 179 are changed to alanine. Although these studies suggest that activation of PKB is necessary for plasma membrane targeting, the precise mechanism of action is not clear.

More recently, Viard et al. (2004) reported that in COS-7 cells, PI3 Kinase acting through PKB promotes translocation of voltage dependent calcium channels to the plasma membrane, this was measured by whole cell electrophysiology and confocal microscopy. Furthermore this effect is specific for channel combinations which include the $Ca_V\beta2a$ subunit. The $Ca_V\beta2a$ subunit was found to contain a putative PKB phosphorylation motif RxRxxS/T in its C-terminus. Mutations of residue 574 in $Ca_V\beta2a$ to alanine or glutamic acid which abolish or mimic phosphorylation respectively were shown to abolish or promote $Ca_V2.2$ trafficking to the plasma membrane and so to mimic the effect of PI3 kinase and PKB. In acutely isolated rat dorsal root ganglion (DRG) neurons, application of IGF-1 induced translocation of transiently transfected $Ca_V2.2$ channels to the plasma membrane and in COS-7 cells introduction of constitutively active PKB which can be myrisoylated at

its N-terminus and therefore localised at the plasma membrane also induced translocation suggesting that PKB may act directly on the $Ca_V2.2/Ca_V\beta2a$ channel complex.

The experiments described here were performed to investigate whether $Ca_V\beta2a$ can be a substrate for PKB both *in vitro* and *in vivo*. By using *in vitro* and *in vivo* phosphorylation assays combined with immunoprecipitation, the amounts of radioactive phosphate incorporated into wild-type $Ca_V\beta2a$ compared to $Ca_V\beta2a$ S574A were measured. Antibodies directed specifically to the phosphorylated form of threonine 308 or serine 473 of PKB were used to probe its activation state after co-transfection with phosphoinositide 3-kinase. Finally, co-immunoprecipitation was used to probe for a direct interaction between $Ca_V\beta2a$ and PKB.

5.2 Results

5.2.1 Expression of PI3 kinase γ induces activation of endogenous protein kinase B in COS-7 cells

The Gβγ sensitive PI3 Kinase γ is composed of a regulatory P101 subunit and a catalytic subunit P110γ (Krugmann et al., 1999). COS-7 cells were transiently transfected with P101 in expression vector pcDNA3 and P110γ in expression vector pMT2. Western blot analysis was performed on whole cell lysates (10μg) three days after transfection. The P101 subunit contained a Glu-Glu epitope tag at its N-terminus (sequence EEEEYMPME) (Grussenmeyer *et al.*, 1985) and this was detected with anti Glu-Glu tag antibodies. P110γ subunits were detected with anti P110 antibodies (Santa Cruz biotechnology). Figure 5.1a shows expression of both subunits compared to untransfected COS-7 cells, in agreement with previous reports, no endogenous P110γ subunits are detected (Murga *et al*,. 1998).

Full activation of PKB requires production of Phosphatidylinositol(3,4)P_2 or Phosphatidylinositol (3,4,5)P_3 which PKB binds via its PH domain causing translocation to the plasma membrane (Burgering *et al.*, 1995; Franke *et al.*, 1997). At the membrane, PKB is phosphorylated at a threonine at position 308 in the kinase loop or T loop by phosphoinositide dependent kinase 1 (PDK1) (Alessi *et al.*, 1997) and at position 473 in the hydrophobic C-terminal domain by a second kinase. The molecular identity of the serine 473 kinase has been controversial for many years, many candidates have been put forward such as PDK1 (Balendran *et al.*, 1999), integrin linked kinase (ILK) (Persad *et al.*, 2001) and even PKB itself (Toker *et al.*, 2000). Recently however, Sarbassov et al. (2005) reported that the large protein kinase mammalian target of rapamycin kinase (mTOR) complexed with another protein Rictor is necessary for serine 473 phosphorylation and that this complex can phosphorylate serine 473 on PKB *in vitro*.

The ability of PI3 kinase γ to activate endogenous PKB in COS-7 cells was assessed using structural and phosphospecific antibodies to PKB. It has been shown previously that PI3 kinase γ expressed in COS-7 cells is active without the need for further activation (Lopez-llasaca *et al.*, 1997) this may be due to the endogenous pool of free G protein βγ subunits reported to be present in COS-7 cells (Stephens et al., 1998). Figure 5.1b shows western blots of whole cell lysates (10μg) from COS-7

Figure 5.1

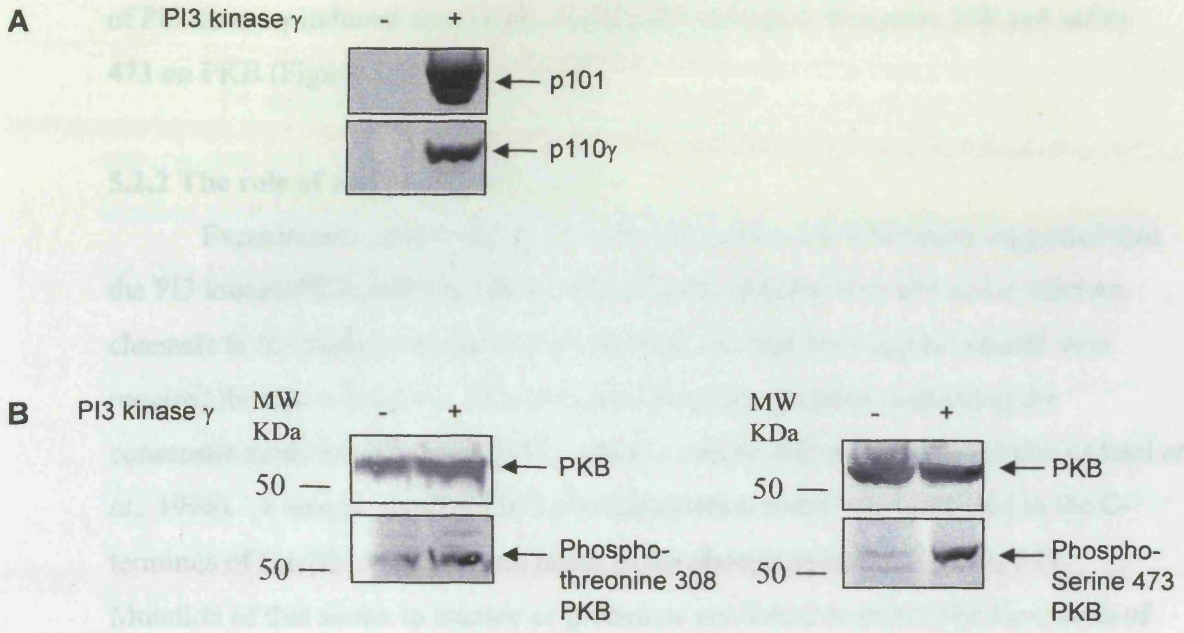

Figure 5.1. Expression of PI3 kinase γ and activation of endogenous protein kinase B in COS-7 cells.
A. Western blot showing expression of P101 (upper panel) and P110γ (lower panel) in transfected COS-7 cells.
B. PI3 kinase γ induces phosphorylation of endogenous PKB. PKB is detected in both transfected and untransfected COS-7 cells (upper panel) but phosphorylation on threonine 308 and serine 473 (lower panels) is only detected when PI3 kinase γ is transfected.

cells transfected with P101 and P110γ. Antibodies specific for the phosphorylated forms of threonine 308 or serine 473 (Upstate biotechnology) of PKB were used to probe the phosphorylation states of these residues after transfection of PI3 kinase γ. PKB is present endogenously in COS-7 cells (Figure 5.1b, top panel) and transfection of PI3 kinase γ induced an increase in phosphorylation at threonine 308 and serine 473 on PKB (Figure 5.1b, lower panel).

5.2.2 The role of serine 574 in $Ca_V\beta 2a$

Experiments performed by Dr Patricia Viard in our laboratory suggested that the PI3 kinase/PKB pathway was involved in the translocation of $Ca_V2.2$ calcium channels to the plasma membrane and furthermore that the $Ca_V\beta 2a$ subunit was required for this to happen. PKB will phosphorylate proteins containing the consensus motif R-x-R-x-x-S/T-F/L, where x can be any amino acid residue (Alessi *et al*,. 1996). A unique putative PKB phosphorylation motif was identified in the C-terminus of $Ca_V\beta 2a$ which would result in the phosphorylation of serine 574. Mutation of this serine to alanine or glutamate abolished or mimicked the effects of transfection of PI3 kinase γ and PKB on Ca_V calcium channel trafficking. Figure 5.2 shows the putative phosphorylation site in $Ca_V\beta 2a$ aligned with some known, published PKB phosphorylation sites.

Figure 5.2

Phosphorylation site	Protein
R A R T S S F	GSK-3β
R A R T S S F	GSK-3α
R T R T D S Y	mTOR
R S R H S S Y	BAD
R R R A V S M	FKHRL1
R G R S A S A	C-RAF
R Q R S T S T	B-RAF
R S R H R S K	$Ca_V\beta 2a$

Figure 5.2. Alignment of proteins containing published PKB phosphorylation sites against the putative site in the C-terminus of $Ca_V\beta 2a$. The sites of potential phosphorylation are marked in red. Taken from Brazil and Hemmings. (2001).

To investigate whether serine 574 of $Ca_V\beta 2a$ is a substrate for PKB, experiments were performed where $Ca_V\beta 2a$ was immunoprecipitated from ^{33}P labelled transfected COS-7 cells and the amounts of ^{33}P incorporated into wildtype $Ca_V\beta 2a$ was compared to $Ca_V\beta 2a$ where serine 574 was changed to alanine.

The $Ca_V\beta 2a$ and $Ca_V\beta 2a$ S574A were modified so that a haemaglutinin (HA) epitope tag was fused to their N-terminus, this was performed by polymerase chain reaction as described in Chapter 2. The $Ca_V\beta 2a$ subunit is palmitoylated at its N-terminus (Chien *et al.*, 1996) and this enhances its ability to traffic $Ca_V\alpha 1$ subunits to the plasma membrane. In Dr Viard's experiments palmitoylation was not required for PI3 kinase induced modulation of Ca_V calcium channels. Experiments were performed nevertheless to try to immunoprecipitated HA tagged wildtype $Ca_V\beta 2a$ from transfected cells. However, western blotting and immunoprecipitation experiments showed that the HA tag could barely be detected by western blotting with anti HA antibodies and the protein could not be captured by anti HA antibodies in immunoprecipitation (not shown). Interestingly, the same construct did behave similarly to $Ca_V\beta 2a$ without an HA tag when expressed in *Xeopus laevis* oocytes with $Ca_V2.2$ and $\alpha 2\delta 2$ (not shown). These result suggest that the lipid modification may hinder antibody binding or the HA tag may be removed during the post-translational modification. In the light of this data and to follow Dr Viard's experiments as closely as possible, these constructs were modified so that they were no longer able to be palmitoylated, this was done by substituting cysteine at positions 3 and 4 for serine (Stephens *et al.*, 2000). Metabolic labelling was performed as described in Chapter 2, COS-7 cells were transfected with $Ca_V\beta 2a$ or $Ca_V\beta 2a$S574A and with or without PI3 kinase γ. Cells were deprived of phosphate for 1 hour prior to labelling with 30μCi/ml [^{33}P] orthophosphate. HA tagged $Ca_V\beta 2a$ subunits were immunoprecipitated using anti HA monoclonal antibodies (Roche Diagnostics).

5.2.3 Mutation of serine 574 to alanine prevents PI3 kinase γ induced phosphorylation of $Ca_V\beta 2a$ in COS-7 cells

Immunoprecipites from ^{33}P labelled COS-7 cells were separated by SDS PAGE, transferred to a PVDF membrane and the amounts of incorporated phosphate were measured using autoradiography. It was necessary to transfer the proteins from the polyacrylamide gel to the membrane as ^{33}P has a much weaker signal than ^{32}P and even a thin layer of gel can retard the signal significantly. Figure 5.3 shows western blot using anti $Ca_V\beta 2$ antibodies (Chien *et al.*, 1996) and autoradiogram of immunoprecipitated ^{33}P labelled $Ca_V\beta 2a$. The amount of precipitated $Ca_V\beta 2$ protein is similar in all conditions (top panel) but the amount of incorporated phosphate is substantially increased in the condition where PI3 kinase γ is cotransfected with wildtype $Ca_V\beta 2a$ (lower panel). The amounts of incorporated phosphate was quantified using ImageQuant 5.2 (Molecular Dynamics, GE Healthcare) and expressed as a percentage of wildtype $Ca_V\beta 2a$ phosphorylation where PI3 kinase γ is not co-transfected (Figure 5.4). Coexpression of PI3 kinase γ caused an 83 ± 35 % (n=3) increase in wildtype $Ca_V\beta 2a$ phosphorylation whereas phosphorylation of $Ca_V\beta 2aS574A$ was reduced by 33 ± 14 % (n=3) when expressed alone and by 14 ± 10 % (n=3) when PI3 kinase was coexpressed.

These results show that in COS-7 cells, coexpression of PI3 kinase γ causes an increase in phosphorylation at position 574 on $Ca_V\beta 2a$. This data does not however implicate PKB in the direct phosphorylation of $Ca_V\beta 2a$, other protein kinases can be activated by PI3 kinase and this putative phosphorylation motif could be a target for other enzymes.

5.2.4 Protein kinase B can associate directly with $Ca_V\beta 2a$

Having shown that coexpression of PI3 kinase γ resulted in increased phosphorylation on serine 574 of $Ca_V\beta 2a$ and in view of the results from Dr Viards experiments in which coexpression of a constitutively active PKB induced trafficking of $Ca_V\beta 2a$ containing voltage dependent calcium channel complexes to the plasma membrane, coimmunoprecipitation experiments were performed to determine whether PKB could interact directly with $Ca_V\beta 2a$. The interaction of protein kinases with their substrates is not considered to be stable or long lasting as rapid rates of

Figure 5.3

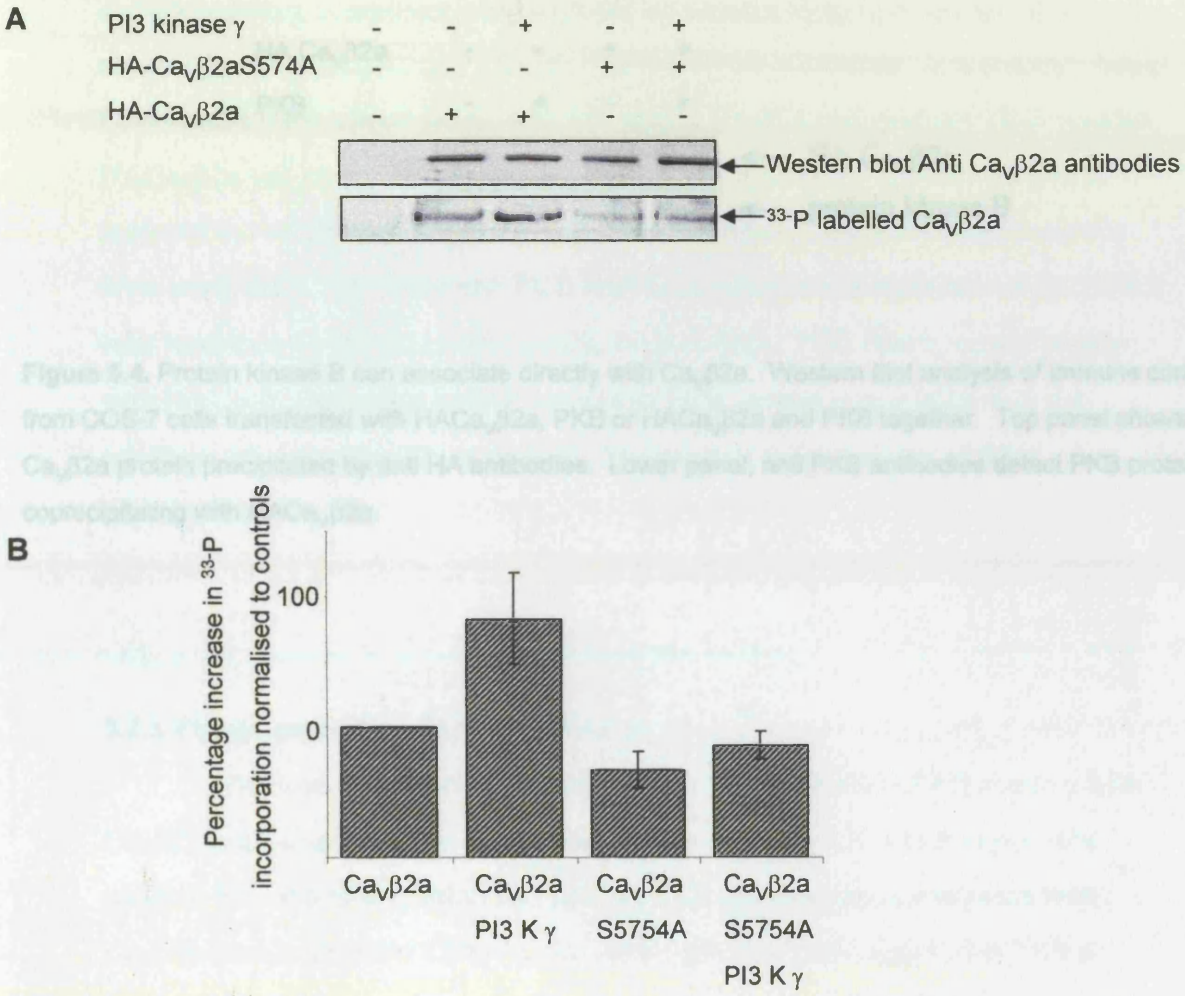

Figure 5.3. A. $Ca_V\beta2a$ S574A prevents PI3 kinase γ induced phosphorylation of $Ca_V\beta2a$ in COS-7 cells. Western blot using anti $Ca_V\beta2a$ antibodies shows $Ca_V\beta2a$ precipitated from ^{33}P labelled COS-7 cells (upper panel). Lower panel, autoradiogram showing ^{33}P incorporation into $Ca_V\beta2a$.
B. Histogram showing mean increase in ^{33}P incorporation into $Ca_V\beta2a$ alone or coexpressed with PI3 kinase γ or $Ca_V\beta2aS574A$ alone or coexpressed with PI3 kinase γ given as a percentage of ^{33}P incorporation into $Ca_V\beta2a$ expressed alone. Data are mean ± SEM of 3 independent experiments.

Figure 5.4

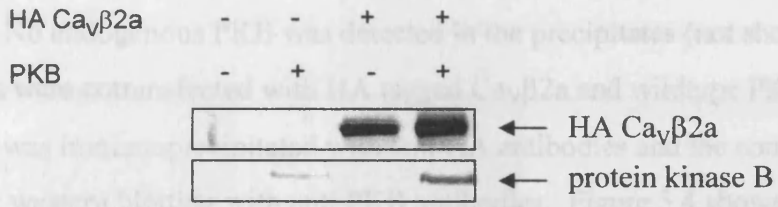

Figure 5.4. Protein kinase B can associate directly with $Ca_V\beta 2a$. Western blot analysis of immune complexes from COS-7 cells transfected with $HACa_V\beta 2a$, PKB or $HACa_V\beta 2a$ and PKB together. Top panel shows $Ca_V\beta 2a$ protein precipitated by anti HA antibodies. Lower panel, anti PKB antibodies detect PKB protein coprecipitating with $HACa_V\beta 2a$.

phosphorylation are often required in intracellular signalling cascades (Brazil and Hemmings., 2001) however PKB has previously been shown to form stable complexes with some of its protein partners (Lee *et al.*, 2001; Zhou *et al.*, 2001).

HA tagged $Ca_V\beta2a$ was immunoprecipitated from transfected COS-7 cells and the resulting complexes were analysed by western blotting with anti PKB antibodies. No endogenous PKB was detected in the precipitates (not shown). Next, COS-7 cells were cotransfected with HA tagged $Ca_V\beta2a$ and wildtype PKB together. $HACa_V\beta2a$ was immunoprecipitated with anti HA antibodies and the complexes analysed by western blotting with anti PKB antibodies. Figure 5.4 shows western blots using anti $Ca_V\beta2a$ and anti PKB antibodies of immunoprecipitates from COS-7 cells transfected with either $HACa_V\beta2a$, PKB or both. PKB clearly coprecipitates with $HACa_V\beta2a$ although a small amount of PKB protein is precipitated in the condition where no $Ca_V\beta2a$ is present. The result is representative of three experiments.

5.2.5 Phosphorylation of $Ca_V\beta2a$ *in vitro*

Previous experiments have shown that cotransfection of PI3 kinase γ with $Ca_V\beta2a$ leads to an increase in phosphorylation on serine 574 which is part of a putative PKB phosphorylation site and that PKB can coimmunoprecipitate with $Ca_V\beta2a$ from transfected COS-7 cells. Although these data suggest that PKB is involved, there is no evidence that it can directly phosphorylate this site in $Ca_V\beta2a$. Further experiments were performed to determine whether $Ca_V\beta2a$ is really a substrate for PKB, this was done by preparing purified $Ca_V\beta2a$ and $Ca_V\beta2a$ C-terminus and incubating these with activated PKB in the presence of ^{32}P ATP.

Initial experiments were performed using an N-terminally His(6) tagged $Ca_V\beta2a$ and $Ca_V\beta2aS574A$ purified from sf9 insect cells infected with a recombinant baculovirus. However, as has been reported previously (Puri et al., 1997) the $Ca_V\beta2$ protein copurified with an unknown protein kinase which caused substantial phosphorylation of $Ca_V\beta2a$ and $Ca_V\beta2aS574A$ without exogenously added PKB (not shown). To try to circumvent this problem, the C-termini (the last 80 amino acid

Figure 5.5

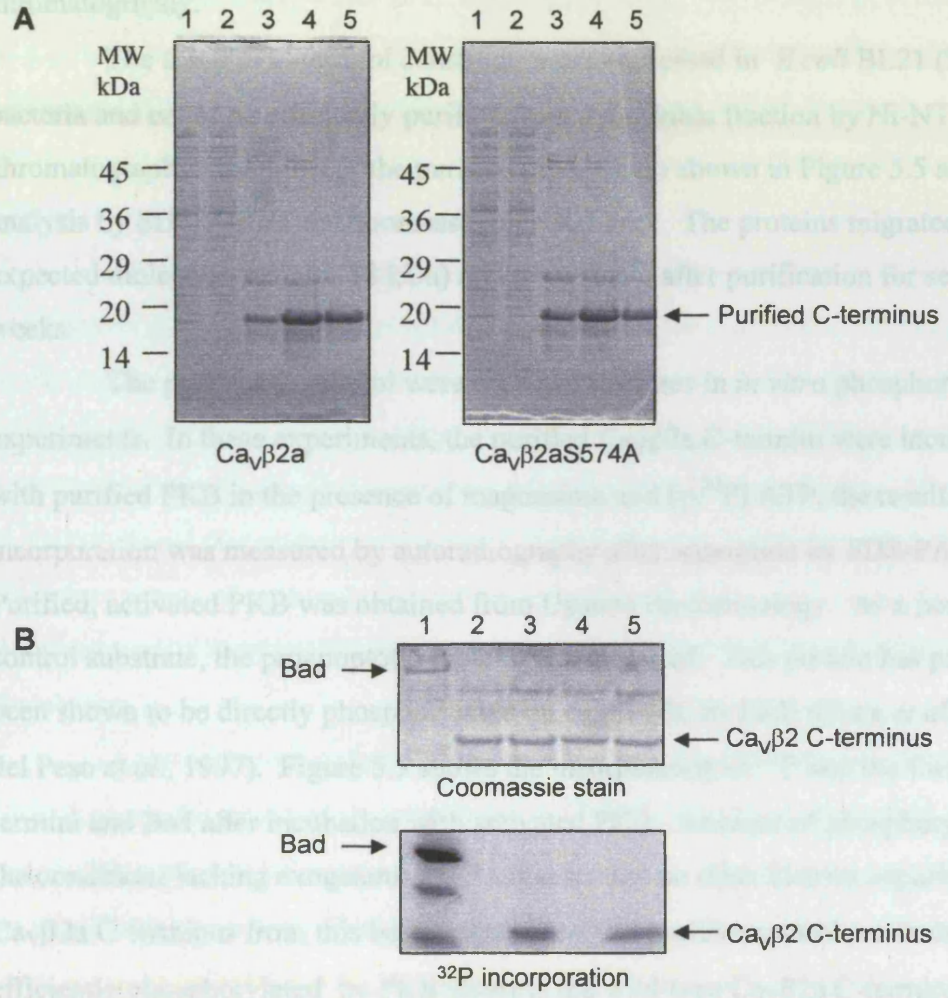

Figure 5.5. A. Coomassie blue stained SDS-PAGE on NuPage 4-12% Bis-Tris gel showing purified $Ca_V\beta2a$ wild-type and S574A C-termini used as substrate for *in vitro* kinase assays. Lane 1, whole lysate; lane 2, flow through; lanes 3,4,5, eluate. B. (upper panel) Coomassie blue stained SDS-PAGE on NuPage 4-12% Bis-Tris gel showing loadings of substrate proteins after phosphorylation reactions. Lane 1, Bad + PKB. Lane 2, $Ca_V\beta2a$ C-terminus only. Lane 3, $Ca_V\beta2a$ C-terminus + PKB. Lane 4, $Ca_V\beta2aS574A$ C-terminus only. Lane 5 $Ca_V\beta2aS574A$ C-terminus + PKB. Autoradiogram of the same gel showing Incorporation of ^{32}P into substrate proteins (Lower panel), S574A mutation causes 14.6 ± 5.6 % (n=3) reduction in phosphorylation.

residues) of $Ca_V\beta 2a$ and $Ca_V\beta 2S574A$ were amplified by PCR as described in Chapter 2 and subcloned into expression vector pET28 for expression in *E.coli.* The pET28 vector encodes a C-terminal His(6) tag which is fused to the $Ca_V\beta$ subunit C-termini so that the resulting proteins can be efficiently purified by Ni-NTA chromatography.

The $Ca_V\beta 2a$ C-termini constructs were expressed in *E.coli* BL21 (DE3) RIL bacteria and could be efficiently purified from the soluble fraction by Ni-NTA chromatography. Samples of the purified proteins are shown in Figure 5.5 after analysis by SDS-PAGE and coomassie blue staining. The proteins migrated at the expected molecular weight (18 kDa) and were stable after purification for several weeks.

The purified C-termini were used as substrates in *in vitro* phosphorylation experiments. In these experiments, the purified $Ca_V\beta 2a$ C-termini were incubated with purified PKB in the presence of magnesium and [γ-^{32}P] ATP, the resulting ^{32}P incorporation was measured by autoradiography after separation by SDS-PAGE. Purified, activated PKB was obtained from Upstate Biotechnology. As a positive control substrate, the proapoptotic protein Bad was used. This protein has previously been shown to be directly phosphorylated on serine 136 by PKB (Datta *et al.*, 1997; del Peso *et al.*, 1997). Figure 5.5 shows the incorporation of ^{32}P into the $Ca_V\beta 2a$ C-termini and Bad after incubation with activated PKB. Absence of phosphorylation in the conditions lacking exogenous PKB suggests that no other kinases copurify with $Ca_V\beta 2a$ C-terminus from this bacterial source. The positive control substrate Bad is efficiently phosphorylated by PKB whereas the wild-type $Ca_V\beta 2a$ C-terminus is phosphorylated to a lesser extent. There was not any substantial reduction in phosphorylation in the S574A mutant, the amount of ^{32}P incorporation was measured using ImageQuant 5.2 software (Molecular dynamics, GE healthcare) and incorporation into the S574A mutant C-terminus was found to reduced by 14.6 ± 5.6 % (n=3) compared to wildtype $Ca_V\beta 2a$ C-terminus. These results suggest that the $Ca_V\beta 2$ C-terminus is a poor substrate for PKB *in vitro*, the small reduction in incorporation seen in the S574A mutant may be due simply to a reduction in the number of serine residues available for phosphorylation in the substrate from 9 to 8, a reduction of 12 %. This would mean however that all available serine residues were substrates for PBK and thus that the all phosphorylation was completely non-specific.

5.3 Discussion

In addition to modulation by the $Ca_V\beta$ subunit, calcium influx through voltage dependent calcium channels can be modulated by other regulatory pathways which are linked to G-protein coupled receptors or receptor tyrosine kinases (Dolphin, 2003; Viard *et al.*, 2004; Viard *et al.*,1999; Blair *et al.*, 1997). Such modulation can be a direct physical interaction as is the case for G-protein $\beta\gamma$ subunits binding to the I-II linkers of the Ca_V 2 class of channel (De Waard *et al.*, 1997; Zamponi *et al.*, 1997) or via signaling intermediates which result in phosphorylation of the channel protein.

Experiments performed by Viard et al. (2004) in our laboratory showed that coexpresssion of PI3 kinase γ promotes voltage dependent calcium channel trafficking to the plasma membrane. The increase in trafficking is dependent upon the presence of the $Ca_V\beta2a$ subunit. The $Ca_V\beta2a$ subunit contains a putative PKB phosphorylation motif in its C-terminus which would result in phosphorylation of serine 574. Viard et al. (2004) found that mutation of serine 574 to alanine or glutamate which should abolish or mimic phosphorylation on this residue abolished or mimicked the effects of PI3 kinase or PKB on trafficking Ca_V calcium channel complexes to the plasma membrane.

Antibodies to the phosphorylated forms of threonine 308 and serine 473 of PKB were used to measure its activation. In COS-7 cells, expression of PI3 kinase γ resulted in activation of endogenous PKB and when $Ca_V\beta2a$ was coexpressed caused an 83 ± 35 % increase in phosphorylation on $Ca_V\beta2a$ compared to $Ca_V\beta2a$ expressed in the absence of PI3 kinase. The increase in $Ca_V\beta2a$ phosphorylation caused by coexpression of PI3 kinase was blocked by mutation of serine 574 on $Ca_V\beta2a$ to alanine suggesting that this residue is involved in the phosphorylation. These results correlate well with the results of electrophysiological and fluorescence confocal microscopy experiments preformed by Viard et al. (2004) and suggest that PKB may act directly on serine 574 of $Ca_V\beta2a$. Further evidence for a direct phosphorylation of $Ca_V\beta2a$ by PKB came from coimmunoprecipitation experiments which showed that PKB can be pulled down with $Ca_V\beta2a$ when both proteins were over expressed in COS-7 cells. However PKB also coprecipitated with $Ca_V\beta2aS574A$ (not shown) a possible explanation for this could be that although the target serine is mutated, the surrounding consensus sequence remains intact and so this serves as the site of

association. In addition, when pull down experiments were performed in reverse using an N-terminally HA tagged PKB construct, no interaction could be detected (not shown). This could be because the N-terminus is involved in the interaction with the $Ca_V\beta$ subunit or because the addition of the epitope tag disrupted the structure of the protein. Neither of these possibilities were investigated further. Experiments performed *in vitro* using the purified C-terminus of $Ca_V\beta2a$ and $Ca_V\beta2aS574A$ also failed to show that PKB can directly phosphorylate serine 574. The results show that the $Ca_V\beta2a$ C-terminus is not a good substrate for PKB *in vitro* as it was phosphorylated substantially less than the positive control substrate.

The PI3 kinase/ PKB pathway has previously been shown to be involved in trafficking and membrane insertion of ion channels and membrane proteins (Kanzaki *et al.*, 1999; Lhullier *et al.*, 2002; Wang *et al.*, 1999; Blair *et al.*, 1997; Viard *et al.*, 2004) although the molecular mechanism remains unclear. In this case, it appears that the PI3 kinase induced trafficking is dependent upon phosphorylation of $Ca_V\beta2a$ on serine 574 and that PKB is involved as the effect can be reproduced by transfection of a constitutively active PKB and abolished by the dominant negative mutant. It remains possible however that other kinases downstream from PKB are involved in phosphorylation of $Ca_V\beta2a$ on serine 574 and further work is necessary to either confirm that serine 574 as a substrate for PKB or to establish their molecular identity of the kinase responsible.

Recent work has revealed that the 14-3-3 family of proteins plays an important role in the function, translocation and membrane insertion of some ion channels (Bunney *et al.*, 2002). The 14-3-3 proteins are phospho-serine / phospho-threonine binding proteins which have been shown to play important roles in many cellular processes such as apoptosis and transcriptional regulation, in addition, they can control subcellular localisation of proteins and modulate protein–protein interactions (Yaffe, 2002; Tzivion *et al.*, 2001; Van Hemert., 2001). Rajan et al. (2002) reported that 14-3-3 proteins were essential for plasma membrane expression of TASK (two-pore-domain, acid-sensitive potassium channel) and only channels which were able to associate with 14-3-3 were localised at the plasma membrane. In addition, the brain chloride intracellular channel protein (Clic4) was shown to bind directly to 14-3-3ζ (Suginta *et al.*, 2001). As 14-3-3 proteins have been shown to bind to phosphorylated serine or threonine residues including those phosphorylated by PKB (Datta et al.,

1997; Del Peso et al., 1997) it is tempting to speculate that 14-3-3 binding to the site around the phosphorylated serine 574 of $Ca_V\beta 2a$ may represent the trafficking mechanism for $Ca_V\alpha 1/Ca_V\beta 2a$ calcium channels. However, most 14-3-3 protein binding partners contain one of two binding motifs (Muslin *et al.*, 1996; Yaffe *et al.*, 1997; Petosa *et al.*, 1998), either **R S X $_P$S X P** or **R X Y/F $_P$S X P** where **X** is any amino acid residue and **$_P$S** is phospho-serine. These motifs are absent in the C-terminus of $Ca_V\beta 2a$ and it is therefore unlikely that $Ca_V\beta 2a$ interacts directly with 14-3-3 proteins although the possibility of interactions occurring via other proteins cannot be ruled out.

In conclusion, experiments described here show that in COS-7 cells $Ca_V\beta 2a$ is phosphorylated on serine 574 in response to PI3 kinase activation. $Ca_V\beta 2a$ will associate with PKB in COS-7 cells and although it is likely that PKB is responsible for phosphorylation of serine 574, further experiments are necessary to both confirm the identity of the serine 574 kinase and shed more light on the molecular mechanism by which PI3 kinase activation leads increased plasma membrane expression of voltage dependent calcium channels.

Chapter 6:

Identification of protein binding partners of $Ca_V\beta$ subunits

6.1 Introduction

The $Ca_V\beta$ subunit is an essential component of the HVA calcium channel complex controlling both trafficking and modulation of the pore forming $\alpha 1$ subunit. Until recently the only function of the auxiliary β subunit was thought to be to modulate the expression, targeting and gating of the $\alpha 1$ subunit. A number of recent studies have provided evidence to suggest that $Ca_V\beta$ subunits can interact with proteins other than the $Ca_V\alpha 1$ and that $Ca_V\beta$ could even act as an independent regulatory protein. The first such report was from Beguin et al. (2001). These workers found that the small Guanosine triphosphatase (GTPase) Gem, a member of the RGK family of G proteins which includes Rem, Rem2 and Rad interacted with $Ca_V\beta 3$ in a yeast two-hybrid assay, immunoprecipitation subsequently confirmed a direct interaction between these two proteins. The GTP-bound form of Gem in the presence of calcium and calmodulin was found to reduce calcium channel activity by preventing the β subunit from trafficking the $Ca_V\alpha 1$ to the plasma membrane. This reduction was in calcium channel activity was found for $Ca_V\beta 1$, 2 and 3 subunits and both L-type and non L-type $\alpha 1$ subunits suggesting, that it is a general mechanism of HVA calcium channel regulation.

Subsequent studies found that two other members of this family Rem and Rad could also associate with $Ca_V\beta$ subunits (Finlin *et al.*, 2003). Coexpression of Rem with cells expressing $Ca_V1.2$ and $Ca_V\beta 2a$ resulted in the abolition of HVA calcium currents, also there was no effect on low voltage activated calcium channels. The site of interaction on the RGK protein family was mapped to a highly conserved polybasic region in the last 32 residues of the C-terminus.

Another novel binding partner for the $Ca_V\beta$ subunit was reported recently by Viard et al., (2004). This work showed that the $Ca_V\beta 2a$ subunit interacts with and can be phosphorylated in its C-terminus by Akt/PKB kinase. Akt is activated by activation of PI3 kinase which recruits it to the plasma membrane. Phosphorylation of $Ca_V\beta 2a$ resulted in increased HVA channel trafficking to the plasma membrane. This mechanism was shown to be specific for the $Ca_V\beta 2a$ subunit and may represent a more specialised mechanism of HVA calcium channel regulation.

Whilst these new interactions appear to be specific for the $Ca_V\beta$ subunit, the functional outcome of the above interactions is still associated with the $Ca_V\alpha 1$

subunit, the result being an increase or decrease in calcium channel activity. Two novel functions of the $Ca_V\beta$ subunit have been reported which seem to be independent of their ability to modulate calcium channel function. Firstly, work by Berggren et al. (2004) showed that in the pancreatic β cells of a $Ca_V\beta3^{-/-}$ mouse, the modulation of L type calcium channels was not affected compared to wild-type, nor was the decrease in $Ca_V\beta3$ compensated for by an increase in expression of other $Ca_V\beta$ subunits. The mutant mice displayed enhanced intracellular calcium oscillation frequency leading to increased glucose induced insulin release and therefore a more efficient glucose homeostasis. The $Ca_V\beta3$ subunit appears to modulate the formation of inositol 1,4,5-trisphosphate ($InsP_3$) and thus modulate the release of calcium from intracellular stores completely independently from modulating $Ca_V\alpha1$ subunits. Secondly, a short isoform of the $Ca_V\beta4$ subunit known as β4c was isolated from cochlea, (Hibino *et al.*, 2003) this variant is truncated between the SH3 and GK like domains. Although the authors suggest that it retains the sequence known as BID and so can interact with the AID of a HVA α1 subunit, more recent structural data has shown that most of the GK module is required for binding to the AID. In addition to this the authors report that β4c has little effect on the current density again suggesting that it may not interact with AID. The short $Ca_V\beta4c$ subunit did however modulate some HVA calcium channel properties as has been described for other short $Ca_V\beta$ subunit isoforms (Cohen *et al.*, 2005). Yeast two-hybrid assays with this short isoform revealed that it could interact with a nuclear protein involved in gene silencing known as chromobox protein 2 (CHCB2), this was confirmed by co-immunoprecipitation. Analysis of $Ca_V\beta4c$ subcellular location revealed that it is targeted to the nucleus of transfected tsA201 cells and can regulate gene silencing activity of CHCB2 although no mechanism was proposed as the short $Ca_V\beta$ subunit did not interact with the methyltansferase enzyme SUV39H1 or transcription factor 1β both of which are involved in gene silencing. The question of whether these functions are primary or secondary to the modulation of HVA calcium channels is still an open one although there is evidence to suggest that under physiological conditions $Ca_V\beta$ subunits can unbind from the α1 (Canti *et al.*, 2001; Restituto *et al.*, 2001; Bichet *et al.*, 2000), leaving them free to perform other roles.

In the light of the results of work from other groups and work in our laboratory which identified Akt/PKB kinase as a binding partner for the $Ca_V\beta 2a$ subunit (Viard et al., 2004), experiments were designed to try to identify other proteins which may interact with $Ca_V\beta$ subunits. A conventional approach would have been to use $Ca_V\beta$ subunits as bait in a yeast two-hybrid assay to screen cDNA libraries of brain or other tissue for potential binding partners. However, this approach, although sensitive, is time consuming and requires substantial amounts of screening, subcloning, cloning and DNA sequencing. As procedures for immunoprecipitation and purification of epitope tagged $Ca_V\beta 1$ and 2 subunits were already in place, these techniques were used to "fish" for β subunit binding partners from a neuronal cell line and from a mouse brain lysate.

6.2 Results

6.2.1 Expression of HA tagged $Ca_V\beta$ subunits in the NG108-15 cell line.

Attempts were made to overexpress $Ca_V\beta$ subunits in NG108-15 cells. NG108-15 is a neuronal cell line formed from the fusion of a mouse neuroblastoma and a rat glioma cell line (Klee *et al.*, 1973). These cells have been widely studied and display electrophysiological and pharmacological properties similar to sympathetic neurons (Tsunoo *et al.*, 1986; Docherty *et al.*, 1989; Filippov *et al.*, 1996 Buisson *et al.*, 1995). The NG108-15 cell line expresses LVA calcium channels when undifferentiated, expression of $Ca_V3.2$ and $Ca_V3.3$ but not $Ca_V3.1$ channels have been detected (Chemin *et al.*, 2002), the expression of LVA channels appears to change after differentiation. Differentiation of NG108-15 cells can be achieved by treatment with isobutylmethylxanthine (50μM) and prostaglandin E1 (10μM). Three to six days after treatment the cells change from being spherical and clustered and begin to express neurite like projections, accompanied by a slowed rate of growth. Many electrophysiological studies have shown that differentiation of NG108-15 cells leads to an increase in the expression of HVA calcium channels (Brown *et al.*, 1989; Caulfield *et al.*,1992; Docherty *et al.*,1992; Schmitt *et al.*,1995). Pharmacological blockers of HVA calcium channels have been used to confirm the presence of N, P/Q L and R type current (Lukyanetz, 1998). Gottschalk et al. (1999) performed RT-PCR analysis on total RNA from undifferentiated NG108-15 cells and showed that all four $Ca_V\beta$ subunits were expressed as were $Ca_V2.2$ and $Ca_V1.2$ $\alpha1$ subunits. These findings make the NG108-15 cell line a reasonable model for searching for $Ca_V\beta$ subunit binding partner proteins as they express all four $Ca_V\beta$ subunits endogenously and are likely therefore to express proteins with which they associate.

6.2.2 Immunoprecipitation of HA tagged proteins

Previous experiments (see chapter 5) used haemaglutinin (HA) tagged $Ca_V\beta 2a$ constructs which could be efficiently precipitated from transfected Cos-7 cells using anti HA monoclonal antibodies. These constructs were modified so that they were no longer able to be palmitoylated, this was done by changing cystine 3 and 4 to serine. The same construct was expressed in NG105-15 cells. In addition to this, an HA tag was introduced into the N-terminus of $Ca_V\beta 1b$. It was necessary to subclone both HA tagged constructs from expression vector pMT2 into pRK5 as preliminary experiments showed that the fluorescent marker protein GFP did not express in NG108-15 cells when it was in pMT2 (not shown). NG108-15 cells in 75cm dishes were transfected 2-4 hours after the start of the differentiation process as described in chapter 2 with 15μg $Ca_V\beta$ subunit DNA or 15μg empty pRK5 vector as a control . Four days after transfection, cells were harvested and HA tagged $Ca_V\beta$ subunits were immunoprcipitated using 4μg anti HA antibody (clone 3F10, Roche diagnostics).

Western blot analysis of whole cell lysates (10μg) from transfected NG108-15 cells was performed using anti $Ca_V\beta$ and anti HA antibodies. Figure 6.1 shows good expression of both $Ca_V\beta 2a$ and $Ca_V\beta 1b$ when lysates were probed with antibodies against the respective subunits, a weak signal at 75 kDa in the negative control lane may represent some endogenous $Ca_V\beta$ subunit. Attempts were made to express the wild-type, $Ca_V\beta 2a$ subunit which could be palmitoylated. As palmitoylation directs $Ca_V\beta 2a$ to the plasma membrane in the absence of a $Ca_V\alpha 1$ (Leroy *et al.,* 2005) it may be able to interact with membrane associated protein partners. However, although this construct induced slowed inactivation kinetics typical of $Ca_V\beta 2a$ when expressed in *Xenopus laevis* oocytes with $Ca_V2.2$ and $\alpha 2\delta 2$, no HA tag could be detected by western blotting and subsequent immunoprecipitation experiments showed that HA tagged wild-type $Ca_V\beta 2a$ could not be captured by anti HA antibodies, suggesting that either the lipid modification hinders antibody binding or the HA motif is modified or removed during the palmitoylation process.

The $Ca_V\beta$ subunits were immunoprecipitated from whole lysates of transfected, differentiated NG108-15 cells with anti HA monoclonal antibodies. Figure 6.2 shows a Coomassie stained SDS PAGE gel of HA tagged $Ca_V\beta 1b$ and $\beta 2a$

Figure 6.1

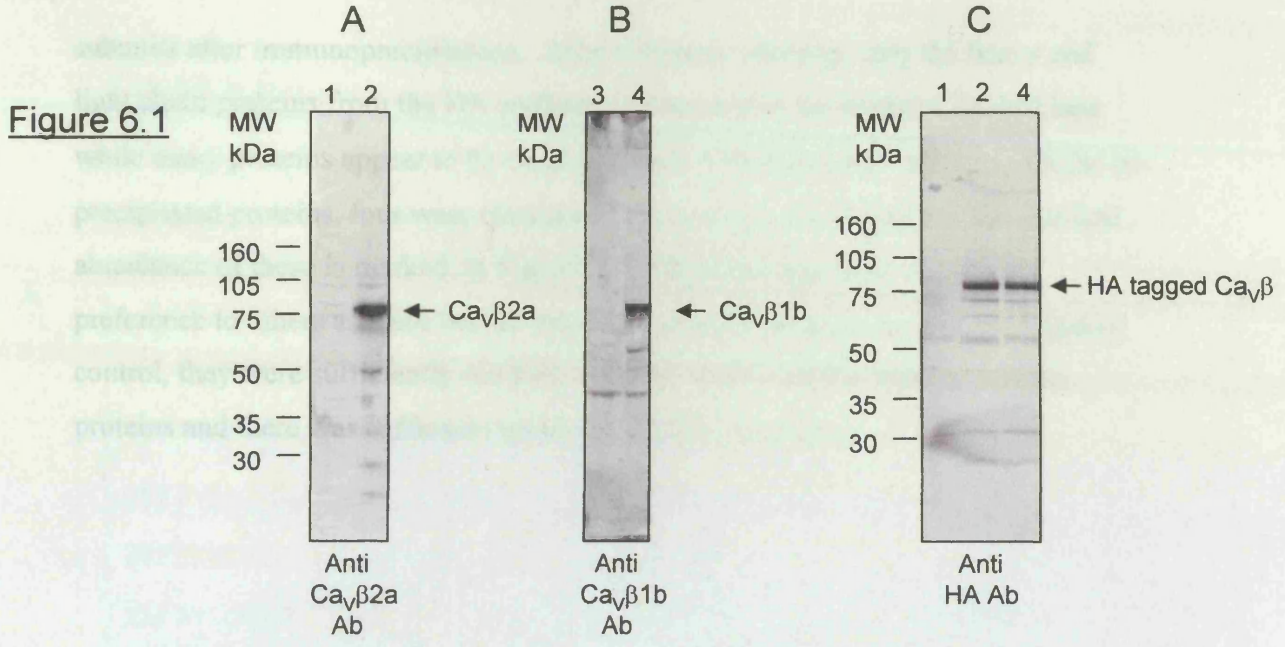

Figure 6.1 Expression of HA tagged $Ca_V\beta 2a$ and $Ca_V\beta 1b$ in differentiated NG108-15 cells. Western blot analysis of whole cell lysates probed with A. Anti $Ca_V\beta 2a$ or B. Anti $Ca_V\beta 1b$ or C. Anti HA antibodies. Cells were transfected with empty vector (Lane 1), HA$\beta 2a$ (lane 2), empty vector (Lane 3), HA$\beta 1b$ (Lane 4). Position of HA tagged $Ca_V\beta$ subunit is indicated.

Figure 6.2

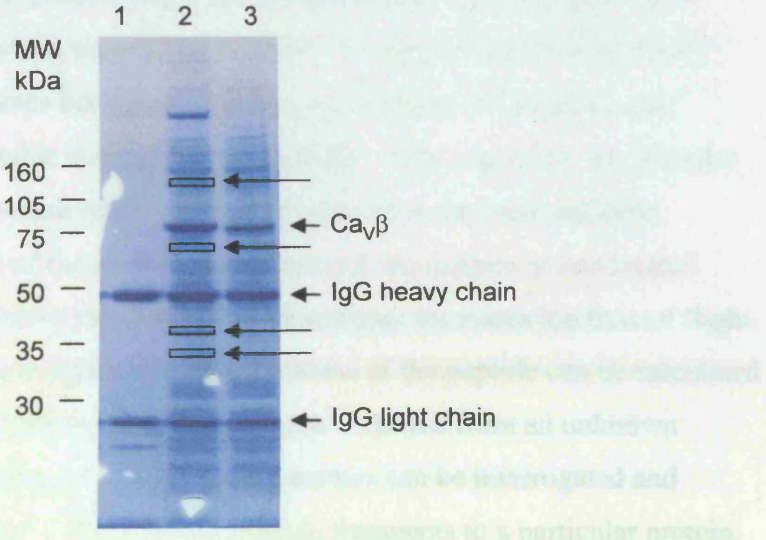

Figure 6.2 Coomassie blue stained SDS-PAGE on NuPage 4-12% Bis-Tris gel showing immunoprecipitated $Ca_V\beta$ subunits and co-precipitated proteins. NG108-15 cells were transfected with empty vector (Lane 1), HA$\beta 2a$ (Lane 2), HA$\beta 1b$ (Lane 3). Positions of the $Ca_V\beta$ subunits, the heavy and light chain antibody fragments and the position of the proteins selected for further analysis are shown.

subunits after immunoprecipitation. After extensive washing, only the heavy and light chain proteins from the HA antibody can be seen in the negative control lane while many proteins appear to be co-precipitated with both $Ca_V\beta$ subunits. Of the co-precipitated proteins, four were chosen as candidates for identification, the size and abundance of these is marked on Figure 6.2. These proteins were chosen in preference to others as there was no trace of a corresponding protein in the negative control, they were sufficiently resolved so as not to be contaminated by nearby proteins and there was sufficient material for further analysis.

6.2.3 Identification of unknown proteins by Peptide Mass Fingerprinting

Peptide mass fingerprinting (PMF) was used to identify the unknown proteins in this study. Proteins are subjected to proteolytic digestion followed by Matrix Assisted Laser Desorption Ionisation Time of Flight (MALDI-TOF) mass spectroscopy. PMF works because each individual protein yields a unique set of peptides after digestion with a proteolytic enzyme. Trypsin is used to completely digest the proteins, it cleaves between lysine (K) and arginine (R) residues and generates peptides of suitable size for further analysis. After digestion, the peptides are mixed with a matrix which readily absorbs energy from the laser and aids desorption and ionisation of the sample. Once ionised, the sample is accelerated through an electric field into a vacuum where an analyser measures the time of flight, as small peptides fly slower than large ones, the mass of the peptide can be calculated from the time of flight. Once a spectrum has been collected from an unknown protein, databases containing fully sequenced genomes can be interrogated and software can be used which will assign the peptide fragments to a particular protein.

In these experiments, Peptide Mass Fingerprinting analysis was carried out by Dr Dinah Rahman (Section of Proteomics, MRC Clinicial Sciences Centre, Imperial College London). The resulting spectra were analysed using Mascot software (Matrix Science, www.matrixscience.com).

Figure 6.3

35 kDa protein. Glyceraldehyde-3-phosphate dehydrogenase – Accession number P09328

A

1 VKVGVNGFGR IGRLVTRAAF SCDKVDIVAI NDPFIDLNYM VYMFQYDSTH

51 GKFNGTVKAE NGKLVINGKP ITIFQERDPV KIKWGDAGAE YVVESTGVFT

101 TMEKAGAHLK GGAKRVIISA PSADAPMFVM GVNHEKYDNS LKIVSNASCT

151 TNCLAPLAKV IHDNFGIVEG LMTTVHAITA TQKTVDGPSG KLWRDGRGAA

201 QNIIPASTGA AKAVGKVIPE LNGKLTGMAF RVPTPNVSVV DLTCRLEKPA

251 KYDDIKKVVK QAAEGPLKGI LGYTEDQVVS CDFNSNSHSS TFDAGAGIAL

301 NDNIVKLISW YDNEYGYSNR VVDLMAYMAS KE

45 kDa protein. Cardiac actin - Accession number Q9DFH5

B

1 MCDDEEVTAL VCDNGSGLVK AGFAGDDAPR AVFPSIVGRPRHQGVMVGMG

51 QKDSYVGDEA QSKRGILTLK YPIEHGIITN WDDMEKIWHH TFYNELRVAP

101 EEHPTLFTEA PLNPKVNREK MTQIMCETFN VPAMYVVIQA VLSLYASGRT

151 TGIVLDSGDG VTHIVPIYEG YALPHAIQRL DLAGRDLTDY LMKILTERGY

201 SFVTTAEREI VRDIKEKLCY VALDFENEMA TAASSSSLEK SYELPDGQVI

251 TIGNERFRCP ETLFQPSFIG MESAGIHETT YNSIMKCDID IRKDLYANNV

301 LSGGTTMYPG IADRMQKEIT ALAPSTMKIK IIVPPERKYS VWIGGSILAS

351 LSTFQQMWIS KQEYDEAGPS IVHRKCF

70kDa protein. Bos taurus serum albumin – Accession number AF542068

C

1 MKWVTFISLL LLFSSAYSRG VFRRDTHKSE IAHRFKDLGE EHFKGLVLIA
51 FSQYLQQCPF DEHVKLVNEL TEFAKTCVAD ESHAGCEKSL HTLFGDELCK
101 VASLRETYGD MADCCEKQEP ERNECFLSHK DDSPDLPKLK PDPNTLCDEF
151 KADEKKFWGK YLYEIARRHP YFYAPELLYY ANKYNGVFQE CCQAEDKGAC
201 LLPKIETMRE KVLTSSARQR LRCASIQKFG ERALKAWSVA RLSQKFPKAE
251 FVEVTKLVTD LTKVHKECCH GDLLECADDR ADLAKYICDN QDTISSKLKE
301 CCDKPLLEKS HCIAEVEKDA IPENLPPLTA DFAEDKDVCK NYQEAKDAFL
351 GSFLYEYSRR HPEYAVSVLL RLAKEYEATL EECCAKDDPH ACYSTVFDKL
401 KHLVDEPQNL IKQNCDQFEK LGEYGFQNAL IVRYTRKVPQ VSTPTLVEVS
451 RSLGKVGTRC CTKPESERMP CTEDYLSLIL NRLCVLHEKT PVSEKVTKCC
501 TESLVNRRPC FSALTPDETY VPKAFDEKLF TFHADICTLP DTEKQIKKQT
551 ALVELLKHKP KATEEQLKTV MENFVAFVDK CCAADDKEAC FAVEGPKLVV
601 STQTALA

100kDa protein. Heterogeneous nuclear ribonucleoprotein U - Accession number Q6IMY8

D

1 MSSSPVNVKK LKVSELKEEL KKRRLSDKGL KADLMDRLQA ALDNEAGGRP
51 AMEPGNGSLD LGGDAAGRSG AGLEQEAAAG AEDDEEEEGI AALDGDQMEL
101 GEENGAAGAA DAGAMEEEEA ASEDENGDDQ GFQEGEDELG DEEEGAGDEN
151 GHGEQQSQPP AAAQQASQQR GPGKEAAGKS SGPTSLFAVT VAPPGARQGQ
201 QQAGGDGKTE QKAGDKKRGV KRPREDHGRG YFEYIEENKY SRAKSPQPPV
251 EEEDEHFDDT VVCLDTYNCD LHFKISRDRL SASSLTMESF AFLWAGGRAS
301 YGVSKGKVCF EMKVTEKIPV RHLYTKDIDI HEVRIGWSLT TSGMLLGEEE
351 FSYGYSLKGI KTCNCETEDY GEKFDENDVI TCFANFETDE VELSYAKNGQ
401 DLGVAFKISK EVLADRPLFP HVLCHNCAVE FNFGQKEKPY FPIPEDCTFI
451 QNVPLEDRVR GPKGPEEKKD CEVVMMIGLP GAGKTTWVTK HAAENPGKYN
501 ILGTNTIMDK MMVAGFKKQM ADTGKLNTLL QRAPQCLGKF IEIAARKKRN
551 FILDQTNVSA AAQRRKMCLF AGFQRKAVVV CPKDEDYKQR TQKKAEVEGK
601 DLPEHAVLKM KGNFTLPEVA ECFDEITYVE LQKEEAQKLL EQYKEESKKA
651 LPPEKKQNTG SKKSNKNKSG KNQFNRGGGH RGRGGFNMRGGNFRGGAPGN
701 RGGYNRRGNM PQRGGGGGSGGIGYPYPRGPVFPGRGGYSNRGNYNRGGMP
751 NRGNYNQNFR GRGNNRGYKN QSQGYNQWQQ GQFWGQKPWS QHYHQGYY

Figure 6.3 Numbers and positions of peptides identified by peptide mass fingerprinting analysis on proteins co-precipitating with $Ca_V\beta 2a$. **A** positions of the 7 peptides generated from the 35kDa protein. Protein identified as Glyceraldehyde-3-phosphate dehydrogenase (P09328). **B** Positions of the 8 peptides generated from the 40 kDa protein. Protein identified as Cardiac actin (Q9DFH5). **C** Positions of the 10 peptides generated from the 70 kDa protein. Protein identified as Bovine Serum Albumin (AF542068). **D** Positions of the 10 peptides generated from the 100 kDa protein. Protein identified as Heterogeneous nuclear ribonucleoprotein U (Q6IMY8).

Spectra were obtained from all four of the unknown proteins submitted for identification. The abundance and positions of the peptides relative to the proteins from which they originate is shown in Figure 6.3. The 35 kilodalton protein was identified as Glyceraldehyde-3-phosphate dehydrogenase, 7 different peptides were identified which represents a coverage of 29%. The 40 kilodalton protein was identified as Actin, 8 peptides were identified representing 23% coverage. The 70 kilodalton protein was identified as Bovine Serum Albumin (BSA), 10 peptides were identified representing 19% coverage. The 100 kilodalton protein was identified as Heterogeneous nuclear ribonucleoprotein U, 10 peptides were identified representing 15% coverage.

In all cases, many peptides were identified, representing significant portions of the proteins from which they originated, it is therefore highly likely that the identifications are correct. However, the presence of BSA and actin in the samples suggests that the samples may have been contaminated during the precipitation or the SDS-PAGE procedure, the relevance of the other two proteins identified is therefore called into question. No further work was carried out on these samples.

6.2.4 Co-precipitation of $Ca_V\beta 1b$ binding partners from mouse brain extract

Co-precipitation of binding partners for $Ca_V\beta 1b$ from the neuronal cell line proved to be unsuccessful. Attempts were made to use already purified $Ca_V\beta 1b$ and fragments of $Ca_V\beta 1b$ to capture potential binding partners from native tissue, in this case mouse brain.

Full length $Ca_V\beta 1b$ was expressed in *E.coli* and purified by Ni-NTA chromatography as has been described previously (Bell *et al.*, 2001). Two further constructs were generated by removing the C-terminus of $Ca_V\beta 1b$ by restriction enzyme digestion of $Ca_V\beta 1b$ cDNA. These constructs are $Ca_V\beta 1b$ C-terminus and $Ca_V\beta 1b$ without C-terminus ($Ca_V\beta 1b\Delta$C-terminus). The two new constructs were expressed in *E.coli* and purified using NI-NTA chromatography. Figure 6.4 (Left panel) shows an SDS PAGE gel containing samples of the purified $Ca_V\beta 1b$ fragments.

Figure 6.4

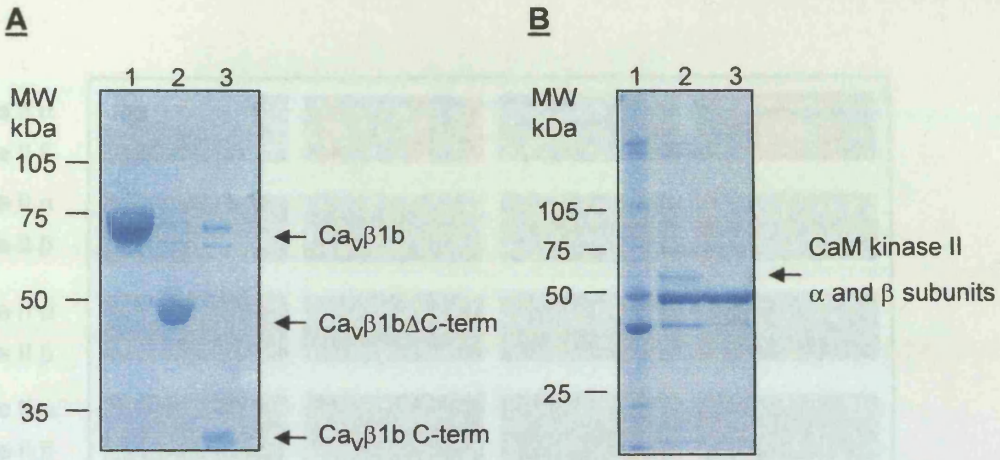

Figure 6.4. A. Coomassie blue stained SDS PAGE gel showing purified proteins used in pull down experiments $Ca_V\beta1b$ (lane 1) $Ca_V\beta1b$ Δ C-terminus (lane 2) $Ca_V\beta1b$ C-terminus (lane 3). **B**. Coomassie blue stained SDS PAGE gel showing protein eluted from $Ca_V\beta1b$ coupled to sepharose beads after incubation with mouse brain extract. Control (lane 1), CaVβ1b (lane 2) CaVβ1b Δ C-terminus (lane 3). Band representing CaM kinase II α and β subunits is indicated.

Figure 6.5

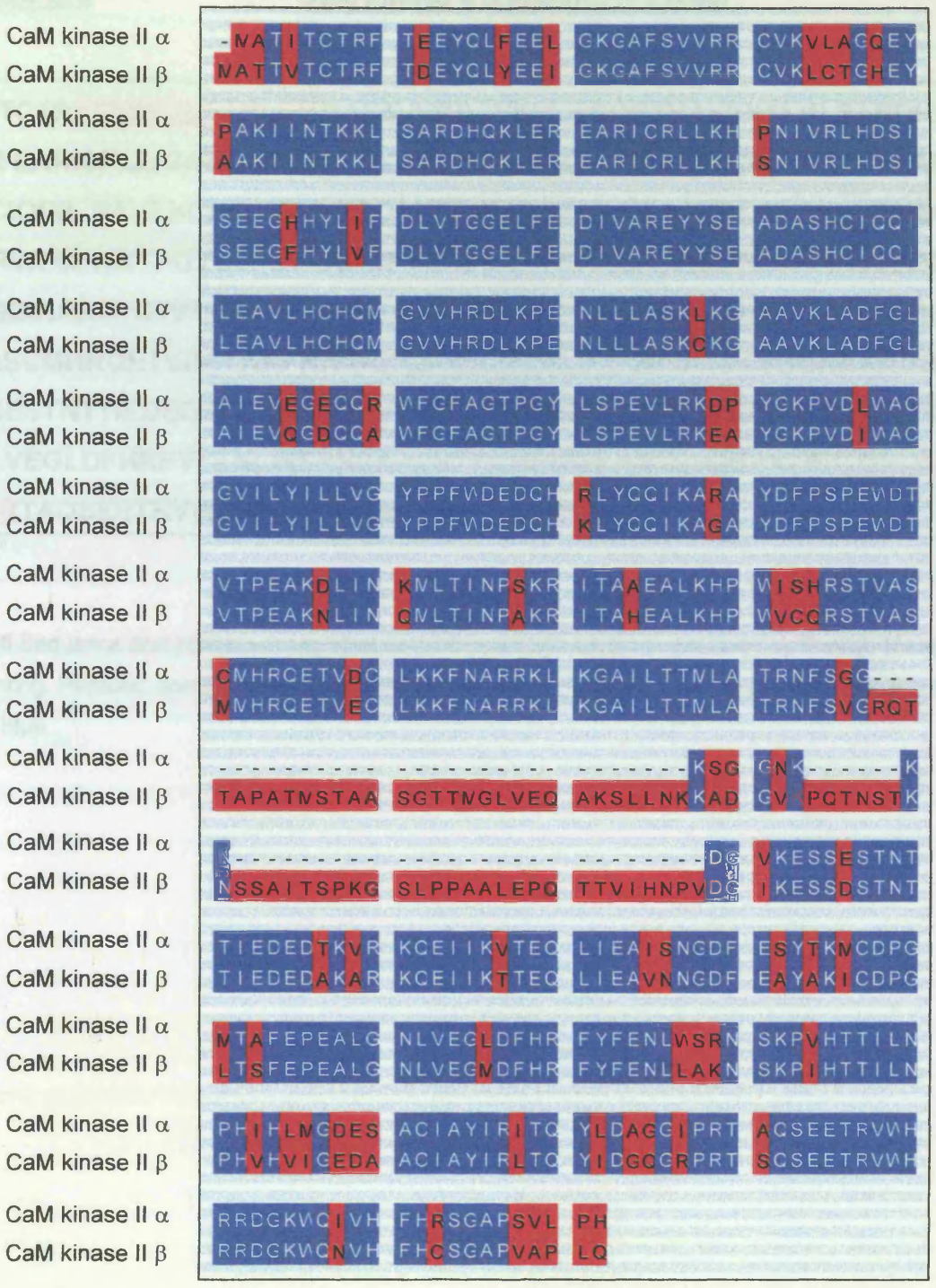

Figure 6.5 Alignment of primary sequences of mouse CaM kinase II α (P11789) and β (CAA45160) subunits, differences in sequence are shown in red.

Figure 6.6 **CaM kinase II α subunit (P11789)**

MATITCTRFTEEYQLFEELGKGAFSVVRRCVKVLAGQEYPAKIINTKKLSARDHQ
KLER EARICRLLKHPNIVRLHDSISEEGHHYLIFDLVTGGELFEDIVAREYYSEAD
ASHCIQQIL EAVLHCHQMGVVHRDLKPENLLLASKLKGAAVKLADFGLAIEVEG
EQQRWFGFAGTPGYLSPEVLRKDPYGKPVDLWACGVILYILLVGYPPFWDEDQH
RLYQQIKARAYDFPSPEWDTVTPEAKDLINKMLTINPSKRITAAEALKHPWISHR
STVASCMHRQETVDCLKKFNARRKLKGAILTTMLATRNFSGGKSGGNKKNDGV
KESSESTNTTIEDEDTKVRKQEIIKVTEQLIEAISNGDFESYTKMCDPGMTAFEPEA
LGNLVEGLDFHRFYFENLWSRNSKPVHTTILNPHIHLMGDESACIAYIRITQYLDA
GGIPRTAQSEETRVWHRRDGKWQIVHFHRSGAPSVLPH

Figure 6.6 Sequence and position of peptides derived from CaM kinase II α subunit by Peptide Mass Fingerprinting. Peptides specific for the α subunit shown in red, peptides common to both α and β subunits shown in blue

Figure 6.7

CaM kinase II β subunit (CAA45160)

MATTVTCTRFTDEYQLYEEIGKGAFSVVRRCVKLCTGHEYAAKIINTKKLSARD
HQKLEREARICRLLKHSNIVRLHDSISEEGFHYLVFDLVTGGELFEDIVARE
YYSEADASHCIQQILEAVLHCHQMGVVHRDLKPENLLLASKCKGAAVKLADFGLAIEV
QGDQQAWFGFAGTPGYLSPEVLRKEAYGKPVDIWACGVILYILLVGYPPFWDED
QHKLYQQIKAGAYDFPSPEWDTVTPEAKNLINQMLTINPAKRITAHEALKHPWV
CQRSTVASMMHRQETVECLKKFNARRKLKGAILTTMLATRNFSVGRQTTAPAT
MSTAASGTTMGLVEQAKSLLNKKADGVKPQTNSTKNSSAITSPKGSLPPAALEP
QTTVIHNPVDGIKESSDSTNTTIEDEDAKARKQEIIKTTEQLIEAVNNGDFEAYAKI
CDPGLTSFEPEALGNLVEGMDFHRFYFENLLAKNSKPIHTTILNPHVHVIGEDAA
CIAYIRLTQYIDGQGRPRTSQSEETRVWHRRDGKWQNVHFHCSGAPVAPLQ

Figure 6.7 Sequence and position of peptides derived from CaM kinase II β subunit by Peptide Mass Fingerprinting. Peptides specific for the β subunit shown in red, peptides common to both α and β subunits shown in blue

Equal amounts of the purified proteins (5mg) were chemically immobilised onto 1 ml HiTrap NHS activated sepharose columns (Amersham biosciences, Little Chalfont, UK) according to manufacturers instructions, as a control one column was activated and blocked but no protein was immobilised. The brains of 10 adult mice were homogenised and prepared as described in chapter 2.2.12. Mouse brain was used for several reasons, firstly $Ca_V\beta 1b$ is expressed highly in brain and this material is likely to contain proteins with which it associates, secondly a full mouse genome sequence is available, this greatly facilitates identification of unknown proteins after MALDI-TOF spectroscopy. Equal amounts of the cleared brain extract were applied to each column. After extensive washing, bound proteins were eluted with 5 volumes of Glycine pH 2.2. Eluted proteins were analysed by SDS PAGE and Coomassie staining.

6.2.5 CaM kinase II interacts with the C-terminus of $Ca_V\beta 1b$

Figure 6.4 (Right panel) shows an SDS PAGE gel containing samples of eluates from beads coupled to $Ca_V\beta 1b$ and $Ca_V\beta 1b\Delta$C-terminus compared to control beads. Some proteins were retained by the column containing no $Ca_V\beta$ subunit, proteins of similar size in the other lanes were considered to be bound non-specifically and were ignored. One band of approximately 60 kDa was of particular interest as it appeared in the eluate from full length $Ca_V\beta 1b$ and in the C-terminus only but not the $Ca_V\beta 1b\Delta$C-terminus. Peptide mass fingerprinting analysis of this protein revealed its identity to be a mixture of CaM kinase II α and β subunits. Figure 6.5 shows an alignment of the primary sequences of mouse CaM kinase II α and β subunits. Both subunits are similar in size and as the CaM kinase II enzyme is a complex of both α and β subunits, it is likely that both subunits could be present together. A total of 13 different peptides were identified, 9 of which were specific to the β subunit, 2 were specific for the α subunit and 2 could be assigned to either α or β. The sequence and positions of the peptides is shown in Figure 6.6 and 6.7, these represent 31% of the CaM kinase II β subunit protein and 10.5% of the α subunit, it is

Figure 6.8

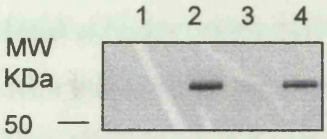

Western blot: Anti CaM Kinase II Ab

Figure 6.8 Western blot analysis of proteins eluted from beads coupled to purified $Ca_V\beta 1b$ subunit domains shown in Figure 6.4.A. Control (lane 1), $Ca_V\beta 1b$ (lane 2), $Ca_V\beta 1b$ Δ c-terminus (lane 3), $Ca_V\beta 1b$ C-terminus (lane 4).

Figure 6.9

$Ca_V\beta 1b$ C-terminus

MATALAASPAPVSNLQGPYLVSGDQPLDRATGEHASVHEYPGELGQPPLYPS
NHPPGRAGTLWALSRQDTFDADTPGSRNSVYTEPGDSCVDMETDSEGPGPG
DPAGGGTPPARQGSWEEEEDYEEEMTDNRNRGRNKARYCAEGGPVLGRNK
NELEGWGQGVYIR

Figure 6.8 Primary sequence of the C-terminus of $Ca_V\beta 1b$ subunit, the positions of putative CaM kinase II phosphorylation sites are marked in red.

therefore highly likely that this identification is correct. To further confirm the presence of CaM Kinase II α subunit, western blotting was performed on the eluates from the pull down experiment using an antibody specific for the CaM kinase II α subunit (Chemicon monoclonal antibody, clone 6G9). CaM kinase II α subunit was not found to be associated with the control beads or the beads containing $Ca_V\beta 1b$ lacking a C-terminus but was it was associated with both the full length $Ca_V\beta 1b$ and the $Ca_V\beta 1b$ C-terminus (Figure 6.8).

Since the Interaction between CaM kinase II and $Ca_V\beta 1b$ appears to be specific to the C-terminus of $Ca_V\beta 1b$, the primary sequence of $Ca_V\beta 1b$ was analysed for the presence of putative CaM kinase II phosphorylation motifs. CaM kinase II can phosphorylate serine or thereonine residues which occur in the consensus sequence φ X R nb X S/T where φ represents a hydrophobic residue, X can be any amino acid and nb is a non-basic residue (Hudmon and Schulman, 2002). Three putative sites were identified, Figure 6.9 shows the primary amino acid sequence of the C-terminus of $Ca_V\beta 1b$ and the position of the three putative CaM kinase II phosphorylation sites.

6.3 Discussion

Recent work has revealed that the $Ca_V\beta$ subunit may have secondary roles within the cell other than enhancing the functional expression and modulating the biophysical properties of HVA calcium channel $\alpha 1$ subunits (Hibino *et al.*, 2003; Viard *et al.*, 2004; Finlin *et al.*, 2003; Beguin *et al.*, 2001).

Purified full length $Ca_V\beta 1b$, $Ca_V\beta 1b\Delta$C-terminus and C-terminus alone were used to pull down potential binding partners from mouse brain lysate. Proteins which appeared to interact specifically with the C-terminus of $Ca_V\beta 1b$ were identified as the α and β subunits of Ca^{2+}/Calmodulin dependent protein kinase II. Western blotting using an antibody against the α subunit confirmed that no α subunit was associated with the $Ca_V\beta$ subunit lacking a C-terminus. A search of the primary sequence of the $Ca_V\beta 1b$ C-terminus revealed three putative CaM kinase II phosphorylation sites.

The Ca^{2+}/Calmodulin dependent kinase II is a multi-subunit serine/threonine kinase which is composed of homo or hetero multimers of α,β,γ or δ subunits. Structural studies have shown each enzyme to be composed of twelve subunits (Kolodziej *et al.*, 2000) although more recent X-ray crystallographic structure showed a tetradecameric arrangement (Hoelz *et al.*, 2003). The holoenzyme is activated by Ca^{2+}/Calmodulin binding which prevents inhibition by the autoregulatory domain, making the ATP binding and substrate binding sites available (Hudmon and Schulman, 2002). CaM kinase II is highly expressed in some parts of the brain, the neuronal α and β subunits can constitute up to 1% of the total protein of the forebrain (Erondu *et al.*, 1985). The enzyme is described as multifunctional and has roles in long term potentiation (LTP) and long term depression (LTD). In addition to this, CaM kinase II is reported to be involved in the regulation of L-type calcium channels in cardiomyocytes (Wu *et al.*, 2003). Activation of CaM kinase II causes an increase in calcium current through L-type channels by increasing the open probability of the channel, this occurs through a phosphorylation dependent mechanism (Dzhura *et al.*, 2000). Recent work by Hudmon et al. (2005) demonstrated that CaM Kinase II can interact with the C-terminus of $Ca_V1.2$ and that the C-terminus of $Ca_V1.2$ is a substrate for CaM kinase II *in vivo* and suggested that this interaction is essential for the calcium dependent facilitation reported previously by other studies.

Results shown here suggest that the neuronal CaM kinase II can interact with the C-terminus of $Ca_V\beta 1b$. Although putative CaM kinase II phosphorylation sites

are present in the C-terminus, it is not known whether it is a substrate for this enzyme. As the $Ca_V\beta$ subunit itself is responsible for modulating the open probability the $Ca_V\alpha1$ subunit (Meir *et al.*, 2000;Wakamori *et al.*,1999) it is possible if not likely that the modulation of $Ca_V\alpha1$ subunit open probability by CaM kinase II occurs via the $Ca_V\beta$ subunit.

Further experiments are necessary to establish the nature of the interaction between neuronal CaM kinase II and $Ca_V\beta1b$. Mutation of the putative CaM kinase II phosphorylation sites in the C-terminus of $Ca_V\beta1b$ would enable phosphorylation experiments to be carried out *in vitro*. The purified mutated $Ca_V\beta$ subunits could be incubated with active CaM kinase II in the presence of radio labelled ATP, decreases in the amounts of phosphate incorporated into the mutants compared to the wildtype $Ca_V\beta$ subunit would show if the C-terminus really is a substrate for this enzyme. In addition, functional experiments could be carried out to investigate the effect of CaM kinase II on HVA $Ca_V\alpha1/Ca_V\beta1b$ subunit combination and to investigate what effects if any mutation of the putative CaM kinase II phosphorylation sites in $Ca_V\beta1b$ may have on HVA calcium channel function. It would also be of interest to know if all $Ca_V\beta$ subunits can interact in this way or if it is limited to $Ca_V\beta1b$. Recent work by Abiria et al. (2005) showed that in tsA-201 cells, CaM kinase II mediated increase in open probability of $Ca_V1.2$ required coexpression of $Ca_V\beta2a$ and furthermore that a fragment of $Ca_V\beta2$ containing a putative CaM kinase II phosphorylation site will complex with CaM kinase II *in vitro*. In addition, CaM kinase II co-precipitated with the $Ca_V\beta2a$ subunit from a transfected cell line suggesting that this enzyme might interact with other $Ca_V\beta$ subunits.

Surface plasmon resonance experiments were performed using purified $Ca_V\beta1b$ and purified CaM kinase II however no interaction was observed (not shown). This may have been due to the very small amounts of CaM kinase II available, such that only low concentrations could be tested or because the K_D for this interaction is so low that it cannot be measured by this method.

Immunoprecipitation of HA tagged $Ca_V\beta1b$ and $Ca_V\beta2a$ subunits from transfected, differentiated NG108-15 cells with anti HA monoclonal antibodies was a highly effective way of capturing the proteins. Analysis of the precipitated proteins by SDS PAGE showed several different proteins associating with the β subunits

which were not pulled down by the beads alone. These proteins were identified successfully by MALDI-TOF spectroscopy however, their identities lead to the conclusion that the samples had been contaminated at some stage during the procedure and no further experiments were carried out. It is possible that the analysis of the immunoprecipitates could have been more successful if two dimensional SDS PAGE had been used, this procedure separates the proteins firstly by charge and then by size (Görg *et al.*, 2000). This may have given rise to cleaner, better resolved samples which may have produced better results.

Chapter 7
General discussion

7.1 General discussion

In this study, an SPR assay was developed to measure the interaction between the cytoplasmic I-II linker of L-type and non L-type Ca^{2+}channels and $Ca_V\beta$ subunits. Interaction between the I-II linker of $Ca_V1.3$, $Ca_V2.1$ and $Ca_V2.2$ and $Ca_V\beta1$, 2a and 3 subunits were tested and the results show that the dissociation constants for these interactions is in the low nanomolar range, between 12.1 and 20nM. This is in agreement with other studies (De Waard *et al.*, 1995; Scott *et al.*, 1996; Geib *et al.*, 2002). However, these authors used only short fragments of the I-II linker containing the AID motif. The results shown here suggest that other residues within the I-II linker do not significantly contribute to the high affinity interaction between the I-II linker and $Ca_V\beta$. The study was then extended to measure the interaction of G protein $\beta\gamma$ subunits with the I-II linker of L-type and non L-type channels. G protein $\beta\gamma$ subunits bound specifically to the $Ca_V2.2$ I-II linker and the K_D for this interaction was calculated to be 62.2 nM, this again is in agreement with previous studies (De Waard *et al.*, 1997). In agreement with Bell et al., (2001) who found that $Ca_V1.3$ was resistant to modulation by G protein $\beta\gamma$ subunits, no interaction between $Ca_V1.3$ I-II linker and G protein $\beta\gamma$ subunits was detected.

It has been shown that both G protein $\beta\gamma$ subunits and $Ca_V\beta$ subunits can bind to residues within the AID motif and there is some controversy over whether both subunits can bind at the same time (Canti *et al.*, 1999; Sandoz *et al.*, 2004; Hummer *et al.*, 2003). Attempts were made to adapt the SPR assay to determine whether one subunit can be displaced from its binding site on the I-II linker by the other subunit or if both subunits can occupy the I-II linker at the same time. However due to the relatively fast dissociation rates of both G protein $\beta\gamma$ and $Ca_V\beta$ subunits it was impossible to arrive at a situation where sites on the I-II linker were fully occupied by one protein or the other. Although the competition experiments were attempted, the results were impossible to interpret and it seems that this assay is not robust enough to address this complicated problem.

The SPR assay was then extended further to examine the effects of mutating the conserved tryptophan and tyrosine residues in the I-II linker on $Ca_V\beta$ subunit binding. These residues have previously been shown to disrupt $Ca_V\beta$ subunit binding (Pragnell *et al.*, 1994; Witcher *et al.*, 1995; De Waard *et al.*, 1995). The results showed that the conserved tryptophan but not the tyrosine is critical for $Ca_V\beta$ subunit

binding although mutation of the tyrosine to phenylalanine or serine reduced the affinity of $Ca_V\beta$ by 5.6 and 24 fold respectively (Leroy *et al.*, 2005; Butcher *et al.*, 2006). Biochemical and functional assays showed that expression of $Ca_V2.2$W391A with $Ca_V\beta1b$ resulted in a substantial reduction in the number of $Ca_V2.2$ channels at the plasma membrane, substantial reduction in whole cell current and altered biophysical properties similar to those of a $Ca_V2.2$ channel expressed without a $Ca_V\beta$ subunit. These findings suggest that $Ca_V\beta$ binding to AID regulates both channel trafficking and the biophysical properties of the channel. However whilst coexpression of $Ca_V\beta2a$ with the $Ca_V2.2$ W391A mutant channel resulted in fewer channels at the plasma membrane, the biophysical properties of the channel appeared to be modulated by $Ca_V\beta2a$ including restoration of voltage dependent G protein inhibition. Mutation of cysteines 3 and 4 serine prevents $Ca_V\beta2a$ from becoming palmitoylated (Chien *et al.*, 1996), this also prevented $Ca_V\beta2a$ from modulating $Ca_V2.2$W391A (Leroy *et al.*, 2005). As palmitoylation directs $Ca_V\beta2a$ to the plasma membrane (Bogdanov *et al.*, 2000), it seems that although the high affinity interaction with AID is lost and the channels can no longer be efficiently trafficked to the plasma membrane, $Ca_V\beta2a$ can still interact with channels in the plasma membrane possibly through low affinity interactions at sites other than AID.

The tyrosine to serine mutant was studied in preference to the phenylalanine mutant as the effects of the serine mutation on $Ca_V\beta$ subunit binding were much greater. Although this mutation reduced $Ca_V\beta$ subunit binding 24 fold, no functional effects were observed when $Ca_V2.2$Y388S was expressed in tsA201 cells with $Ca_V\beta1b$ and the mutated channels were efficiently trafficked to the plasma membrane. However, in a *Xenopus laevis* oocyte expression system where the amounts of DNA introduced into each oocyte can be more tightly controlled, experiments performed by Professor Annette Dolphin (Department of Pharmacology, University College London) showed that a 50 fold reduction in the amount of $Ca_V\beta1b$ DNA injected into the oocytes abolished the influence of $Ca_V\beta1b$ on $Ca_V2.2$Y388S whilst the same dilution had no effect on the wildtype channel (Butcher *et al.*, 2006). These findings suggest that a high affinity interaction between AID and $Ca_V\beta$ is not required for any of the modulatory effects of $Ca_V\beta$ but that $Ca_V\beta$ subunit occupancy of the AID site is important. In overexpression systems such as the one used in this study, it is possible

due to its size and cytoplasmic localisation that $Ca_V\beta$ subunits are produced at substantially higher levels relative to $Ca_V\alpha1$ subunits. These results also show the limitations of using overexpression systems to study the function of protein complexes in which there are large differences in the size and nature of the protein components and where the stoichiometry of interaction is important to the function of the complex.

The second part of this work focused specifically on the $Ca_V\beta2a$ subunit. It was recently reported that activation of phosphoinositide 3-kinase (PI3 kinase) promotes translocation of VDCC's to the plasma membrane (Viard *et al.*, 2004). This mechanism was shown to involve protein kinase B and be specific for channels containing the $Ca_V\beta2a$ subunit. The experiments described here show that PKB will co-precipitate with $Ca_V\beta2a$ from transfected COS-7 cells and that transfection of PI3 kinase causes an increase in $Ca_V\beta2a$ phosphorylation, an increase which is blocked by mutation of serine 574 in $Ca_V\beta2a$ to alanine. It was not possible to demonstrate direct phosphorylation of serine 574 in $Ca_V\beta2a$ using an *in vitro* assay, the purified C-terminal region of $Ca_V\beta2a$ appeared to be a poor substrate for PKB and thus, whether PKB is the kinase responsible for the increased phosphorylation observed *in vivo* is still an open question.

Finally, taking advantage of epitope tagged constructs, purified proteins and immunoprecipitation assays which had been developed previously, a proteomic approach was used to try to identify proteins which coprecipitated with $Ca_V\beta$ subunits. Peptide mass fingerprinting was used to identify proteins which bound to $Ca_V\beta1b$ from a mouse brain lysate. Ca^{2+}/calmodulin dependent kinase II was found interact with the C-terminus of $Ca_V\beta1b$ and inspection of the primary sequence of $Ca_V\beta1b$ revealed three putative CaM kinase II phosphorylation sites. It is known that CaM kinase II can regulate L-type Ca^{2+} channels in cardiomyocytes by increasing the open probability of the channels and that it can interact with the C-terminus of $Ca_V1.2$ (Wu *et al.*, 2003; Dzhura *et al.*, 2000; Hudmon *et al.*, 2005) but further experiments are necessary to determine whether the interaction of CaM kinase II with $Ca_V\beta1b$ is relevant to Ca^{2+} channel function.

7.2 Future work

Mutation of tryptophan to alanine in AID of HVA channels abolishes $Ca_V\beta$ subunit binding (De Waard *et al.*, 1995) and also prevents $Ca_V\beta$ subunit modulation of $Ca_V2.2$ channels containing this mutation (Leroy *et al.*, 2005). However, when the $Ca_V\beta$ subunit is directed to the plasma membrane as is the case for palmitoylated $Ca_V\beta2a$, modulation of the mutated channels can occur, possibly via low affinity interactions at sites other than AID (Leroy *et al.*, 2005). In future, it would be of interest to identify the regions of $Ca_V\beta$ responsible for these lower affinity interactions as well as the sites on the pore forming $\alpha1$ subunit with which they interact. Using a combination of mutagenesis and functional experiments, further mutations could be introduced into $Ca_V2.2W391A$ to try to remove modulation by palmitoylated $Ca_V\beta2$. As additional $Ca_V\beta$ subunit binding sites have already been reported on the N- and C-termini and elsewhere within the I-II linker (Walker *et al.*, 1999; Stephens *et al.*, 2000; Maltez *et al.*, 2005), these regions would be of particular interest. In addition, constructs containing isolated domains such as SH3 alone, GK alone or C-terminus alone could be used in combination with wild type $\alpha1$ subunits to look for any modulatory effects which these domains or combinations of domains may impart upon the channel. The confirmation of the $Ca_V\beta$ subunit structure has made this approach more reliable as the boundaries between the $Ca_V\beta$ subunit domains are now well-defined.

In the final part of this work, a protein from a mouse brain lysate which interacted specifically with the C-terminus of $Ca_V\beta1b$ was identified by Peptide mass fingerprinting as CaM kinase II. The presence of CaM kinase II was further confirmed by western blotting using antibodies to the CaM kinase II α subunit. Further experiments should be performed to determine whether CaM kinase II can phosphorylate any of the three putative CaM kinase II phosphorylation sites present in the C-terminus of $Ca_V\beta1b$. This could be done by mutating the putative sites in the C-terminus and performing *in vitro* phosphorylation experiments. The investigation could then be extended so that these sites within the full length $Ca_V\beta1b$ are mutated and metabolic labelling experiments could be performed which would show whether the C-terminus of $Ca_V\beta$ is a substrate for CaM kinase II under more physiological conditions.

Recent work by Abiria et al. (2005) showed that in tsA-201 cells, CaM kinase II mediated increase in open probability of $Ca_V1.2$ required coexpression of $Ca_V\beta2a$ and furthermore that a fragment of $Ca_V\beta2$ containing a putative CaM kinase II phosphorylation site will complex with CaM kinase II *in vitro*. Further experiments should be performed to determine whether all $Ca_V\beta$ subunits can interact with CaM kinase II in this way or whether this interaction is specific for $Ca_V\beta1b$.

Finally, it would be important to know the functional outcome of $Ca_V\beta1b$ interaction with or phosphorylation by CaM kinase II. Electrophysiological experiments could be performed using a cell line transfected with CaM kinase II, an HVA calcium channel $\alpha1$ subunit and $Ca_V\beta1b$ and these recordings compared to those made under the same conditions using $Ca_V\beta1b$ containing the appropriate mutations in its C-terminus.

Publications as Author

Butcher, A. J., Leroy, J., Richards, M. W., Pratt, W. S., & Dolphin, A. C. (2006). The importance of occupancy rather than affinity of CaV(beta) subunits for the calcium channel I-II linker in relation to calcium channel function. *J.Physiol* **574**, 387-398.

Martin, S. W., Butcher, A. J., Berrow, N. S., Richards, M. W., Paddon, R. E., Turner, D. J., Dolphin, A. C., Sihra, T. S., & Fitzgerald, E. M. (2006). Phosphorylation sites on calcium channel alpha1 and beta subunits regulate ERK-dependent modulation of neuronal N-type calcium channels. *Cell Calcium* **39**, 275-292.

Leroy, J., Richards, M. W., Butcher, A. J., Nieto-Rostro, M., Pratt, W. S., Davies, A., & Dolphin, A. C. (2005). Interaction via a key tryptophan in the I-II linker of N-type calcium channels is required for beta1 but not for palmitoylated beta2, implicating an additional binding site in the regulation of channel voltage-dependent properties. *J.Neurosci.* **25**, 6984-6996.

Richards, M. W., Butcher, A. J., & Dolphin, A. C. (2004). Ca2+ channel beta-subunits: structural insights AID our understanding. *Trends Pharmacol.Sci.* **25**, 626-632.

Viard, P., Butcher, A. J., Halet, G., Davies, A., Nurnberg, B., Heblich, F., & Dolphin, A. C. (2004). PI3K promotes voltage-dependent calcium channel trafficking to the plasma membrane. *Nat.Neurosci.* **7**, 939-946.

Page, K. M., Heblich, F., Davies, A., Butcher, A. J., Leroy, J., Bertaso, F., Pratt, W. S., & Dolphin, A. C. (2004). Dominant-negative calcium channel suppression by truncated constructs involves a kinase implicated in the unfolded protein response. *J.Neurosci.* **24**, 5400-5409.

Canti, C., Davies, A., Berrow, N. S., Butcher, A. J., Page, K. M., & Dolphin, A. C. (2001). Evidence for two concentration-dependent processes for beta-subunit effects on alpha1B calcium channels. *Biophys.J.* **81**, 1439-1451.

Bell, D. C., Butcher, A. J., Berrow, N. S., Page, K. M., Brust, P. F., Nesterova, A., Stauderman, K. A., Seabrook, G. R., Nurnberg, B., & Dolphin, A. C. (2001). Biophysical properties, pharmacology, and modulation of human, neuronal L-type (alpha(1D), Ca(V)1.3) voltage-dependent calcium currents. *J.Neurophysiol.* **85**, 816-827.

References

Abiria, S. A., Grueter, C. E., Dzhura, I., Thiel, W., Zhang, R., Anderson, M. E., Colbran, R. J., (2005) Calcium/calmodulin dependent protein kinase II (CAMKII) interacts with L-type calcium channel (LTCC) beta subunits. *Soc Neurosci Abstr,* Prog.No. 726.13.

Agler, H. L., Evans, J., Tay, L. H., Anderson, M. J., Colecraft, H. M., & Yue, D. T. (2005). G protein-gated inhibitory module of N-type (ca(v)2.2) Ca^{2+} channels. *Neuron* **46**, 891-904.

Albert, A. P. & Large, W. A. (2002). Activation of store-operated channels by noradrenaline via protein kinase C in rabbit portal vein myocytes. *J.Physiol* **544**, 113-125.

Alessi, D. R., James, S. R., Downes, C. P., Holmes, A. B., Gaffney, P. R., Reese, C. B., & Cohen, P. (1997). Characterization of a 3-phosphoinositide-dependent protein kinase which phosphorylates and activates protein kinase Balpha. *Curr.Biol.* **7**, 261-269.

Arias, J. M., Murbartian, J., Vitko, I., Lee, J. H., & Perez-Reyes, E. (2005). Transfer of beta subunit regulation from high to low voltage-gated Ca^{2+} channels. *FEBS Lett.* **579**, 3907-3912.

Arikkath, J. & Campbell, K. P. (2003). Auxiliary subunits: essential components of the voltage-gated calcium channel complex. *Curr.Opin.Neurobiol.* **13**, 298-307.

Baimbridge, K. G., Celio, M. R., & Rogers, J. H. (1992). Calcium-binding proteins in the nervous system. *Trends Neurosci.* **15**, 303-308.

Baksh, S. & Michalak, M. (1991). Expression of calreticulin in Escherichia coli and identification of its Ca^{2+} binding domains. *J.Biol.Chem.* **266**, 21458-21465.

Balendran, A., Casamayor, A., Deak, M., Paterson, A., Gaffney, P., Currie, R., Downes, C. P., & Alessi, D. R. (1999). PDK1 acquires PDK2 activity in the presence of a synthetic peptide derived from the carboxyl terminus of PRK2. *Curr.Biol.* **9**, 393-404.

Ball, S. L., Powers, P. A., Shin, H. S., Morgans, C. W., Peachey, N. S., & Gregg, R. G. (2002). Role of the beta(2) subunit of voltage-dependent calcium channels in the retinal outer plexiform layer. *Invest Ophthalmol.Vis.Sci.* **43**, 1595-1603.

Barclay, J., Balaguero, N., Mione, M., Ackerman, S. L., Letts, V. A., Brodbeck, J., Canti, C., Meir, A., Page, K. M., Kusumi, K., Perez-Reyes, E., Lander, E. S., Frankel, W. N., Gardiner, R. M., Dolphin, A. C., & Rees, M. (2001). Ducky mouse phenotype of epilepsy and ataxia is associated with mutations in the Cacna2d2 gene and decreased calcium channel current in cerebellar Purkinje cells. *J.Neurosci.* **21**, 6095-6104.

Bean, B. P. (1989). Neurotransmitter inhibition of neuronal calcium currents by changes in channel voltage dependence. *Nature* **340**, 153-156.

Beguin, P., Nagashima, K., Gonoi, T., Shibasaki, T., Takahashi, K., Kashima, Y., Ozaki, N., Geering, K., Iwanaga, T., & Seino, S. (2001). Regulation of Ca^{2+} channel expression at the cell surface by the small G-protein kir/Gem. *Nature* **411**, 701-706.

Bell, D. C., Butcher, A. J., Berrow, N. S., Page, K. M., Brust, P. F., Nesterova, A., Stauderman, K. A., Seabrook, G. R., Nurnberg, B., & Dolphin, A. C. (2001). Biophysical properties, pharmacology, and modulation of human, neuronal L-type (alpha(1D), Ca(V)1.3) voltage-dependent calcium currents. *J.Neurophysiol.* **85**, 816-827.

Berggren, P. O., Yang, S. N., Murakami, M., Efanov, A. M., Uhles, S., Kohler, M., Moede, T., Fernstrom, A., Appelskog, I. B., Aspinwall, C. A., Zaitsev, S. V., Larsson, O., de Vargas, L. M., Fecher-Trost, C., Weissgerber, P., Ludwig, A., Leibiger, B., Juntti-Berggren, L., Barker, C. J., Gromada, J., Freichel, M., Leibiger, I. B., & Flockerzi, V.

(2004). Removal of Ca^{2+} channel beta3 subunit enhances Ca^{2+} oscillation frequency and insulin exocytosis. *Cell* **119**, 273-284.

Berrou, L., Bernatchez, G., & Parent, L. (2001). Molecular determinants of inactivation within the I-II linker of alpha1E (CaV2.3) calcium channels. *Biophys.J.* **80**, 215-228.

Berrou, L., Klein, H., Bernatchez, G., & Parent, L. (2002). A specific tryptophan in the I-II linker is a key determinant of beta-subunit binding and modulation in Ca(V)2.3 calcium channels. *Biophys.J.* **83**, 1429-1442.

Berrou, L., Dodier, Y., Raybaud, A., Tousignant, A., Dafi, O., Pelletier, J. N., & Parent, L. (2005). The C-terminal residues in the alpha-interacting domain (AID) helix anchor CaV beta subunit interaction and modulation of CaV2.3 channels. *J.Biol.Chem.* **280**, 494-505.

Berrow, N. S., Campbell, V., Fitzgerald, E. M., Brickley, K., & Dolphin, A. C. (1995). Antisense depletion of beta-subunits modulates the biophysical and pharmacological properties of neuronal calcium channels. *J.Physiol* **482 (Pt 3)**, 481-491.

Bertani, G. (1951). Studies on lysogenesis. I. The mode of phage liberation by lysogenic Escherichia coli. *J.Bacteriol.* **62**, 293-300.

Bichet, D., Cornet, V., Geib, S., Carlier, E., Volsen, S., Hoshi, T., Mori, Y., & De Waard, M. (2000). The I-II loop of the Ca^{2+} channel alpha1 subunit contains an endoplasmic reticulum retention signal antagonized by the beta subunit. *Neuron* **25**, 177-190.

Birnbaumer, L., Campbell, K. P., Catterall, W. A., Harpold, M. M., Hofmann, F., Horne, W. A., Mori, Y., Schwartz, A., Snutch, T. P., Tanabe, T., & (1994). The naming of voltage-gated calcium channels. *Neuron* **13**, 505-506.

Birnbaumer, L., Qin, N., Olcese, R., Tareilus, E., Platano, D., Costantin, J., & Stefani, E. (1998). Structures and functions of calcium channel beta subunits. *J.Bioenerg.Biomembr.* **30**, 357-375.

Blair, L. A. & Marshall, J. (1997). IGF-1 modulates N and L calcium channels in a PI 3-kinase-dependent manner. *Neuron* **19**, 421-429.

Blume-Jensen, P. & Hunter, T. (2001). Oncogenic kinase signalling. *Nature* **411**, 355-365.

Bogdanov, Y., Brice, N. L., Canti, C., Page, K. M., Li, M., Volsen, S. G., & Dolphin, A. C. (2000). Acidic motif responsible for plasma membrane association of the voltage-dependent calcium channel beta1b subunit. *Eur.J.Neurosci.* **12**, 894-902.

Bolotina, V. M. (2004). Store-operated channels: diversity and activation mechanisms. *Sci.STKE.* 2004, e34.

Bootman, M. D., Collins, T. J., Peppiatt, C. M., Prothero, L. S., MacKenzie, L., De Smet, P., Travers, M., Tovey, S. C., Seo, J. T., Berridge, M. J., Ciccolini, F., & Lipp, P. (2001). Calcium signalling--an overview. *Semin.Cell Dev.Biol.* **12**, 3-10.

Bourinet, E., Soong, T. W., Sutton, K., Slaymaker, S., Mathews, E., Monteil, A., Zamponi, G. W., Nargeot, J., & Snutch, T. P. (1999). Splicing of alpha 1A subunit gene generates phenotypic variants. *Nat.Neurosci.* **2**, 407-415.

Brazil, D. P. & Hemmings, B. A. (2001). Ten years of protein kinase B signalling: a hard Akt to follow. *Trends Biochem.Sci.* **26**, 657-664.

Brice, N. L. & Dolphin, A. C. (1999). Differential plasma membrane targeting of voltage-dependent calcium channel subunits expressed in a polarized epithelial cell line. *J.Physiol* **515 (Pt 3)**, 685-694.

Brock, C., Schaefer, M., Reusch, H. P., Czupalla, C., Michalke, M., Spicher, K., Schultz, G., & Nurnberg, B. (2003). Roles of G beta gamma in membrane recruitment and activation of p110 gamma/p101 phosphoinositide 3-kinase gamma. *J.Cell Biol.* **160**, 89-99.

Buisson, B., Laflamme, L., Bottari, S. P., de Gasparo, M., Gallo-Payet, N., & Payet, M. D. (1995). A G protein is involved in the angiotensin AT2 receptor inhibition of the T-type calcium current in non-differentiated NG108-15 cells. *J.Biol.Chem.* **270**, 1670-1674.

Bunney, T. D., van den Wijngaard, P. W., & de Boer, A. H. (2002). 14-3-3 protein regulation of proton pumps and ion channels. *Plant Mol.Biol.* **50**, 1041-1051.

Burgering, B. M. & Coffer, P. J. (1995). Protein kinase B (c-Akt) in phosphatidylinositol-3-OH kinase signal transduction. *Nature* **376**, 599-602.

Burgess, D. L., Gefrides, L. A., Foreman, P. J., & Noebels, J. L. (2001). A cluster of three novel Ca^{2+} channel gamma subunit genes on chromosome 19q13.4: evolution and expression profile of the gamma subunit gene family. *Genomics* **71**, 339-350.

Butcher, A. J., Leroy, J., Richards, M. W., Pratt, W. S., & Dolphin, A. C. (2006). The importance of occupancy rather than affinity of $Ca_V\{beta\}$ subunits for the calcium channel I-II linker in relation to calcium channel function. *J.Physiol.* **574**, 387-392.

Campbell, K. P., Sharp, A. H., & Leung, A. T. (1989). 32,000-Dalton subunit of the 1,4-dihydropyridine receptor. *Ann.N.Y.Acad.Sci.* **560**, 251-257.

Canti, C., Page, K. M., Stephens, G. J., & Dolphin, A. C. (1999). Identification of residues in the N terminus of alpha1B critical for inhibition of the voltage-dependent calcium channel by Gbeta gamma. *J.Neurosci.* **19**, 6855-6864.

Canti, C., Bogdanov, Y., & Dolphin, A. C. (2000). Interaction between G proteins and accessory subunits in the regulation of 1B calcium channels in Xenopus oocytes. *J.Physiol* **527 Pt 3**, 419-432.

Canti, C., Davies, A., Berrow, N. S., Butcher, A. J., Page, K. M., & Dolphin, A. C. (2001). Evidence for two concentration-dependent processes for beta-subunit effects on alpha1B calcium channels. *Biophys.J.* **81**, 1439-1451.

Canti, C., Nieto-Rostro, M., Foucault, I., Heblich, F., Wratten, J., Richards, M. W., Hendrich, J., Douglas, L., Page, K. M., Davies, A., & Dolphin, A. C. (2005). The metal-ion-dependent adhesion site in the Von Willebrand factor-A domain of alpha2delta subunits is key to trafficking voltage-gated Ca^{2+} channels. *Proc.Natl.Acad.Sci.U.S.A* **102**, 11230-11235.

Carbone, E. & Lux, H. D. (1984). A low voltage-activated, fully inactivating Ca channel in vertebrate sensory neurones. *Nature* **310**, 501-502.

Carbone, E. & Lux, H. D. (1984). A low voltage-activated calcium conductance in embryonic chick sensory neurons. *Biophys.J.* **46**, 413-418.

Castellano, A., Wei, X., Birnbaumer, L., & Perez-Reyes, E. (1993). Cloning and expression of a third calcium channel beta subunit. *J.Biol.Chem.* **268**, 3450-3455.

Catterall, W. A. (1999). Interactions of presynaptic Ca^{2+} channels and snare proteins in neurotransmitter release. *Ann.N.Y.Acad.Sci.* **868**, 144-159.

Catterall, W. A. (2000). Structure and regulation of voltage-gated Ca^{2+} channels. *Annu.Rev.Cell Dev.Biol.* **16**, 521-555.

Caulfield, M. P. & Brown, D. A. (1992). Cannabinoid receptor agonists inhibit Ca current in NG108-15 neuroblastoma cells via a pertussis toxin-sensitive mechanism. *Br.J.Pharmacol.* **106**, 231-232.

Cens, T., Restituito, S., Vallentin, A., & Charnet, P. (1998). Promotion and inhibition of L-type Ca2+ channel facilitation by distinct domains of the subunit. *J.Biol.Chem.* **273**, 18308-18315.

Chaga, G. S. (2001). Twenty-five years of immobilized metal ion affinity chromatography: past, present and future. *J.Biochem.Biophys.Methods* **49**, 313-334.

Chemin, J., Monteil, A., Perez-Reyes, E., Bourinet, E., Nargeot, J., & Lory, P. (2002). Specific contribution of human T-type calcium channel isotypes (alpha(1G), alpha(1H) and alpha(1I)) to neuronal excitability. *J.Physiol* **540**, 3-14.

Chen, L., Chetkovich, D. M., Petralia, R. S., Sweeney, N. T., Kawasaki, Y., Wenthold, R. J., Bredt, D. S., & Nicoll, R. A. (2000). Stargazin regulates synaptic targeting of AMPA receptors by two distinct mechanisms. *Nature* **408**, 936-943.

Chen, Y. H., Li, M. H., Zhang, Y., He, L. L., Yamada, Y., Fitzmaurice, A., Shen, Y., Zhang, H., Tong, L., & Yang, J. (2004). Structural basis of the alpha1-beta subunit interaction of voltage-gated Ca^{2+} channels. *Nature* **429**, 675-680.

Cheng, J. Q., Ruggeri, B., Klein, W. M., Sonoda, G., Altomare, D. A., Watson, D. K., & Testa, J. R. (1996). Amplification of AKT2 in human pancreatic cells and inhibition of AKT2 expression and tumorigenicity by antisense RNA. *Proc.Natl.Acad.Sci.U.S.A* **93**, 3636-3641.

Chien, A. J., Gao, T., Perez-Reyes, E., & Hosey, M. M. (1998). Membrane targeting of L-type calcium channels. Role of palmitoylation in the subcellular localization of the beta2a subunit. *J.Biol.Chem.* **273**, 23590-23597.

Chien, A. J. & Hosey, M. M. (1998). Post-translational modifications of beta subunits of voltage-dependent calcium channels. *J.Bioenerg.Biomembr.* **30**, 377-386.

Chu, P. J., Robertson, H. M., & Best, P. M. (2001). Calcium channel gamma subunits provide insights into the evolution of this gene family. *Gene* **280**, 37-48.

Clapham, D. E. (1995). Calcium signaling. *Cell* **80**, 259-268.

Cohen, R. M., Foell, J. D., Balijepalli, R. C., Shah, V., Hell, J. W., & Kamp, T. J. (2005). Unique modulation of L-type Ca2+ channels by short auxiliary beta1d subunit present in cardiac muscle. *Am.J.Physiol Heart Circ.Physiol* **288**, H2363-H2374.

Colecraft, H. M., Alseikhan, B., Takahashi, S. X., Chaudhuri, D., Mittman, S., Yegnasubramanian, V., Alvania, R. S., Johns, D. C., Marban, E., & Yue, D. T. (2002). Novel functional properties of Ca^{2+} channel beta subunits revealed by their expression in adult rat heart cells. *J.Physiol* **541**, 435-452.

Colledge, M., Dean, R. A., Scott, G. K., Langeberg, L. K., Huganir, R. L., & Scott, J. D. (2000). Targeting of PKA to glutamate receptors through a MAGUK-AKAP complex. *Neuron* **27**, 107-119.

Collin, T., Lory, P., Taviaux, S., Courtieu, C., Guilbault, P., Berta, P., & Nargeot, J. (1994). Cloning, chromosomal location and functional expression of the human voltage-dependent calcium-channel beta 3 subunit. *Eur.J.Biochem.* **220**, 257-262.

Cormack, B. P., Bertram, G., Egerton, M., Gow, N. A., Falkow, S., & Brown, A. J. (1997). Yeast-enhanced green fluorescent protein (yEGFP) a reporter of gene expression in Candida albicans. *Microbiology* **143 (Pt 2)**, 303-311.

Cribbs, L. L., Lee, J. H., Yang, J., Satin, J., Zhang, Y., Daud, A., Barclay, J., Williamson, M. P., Fox, M., Rees, M., & Perez-Reyes, E. (1998). Cloning and characterization of alpha1H from human heart, a member of the T-type Ca^{2+} channel gene family. *Circ.Res.* **83**, 103-109.

Cross, D. A., Alessi, D. R., Cohen, P., Andjelkovich, M., & Hemmings, B. A. (1995). Inhibition of glycogen synthase kinase-3 by insulin mediated by protein kinase B. *Nature* **378**, 785-789.

Curtis, B. M. & Catterall, W. A. (1983). Solubilization of the calcium antagonist receptor from rat brain. *J.Biol.Chem.* **258**, 7280-7283.

Curtis, B. M. & Catterall, W. A. (1985). Phosphorylation of the calcium antagonist receptor of the voltage-sensitive calcium channel by cAMP-dependent protein kinase. *Proc.Natl.Acad.Sci.U.S.A* **82**, 2528-2532.

Datta, S. R., Dudek, H., Tao, X., Masters, S., Fu, H., Gotoh, Y., & Greenberg, M. E. (1997). Akt phosphorylation of BAD couples survival signals to the cell-intrinsic death machinery. *Cell* **91**, 231-241.

de Boer, H. A., Comstock, L. J., Hui, A., Wong, E., & Vasser, M. (1983). Portable Shine-Dalgarno regions; nucleotides between the Shine-Dalgarno sequence and the start codon affect the translation efficiency. *Gene Amplif.Anal.* **3**, 103-116.

De Waard, M., Pragnell, M., & Campbell, K. P. (1994). Ca^{2+} channel regulation by a conserved beta subunit domain. *Neuron* **13**, 495-503.

De Waard, M., Witcher, D. R., Pragnell, M., Liu, H., & Campbell, K. P. (1995). Properties of the alpha 1-beta anchoring site in voltage-dependent Ca^{2+} channels. *J.Biol.Chem.* **270**, 12056-12064.

De Waard, M., Scott, V. E., Pragnell, M., & Campbell, K. P. (1996). Identification of critical amino acids involved in alpha1-beta interaction in voltage-dependent Ca^{2+} channels. *FEBS Lett.* **380**, 272-276.

De Waard, M., Liu, H., Walker, D., Scott, V. E., Gurnett, C. A., & Campbell, K. P. (1997). Direct binding of G-protein beta gamma complex to voltage-dependent calcium channels. *Nature* **385**, 446-450.

De, M. V., Stier, G., Blandin, S., & de Marco, A. (2004). The solubility and stability of recombinant proteins are increased by their fusion to NusA. *Biochem.Biophys.Res.Commun.* **322**, 766-771.

del Peso, L., Gonzalez-Garcia, M., Page, C., Herrera, R., & Nunez, G. (1997). Interleukin-3-induced phosphorylation of BAD through the protein kinase Akt. *Science* **278**, 687-689.

Dietrich, D., Kirschstein, T., Kukley, M., Pereverzev, A., von der, B. C., Schneider, T., & Beck, H. (2003). Functional specialization of presynaptic Cav2.3 Ca^{2+} channels. *Neuron* **39**, 483-496.

Ding, Q., Gros, R., Chorazyczewski, J., Ferguson, S. S., & Feldman, R. D. (2005). Isoform-specific regulation of adenylyl cyclase function by disruption of membrane trafficking. *Mol.Pharmacol.* **67**, 564-571.

Docherty, R. J. & McFadzean, I. (1989). Noradrenaline-induced inhibition of voltage-sensitive calcium currents in NG108-15 hybrid cells. *Eur.J.Neurosci.* **1**, 132-140.

Dolphin, A. C. (1999). L-type calcium channel modulation. *Adv.Second Messenger Phosphoprotein Res.* **33**, 153-177.

Dolphin, A. C. (2003). Beta subunits of voltage-gated calcium channels. *J.Bioenerg.Biomembr.* **35**, 599-620.

Douglas, K. T. (1987). Mechanism of action of glutathione-dependent enzymes. *Adv.Enzymol.Relat Areas Mol.Biol.* **59**, 103-167.

Doyle, D. A., Morais, C. J., Pfuetzner, R. A., Kuo, A., Gulbis, J. M., Cohen, S. L., Chait, B. T., & MacKinnon, R. (1998). The structure of the potassium channel: molecular basis of K^+ conduction and selectivity. *Science* **280**, 69-77.

Dubel, S. J., Starr, T. V., Hell, J., Ahlijanian, M. K., Enyeart, J. J., Catterall, W. A., & Snutch, T. P. (1992). Molecular cloning of the alpha-1 subunit of an omega-conotoxin-sensitive calcium channel. *Proc.Natl.Acad.Sci.U.S.A* **89**, 5058-5062.

Dunlap, K., Luebke, J. I., & Turner, T. J. (1995). Exocytotic Ca^{2+} channels in mammalian central neurons. *Trends Neurosci.* **18**, 89-98.

Dzhura, I., Wu, Y., Colbran, R. J., Balser, J. R., & Anderson, M. E. (2000). Calmodulin kinase determines calcium-dependent facilitation of L-type calcium channels. *Nat.Cell Biol.* **2**, 173-177.

Ellis, S. B., Williams, M. E., Ways, N. R., Brenner, R., Sharp, A. H., Leung, A. T., Campbell, K. P., McKenna, E., Koch, W. J., Hui, A., & . (1988). Sequence and expression of mRNAs encoding the alpha 1 and alpha 2 subunits of a DHP-sensitive calcium channel. *Science* **241**, 1661-1664.

Erondu, N. E. & Kennedy, M. B. (1985). Regional distribution of type II Ca^{2+}/calmodulin-dependent protein kinase in rat brain. *J.Neurosci.* **5**, 3270-3277.

Ertel, E. A., Campbell, K. P., Harpold, M. M., Hofmann, F., Mori, Y., Perez-Reyes, E., Schwartz, A., Snutch, T. P., Tanabe, T., Birnbaumer, L., Tsien, R. W., & Catterall, W. A. (2000). Nomenclature of voltage-gated calcium channels. *Neuron* **25**, 533-535.

Escayg, A., Jones, J. M., Kearney, J. A., Hitchcock, P. F., & Meisler, M. H. (1998). Calcium channel beta 4 (CACNB4): human ortholog of the mouse epilepsy gene lethargic. *Genomics* **50**, 14-22.

Exner, T., Jensen, O. N., Mann, M., Kleuss, C., & Nurnberg, B. (1999). Posttranslational modification of Galphao1 generates Galphao3, an abundant G protein in brain. *Proc.Natl.Acad.Sci.U.S.A* **96**, 1327-1332.

Fasman, G. D. (1989). Protein conformational prediction. *Trends Biochem.Sci.* **14**, 295-299.

Fatt, P. & Katz, B. (1953). The electrical properties of crustacean muscle fibres. *J.Physiol* **120**, 171-204.

Felix, J. A., Woodruff, M. L., & Dirksen, E. R. (1996). Stretch increases inositol 1,4,5-trisphosphate concentration in airway epithelial cells. *Am.J.Respir.Cell Mol.Biol.* **14**, 296-301.

Felix, R., Gurnett, C. A., De Waard, M., & Campbell, K. P. (1997). Dissection of functional domains of the voltage-dependent Ca^{2+} channel alpha2delta subunit. *J.Neurosci.* **17**, 6884-6891.

Filippov, A. K. & Brown, D. A. (1996). Activation of nucleotide receptors inhibits high-threshold calcium currents in NG108-15 neuronal hybrid cells. *Eur.J.Neurosci.* **8**, 1149-1155.

Finlin, B. S., Crump, S. M., Satin, J., & Andres, D. A. (2003). Regulation of voltage-gated calcium channel activity by the Rem and Rad GTPases. *Proc.Natl.Acad.Sci.U.S.A* **100**, 14469-14474.

Franke, T. F., Yang, S. I., Chan, T. O., Datta, K., Kazlauskas, A., Morrison, D. K., Kaplan, D. R., & Tsichlis, P. N. (1995). The protein kinase encoded by the Akt proto-oncogene is a target of the PDGF-activated phosphatidylinositol 3-kinase. *Cell* **81**, 727-736.

Franke, T. F., Kaplan, D. R., Cantley, L. C., & Toker, A. (1997). Direct regulation of the Akt proto-oncogene product by phosphatidylinositol-3,4-bisphosphate. *Science* **275**, 665-668.

Freise, D., Held, B., Wissenbach, U., Pfeifer, A., Trost, C., Himmerkus, N., Schweig, U., Freichel, M., Biel, M., Hofmann, F., Hoth, M., & Flockerzi, V. (2000). Absence of the gamma subunit of the skeletal muscle dihydropyridine receptor increases L-type Ca^{2+} currents and alters channel inactivation properties. *J.Biol.Chem.* **275**, 14476-14481.

Fujita, Y., Mynlieff, M., Dirksen, R. T., Kim, M. S., Niidome, T., Nakai, J., Friedrich, T., Iwabe, N., Miyata, T., Furuichi, T., & . (1993). Primary structure and functional expression of the omega-conotoxin-sensitive N-type calcium channel from rabbit brain. *Neuron* **10**, 585-598.

Fukata, Y., Tzingounis, A. V., Trinidad, J. C., Fukata, M., Burlingame, A. L., Nicoll, R. A., & Bredt, D. S. (2005). Molecular constituents of neuronal AMPA receptors. *J.Cell Biol.* **169**, 399-404.

Funke, L., Dakoji, S., & Bredt, D. S. (2005). Membrane-associated guanylate kinases regulate adhesion and plasticity at cell junctions. *Annu.Rev.Biochem.* **74**, 219-245.

Garner, C. C., Nash, J., & Huganir, R. L. (2000). PDZ domains in synapse assembly and signalling. *Trends Cell Biol.* **10**, 274-280.

Geib, S., Sandoz, G., Mabrouk, K., Matavel, A., Marchot, P., Hoshi, T., Villaz, M., Ronjat, M., Miquelis, R., Leveque, C., & De Waard, M. (2002). Use of a purified and functional recombinant calcium-channel beta4 subunit in surface-plasmon resonance studies. *Biochem.J.* **364**, 285-292.

Gerster, U., Neuhuber, B., Groschner, K., Striessnig, J., & Flucher, B. E. (1999). Current modulation and membrane targeting of the calcium channel alpha1C subunit are independent functions of the beta subunit. *J.Physiol* **517 (Pt 2)**, 353-368.

Gluzman, Y. (1981). SV40-transformed simian cells support the replication of early SV40 mutants. *Cell* **23**, 175-182.

Gorg, A., Weiss, W., & Dunn, M. J. (2004). Current two-dimensional electrophoresis technology for proteomics. *Proteomics.* **4**, 3665-3685.

Gottschalk, W., Kim, D. S., Chin, H., & Stanley, E. F. (1999). High-voltage-activated calcium channel messenger RNA expression in the 140-3 neuroblastoma-glioma cell line. *Neuroscience* **94**, 975-983.

Green, N. M. (1990). Avidin and streptavidin. *Methods Enzymol.* **184**, 51-67.

Green, P. J., Warre, R., Hayes, P. D., McNaughton, N. C., Medhurst, A. D., Pangalos, M., Duckworth, D. M., & Randall, A. D. (2001). Kinetic modification of the alpha(1I) subunit-mediated T-type Ca(2+) channel by a human neuronal Ca^{2+} channel gamma subunit. *J.Physiol* **533**, 467-478.

Gregg, R. G., Messing, A., Strube, C., Beurg, M., Moss, R., Behan, M., Sukhareva, M., Haynes, S., Powell, J. A., Coronado, R., & Powers, P. A. (1996). Absence of the beta subunit (cchb1) of the skeletal muscle dihydropyridine receptor alters expression of the alpha 1 subunit and eliminates excitation-contraction coupling. *Proc.Natl.Acad.Sci.U.S.A* **93**, 13961-13966.

Gurnett, C. A., De Waard, M., & Campbell, K. P. (1996). Dual function of the voltage-dependent Ca^{2+} channel alpha 2 delta subunit in current stimulation and subunit interaction. *Neuron* **16**, 431-440.

Haase, H., Kresse, A., Hohaus, A., Schulte, H. D., Maier, M., Osterziel, K. J., Lange, P. E., & Morano, I. (1996). Expression of calcium channel subunits in the normal and diseased human myocardium. *J.Mol.Med.* **74**, 99-104.

Hagiwara, S., Ozawa, S., & Sand, O. (1975). Voltage clamp analysis of two inward current mechanisms in the egg cell membrane of a starfish. *J.Gen.Physiol* **65**, 617-644.

Hall, D. (2001). Use of optical biosensors for the study of mechanistically concerted surface adsorption processes. *Anal.Biochem.* **288**, 109-125.

Hanada, T., Lin, L., Tibaldi, E. V., Reinherz, E. L., & Chishti, A. H. (2000). GAKIN, a novel kinesin-like protein associates with the human homologue of the Drosophila discs large tumor suppressor in T lymphocytes. *J.Biol.Chem.* **275**, 28774-28784.

Hanlon, M. R., Berrow, N. S., Dolphin, A. C., & Wallace, B. A. (1999). Modelling of a voltage-dependent Ca2+ channel beta subunit as a basis for understanding its functional properties. *FEBS Lett.* **445**, 366-370.

Harris, B. Z. & Lim, W. A. (2001). Mechanism and role of PDZ domains in signaling complex assembly. *J.Cell Sci.* **114**, 3219-3231.

Haslam, R. J., Koide, H. B., & Hemmings, B. A. (1993). Pleckstrin domain homology. *Nature* **363**, 309-310.

Heizmann, C. W. & Hunziker, W. (1991). Intracellular calcium-binding proteins: more sites than insights. *Trends Biochem.Sci.* **16**, 98-103.

Helton, T. D. & Horne, W. A. (2002). Alternative splicing of the beta 4 subunit has alpha1 subunit subtype-specific effects on Ca^{2+} channel gating. *J.Neurosci.* **22**, 1573-1582.

Herlitze, S., Hockerman, G. H., Scheuer, T., & Catterall, W. A. (1997). Molecular determinants of inactivation and G protein modulation in the intracellular loop connecting domains I and II of the calcium channel alpha1A subunit. *Proc.Natl.Acad.Sci.U.S.A* **94**, 1512-1516.

Hibino, H., Pironkova, R., Onwumere, O., Rousset, M., Charnet, P., Hudspeth, A. J., & Lesage, F. (2003). Direct interaction with a nuclear protein and regulation of gene silencing by a variant of the Ca^{2+}-channel beta 4 subunit. *Proc.Natl.Acad.Sci.U.S.A* **100**, 307-312.

Hille, B. (2001). Ion Channels of Excitable Membranes. Massachusetts: Sinauer Associates Inc..

Hobom, M., Dai, S., Marais, E., Lacinova, L., Hofmann, F., & Klugbauer, N. (2000). Neuronal distribution and functional characterization of the calcium channel alpha2delta-2 subunit. *Eur.J.Neurosci.* **12**, 1217-1226.

Hochuli, E. (1988). Large-scale chromatography of recombinant proteins. *J.Chromatogr.* **444**, 293-302.

Hoelz, A., Nairn, A. C., & Kuriyan, J. (2003). Crystal structure of a tetradecameric assembly of the association domain of Ca^{2+}/calmodulin-dependent kinase II. *Mol.Cell* **11**, 1241-1251.

Hoth, M. & Penner, R. (1992). Depletion of intracellular calcium stores activates a calcium current in mast cells. *Nature* **355**, 353-356.

Huang, L., Bhattacharjee, A., Taylor, J. T., Zhang, M., Keyser, B. M., Marrero, L., & Li, M. (2004). [Ca2+]i regulates trafficking of Cav1.3 (alpha1D Ca^{2+} channel) in insulin-secreting cells. *Am.J.Physiol Cell Physiol* **286**, C213-C221.

Hudmon, A. & Schulman, H. (2002). Structure-function of the multifunctional Ca^{2+}/calmodulin-dependent protein kinase II. *Biochem.J.* **364**, 593-611.

Hudmon, A., Schulman, H., Kim, J., Maltez, J. M., Tsien, R. W., & Pitt, G. S. (2005). CaMKII tethers to L-type Ca2+ channels, establishing a local and dedicated integrator of Ca2+ signals for facilitation. *J.Cell Biol.* **171**, 537-547.

Huguenard, J. R. (1996). Low-threshold calcium currents in central nervous system neurons. *Annu.Rev.Physiol* **58**, 329-348.

Hullin, R., Singer-Lahat, D., Freichel, M., Biel, M., Dascal, N., Hofmann, F., & Flockerzi, V. (1992). Calcium channel beta subunit heterogeneity: functional expression of cloned cDNA from heart, aorta and brain. *EMBO J.* **11**, 885-890.

Hullin, R., Asmus, F., Ludwig, A., Hersel, J., & Boekstegers, P. (1999). Subunit expression of the cardiac L-type calcium channel is differentially regulated in diastolic heart failure of the cardiac allograft. *Circulation* **100**, 155-163.

Hullin, R., Khan, I. F., Wirtz, S., Mohacsi, P., Varadi, G., Schwartz, A., & Herzig, S. (2003). Cardiac L-type calcium channel beta-subunits expressed in human heart have differential effects on single channel characteristics. *J.Biol.Chem.* **278**, 21623-21630.

Hummer, A., Delzeith, O., Gomez, S. R., Moreno, R. L., Mark, M. D., & Herlitze, S. (2003). Competitive and synergistic interactions of G protein beta(2) and $Ca^{(2+)}$ channel beta(1b) subunits with Ca(v)2.1 channels, revealed by mammalian two-hybrid and fluorescence resonance energy transfer measurements. *J.Biol.Chem.* **278**, 49386-49400.

Ikeda, S. R. & Schofield, G. G. (1989). Somatostatin blocks a calcium current in rat sympathetic ganglion neurones. *J.Physiol* **409**, 221-240.

Ikeda, S. R. (1991). Double-pulse calcium channel current facilitation in adult rat sympathetic neurones. *J.Physiol* **439**, 181-214.

Jay, S. D., Ellis, S. B., McCue, A. F., Williams, M. E., Vedvick, T. S., Harpold, M. M., & Campbell, K. P. (1990). Primary structure of the gamma subunit of the DHP-sensitive calcium channel from skeletal muscle. *Science* **248**, 490-492.

Jay, S. D., Sharp, A. H., Kahl, S. D., Vedvick, T. S., Harpold, M. M., & Campbell, K. P. (1991). Structural characterization of the dihydropyridine-sensitive calcium channel alpha 2-subunit and the associated delta peptides. *J.Biol.Chem.* **266**, 3287-3293.

Jiang, Y., Lee, A., Chen, J., Ruta, V., Cadene, M., Chait, B. T., & MacKinnon, R. (2003). X-ray structure of a voltage-dependent K^+ channel. *Nature* **423**, 33-41.

Keen, M., Kelly, E., Krane, A., Austin, A., Wiltshire, R., Taylor, N., Docherty, K., & MacDermot, J. (1992). Cyclic AMP produces desensitization of prostacyclin and adenosine A2 receptors in hybrid cell lines but does not affect Gs function. *Biochim.Biophys.Acta* **1134**, 157-163.

Kim, D., Song, I., Keum, S., Lee, T., Jeong, M. J., Kim, S. S., McEnery, M. W., & Shin, H. S. (2001). Lack of the burst firing of thalamocortical relay neurons and resistance to absence seizures in mice lacking alpha(1G) T-type $Ca^{(2+)}$ channels. *Neuron* **31**, 35-45.

Kim, E., Naisbitt, S., Hsueh, Y. P., Rao, A., Rothschild, A., Craig, A. M., & Sheng, M. (1997). GKAP, a novel synaptic protein that interacts with the guanylate kinase-like domain of the PSD-95/SAP90 family of channel clustering molecules. *J.Cell Biol.* **136**, 669-678.

Kinoshita, M., Nukada, T., Asano, T., Mori, Y., Akaike, A., Satoh, M., & Kaneko, S. (2001). Binding of G alpha(o) N terminus is responsible for the voltage-resistant inhibition of alpha(1A) (P/Q-type, Ca(v)2.1) $Ca^{(2+)}$ channels. *J.Biol.Chem.* **276**, 28731-28738.

Klee, W. A. & Nirenberg, M. (1974). A neuroblastoma times glioma hybrid cell line with morphine receptors. *Proc.Natl.Acad.Sci.U.S.A* **71**, 3474-3477.

Klugbauer, N., Lacinova, L., Marais, E., Hobom, M., & Hofmann, F. (1999). Molecular diversity of the calcium channel alpha2delta subunit. *J.Neurosci.* **19**, 684-691.

Klugbauer, N., Dai, S., Specht, V., Lacinova, L., Marais, E., Bohn, G., & Hofmann, F. (2000). A family of gamma-like calcium channel subunits. *FEBS Lett.* **470**, 189-197.

Koch, W. J., Ellinor, P. T., & Schwartz, A. (1990). cDNA cloning of a dihydropyridine-sensitive calcium channel from rat aorta. Evidence for the existence of alternatively spliced forms. *J.Biol.Chem.* **265**, 17786-17791.

Kollmar, R., Fak, J., Montgomery, L. G., & Hudspeth, A. J. (1997). Hair cell-specific splicing of mRNA for the alpha1D subunit of voltage-gated Ca^{2+} channels in the chicken's cochlea. *Proc.Natl.Acad.Sci.U.S.A* **94**, 14889-14893.

Kolodziej, S. J., Hudmon, A., Waxham, M. N., & Stoops, J. K. (2000). Three-dimensional reconstructions of calcium/calmodulin-dependent (CaM) kinase IIalpha and truncated CaM kinase IIalpha reveal a unique organization for its structural core and functional domains. *J.Biol.Chem.* **275**, 14354-14359.

Koschak, A., Reimer, D., Walter, D., Hoda, J. C., Heinzle, T., Grabner, M., & Striessnig, J. (2003). Cav1.4alpha1 subunits can form slowly inactivating dihydropyridine-sensitive L-type Ca2+ channels lacking Ca^{2+}-dependent inactivation. *J.Neurosci.* **23**, 6041-6049.

Kretsinger, R. H. (1980). Structure and evolution of calcium-modulated proteins. *CRC Crit Rev.Biochem.* **8**, 119-174.

Krugmann, S., Hawkins, P. T., Pryer, N., & Braselmann, S. (1999). Characterizing the interactions between the two subunits of the p101/p110gamma phosphoinositide 3-kinase and their role in the activation of this enzyme by G beta gamma subunits. *J.Biol.Chem.* **274**, 17152-17158.

Lacinova, L., Klugbauer, N., & Hofmann, F. (2000). Low voltage activated calcium channels: from genes to function. *Gen.Physiol Biophys.* **19**, 121-136.

Laemmli, U. K. (1970). Cleavage of structural proteins during the assembly of the head of bacteriophage T4. *Nature* **227**, 680-685.

Lee, J. H., Daud, A. N., Cribbs, L. L., Lacerda, A. E., Pereverzev, A., Klockner, U., Schneider, T., & Perez-Reyes, E. (1999). Cloning and expression of a novel member of the low voltage-activated T-type calcium channel family. *J.Neurosci.* **19**, 1912-1921.

Lee, R. Y., Hench, J., & Ruvkun, G. (2001). Regulation of C. elegans DAF-16 and its human ortholog FKHRL1 by the daf-2 insulin-like signaling pathway. *Curr.Biol.* **11**, 1950-1957.

Leroy, J., Richards, M. W., Butcher, A. J., Nieto-Rostro, M., Pratt, W. S., Davies, A., & Dolphin, A. C. (2005). Interaction via a key tryptophan in the I-II linker of N-type calcium channels is required for beta1 but not for palmitoylated beta2, implicating an additional binding site in the regulation of channel voltage-dependent properties. *J.Neurosci.* **25**, 6984-6996.

Letts, V. A., Felix, R., Biddlecome, G. H., Arikkath, J., Mahaffey, C. L., Valenzuela, A., Bartlett, F. S., Mori, Y., Campbell, K. P., & Frankel, W. N. (1998). The mouse stargazer gene encodes a neuronal Ca^{2+} channel gamma subunit. *Nat.Genet.* **19**, 340-347.

Lewit-Bentley, A. & Rety, S. (2000). EF-hand calcium-binding proteins. *Curr.Opin.Struct.Biol.* **10**, 637-643.

Lhuillier, L. & Dryer, S. E. (2002). Developmental regulation of neuronal K(Ca) channels by TGFbeta1: an essential role for PI3 kinase signaling and membrane insertion. *J.Neurophysiol.* **88**, 954-964.

Liu, H., Felix, R., Gurnett, C. A., De Waard, M., Witcher, D. R., & Campbell, K. P. (1996). Expression and subunit interaction of voltage-dependent Ca^{2+} channels in PC12 cells. *J.Neurosci.* **16**, 7557-7565.

Llinas, R. & Yarom, Y. (1981). Electrophysiology of mammalian inferior olivary neurones in vitro. Different types of voltage-dependent ionic conductances. *J.Physiol* **315**, 549-567.

Lopez-Ilasaca, M., Crespo, P., Pellici, P. G., Gutkind, J. S., & Wetzker, R. (1997). Linkage of G protein-coupled receptors to the MAPK signaling pathway through PI 3-kinase gamma. *Science* **275**, 394-397.

Ludwig, A., Flockerzi, V., & Hofmann, F. (1997). Regional expression and cellular localization of the alpha1 and beta subunit of high voltage-activated calcium channels in rat brain. *J.Neurosci.* **17**, 1339-1349.

Lukyanetz, E. A. (1998). Diversity and properties of calcium channel types in NG108-15 hybrid cells. *Neuroscience* **87**, 265-274.

Maltez, J. M., Nunziato, D. A., Kim, J., & Pitt, G. S. (2005). Essential Ca(V)beta modulatory properties are AID-independent. *Nat.Struct.Mol.Biol.* **12**, 372-377.

Martinez-Lara, E., Leaver, M., & George, S. (2002). Evidence from heterologous expression of glutathione S-transferases A and A1 of the plaice (Pleuronectes platessa) that their endogenous role is in detoxification of lipid peroxidation products. *Mar.Environ.Res.* **54**, 263-266.

McFadzean, I., Mullaney, I., Brown, D. A., & Milligan, G. (1989). Antibodies to the GTP binding protein, Go, antagonize noradrenaline-induced calcium current inhibition in NG108-15 hybrid cells. *Neuron* **3**, 177-182.

McGee, A. W. & Bredt, D. S. (1999). Identification of an intramolecular interaction between the SH3 and guanylate kinase domains of PSD-95. *J.Biol.Chem.* **274**, 17431-17436.

McGee, A. W., Dakoji, S. R., Olsen, O., Bredt, D. S., Lim, W. A., & Prehoda, K. E. (2001). Structure of the SH3-guanylate kinase module from PSD-95 suggests a mechanism for regulated assembly of MAGUK scaffolding proteins. *Mol.Cell* **8**, 1291-1301.

McRory, J. E., Hamid, J., Doering, C. J., Garcia, E., Parker, R., Hamming, K., Chen, L., Hildebrand, M., Beedle, A. M., Feldcamp, L., Zamponi, G. W., & Snutch, T. P. (2004). The CACNA1F gene encodes an L-type calcium channel with unique biophysical properties and tissue distribution. *J.Neurosci.* **24**, 1707-1718.

Meir, A., Bell, D. C., Stephens, G. J., Page, K. M., & Dolphin, A. C. (2000). Calcium channel beta subunit promotes voltage-dependent modulation of alpha 1 B by G beta gamma. *Biophys.J.* **79**, 731-746.

Michalak, M., Mariani, P., & Opas, M. (1998). Calreticulin, a multifunctional Ca2+ binding chaperone of the endoplasmic reticulum. *Biochem.Cell Biol.* **76**, 779-785.

Mintz, I. M., Venema, V. J., Swiderek, K. M., Lee, T. D., Bean, B. P., & Adams, M. E. (1992). P-type calcium channels blocked by the spider toxin omega-Aga-IVA. *Nature* **355**, 827-829.

Mintz, I. M., Sabatini, B. L., & Regehr, W. G. (1995). Calcium control of transmitter release at a cerebellar synapse. *Neuron* **15**, 675-688.

Morad, M., Sanders, C., & Weiss, J. (1981). The inotropic actions of adrenaline on frog ventricular muscle: relaxing versus potentiating effects. *J.Physiol* **311**, 585-604.

Mori, Y., Friedrich, T., Kim, M. S., Mikami, A., Nakai, J., Ruth, P., Bosse, E., Hofmann, F., Flockerzi, V., Furuichi, T., & (1991). Primary structure and functional expression from complementary DNA of a brain calcium channel. *Nature* **350**, 398-402.

Mori, Y., Niidome, T., Fujita, Y., Mynlieff, M., Dirksen, R. T., Beam, K. G., Iwabe, N., Miyata, T., Furutama, D., Furuichi, T., & (1993). Molecular diversity of voltage-dependent calcium channel. *Ann.N.Y.Acad.Sci.* **707**, 87-108.

Moss, F. J., Viard, P., Davies, A., Bertaso, F., Page, K. M., Graham, A., Canti, C., Plumpton, M., Plumpton, C., Clare, J. J., & Dolphin, A. C. (2002). The novel product of a five-exon stargazin-related gene abolishes Ca(V)2.2 calcium channel expression. *EMBO J.* **21**, 1514-1523.

Murakami, M., Yamamura, H., Murakami, A., Okamura, T., Nunoki, K., Mitui-Saito, M., Muraki, K., Hano, T., Imaizumi, Y., Flockerzi, T., & Yanagisawa, T. (2000). Conserved smooth muscle contractility and blood pressure increase in response to high-salt diet in mice lacking the beta3 subunit of the voltage-dependent calcium channel. *J.Cardiovasc.Pharmacol.* **36 Suppl 2**, S69-S73.

Murakami, M., Yamamura, H., Suzuki, T., Kang, M. G., Ohya, S., Murakami, A., Miyoshi, I., Sasano, H., Muraki, K., Hano, T., Kasai, N., Nakayama, S., Campbell, K. P., Flockerzi, V., Imaizumi, Y., Yanagisawa, T., & Iijima, T. (2003). Modified cardiovascular L-type channels in mice lacking the voltage-dependent Ca^{2+} channel beta3 subunit. *J.Biol.Chem.* **278**, 43261-43267.

Murata, K., Odahara, N., Kuniyasu, A., Sato, Y., Nakayama, H., & Nagayama, K. (2001). Asymmetric arrangement of auxiliary subunits of skeletal muscle voltage-gated l-type Ca(2+) channel. *Biochem.Biophys.Res.Commun.* **282**, 284-291.

Murga, C., Laguinge, L., Wetzker, R., Cuadrado, A., & Gutkind, J. S. (1998). Activation of Akt/protein kinase B by G protein-coupled receptors. A role for alpha and beta gamma subunits of heterotrimeric G proteins acting through phosphatidylinositol-3-OH kinasegamma. *J.Biol.Chem.* **273**, 19080-19085.

Muslin, A. J., Tanner, J. W., Allen, P. M., & Shaw, A. S. (1996). Interaction of 14-3-3 with signaling proteins is mediated by the recognition of phosphoserine. *Cell* **84**, 889-897.

Nallamsetty, S. & Waugh, D. S. (2006). Solubility-enhancing proteins MBP and NusA play a passive role in the folding of their fusion partners. *Protein Expr.Purif.* **45**, 175-182.

Neher, E. (1995). The use of fura-2 for estimating Ca buffers and Ca fluxes. *Neuropharmacology* **34**, 1423-1442.

Neuhuber, B., Gerster, U., Mitterdorfer, J., Glossmann, H., & Flucher, B. E. (1998). Differential effects of Ca^{2+} channel beta1a and beta2a subunits on complex formation with alpha1S and on current expression in tsA201 cells. *J.Biol.Chem.* **273**, 9110-9118.

Newcomb, R., Szoke, B., Palma, A., Wang, G., Chen, X., Hopkins, W., Cong, R., Miller, J., Urge, L., Tarczy-Hornoch, K., Loo, J. A., Dooley, D. J., Nadasdi, L., Tsien, R. W., Lemos, J., & Miljanich, G. (1998). Selective peptide antagonist of the class E calcium channel from the venom of the tarantula Hysterocrates gigas. *Biochemistry* **37**, 15353-15362.

Nicholson, K. M. & Anderson, N. G. (2002). The protein kinase B/Akt signalling pathway in human malignancy. *Cell Signal.* **14**, 381-395.

Nicoll, R. A., Tomita, S., & Bredt, D. S. (2006). Auxiliary subunits assist AMPA-type glutamate receptors. *Science* **311**, 1253-1256.

Nowycky, M. C., Fox, A. P., & Tsien, R. W. (1985). Three types of neuronal calcium channel with different calcium agonist sensitivity. *Nature* **316**, 440-443.

Nygren, P. A., Stahl, S., & Uhlen, M. (1994). Engineering proteins to facilitate bioprocessing. *Trends Biotechnol.* **12**, 184-188.

Opatowsky, Y., Chomsky-Hecht, O., Kang, M. G., Campbell, K. P., & Hirsch, J. A. (2003). The voltage-dependent calcium channel beta subunit contains two stable interacting domains. *J.Biol.Chem.* **278**, 52323-52332.

Opatowsky, Y., Chen, C. C., Campbell, K. P., & Hirsch, J. A. (2004). Structural analysis of the voltage-dependent calcium channel beta subunit functional core and its complex with the alpha 1 interaction domain. *Neuron* **42**, 387-399.

Ophoff, R. A., Terwindt, G. M., Vergouwe, M. N., van Eijk, R., Oefner, P. J., Hoffman, S. M., Lamerdin, J. E., Mohrenweiser, H. W., Bulman, D. E., Ferrari, M., Haan, J., Lindhout, D., van Ommen, G. J., Hofker, M. H., Ferrari, M. D., & Frants, R. R. (1996). Familial hemiplegic migraine and episodic ataxia type-2 are caused by mutations in the Ca^{2+} channel gene CACNL1A4. *Cell* **87**, 543-552.

Pawson, T. (1994). SH2 and SH3 domains in signal transduction. *Adv.Cancer Res.* **64**, 87-110.

Perez-Reyes, E., Castellano, A., Kim, H. S., Bertrand, P., Baggstrom, E., Lacerda, A. E., Wei, X. Y., & Birnbaumer, L. (1992). Cloning and expression of a cardiac/brain beta subunit of the L-type calcium channel. *J.Biol.Chem.* **267**, 1792-1797.

Perez-Reyes, E., Cribbs, L. L., Daud, A., Lacerda, A. E., Barclay, J., Williamson, M. P., Fox, M., Rees, M., & Lee, J. H. (1998). Molecular characterization of a neuronal low-voltage-activated T-type calcium channel. *Nature* **391**, 896-900.

Persad, S., Attwell, S., Gray, V., Mawji, N., Deng, J. T., Leung, D., Yan, J., Sanghera, J., Walsh, M. P., & Dedhar, S. (2001). Regulation of protein kinase B/Akt-serine 473 phosphorylation by integrin-linked kinase: critical roles for kinase activity and amino acids arginine 211 and serine 343. *J.Biol.Chem.* **276**, 27462-27469.

Petosa, C., Masters, S. C., Bankston, L. A., Pohl, J., Wang, B., Fu, H., & Liddington, R. C. (1998). 14-3-3zeta binds a phosphorylated Raf peptide and an unphosphorylated peptide via its conserved amphipathic groove. *J.Biol.Chem.* **273**, 16305-16310.

Pichler, M., Cassidy, T. N., Reimer, D., Haase, H., Kraus, R., Ostler, D., & Striessnig, J. (1997). Beta subunit heterogeneity in neuronal L-type Ca^{2+} channels. *J.Biol.Chem.* **272**, 13877-13882.

Powers, P. A., Liu, S., Hogan, K., & Gregg, R. G. (1992). Skeletal muscle and brain isoforms of a beta-subunit of human voltage-dependent calcium channels are encoded by a single gene. *J.Biol.Chem.* **267**, 22967-22972.

Pragnell, M., De Waard, M., Mori, Y., Tanabe, T., Snutch, T. P., & Campbell, K. P. (1994). Calcium channel beta-subunit binds to a conserved motif in the I-II cytoplasmic linker of the alpha 1-subunit. *Nature* **368**, 67-70.

Puri, T. S., Gerhardstein, B. L., Zhao, X. L., Ladner, M. B., & Hosey, M. M. (1997). Differential effects of subunit interactions on protein kinase. *Biochemistry* **36**, 9605-9615.

Qian, J. & Noebels, J. L. (2000). Presynaptic Ca(2+) influx at a mouse central synapse with Ca(2+) channel subunit mutations. *J.Neurosci.* **20**, 163-170.

Qin, N., Platano, D., Olcese, R., Stefani, E., & Birnbaumer, L. (1997). Direct interaction of g betagamma with a C-terminal g betagamma-binding domain of the Ca^{2+} channel alpha1 subunit is responsible for channel inhibition by G protein-coupled receptors. *Proc.Natl.Acad.Sci.U.S.A* **94**, 8866-8871.

Qin, N., Platano, D., Olcese, R., Costantin, J. L., Stefani, E., & Birnbaumer, L. (1998). Unique regulatory properties of the type 2a Ca^{2+} channel beta subunit caused by palmitoylation. *Proc.Natl.Acad.Sci.U.S.A* **95**, 4690-4695.

Qin, N., Yagel, S., Momplaisir, M. L., Codd, E. E., & D'Andrea, M. R. (2002). Molecular cloning and characterization of the human voltage-gated calcium channel alpha(2)delta-4 subunit. *Mol.Pharmacol.* **62**, 485-496.

Rajan, S., Preisig-Muller, R., Wischmeyer, E., Nehring, R., Hanley, P. J., Renigunta, V., Musset, B., Schlichthorl, G., Derst, C., Karschin, A., & Daut, J. (2002). Interaction with 14-3-3 proteins promotes functional expression of the potassium channels TASK-1 and TASK-3. *J.Physiol* **545**, 13-26.

Rameh, L. E. & Cantley, L. C. (1999). The role of phosphoinositide 3-kinase lipid products in cell function. *J.Biol.Chem.* **274**, 8347-8350.

Randall, A. & Tsien, R. W. (1995). Pharmacological dissection of multiple types of Ca^{2+} channel currents in rat cerebellar granule neurons. *J.Neurosci.* **15**, 2995-3012.

Restituito, S., Cens, T., Barrere, C., Geib, S., Galas, S., De Waard, M., & Charnet, P. (2000). The [beta]2a subunit is a molecular groom for the Ca^{2+} channel inactivation gate. *J.Neurosci.* **20**, 9046-9052.

Reuter, H. (1983). Calcium channel modulation by neurotransmitters, enzymes and drugs. *Nature* **301**, 569-574.

Richards, M. W., Butcher, A. J., & Dolphin, A. C. (2004). Ca^{2+} channel beta-subunits: structural insights AID our understanding. *Trends Pharmacol.Sci.* **25**, 626-632.

Rouach, N., Byrd, K., Petralia, R. S., Elias, G. M., Adesnik, H., Tomita, S., Karimzadegan, S., Kealey, C., Bredt, D. S., & Nicoll, R. A. (2005). TARP gamma-8 controls hippocampal AMPA receptor number, distribution and synaptic plasticity. *Nat.Neurosci.* **8**, 1525-1533.

Rousset, M., Cens, T., Restituito, S., Barrere, C., Black, J. L., III, McEnery, M. W., & Charnet, P. (2001). Functional roles of gamma2, gamma3 and gamma4, three new Ca2+ channel subunits, in P/Q-type Ca^{2+} channel expressed in Xenopus oocytes. *J.Physiol* **532**, 583-593.

Ruggeri, B. A., Huang, L., Wood, M., Cheng, J. Q., & Testa, J. R. (1998). Amplification and overexpression of the AKT2 oncogene in a subset of human pancreatic ductal adenocarcinomas. *Mol.Carcinog.* **21**, 81-86.

Ruth, P., Rohrkasten, A., Biel, M., Bosse, E., Regulla, S., Meyer, H. E., Flockerzi, V., & Hofmann, F. (1989). Primary structure of the beta subunit of the DHP-sensitive calcium channel from skeletal muscle. *Science* **245**, 1115-1118.

Sandoz, G., Lopez-Gonzalez, I., Grunwald, D., Bichet, D., Altafaj, X., Weiss, N., Ronjat, M., Dupuis, A., & De Waard, M. (2004). Cavbeta-subunit displacement is a key step to induce the reluctant state of P/Q calcium channels by direct G protein regulation. *Proc.Natl.Acad.Sci.U.S.A* **101**, 6267-6272.

Sarbassov, D. D., Guertin, D. A., Ali, S. M., & Sabatini, D. M. (2005). Phosphorylation and regulation of Akt/PKB by the rictor-mTOR complex. *Science* **307**, 1098-1101.

Schmitt, H. & Meves, H. (1994). Bovine serum albumin selectively increases the low-voltage-activated calcium current of NG108-15 neuroblastoma x glioma cells. *Brain Res.* **656**, 375-380.

Scholze, A., Plant, T. D., Dolphin, A. C., & Nurnberg, B. (2001). Functional expression and characterization of a voltage-gated CaV1.3 (alpha1D) calcium channel subunit from an insulin-secreting cell line. *Mol.Endocrinol.* **15**, 1211-1221.

Schwartz, L. M., McCleskey, E. W., & Almers, W. (1985). Dihydropyridine receptors in muscle are voltage-dependent but most are not functional calcium channels. *Nature* **314**, 747-751.

Scott, V. E., De Waard, M., Liu, H., Gurnett, C. A., Venzke, D. P., Lennon, V. A., & Campbell, K. P. (1996). Beta subunit heterogeneity in N-type Ca^{2+} channels. *J.Biol.Chem.* **271**, 3207-3212.

Seagar, M. & Takahashi, M. (1998). Interactions between presynaptic calcium channels and proteins implicated in synaptic vesicle trafficking and exocytosis. *J.Bioenerg.Biomembr.* **30**, 347-356.

Sekulic, A., Hudson, C. C., Homme, J. L., Yin, P., Otterness, D. M., Karnitz, L. M., & Abraham, R. T. (2000). A direct linkage between the phosphoinositide 3-kinase-AKT signaling pathway and the mammalian target of rapamycin in mitogen-stimulated and transformed cells. *Cancer Res.* **60**, 3504-3513.

Sharp, A. H., Black, J. L., III, Dubel, S. J., Sundarraj, S., Shen, J. P., Yunker, A. M., Copeland, T. D., & McEnery, M. W. (2001). Biochemical and anatomical evidence for specialized voltage-dependent calcium channel gamma isoform expression in the epileptic and ataxic mouse, stargazer. *Neuroscience* **105**, 599-617.

Shin, H., Hsueh, Y. P., Yang, F. C., Kim, E., & Sheng, M. (2000). An intramolecular interaction between Src homology 3 domain and guanylate kinase-like domain required for channel clustering by postsynaptic density-95/SAP90. *J.Neurosci.* **20**, 3580-3587.

Singer, D., Biel, M., Lotan, I., Flockerzi, V., Hofmann, F., & Dascal, N. (1991). The roles of the subunits in the function of the calcium channel. *Science* **253**, 1553-1557.

Skryma, R., Mariot, P., Bourhis, X. L., Coppenolle, F. V., Shuba, Y., Vanden Abeele, F., Legrand, G., Humez, S., Boilly, B., & Prevarskaya, N. (2000). Store depletion and store-operated Ca^{2+} current in human prostate cancer LNCaP cells: involvement in apoptosis. *J.Physiol* **527 Pt 1**, 71-83.

Soldatov, N. M., Oz, M., O'Brien, K. A., Abernethy, D. R., & Morad, M. (1998). Molecular determinants of L-type Ca^{2+} channel inactivation. Segment exchange analysis of the carboxyl-terminal cytoplasmic motif encoded by exons 40-42 of the human alpha1C subunit gene. *J.Biol.Chem.* **273**, 957-963.

Spaetgens, R. L. & Zamponi, G. W. (1999). Multiple structural domains contribute to voltage-dependent inactivation of rat brain alpha(1E) calcium channels. *J.Biol.Chem.* **274**, 22428-22436.

Staros, J. V., Wright, R. W., & Swingle, D. M. (1986). Enhancement by N-hydroxysulfosuccinimide of water-soluble carbodiimide-mediated coupling reactions. *Anal.Biochem.* **156**, 220-222.

Stea, A., Tomlinson, W. J., Soong, T. W., Bourinet, E., Dubel, S. J., Vincent, S. R., & Snutch, T. P. (1994). Localization and functional properties of a rat brain alpha 1A calcium channel reflect similarities to neuron. *Proc.Natl.Acad.Sci.U.S.A* **91**, 10576-10580.

Stephens, G. J., Canti, C., Page, K. M., & Dolphin, A. C. (1998). Role of domain I of neuronal Ca2+ channel alpha1 subunits in G protein modulation. *J.Physiol* **509 (Pt 1)**, 163-169.

Stephens, G. J., Page, K. M., Bogdanov, Y., & Dolphin, A. C. (2000). The alpha1B Ca^{2+} channel amino terminus contributes determinants for beta subunit-mediated voltage-dependent inactivation properties. *J.Physiol* **525 Pt 2**, 377-390.

Stephens, L. R., Eguinoa, A., Erdjument-Bromage, H., Lui, M., Cooke, F., Coadwell, J., Smrcka, A. S., Thelen, M., Cadwallader, K., Tempst, P., & Hawkins, P. T. (1997). The G beta gamma sensitivity of a PI3K is dependent upon a tightly associated adaptor, p101. *Cell* **89**, 105-114.

Stotz, S. C., Hamid, J., Spaetgens, R. L., Jarvis, S. E., & Zamponi, G. W. (2000). Fast inactivation of voltage-dependent calcium channels. A hinged-lid mechanism? *J.Biol.Chem.* **275**, 24575-24582.

Stotz, S. C. & Zamponi, G. W. (2001). Structural determinants of fast inactivation of high voltage-activated Ca(2+) channels. *Trends Neurosci.* **24**, 176-181.

Stoyanov, B., Volinia, S., Hanck, T., Rubio, I., Loubtchenkov, M., Malek, D., Stoyanova, S., Vanhaesebroeck, B., Dhand, R., Nurnberg, B., & . (1995). Cloning and characterization of a G protein-activated human phosphoinositide-3 kinase. *Science* **269**, 690-693.

Strom, T. M., Nyakatura, G., Apfelstedt-Sylla, E., Hellebrand, H., Lorenz, B., Weber, B. H., Wutz, K., Gutwillinger, N., Ruther, K., Drescher, B., Sauer, C., Zrenner, E., Meitinger, T., Rosenthal, A., & Meindl, A. (1998). An L-type calcium-channel gene mutated in incomplete X-linked congenital stationary night blindness. *Nat.Genet.* **19**, 260-263.

Su, Z., Csutora, P., Hunton, D., Shoemaker, R. L., Marchase, R. B., & Blalock, J. E. (2001). A store-operated nonselective cation channel in lymphocytes is activated directly by Ca^{2+} influx factor and diacylglycerol. *Am.J.Physiol Cell Physiol* **280**, C1284-C1292.

Suginta, W., Karoulias, N., Aitken, A., & Ashley, R. H. (2001). Chloride intracellular channel protein CLIC4 (p64H1) binds directly to brain dynamin I in a complex containing actin, tubulin and 14-3-3 isoforms. *Biochem.J.* **359**, 55-64.

Swick, A. G., Janicot, M., Cheneval-Kastelic, T., McLenithan, J. C., & Lane, M. D. (1992). Promoter-cDNA-directed heterologous protein expression in Xenopus laevis oocytes. *Proc.Natl.Acad.Sci.U.S.A* **89**, 1812-1816.

Takahashi, M. & Catterall, W. A. (1987). Dihydropyridine-sensitive calcium channels in cardiac and skeletal muscle membranes: studies with antibodies against the alpha subunits. *Biochemistry* **26**, 5518-5526.

Takahashi, M., Seagar, M. J., Jones, J. F., Reber, B. F., & Catterall, W. A. (1987). Subunit structure of dihydropyridine-sensitive calcium channels from skeletal muscle. *Proc.Natl.Acad.Sci.U.S.A* **84**, 5478-5482.

Takahashi, S. X., Mittman, S., & Colecraft, H. M. (2003). Distinctive modulatory effects of five human auxiliary beta2 subunit splice variants on L-type calcium channel gating. *Biophys.J.* **84**, 3007-3021.

Takahashi, S. X., Miriyala, J., & Colecraft, H. M. (2004). Membrane-associated guanylate kinase-like properties of beta-subunits required for modulation of voltage-dependent Ca2+ channels. *Proc.Natl.Acad.Sci.U.S.A* **101**, 7193-7198.

Tanabe, T., Takeshima, H., Mikami, A., Flockerzi, V., Takahashi, H., Kangawa, K., Kojima, M., Matsuo, H., Hirose, T., & Numa, S. (1987). Primary structure of the receptor for calcium channel blockers from skeletal muscle. *Nature* **328**, 313-318.

Testa, J. R. & Bellacosa, A. (2001). AKT plays a central role in tumorigenesis. *Proc.Natl.Acad.Sci.U.S.A* **98**, 10983-10985.

Tomita, S., Adesnik, H., Sekiguchi, M., Zhang, W., Wada, K., Howe, J. R., Nicoll, R. A., & Bredt, D. S. (2005). Stargazin modulates AMPA receptor gating and trafficking by distinct domains. *Nature* **435**, 1052-1058.

Tsunoo, A., Yoshii, M., & Narahashi, T. (1986). Block of calcium channels by enkephalin and somatostatin in neuroblastoma-glioma hybrid NG108-15 cells. *Proc.Natl.Acad.Sci.U.S.A* **83**, 9832-9836.

Tzivion, G., Shen, Y. H., & Zhu, J. (2001). 14-3-3 proteins; bringing new definitions to scaffolding. *Oncogene* **20**, 6331-6338.

van Hemert, M. J., Steensma, H. Y., & van Heusden, G. P. (2001). 14-3-3 proteins: key regulators of cell division, signalling and apoptosis. *Bioessays* **23**, 936-946.

Van Petegem, F., Clark, K. A., Chatelain, F. C., & Minor, D. L., Jr. (2004). Structure of a complex between a voltage-gated calcium channel beta-subunit and an alpha-subunit domain. *Nature* **429**, 671-675.

Vendel, A. C., Rithner, C. D., Lyons, B. A., & Horne, W. A. (2006). Solution structure of the N-terminal A domain of the human voltage-gated Ca^{2+} channel beta4a subunit. *Protein Sci.* **15**, 378-383.

Viard, P., Exner, T., Maier, U., Mironneau, J., Nurnberg, B., & Macrez, N. (1999). Gbetagamma dimers stimulate vascular L-type Ca^{2+} channels via phosphoinositide 3-kinase. *FASEB J.* **13**, 685-694.

Viard, P., Butcher, A. J., Halet, G., Davies, A., Nurnberg, B., Heblich, F., & Dolphin, A. C. (2004). PI3K promotes voltage-dependent calcium channel trafficking to the plasma membrane. *Nat.Neurosci.* **7**, 939-946.

Wakamori, M., Mikala, G., & Mori, Y. (1999). Auxiliary subunits operate as a molecular switch in determining gating behaviour of the unitary N-type Ca^{2+} channel current in Xenopus oocytes. *J.Physiol* **517 (Pt 3)**, 659-672.

Walker, D. & De Waard, M. (1998). Subunit interaction sites in voltage-dependent Ca^{2+} channels: role in channel function. *Trends Neurosci.* **21**, 148-154.

Walker, D., Bichet, D., Geib, S., Mori, E., Cornet, V., Snutch, T. P., Mori, Y., & De Waard, M. (1999). A new beta subtype-specific interaction in alpha1A subunit controls P/Q-type Ca2+ channel activation. *J.Biol.Chem.* **274**, 12383-12390.

Wang, L., Hayashi, H., & Ebina, Y. (1999). Transient effect of platelet-derived growth factor on GLUT4 translocation in 3T3-L1 adipocytes. *J.Biol.Chem.* **274**, 19246-19253.

Wang, M. C., Velarde, G., Ford, R. C., Berrow, N. S., Dolphin, A. C., & Kitmitto, A. (2002). 3D structure of the skeletal muscle dihydropyridine receptor. *J.Mol.Biol.* **323**, 85-98.

Wang, M. C., Collins, R. F., Ford, R. C., Berrow, N. S., Dolphin, A. C., & Kitmitto, A. (2004). The three-dimensional structure of the cardiac L-type voltage-gated calcium channel: comparison with the skeletal muscle form reveals a common architectural motif. *J.Biol.Chem.* **279**, 7159-7168.

Wei, S. K., Colecraft, H. M., DeMaria, C. D., Peterson, B. Z., Zhang, R., Kohout, T. A., Rogers, T. B., & Yue, D. T. (2000). Ca^{2+} channel modulation by recombinant auxiliary beta subunits expressed in young adult heart cells. *Circ.Res.* **86**, 175-184.

Weick, J. P., Groth, R. D., Isaksen, A. L., & Mermelstein, P. G. (2003). Interactions with PDZ proteins are required for L-type calcium channels to activate cAMP response element-binding protein-dependent gene expression. *J.Neurosci.* **23**, 3446-3456.

Weston, C. R. & Davis, R. J. (2001). Signal transduction: Signaling specificity – a complex affair. *Science* **292**, 2439-2440.

Williams, M. E., Brust, P. F., Feldman, D. H., Patthi, S., Simerson, S., Maroufi, A., McCue, A. F., Velicelebi, G., Ellis, S. B., & Harpold, M. M. (1992). Structure and functional expression of an omega-conotoxin-sensitive human N-type calcium channel. *Science* **257**, 389-395.

Witcher, D. R., De Waard, M., Liu, H., Pragnell, M., & Campbell, K. P. (1995). Association of native Ca^{2+} channel beta subunits with the alpha 1 subunit interaction domain. *J.Biol.Chem.* **270**, 18088-18093.

Wolf, M., Eberhart, A., Glossmann, H., Striessnig, J., & Grigorieff, N. (2003). Visualization of the domain structure of an L-type Ca^{2+} channel using electron cryo-microscopy. *J.Mol.Biol.* **332**, 171-182.

Wu, L., Bauer, C. S., Zhen, X. G., Xie, C., & Yang, J. (2002). Dual regulation of voltage-gated calcium channels by PtdIns(4,5)P2. *Nature* **419**, 947-952.

Wu, Y., Kimbrough, J. T., Colbran, R. J., & Anderson, M. E. (2004). Calmodulin kinase is functionally targeted to the action potential plateau for regulation of L-type Ca^{2+} current in rabbit cardiomyocytes. *J.Physiol* **554**, 145-155.

Yaffe, M. B. (2002). How do 14-3-3 proteins work?-- Gatekeeper phosphorylation and the molecular anvil hypothesis. *FEBS Lett.* **513**, 53-57.

Yokoyama, C. T., Westenbroek, R. E., Hell, J. W., Soong, T. W., Snutch, T. P., & Catterall, W. A. (1995). Biochemical properties and subcellular distribution of the neuronal class E calcium channel alpha 1 subunit. *J.Neurosci.* **15**, 6419-6432.

Yu, F. H. & Catterall, W. A. (2003). Overview of the voltage-gated sodium channel family. *Genome Biol.* **4**, 207.

Zamponi, G. W., Bourinet, E., Nelson, D., Nargeot, J., & Snutch, T. P. (1997). Crosstalk between G proteins and protein kinase C mediated by the calcium channel alpha1 subunit. *Nature* **385**, 442-446.

Zhang, J. F., Ellinor, P. T., Aldrich, R. W., & Tsien, R. W. (1994). Molecular determinants of voltage-dependent inactivation in calcium channels. *Nature* **372**, 97-100.

Zhou, B. P., Liao, Y., Xia, W., Zou, Y., Spohn, B., & Hung, M. C. (2001). HER-2/neu induces p53 ubiquitination via Akt-mediated MDM2 phosphorylation. *Nat.Cell Biol.* **3**, 973-982.

Zhuchenko, O., Bailey, J., Bonnen, P., Ashizawa, T., Stockton, D. W., Amos, C., Dobyns, W. B., Subramony, S. H., Zoghbi, H. Y., & Lee, C. C. (1997). Autosomal dominant cerebellar ataxia (SCA6) associated with small polyglutamine expansions in the alpha 1A-voltage-dependent calcium channel. *Nat.Genet.* **15**, 62-69.